



LUND UNIVERSITY

Pre- and postsynaptic dysregulation of dopamine signalling in Parkinson's disease

Sahin, Gurdal

2018

Document Version:

Publisher's PDF, also known as Version of record

[Link to publication](#)

Citation for published version (APA):

Sahin, G. (2018). *Pre- and postsynaptic dysregulation of dopamine signalling in Parkinson's disease*. [Doctoral Thesis (compilation), Department of Experimental Medical Science]. Lund University: Faculty of Medicine.

Total number of authors:

1

Creative Commons License:

GNU LGPL

General rights

Unless other specific re-use rights are stated the following general rights apply:

Copyright and moral rights for the publications made accessible in the public portal are retained by the authors and/or other copyright owners and it is a condition of accessing publications that users recognise and abide by the legal requirements associated with these rights.

- Users may download and print one copy of any publication from the public portal for the purpose of private study or research.
- You may not further distribute the material or use it for any profit-making activity or commercial gain
- You may freely distribute the URL identifying the publication in the public portal

Read more about Creative commons licenses: <https://creativecommons.org/licenses/>

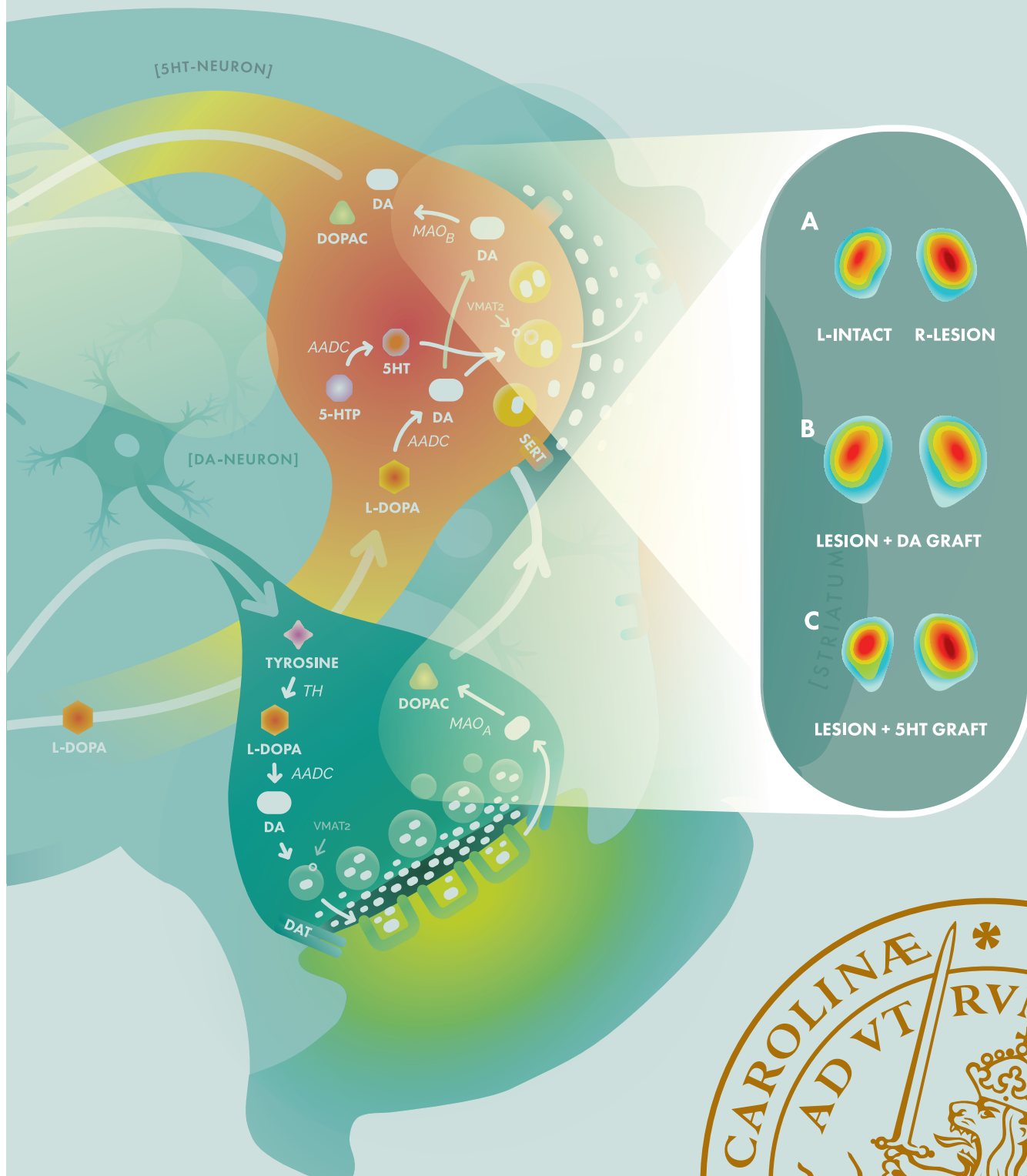
Take down policy

If you believe that this document breaches copyright please contact us providing details, and we will remove access to the work immediately and investigate your claim.

LUND UNIVERSITY

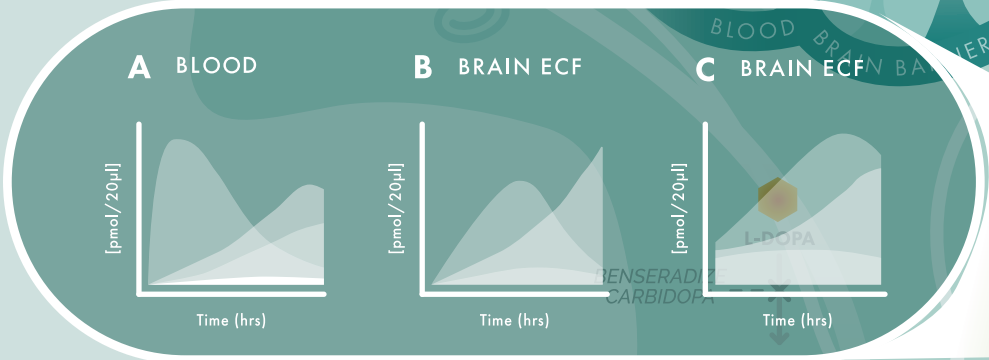
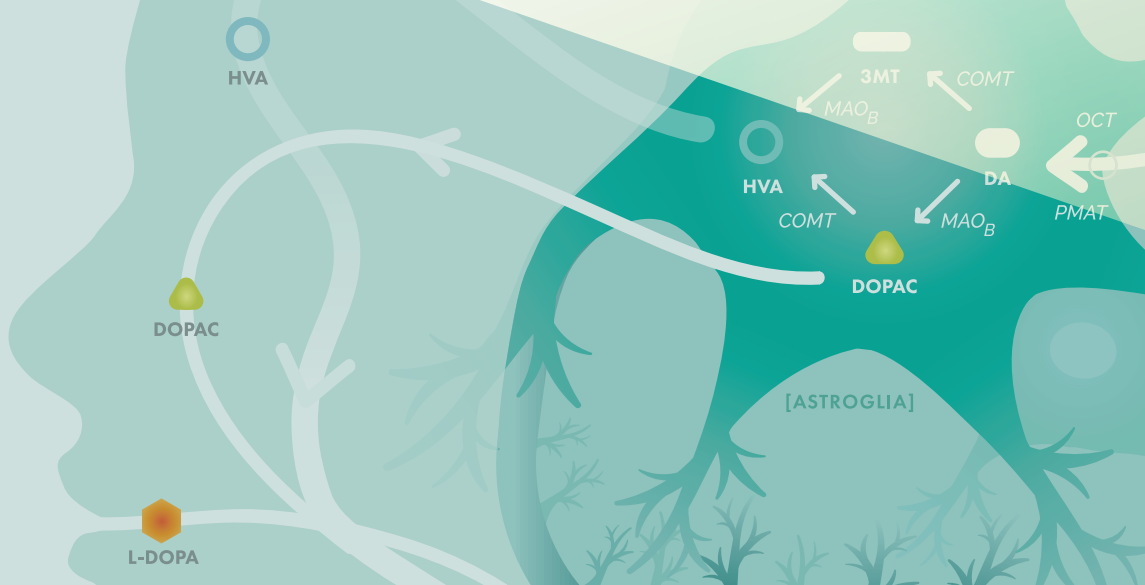
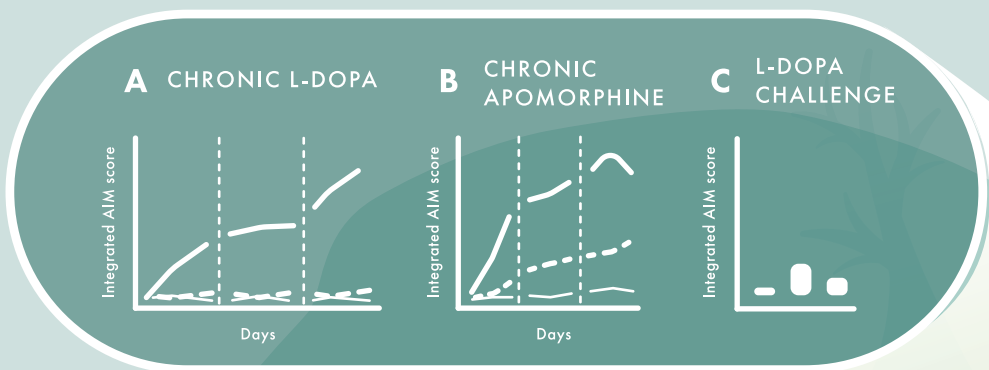
PO Box 117
221 00 Lund
+46 46-222 00 00

Pre- and postsynaptic dysregulation of dopamine signaling in Parkinson's disease



Gürdal Şahin
Lund University 2018





Pre- and postsynaptic dysregulation of dopamine signaling
in Parkinson's disease

Pre- and postsynaptic dysregulation of dopamine signaling in Parkinson's disease

Gürdal Şahin



LUND
UNIVERSITY

DOCTORAL DISSERTATION

By due permission of the Faculty of Medicine, Lund University, Sweden

This thesis will be defended at BMC I:11345 on June 12, 2018 at 9:00

Faculty opponent

Philippe De Deurwaerdère

Organization LUND UNIVERSITY Brain Repair and Imaging in Neural Systems (B.R.A.I.N.S), Department of Experimental Medical Science, BMC D11, 22184 Lund, Sweden		Document name DOCTORAL DISSERTATION	
Author(s) Gürdal Şahin		Date of issue June 12, 2018	
Title and subtitle Pre- and postsynaptic dysregulation of dopamine signaling in Parkinson's disease			
Abstract Dopamine (DA) is an important neurotransmitter that plays a fundamental role in motor control. Deficiency of DA in certain areas of the brain has been found to be the underlying pathophysiological mechanism for Parkinson's disease (PD), which is mainly characterized by motor symptoms such as muscular rigidity, slowness in movement, tremor and postural instability. Treatment of PD relies on strategies restoring this DA deficiency. L-DOPA is a naturally occurring precursor in the DA synthesis machinery, and has been shown to be the most effective therapy for PD to date. However, its use has many long-term complications such as motor fluctuations and L-DOPA-induced dyskinesia (LID). The underlying mechanisms for these complications has yet to be clarified but is thought to be mainly a result of the malfunctioning DA system. This thesis aims to investigate the mechanisms behind this dysfunctional DA signaling at multiple levels from the blood-brain barrier (BBB) transport kinetics of L-DOPA and its metabolites as well as the role of presynaptic DA and 5-HT neurons in the postsynaptic striatal responses in animal models of PD. The first study provided direct evidence that the status of the presynaptic DA-releasing compartment is a critical determinant of both the induction and maintenance of LID. The second study suggested that differential DA receptor activation rather than the excessive DA release could be the underlying mechanism for LID. In the third study, we used a prediction model, which provided a valuable tool to assess BBB transport kinetics of L-DOPA under therapeutic administration conditions. Altogether, this thesis provided evidence that presynaptic sites have a critical role in determining LID and sheds new light into DA release mechanisms by serotonin neurons. Of notable clinical relevance, our findings could help us to better understand mechanisms behind L-DOPA-induced motor complications and response variability among individuals, and thus, have crucial implications for both neurorestorative approaches and development of drugs targeting serotonergic system for the management of LID.			
Key words: [¹⁸ F]fallypride, 3-OMD, AAV, blood-brain barrier, dyskinesia, HVA, L-DOPA, microdialysis, modeling, Parkinson's disease, pharmacokinetics, positron-emission tomography, prediction, RNA interference, shRNA			
Classification system and/or index terms (if any)			
Supplementary bibliographical information		Language English	
ISSN and key title 1652-8220		ISBN 978-91-7619-659-5	
Recipient's notes	Number of pages 148	Price	

I, the undersigned, being the copyright owner of the abstract of the above-mentioned dissertation, hereby grant to all reference sources permission to publish and disseminate the abstract of the above-mentioned dissertation.

Signature



Date: May 8, 2018

*From the Brain Repair and Imaging in Neural Systems, B.R.A.I.N.S unit
Department of Experimental Medical Science, Faculty of Medicine,
Lund University, Lund, Sweden*

Pre- and postsynaptic dysregulation of dopamine signaling in Parkinson's disease

Gürdal Şahin, MD

2018



LUND
UNIVERSITY

The cover figure demonstrates the metabolism of L-DOPA and dopamine in the periphery and the central nervous system.

The cover figure and the artwork are designed by Gürdal Şahin, illustrated by Nikki Schmidt.

Page layout by Gürdal Şahin

© Gürdal Şahin

Paper 1 © National Academy of Sciences

Paper 2 © Public Library of Science (PLOS)

Paper 3 © by the authors (Manuscript unpublished)

Faculty of Medicine
Department of Experimental Medical Science

ISSN 1652-8220

ISBN 978-91-7619-659-5

Lund University, Faculty of Medicine Doctoral Dissertation Series 2018:93

Printed in Sweden by Media-Tryck, Lund University
Lund 2018



MADE IN SWEDEN 

Media-Tryck is an environmentally certified and ISO 14001 certified provider of printed material. Read more about our environmental work at www.mediatryck.lu.se

to Gülşen, Ada and Maya

On a long and narrow path, I am walking day and night

Aşık Veysel Şatırođlu (1894 – 1973)

Anatolian minstrel

Table of Contents

List of figures	10
Abbreviations	12
Original papers	15
Published papers outside the thesis	16
Summary	17
Sammanfattning på svenska	18
Türkçe özet	19
Introduction	21
A historical perspective on the biochemistry of dopamine	21
Basic physiology of the basal ganglia	23
Pathophysiology of Parkinson's disease	29
L-DOPA: From peripheral kinetics to central actions and complications ...	31
Effect of L-DOPA on natural history of PD.....	37
Aims	41
Materials and methods.....	43
Animals	43
Experimental protocols	43
Animal models of PD used in the thesis	44
Surgical procedures	45
Behavioral tests	51
PET Imaging (<i>Paper II</i>)	52
Postmortem analyses	53
Statistical analysis	56
Mathematical modeling for prediction of brain ECF levels of L-DOPA and its metabolites (<i>Paper III</i>)	56

Results	59
Presynaptic dopaminergic compartment determines LID (<i>Paper I</i>)	59
Postsynaptic differential receptor occupancy underlies LID (<i>Paper II</i>)	64
BBB transport kinetics L-DOPA towards optimization of therapeutic and diagnostic use (<i>Paper III</i>).....	69
Discussion and future directions	75
Acknowledgements	81
References	85
Paper I.....	97
Paper II	113
Paper III.....	133

List of figures

- Figure 1.** Biosynthesis and metabolism of L-DOPA.
- Figure 2.** Basal ganglia connections and striatal architecture.
- Figure 3.** The role of the basal ganglia in the selection of desired motor programs.
- Figure 4.** Immunohistochemical staining of TH in a healthy rat brain.
- Figure 5.** The role of the 5-HT neurons in the synthesis and release of DA.
- Figure 6.** Peripheral and central events following administration of L-DOPA.
- Figure 7.** Illustration of ventral mesencephalon in rat embryo.
- Figure 8.** The microdialysis setup coupled to an online HPLC system in a rat.
- Figure 9.** Schematic illustration of microdialysis.
- Figure 10.** Illustration of simultaneous blood sampling and brain microdialysis.
- Figure 11.** Abnormal involuntary movements in a rat induced by L-DOPA.
- Figure 12.** Down-regulation of TH by rAAV-mediated shRNA expression.
- Figure 13.** Three-phase microdialysis protocol.
- Figure 14.** Chronic L-DOPA and apomorphine injections to induce dyskinesia.
- Figure 15.** Behavioral characterization of the dyskinetic animals grafted with DA-rich or 5-HT-rich tissues.
- Figure 16.** Quantification of the releasable pool of DA in baseline and after administration L-DOPA.
- Figure 17.** Online microdialysis in baseline conditions before and after L-DOPA in freely moving awake animals.
- Figure 18.** Assessment of striatal D₂R occupancy using PET imaging.
- Figure 19.** In vitro receptor binding assay for D₂R and D₁R using a generalized non-linear model.
- Figure 20.** Experimental design of simultaneous blood sampling and online microdialysis.

Figure 21. Blood and brain ECF levels of DOPA and its metabolites after 12 mg/kg L-DOPA.

Figure 22. The representative examples with accurate, over-, and underestimation of the DOPA in blood and brain.

Figure 23. The performance of our predictive model with different input values and target ECF metabolites.

Figure 24. False DA neurotransmission via serotonergic terminals as a proposed mechanism for LID in PD.

Abbreviations

3-OMD = 3-*O*-methyl-DOPA
5-HIAA = 5-hydroxyindolacetic acid
5-HT (serotonin) = 5-hydroxytryptamine
5-HTP = 5-hydroxytryptophan
6-OHDA = 6-hydroxydopamine
AADC = aromatic amino acid decarboxylase
AAV = adeno-associated virus
AIMs = abnormal involuntary movements
AP = anteroposterior
BBB = blood-brain barrier
BG = basal ganglia
BH₄ = 5,6,7,8-tetrahydrobiopterin
BP = binding potential
COMT = catechol-*O*-methyltransferase
D₁R = D₁ subtype DA receptors
D₂R = D₂ subtype DA receptors
DA = dopamine
DAB = 3,3-diaminobenzidine
DAT = dopamine transporter
DOPAC = 3,4-dihydroxyphenylacetic acid
DV = dorsoventral
ECF = extracellular fluid
GABA = gamma-aminobutyric acid
GCH1 = GTP cyclohydrolase 1
GID = graft-induced dyskinesia
GP = globus pallidus
GPe = external segment of globus pallidus
GPi = internal segment of globus pallidus
HPLC = high performance liquid chromatography

HVA = homovanillic acid
i.p. = intraperitoneal
L-DOPA = L-3,4-dihydroxyphenylalanine
LAT1 = L-type amino acid transporter-1
LID = L-DOPA-induced dyskinesia
MAO = monoamine oxidase
MD = microdialysis
MFB = medial forebrain bundle
ML = mediolateral
mRL = modified ringer lactate
MSN = medium spiny neuron
NA = noradrenaline
NET = noradrenaline transporter
NSD-1015 = 3-hydroxybenzylhydrazine
OCT-3 = organic cation transporter-3
OMD = online microdialysis
PD = Parkinson's disease
PET = positron emission tomography
PFA = paraformaldehyde
PMAT = plasma membrane monoamine transporter
PPN = pedunculo-pontine nucleus
RMSE = root mean squared error
s.c. = subcutaneous
SERT = serotonin transporter
sh = short-hairpin RNA-mediated construct
shTH = TH knockdown by sh
shTHscr = the scrambled sequence of the shTH
SN = substantia nigra
SNc = substantia nigra pars compacta
SNr = substantia nigra pars reticulata
STN = subthalamic nucleus
TH = tyrosine hydroxylase
UPDRS = unified Parkinson's disease rating scale
VMAT₂ = vesicular monoamine transporter 2
VT = volume transmission
WT = wiring transfer

Original papers

- I. Ulusoy A*, **Sahin G***, Kirik D (2010). Presynaptic dopaminergic compartment determines the susceptibility to L-DOPA-induced dyskinesia in rats. *Proceedings of the National Academy of Sciences of the United States of America*. Jul;107(29):13159-64. *equal contribution
- II. **Sahin G**, Thompson LH, Lavisse S, Ozgur M, Rbah-Vidal L, Dolle F, Hantraye P, Kirik D (2014). Differential dopamine receptor occupancy underlies L-DOPA-induced dyskinesia in a rat model of Parkinson's disease. *PloS one* 9:e90759.
- III. **Sahin G**, Soneson C, Fontes M and Kirik D (2018). Predictive analysis of L-DOPA metabolism in a model of simultaneous blood sampling and microdialysis in healthy rats. *Manuscript unpublished*.

Published papers outside the thesis

Original papers

1. Cederfjall E, Nilsson N, **Sahin G**, Chu Y, Nikitidou E, Bjorklund T, Kordower JH, Kirik D (2013). Continuous DOPA synthesis from a single AAV: dosing and efficacy in models of Parkinson's disease. *Scientific reports* 3:2157.
2. Febbraro F, **Sahin G**, Farran A, Soares S, Jensen PH, Kirik D, Romero-Ramos M (2013). Ser129D mutant alpha-synuclein induces earlier motor dysfunction while S129A results in distinctive pathology in a rat model of Parkinson's disease. *Neurobiology of disease* 56:47-58.
3. Cederfjall E, **Sahin G**, Kirik D, Bjorklund T (2012). Design of a single AAV vector for coexpression of TH and GCH1 to establish continuous DOPA synthesis in a rat model of Parkinson's disease. *Molecular therapy: the journal of the American Society of Gene Therapy* 20:1315-1326.
4. Lastres-Becker I, Ulusoy A, Innamorato NG, **Sahin G**, Rabano A, Kirik D, Cuadrado A (2012). Alpha-synuclein expression and Nrf2 deficiency cooperate to aggravate protein aggregation, neuronal death and inflammation in early-stage Parkinson's disease. *Human molecular genetics* 21:3173-3192.

Review article

5. Cederfjall E, **Sahin G**, Kirik D (2012). Key factors determining the efficacy of gene therapy for continuous DOPA delivery in the Parkinsonian brain. *Neurobiology of disease* 48:222-227.

Book chapter

6. **Sahin G** and Kirik D (2012). Efficacy of L-DOPA therapy in Parkinson's disease. CAB International. *Amino Acids in Human Nutrition and Health* (ed. J.P.F. D'Mello). ISBN: 9781845937980.

Summary

Dopamine (DA) is an important neurotransmitter that plays a fundamental role in motor control. Deficiency of DA in certain areas of the brain has been found to be the underlying pathophysiological mechanism for Parkinson's disease (PD), which is mainly characterized by motor symptoms such as muscular rigidity, slowness in movements, tremor and postural instability. Treatment of PD relies on strategies restoring this DA deficiency. L-DOPA is a naturally occurring precursor in the DA synthesis machinery, and has been shown to be the most effective therapy for PD to date. However, its use has many long-term complications such as motor fluctuations and L-DOPA-induced dyskinesia (LID). The underlying mechanisms for these complications has yet to be clarified but is thought to be mainly a result of the malfunctioning DA system. This thesis aims to investigate the mechanisms behind this dysfunctional DA signaling at multiple levels from the blood-brain barrier (BBB) transport kinetics of L-DOPA and its metabolites as well as the role of presynaptic DA and 5-HT neurons in the postsynaptic striatal responses in animal models of PD. The first study provided direct evidence that the status of the presynaptic DA-releasing compartment is a critical determinant of both the induction and maintenance of LID. The second study suggested that differential DA receptor activation rather than the excessive DA release could be the underlying mechanism for LID. In the third study, we used a prediction model, which provided a valuable tool to assess BBB transport kinetics of L-DOPA under therapeutic administration conditions. Altogether, this thesis provided evidence that presynaptic sites have a critical role in determining LID and sheds new light into DA release mechanisms by serotonin neurons. Of notable clinical relevance, our findings could help us to better understand mechanisms behind L-DOPA-induced motor complications and response variability among individuals, and thus, have crucial implications for both neurorestorative approaches and development of drugs targeting serotonergic system for the management of LID.

Sammanfattning på svenska

Dopamin (DA) är en viktig signalsubstans med en avgörande roll för motorisk kontroll. Dopaminförlust i vissa delar av hjärnan har visat sig vara den bakomliggande orsaken för de patologiska mekanismerna vid Parkinsons sjukdom (PS), som huvudsakligen kännetecknas av motoriska symptom. Till dessa hör muskelstelhet, förlångsammad rörelseförmåga, tremor och postural instabilitet. Behandling av PS syftar till att återställa den rådande DA-bristen. L-DOPA är ett protein i DA-syntesprocessen som än idag är den mest effektiva behandlingen för PS. Dock medför en L-DOPA behandling långsiktiga komplikationer såsom motorfluktuationer och L-DOPA-inducerad dyskinesi (LID). De underliggande orsakerna till dessa komplikationer är ännu oklara, men dysfunktion i DA-systemet kan vara en förklaring. Syftet med följande avhandling var att undersöka mekanismerna bakom DA-signaleringsdysfunktion på ett flertal plan. Vi har undersökt transportkinetik av L-DOPA och dess metaboliter över blodhjärnbarriären samt funktionen av presynaptiska DA- och serotonin neuroner vid postsynaptisk striatal respons i djurmodeller av PS. I vår första studie kunde vi demonstrera att tillståndet för det presynaptiska DA-frisättande utrymmet är avgörande för både induktionen och underhållet av LID. Vår andra studie antydde att den differentiella DA-receptoraktivering snarare än överdriven DA-frisättning kan vara en underliggande mekanism för LID. I den tredje studien användes en prediktionsmodell som ett verktyg för att bedöma blodhjärnbarriärens transportkinetik för L-DOPA under terapeutiska administreringsförhållanden. Sammanfattningsvis har denna avhandling bidragit med evidens att det presynaptiska utrymmet spelar en avgörande roll i fastställandet av LID och öppnar möjligheten för DA-frisättningsmekanismer genom serotoninneuroner. Den kliniska relevansen av våra fynd är ökad förståelse av mekanismerna bakom L-DOPA-inducerade motorkomplikationer och responsvariabilitet bland individer, vilket kan ha avgörande betydelse både för utveckling av neurorestorativa behandlingar samt läkemedel som riktar sig mot serotonerga systemet för hantering av LID.

Türkçe özet

Dopamin (DA), hareketin kontrolünde temel işlev gören önemli bir beyin kimyasalıdır. Beynin belli bazı bölgelerindeki DA eksikliği Parkinson hastalığına (PH) sebep olur. PH kendini kaslarda sertleşme, hareketlerde yavaşlama, titremeler ve denge bozuklukları ile gösterir. PH'nin tedavisinde DA eksikliği giderilmeye çalışılır ve DA üretim zincirinde doğal bir ara ürün olarak yer alan L-DOPA, günümüze dek geliştirilmiş en etkili PH ilacıdır. Ancak, L-DOPA'nın uzun süreli kullanımı motor dalgalanmalar ve diskineziler (istemsiz hareketler) şeklinde komplikasyonlara neden olur. L-DOPA'ya bağlı diskinezilerin oluş mekanizmaları tam olarak bilinmese de yapılan çalışmalar DA sistemindeki işlev bozukluğundan kaynaklandığına işaret etmektedir. Bu tez çalışması, söz konusu bozuk DA sinyal iletiminin altında yatan mekanizmaları birçok seviyede araştırmayı amaçlamaktadır. Buna yönelik olarak L-DOPA ve ürünlerinin kan-beyin bariyerinden (KBB) aktarım dinamiklerini, DA ve serotonin nöronlarının L-DOPA'nın beyindeki etkilerine katkısını ve beyinde hareketin ince planda kontrolünden sorumlu nöronların yanıtlarını farklı deney düzenekleri kullanarak PH'nin sıçan modelinde ele aldık. İlk çalışmamız diskinezilerin tetiklenmesi ve idamesinde bizzat DA üreten nöronların karar verici olduğunu gösterdi. İkinci çalışmamız, daha önce düşünülenin aksine tedaviye bağlı yüksek DA seviyelerinin değil, DA'nın farklı uyarım mekanizmalarının diskinezilere yol açtığını ortaya koydu. Son çalışmada ise L-DOPA'nın KBB'den geçiş yollarını araştıran ve sadece kan seviyelerine bakarak beyindeki miktarlarını tahmin etmemize olanak tanıyan bir model geliştirdik. Sonuç olarak bu tez çalışması, DA üreten nöronların diskinezilerdeki kritik rolüne ve serotonin nöronlarının DA sistemi üzerindeki etkilerine ışık tutmaktadır. Elde edilen bulgular, L-DOPA'ya bağlı diskinezilere neden olan mekanizmaların ve değişken hasta yanıtlarının daha iyi anlaşılmasına, dolayısıyla yeni tedavi yöntemleri ve ilaçların geliştirilmesine katkı sağlayacaktır.

Introduction

A historical perspective on the biochemistry of dopamine

This thesis deals with the central dopamine (DA) system at different levels. DA is a neurotransmitter that plays a key role in motor function and is produced in DA-containing neurons that are principally located in the mesencephalon and diencephalon. DA was first independently synthesized from vanillin in 1910 with a given name 3,4-dihydroxy- β -phenylethylamine (Barger & Dale, 1910). According to Stanley Fahn, the name dopamine was suggested by Sir Henry Dale in 1952 'in order to stress its chemical relationship to DOPA' (Shepherd & West, 1952; Fahn, 2015). L-3,4-dihydroxyphenylalanine (L-DOPA) was first isolated from the broad bean, *Vicia faba* in 1913 at Hoffmann-LaRoche by Markus Guggenheim, who self-ingested 2.5 g and developed nausea and vomiting (Guggenheim, 1913). L-DOPA was first chemically synthesized in 1921 (Waser & Lewandowski, 1921).

In the following years, L-DOPA and DA were studied as possible precursors for epinephrine in regard to interest in the adrenal medulla. Subsequently, the monoamine oxidase (MAO), the inactivating enzyme for the monoamines i.e. norepinephrine, serotonin and DA and the enzyme converting L-DOPA to DA, DOPA decarboxylase, were discovered in 1937 and 1939, respectively (Blaschko *et al.*, 1937; Blaschko, 1939; Holtz, 1939). After several years of research on DA in different tissues such as the adrenal medulla, heart, kidney, sympathetic nerves and urine, Oleh Hornykiewicz, a post-doctoral fellow, from Blaschko's lab in Oxford, showed direct effect of DA on blood pressure in 1956 (Hornykiewicz, 1958; 2002a). He also found that L-DOPA has the same effect.

However, researchers had to wait until the discovery of tyrosine hydroxylase (TH) enzyme to be able to understand how L-DOPA was synthesized (Nagatsu *et al.*, 1964). TH is the rate-limiting step in the synthesis of DA and converts L-tyrosine to L-DOPA. The final product of DA metabolism was found to be homovanillic acid (HVA), which is formed by the combined effects of MAO and catechol-O-methyltransferase (COMT) enzymes (Shaw *et al.*, 1957). Details of the chemical

synthesis and metabolism of DA, including the cofactors are illustrated in Figure 1 (Sahin & Kirik, 2012).

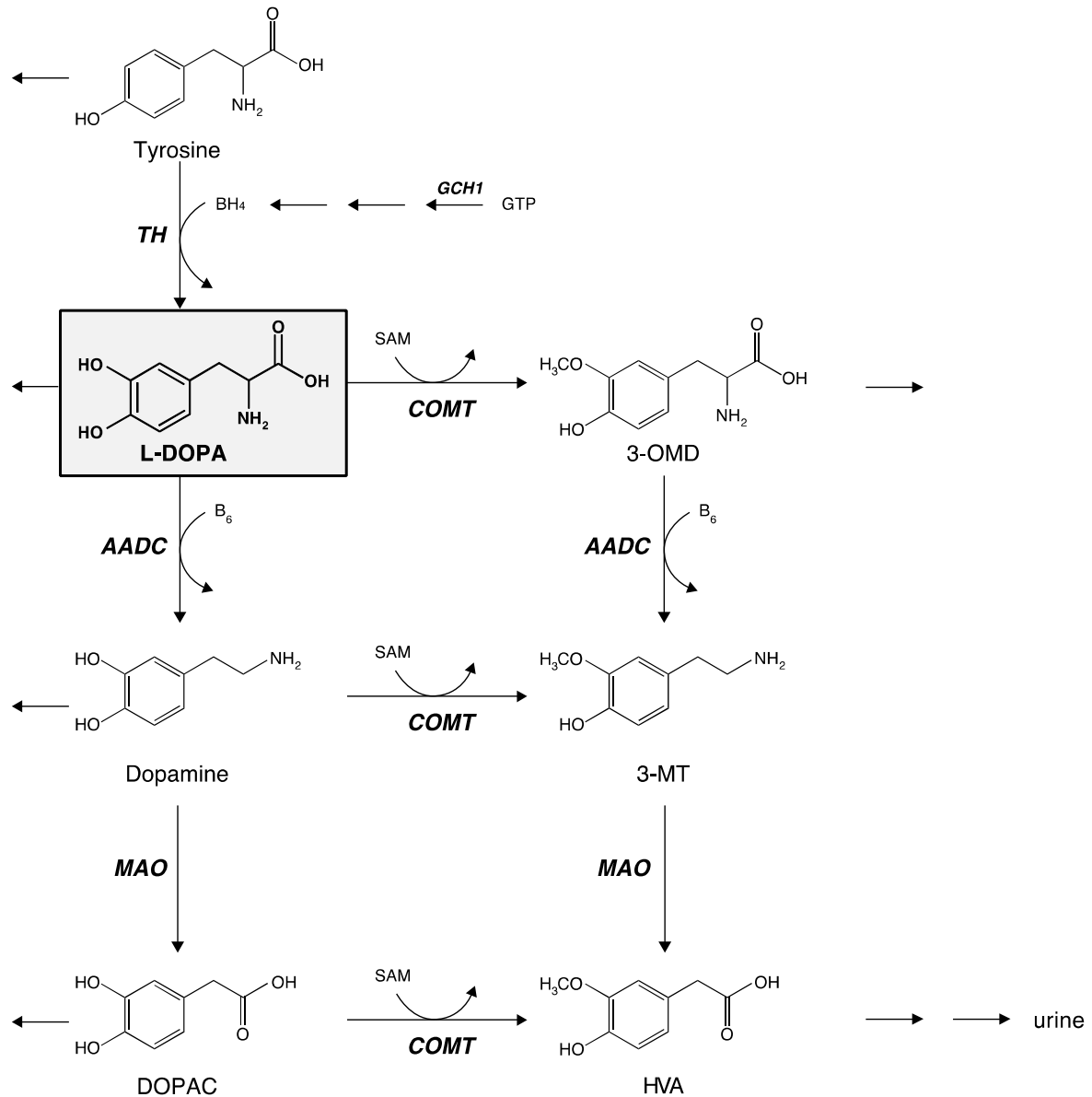


Figure 1

Biosynthesis and metabolism of dopamine (DA). Tyrosine, an essential amino acid obtained from dietary proteins, is converted to DOPA by the TH enzyme. Activity of the TH enzyme is dependent on the presence of tetrahydrobiopterin (BH₄), which acts as a cofactor and is synthesized from guanosine triphosphate (GTP) in a three-step enzymatic reaction. GTP cyclohydrolase 1 (GCH1) is the first and the rate-limiting enzyme in BH₄ biosynthesis. DOPA is either immediately converted into DA by the pyridoxine- (B₆) dependent aromatic amino acid decarboxylase (AADC) enzyme, or methylated to form 3-O-methyl-DOPA (3-OMD). The enzyme known as catechol-O- methyltransferase (COMT) catalyzes this methylation and S-adenosylmethionine (SAM) serves as the donor compound for the methyl group. DA is metabolized to form either 3,4-dihydroxyphenylacetic acid (DOPAC) by the monoamine oxidase (MAO) or 3-methoxytyramine (3-MT) by the COMT enzymes. The end product of this metabolic pathway is homovanillic acid (HVA). The arrows on the left and right of the figure represent other synthesis and/or metabolism pathways, e.g. tyramine from tyrosine, melanin from DOPA, or norepinephrine from DA. Figure is reprinted from (Sahin & Kirik, 2012).

In 1957, it was identified that DA was present in the brains of rats and other animals (Montagu, 1957; Weil-Malherbe & Bone, 1957). At the same time period, the antipsychotic action of reserpine was discovered and Arvid Carlsson (who was one of three to be awarded the Nobel Prize in Physiology or Medicine in 2000) started to study this potent drug that was able to deplete neurotransmitters. In 1957, Carlsson administered DOPA to reserpine-treated rabbits and mice in order to understand its action and discovered that this amino acid had a central stimulant action and was able to reverse the akinetic and sedative actions of reserpine (Carlsson *et al.*, 1957). Following this, Carlsson showed that DA was a normal brain constituent and mapped its regional distribution (mainly in basal ganglia). Further historical details have been reviewed by Iversen et al and Stanley Fahn (Iversen & Iversen, 2007; Fahn, 2015).

Basic physiology of the basal ganglia

The basal ganglia (BG) are a group of subcortical nuclei that are located in the mid- and forebrain region of mammals, birds and reptiles. BG are strongly interconnected with the cerebral cortex, thalamus, brainstem and the cerebellum. The BG have been associated with a variety of functions such as the control of voluntary motor movements, eye movements, cognition, emotion, and learning routine behaviors or 'habits'. In this section, the motor functions related to BG will be reviewed.

As one of the brain's fundamental processing units, the BG are a sophisticated system that contain, including among others, ascending DA projections as important integral elements (Lindvall & Bjorklund, 1974). The primary afferent structure of the BG is the striatum, which is single structure in rodents and consists of two structures in primates (the caudate and putamen). Other components of the BG are globus pallidus (GP), subthalamic nucleus (STN) and substantia nigra (SN).

Neuroanatomical organization of the BG

The striatum receives primary input from the cerebral cortex (glutamatergic), parafascicular nucleus of the thalamus (glutamatergic) and substantia nigra pars compacta (SNc) (dopaminergic) (Figure 2A). Acetylcholinergic inputs from pedunculo-pontine nuclei (PPN), serotonergic inputs from nucleus raphe and noradrenergic inputs from the locus coeruleus end also in the striatum (Albin *et al.*, 1989). The striatum contains both projection neurons and several populations of interneurons (Figure 2B). The major type of the projection neurons is the

medium spiny neuron (MSN) that accounts for 90-95% of the total neuronal population of the striatum. These gamma-aminobutyric acid (GABA) neurons are further subdivided into two major populations, depending on their projection preferences and receptor expression patterns. MSNs of the direct pathway project preferentially to the output nuclei of the BG and express the D₁ subtype of DA receptors (D₁R), dynorphin and substance P. MSNs of the indirect pathway, however, project almost exclusively to the GP externa, and express D₂ subtype of DA receptors (D₂R) and enkephalin.

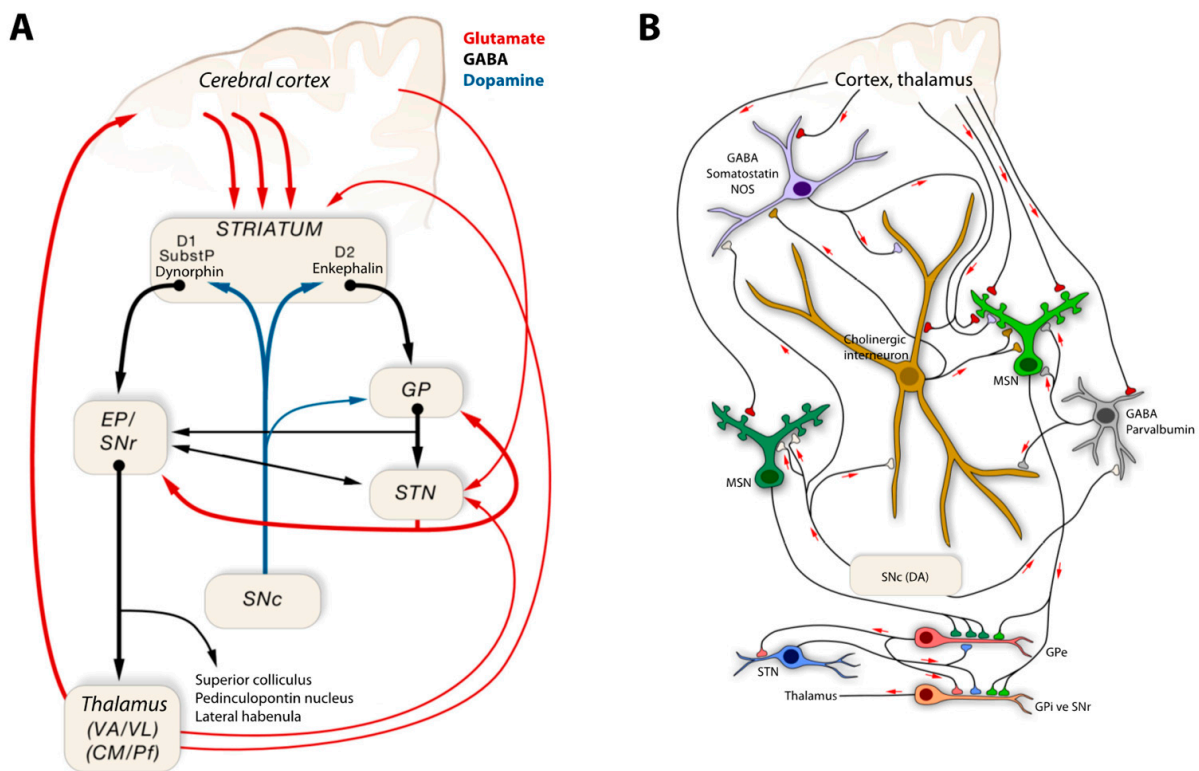


Figure 2

BG connections (A) and striatal architecture (B). The BG are comprised of a group of nuclei located deep in the brain: The striatum includes caudate nucleus and the putamen and, receives dopaminergic input from substantia nigra pars reticulata (SNc), and glutamatergic input from both the cortex and the thalamus. GABAergic striatal neurons (medium spiny neurons, MSN) send further projections directly to substantia nigra reticulata (SNr) and globus pallidus interna (GPi) (in rodents to entopeduncular nucleus (EP), the rodent homologue of GPi). The MSNs constituting this direct pathway express D₁ subtype of DA receptors (D₁R), substance P and dynorphin (light green MSN on panel B). Alternatively, MSNs expressing mainly D₂ subtype of DA receptors (D₂R) and enkephalin (dark green MSNs on panel B) project to GPi/SNr indirectly via globus pallidus externa (GPe) and subthalamic nucleus (STN). GPi/SNr, as being the output structures of the BG send inhibitory fibers to the thalamus (VA/VL: Ventral lateral/anterior, CM: Centromedian, Pf: Parafascicular nuclei of the thalamus), which finally closes to loop by projecting back to the cortex. Despite MSNs constitute 90-95% of all neurons in the striatum there are cholinergic and GABAergic interneurons (B). There are different types GABAergic interneurons expressing parvalbumin, TH, somatostatin, neuropeptide-y. Figure by Bengt Mattsson. Reprinted with permission from (Cakmakli & Topcuoglu, 2011).

Functional perspective: What do basal ganglia do?

According to the classical anatomical model of BG (Wichmann & DeLong, 2007), the striatum receives input (mainly dopaminergic but also other types) that modulates the function of MSNs with the help of interneurons. Striatum then sends information to the thalamus either directly via SNr/GPi or indirectly via GPe and STN. While the direct pathway mainly eases movement, the indirect pathway counterbalances it. This filtered information is then sent back to the cortex to fine-tune the motor patterns that are being sent to the structures located lower in the hierarchical organization for motor control. However, this anatomical model fails to explain certain motor finding and leaves a number of paradoxes with regards to the mechanism of action of surgical interventions for PD (Marsden & Obeso, 1994).

Focused attention

Damage to the BG typically leads to motor bradykinesia (slowness in movements) and a kind of psychic akinesia termed abulia, in which there is apathy but not dysphoria. Moreover, a disconnection of input from output is commonly seen, so that neither thought nor sensory information are linked to mental or physical action. In 1998, Charles David Marsden has proposed that a form of focused attention is necessary for the automatic binding of input to output (Brown & Marsden, 1998). Only with such attention to an object or situation will lead to the calling up and operation of a motor program (or sequence of thoughts). Under normal conditions, this attention operates at an automatic (subconscious) level except during the most demanding tasks when it may be sensed as a feeling of super-attention. The existence of such attention deficits in diseases of the BG is revealed by the observation of paradoxical kinesis, whereby patients with PD are so akinetic that they can barely move can deftly sidestep an oncoming car or flee from a fire. This phenomenon is thought to be a general property of the motor system (Ballanger *et al.*, 2006). According to Marsden, the major function of the BG is ‘to facilitate the synchronization of cortical activity underlying selection and initiating of an appropriate movement, or indeed an appropriate sequence of thoughts’ (Brown & Marsden, 1998). The physiological basis for this cortical synchronization is out of the scope of this thesis and will not be covered here.

Model of focused selection and inhibition of competing motor programs

Based on the hypothesis above, a new model of focused selection has been developed (Mink, 1996; DeLong & Wichmann, 2009) (Figure 3). This model states that the BG do not generate movements. Instead, the BG acts broadly to inhibit competing motor programs that would otherwise constrain the desired movement when voluntary movement is generated by the cerebral cortical and cerebellar mechanisms. Simultaneously, inhibition is removed focally from the

anticipated motor programs to ease the desired movement. The inability to inhibit competing motor programs results in slow movements (bradykinesia), abnormal postures and involuntary muscle activity (rigidity, tremor) that constitute the cardinal symptoms of PD.

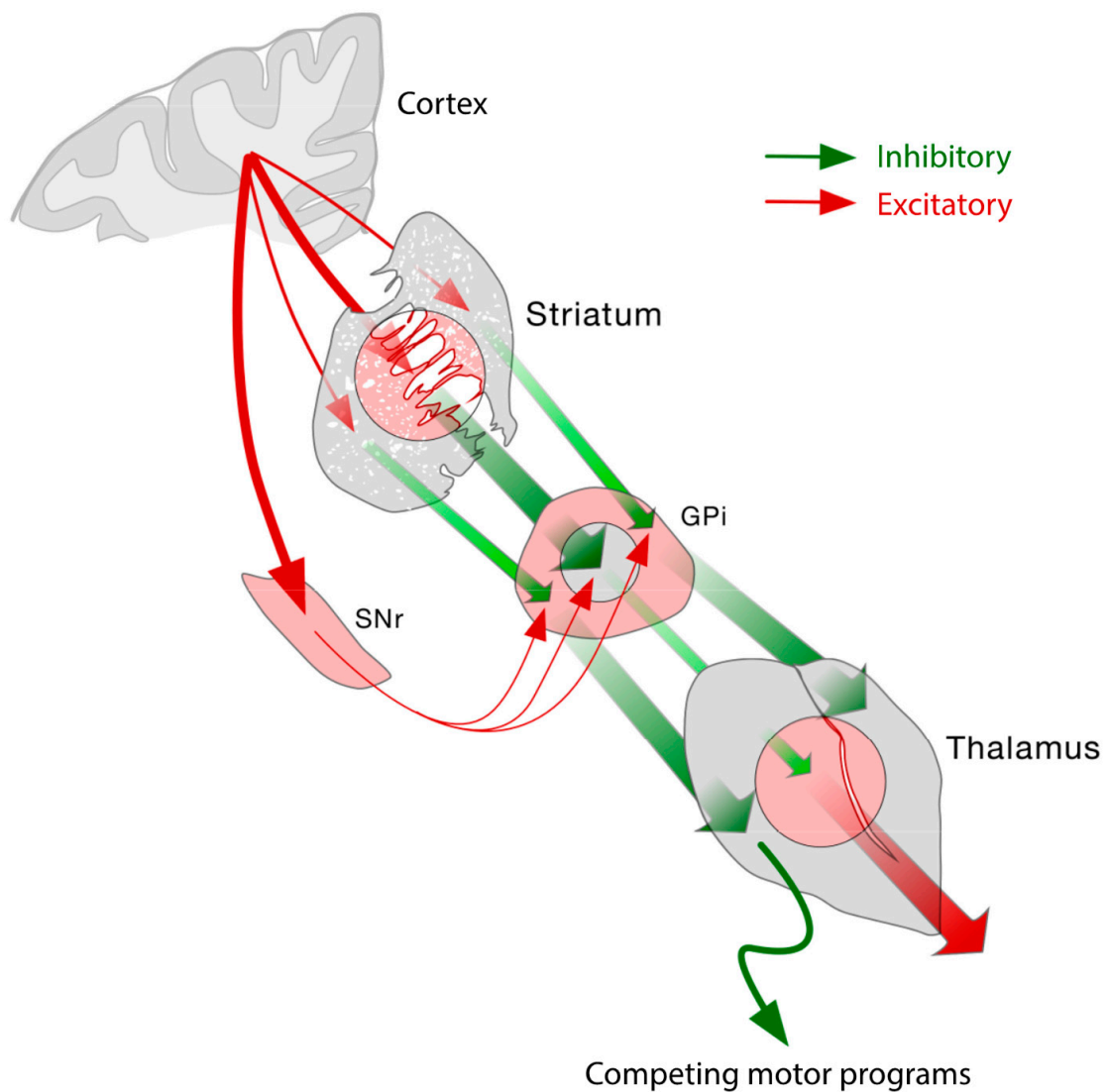


Figure 3
The role of the basal ganglia in the selection of desired motor programs according to the model of focused selection and inhibition of competing motor programs. Figure by Bengt Mattsson. Reprinted with permission from (Tokcaer, 2011).

What is the role of DA in the focused selection model?

DA has contributory actions on aforementioned selection process in two ways. First, by setting a threshold for start of the action and second acting by as a teaching signal (Chakravarthy *et al.*, 2010). In the first mechanism, lower levels of impulse are required to induce a particular behavior when dopaminergic activity is high. As a result, while high levels of DA lead to facilitation of motor activity and impulsive behaviors, low levels lead to reduced reactions. This mechanism has been used to explain paradoxical kinesia in PD and effects of drugs modifying DA release (Jankovic, 2008; Pattij & Vanderschuren, 2008). The second mechanism, the teaching signal suggests that when an action is followed by an increase in the dopaminergic activity, the BG circuit connections are changed in a way making similar responses easier to induce with similar settings in the future. In this way, DA plays a rewarding role (Floresco, 2015).

DA, in general, is not a stimulator or inhibitor, but a modulator. In other words, this implies that DA does not determinedly alter the neural activity of MSNs, but rather affects the level of individual MSNs for controlling the motivational state (Nicola *et al.*, 2000; Ikemoto *et al.*, 2015).

Nigrostriatal DA signaling

DA neurons, which are located mainly in the ventral midbrain, can be easily detected with TH immunoreactivity (Lindvall *et al.*, 1984; Williams & Goldman-Rakic, 1998) (Figure 4). Three major groups of dopaminergic pathways innervate the forebrain and the BG and are designated as A8, A9, and A10, according to the nomenclature of Dahlström and Fuxe (1964). These correspond to the DA cells of the substantia nigra (SN, A9) projecting to striatal areas, ventral tegmental area (VTA, A10) and the retrorubral area (RRA, A8) neurons projecting to the limbic and cortical areas (Björklund & Lindvall, 1984). Moreover, the non-nigral DA neurons, namely from A11 to A17 are located in hypothalamus, zona incerta, arcuate nucleus, olfactory bulb and retina (Dahlstrom & Fuxe, 1964; Björklund & Lindvall, 1984; T. *et al.*, 1984; Albanese *et al.*, 1986).

DA neurons exhibit two main activity patterns: tonic vs. phasic (Grace & Bunney, 1984a; b). Under resting conditions and during sleep, they are tonically active and regularly spike at ≈ 4 Hz frequency. In response to a stimulus such as a reward (e.g., food) or a sensory stimulus that predicts a reward, they display phasic activity with a firing frequency of ≈ 15 Hz. (Mirenowicz & Schultz, 1996; Hyland *et al.*, 2002). Grace and Bunney hypothesized that ‘bursting would be more potent than tonic activity to induce DA release in distant striatal regions’.

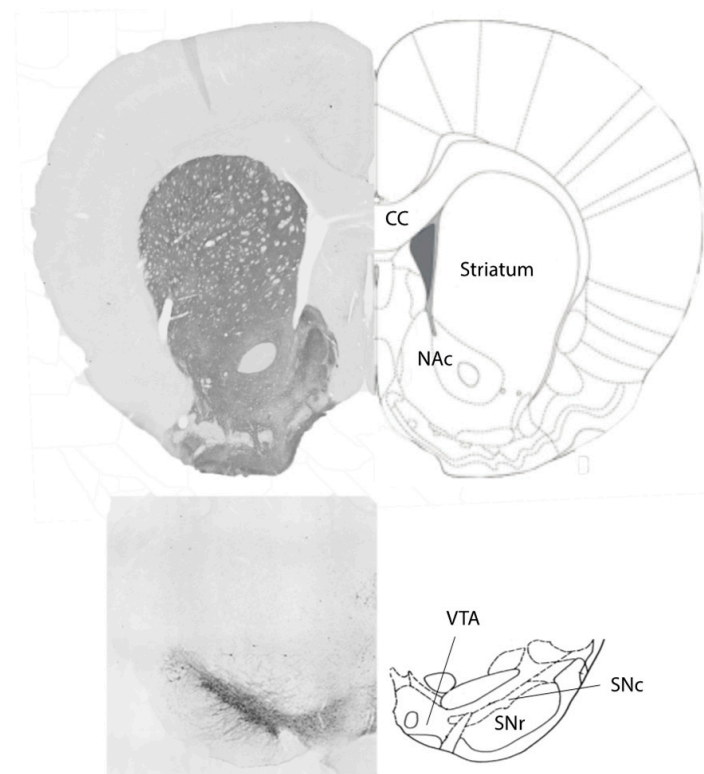


Figure 4

Immunohistochemical staining of TH in a healthy rat brain. Substantia nigra pars compacta (SNc) includes A9 DA neurons, which are visible by dark immunoreactivity in the lower left panel. These neurons project to the striatum that can be visualized by terminal fiber staining (upper left). Ventral tegmental area (VTA), on the other hand, includes A10 neurons that project to the nucleus accumbens (NAc) (CC: corpus callosum). Microscopic images by Ayşe Ulusoy, figure by Gürdal Şahin.

Nigral DA neurons communicate with striatal MSNs through two different types of contact: (1) While asynaptic varicosities mainly utilize volume transmission (VT) that takes place via the extracellular fluid, (2) synaptic contact, however, use wiring transmission (WT) (Agnati *et al.*, 1986). Observations with electron microscopy showed that VT, involving leaking DA synapses and asynaptic DA varicosities, is the major mode of communication for extrasynaptic striatal DA receptors (Zoli *et al.*, 1999; Jansson *et al.*, 2002). Under normal conditions, these receptors (mainly D₁R) are activated selectively after burst discharges. In contrast, DA released from synaptic contacts continuously stimulates D₂R containing sites in a tonic manner (Gonon, 1997; Grace, 2000; Floresco *et al.*, 2003; Goto & Grace, 2005; Hikida *et al.*, 2010; Grieder *et al.*, 2012).

DA is normally synthesized from essential amino acid, tyrosine in a two-step enzymatic reaction. First, TH enzyme attaches a hydroxyl group to the tyrosine to produce L-DOPA. This enzyme uses oxygen, tetrahydrobiopterin and Fe⁺² as cofactors (Ramsey & Fitzpatrick, 2000). In the next step, L-DOPA is decarboxylated to DA by aromatic acid decarboxylase (AADC) enzyme. The cofactor for AADC enzyme is pyridoxal phosphate. While TH is the main rate-

limiting step in the biosynthesis of DA, an increase in the extracellular DA levels that is sensed by DA auto-receptors at the presynaptic site- regulates both the TH and the AADC, resulting in decreased synthesis (Wolf & Roth, 1990; Lindgren *et al.*, 2001).

Cytosolic DA is then translocated immediately into the vesicles by VMAT₂ (Peter *et al.*, 1995; Wimalasena, 2011; Sames *et al.*, 2013). These synaptic vesicles have an acidic lumen that prevents auto-oxidation of DA, besides preventing enzymatic degradation (Guillot & Miller, 2009). VMAT₂ is present not only in DA neurons but also in norepinephrine, serotonin and histamine cells (Wimalasena, 2011; Sames *et al.*, 2013). Upon its release, DA is efficiently taken up by the dopamine transporter (DAT) located outside the release sites (Pickel *et al.*, 1996). This action results in the termination of neurotransmission.

Pathophysiology of Parkinson's disease

Parkinson's disease (PD) is a neurodegenerative disorder, affecting 1-2% of the population over the age of 60 years. The mean age of onset is 57 years, although it may also be seen at younger ages (Koller *et al.*, 1987). PD was first described by James Parkinson in a monograph [Parkinson J, 1817, An Essay on the Shaking Palsy] (Lees, 2017). Clinical features at onset typically include asymmetric bradykinesia (slowness in movements), rigidity (stiffness in the muscles) and tremor (shaking) at rest. These motor symptoms appear when \approx 30% of the SNc neurons have degenerated and striatal terminal density is decreased by 50-70% [reviewed in (Hornykiewicz, 2002b; Lang, 2007; Burke & O'Malley, 2013)]. In parallel to this, motor function is unchanged in 6-hydroxydopamine (6-OHDA)-lesion rat model of PD until 60% of the DAT immunoreactivity is lost and tissue DA levels are decreased by 80% (Abercrombie *et al.*, 1990; Lee *et al.*, 2008). These findings suggest compensatory mechanisms to preserve motor function during the neurodegenerative process.

In addition to DA neurons, other neuronal populations are also known to be affected resulting in deficits in noradrenergic, serotonergic and cholinergic neurotransmission [reviewed elsewhere with possible therapeutic implications in (Shutov & Dondova, 2008; Huot *et al.*, 2011; Fox, 2013; Huot & Fox, 2013; Stayte & Vissel, 2014; Buddhala *et al.*, 2015; Ohno *et al.*, 2015; Politis & Niccolini, 2015; Villalba *et al.*, 2015; Freitas & Fox, 2016)]. These changes are accepted as a basis for the development of non-motor symptoms including cognitive decline, sleep abnormalities and depression as well as gastrointestinal and genitourinary disturbances.

DA deficiency in PD cannot be replaced by direct peripheral administration of DA since it has a very short half-life in blood and is polar, thus unable to diffuse across the blood-brain barrier (BBB) (Cotzias, 1968). Instead, dopaminergic drugs (i.e. L-DOPA and DA agonists) are used for replacement therapy and they are shown to improve motor function, significantly reduce both morbidity and mortality of the affected individuals and improve quality of life (Rajput, 2001). Upon oral administration, L-DOPA crosses BBB via the L-type amino acid transporter 1 (LAT1), augmenting DA release from surviving nigrostriatal terminals in the early stages of the disease. However, as the disease progresses, other cell types harness the AADC capacity and start to take part in handling exogenously administered L-DOPA and its conversion to DA. In particular, serotonin (5-hydroxytryptamine, 5-HT) neurons conserves critical steps in the biosynthesis of DA, i.e. AADC and VMAT₂, could not only synthesize DA but also store and release it into the striatum (Arai *et al.*, 1996; Yamada *et al.*, 2007) (Figure 5).

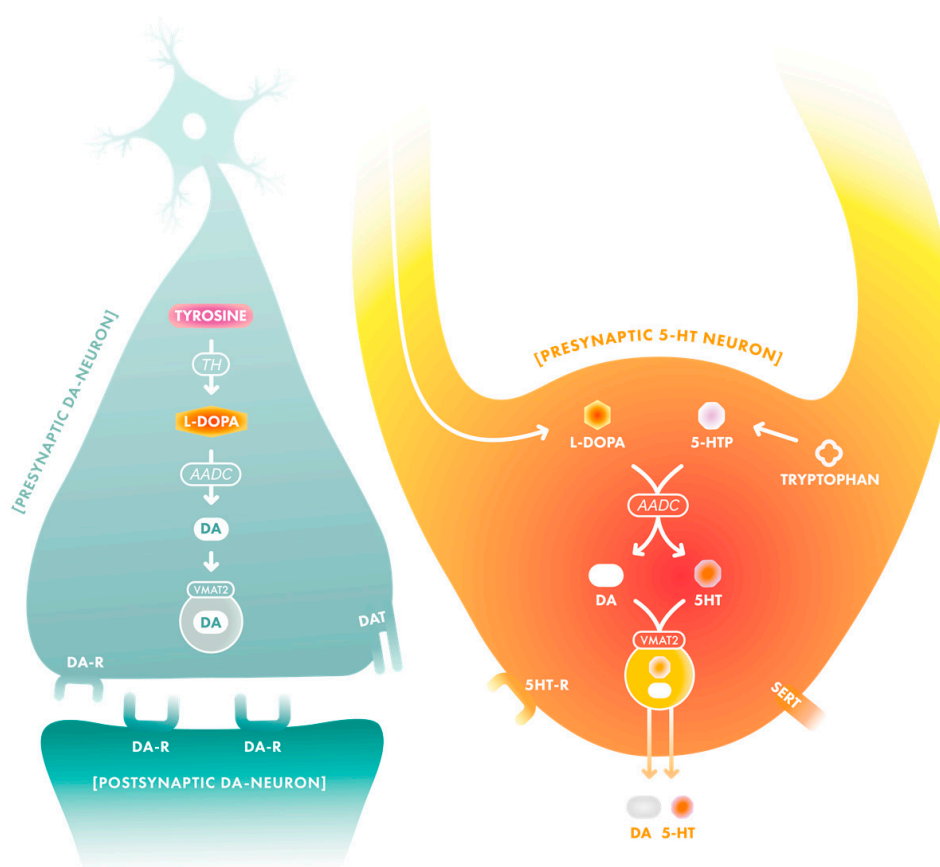


Figure 5

The role of the 5-HT neurons in the synthesis and release of DA from exogenous L-DOPA in advanced PD. 5-HT neurons possess the capacity of decarboxylating L-DOPA into DA, storing DA in the vesicles via VMAT₂ and releasing into the extracellular space (DA-R: Dopamine receptors, 5HT-R: Serotonin receptors, SERT: serotonin transporter). However, they lack the DA auto-receptors and DAT, and thus cannot maintain DA homeostasis. Figure is designed by Gürdal Şahin and illustrated by Nikki Schmidt.

L-DOPA: From peripheral kinetics to central actions and complications

Historical aspects

Striatal DA deficiency in PD has been described by Ehringer and Hornykiewicz a few years after the discovery of the role DA by Arvid Carlsson (Ehringer & Hornykiewicz, 1960). In the following year, Birkmayer and Hornykiewicz showed that a single intravenous injection of L-DOPA resulted in marked resolution of akinesia in PD patients [reprinted in English, (Birkmayer & Hornykiewicz, 2001)]. Finally, Cotzias found that oral administration of D, L-DOPA at a dose of 3-16 g/day was effective but 4 patients developed agranulocytopenia (Cotzias *et al.*, 1967). Subsequently, he showed that the use of L-form was less toxic than the racemic D, L-DOPA mixture (Cotzias, 1968). These clinical studies established the efficacy of L-DOPA therapy in PD and in 1970 the US Food & Drug Administration approved L-DOPA as a treatment for PD. It was only in 1975 when post-mortem analysis of brain tissue from L-DOPA treated PD patients were found to have elevated levels of DA compared to untreated patients and thus the effectiveness of L-DOPA was found to result from its metabolism to DA in the brain (Lloyd *et al.*, 1975). The first double-blind placebo-controlled study showing efficacy of L-DOPA with the development of choreiform movements was reported in 1969 (Birkmayer & Hornykiewicz, 1998). In the same year, the combined use of L-DOPA with decarboxylase inhibitor RO4-4602 (benserazide) was shown to be more effective than L-DOPA alone (Birkmayer, 1969). Following the discovery of carbidopa, as the second AADC inhibitor (Markham *et al.*, 1974), L-DOPA-benserazide (Madopar[®]) and Carbidopa-L-DOPA (Sinemet[®]) commercialized in 1975. Two COMT inhibitors were then found to be orally active in 1989 (Mannisto & Kaakkola, 1989). The first COMT inhibitor, tolcapone, became commercially available in 1998 (Tasmar[®]) (Adler *et al.*, 1998) and the first combination carbidopa-L-DOPA-entacapone formulation (Stalevo[®]) became commercially available in 2003. Thereafter, a carbidopa/L-DOPA gel formulation for enteral infusion (Duodopa[®]) has been shown to provide more consistent clinical effects and reduce motor complications in advanced patients (Nyholm, 2006).

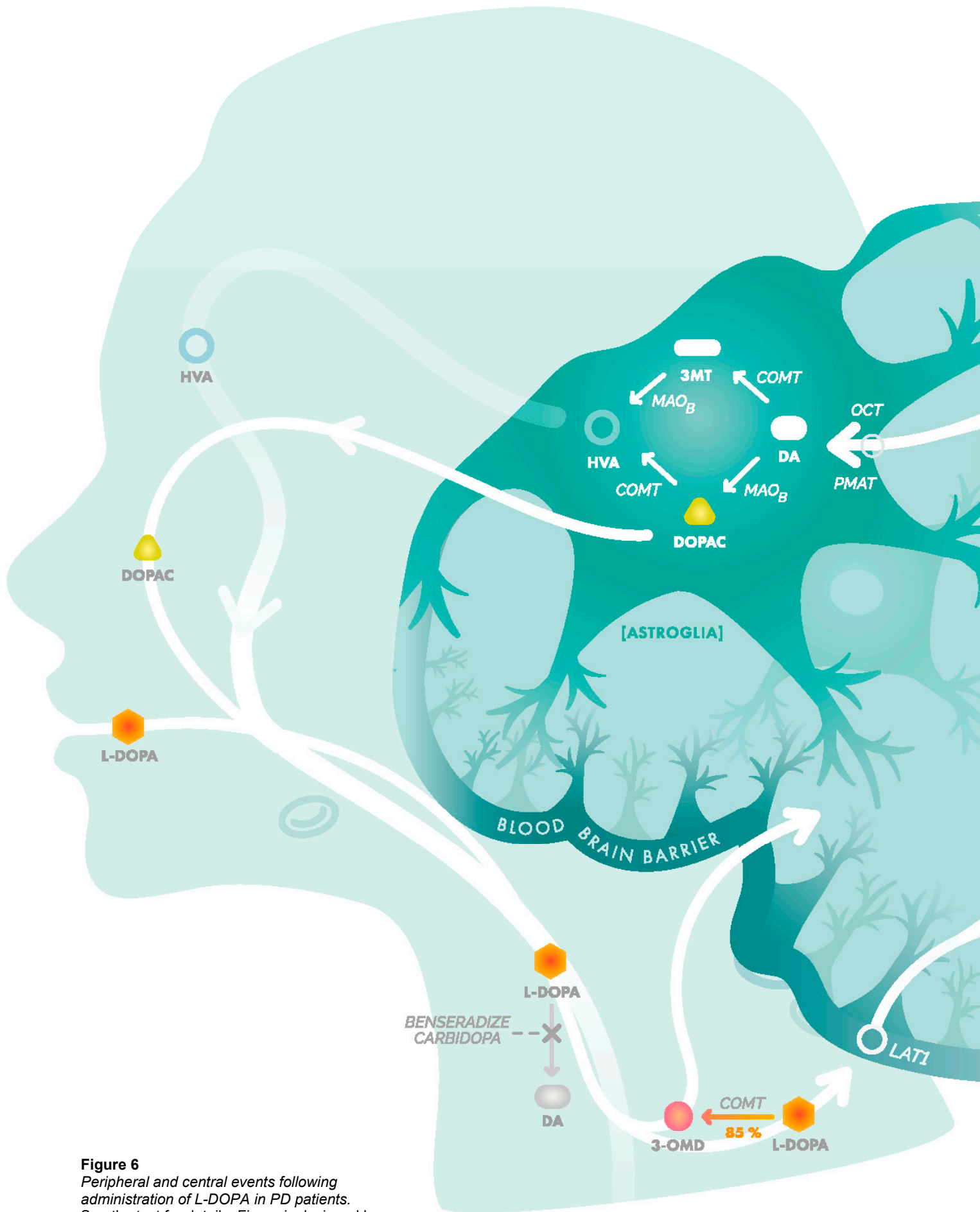
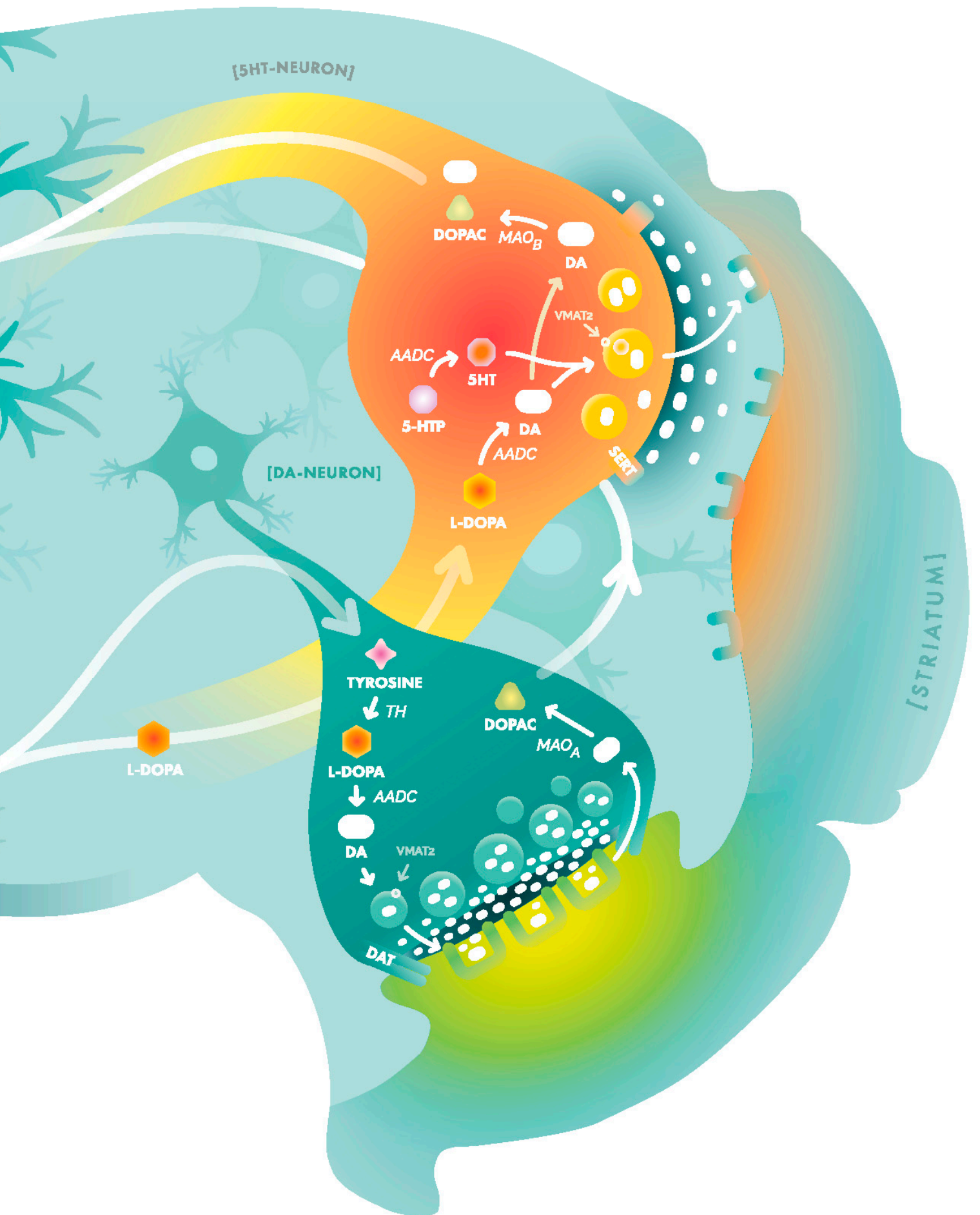


Figure 6
 Peripheral and central events following administration of L-DOPA in PD patients. See the text for details. Figure is designed by Gürdal Şahin and illustrated by Nikki Schmidt.



Pharmacokinetics and pharmacodynamics

Pharmacokinetics is defined as the study of the time course of drug absorption, distribution, metabolism, and excretion. Pharmacodynamics, on the other hand, refers to the relationship between drug concentration at the site of action and the clinical consequence, including the therapeutic and adverse effects (Spruill *et al.*, 2014). This part includes peripheral and central effects of L-DOPA from a clinical point of view. I will include my personal experience as a neurologist with regard to common problems associated with L-DOPA therapy that I have encountered and solutions to them in the clinical practice dealing with the patients with PD.

L-DOPA is probably the most effective drug that has ever been developed (LeWitt, 2015). Peripheral blockage of conversion of L-DOPA to DA -by using benserazide and carbidopa- enhances bioavailability, tolerability and clinical effectiveness of L-DOPA (Hornykiewicz, 2010). Its feature of being ‘a natural intermediate in human metabolism’ makes it easier for patients to accept it as a medication. Before prescribing L-DOPA to my PD patients, I always give brief information about the importance of DA for human motor control, pathophysiology of PD, mechanisms behind motor and non-motor symptoms, DA replacement strategies, and L-DOPAs peripheral and central effects. Besides generating a strong patient-doctor relationship, this ‘trivial’ lecture gives me a priceless chance to explain possible peripheral side effects, long-term complications and measures to avoid many unwanted effects e.g. its interaction with proteins in the meal.

L-DOPA has an extended and complex path from its oral administration to the site of action in the brain (Figure 6). In the clinical practice, L-DOPA is only available in a fixed-combination formulation with one of the two AADC inhibitors (benserazide or carbidopa). The therapeutic efficacy and side effect profile of these two AADC inhibitors have been well-studied and was not found to be significantly different (Greenacre *et al.*, 1976). 80-90 % of gastrointestinal absorption of L-DOPA occurs in the duodenum and the proximal part of the jejunum via human L-type amino acid transporter-1 (LAT1) that is located in the gut wall and at the BBB (Wade *et al.*, 1973). Gastric emptying may be delayed by food (especially fat), resulting in increase in the t_{max} (time to reach maximum serum concentration) of L-DOPA (Baruzzi *et al.*, 1987). L-DOPA competes with other amino acids derived from the diet for this transport system (Nutt & Fellman, 1984; Leenders *et al.*, 1986). These findings have important implications for clinical use and patients are advised to take L-DOPA on an empty stomach and not to eat for least 30 minutes after ingestion of the tablets to increase its bioavailability. Moreover, dietary manipulations, including rescheduling of protein intake or protein restriction (e.g. 0.8 g of protein/kg) were found to be simple and

effective add-on measures for the treatment of advanced PD patients (Karstaedt & Pincus, 1992).

In the presence of an AADC inhibitor, a major part of the orally administered L-DOPA is cleared either by first-pass hepatic metabolism or by skeletal muscle distribution and metabolized by COMT enzyme to form 3-*O*-methyl-DOPA (3-OMD) (Figure 1 and 6). Under these circumstances, about 5 to 10% of the administered L-DOPA reaches the brain (Kaakkola, 2000). 3-OMD is a neutral amino acid with a 15h half-life (15h) that crosses the BBB but does not bind to the DA receptor. Therefore, it has no antiparkinsonian activity. The clinical efficacy of L-DOPA can also be improved by co-administration of a COMT inhibitor, which reduces *O*-methylation in the gastrointestinal tract, increases L-DOPA absorption and extends its half-life (Nutt *et al.*, 1994). The first available COMT inhibitor was tolcapone, but its usage was limited due to hepatic toxicity. At present, entacapone is the most widely used COMT inhibitor and when combined together with L-DOPA, it increases ‘on’ time and reduces ‘off’ time (Heikkinen *et al.*, 2001).

Once L-DOPA reaches to brain, it generates DA with the help of central AADC activity. This decarboxylation capacity exists in the brains of PD patients even in the advanced stages. In the absence of DA terminals, the conversion of L-DOPA to DA occurs both in neuronal (serotonergic nerve terminals and interneurons in the striatum) and non-neuronal (glial cells and endothelium) compartments (Melamed *et al.*, 1981; Mura *et al.*, 1995; Arai *et al.*, 1996).

Upon its synthesis, DA is transported from the cytoplasm to storage vesicles with the help of VMAT₂. Activation of DA neurons causes an influx of calcium ions that give rise to the fusion of synaptic vesicles with the plasma membrane. The content of the vesicles i.e. DA, is then released into the synaptic cleft stimulates its specific receptors located on both pre- and post-synaptic sites. The action of DA is stopped by the reuptake into pre-synaptic sites by the way of DAT. In addition, astroglial cells and non-dopaminergic neurons may take up and metabolize extracellular DA by other transport mechanisms such as, noradrenaline transporter; (NET), serotonin transporter (SERT) organic cation transporter-3 (OCT-3) and plasma membrane monoamine transporter (PMAT) (De Deurwaerdere *et al.*, 2017; Miguez *et al.*, 2017). MAO and COMT metabolize DA. While the MAO enzyme forms DOPAC both intra-neuronally and extra-neuronally, HVA is the major end product of DA metabolism in the brain and produced exclusively in the non-neuronal compartments via the COMT enzyme (Kopin, 1985).

L-DOPA-induced complications

There is a well-known response pattern to L-DOPA therapy observed in PD patients. Fortunately, patients do not usually show any signs of clinical improvement in the very early stages of treatment. This period only takes about a few weeks. Thereafter, they go into an excellent phase with stable and smooth response to L-DOPA, which is called the ‘honeymoon period’ that typically lasts between 2 to 5 years (Melamed *et al.*, 2007).

However as the disease progresses, PD patients go into the next stage of the L-DOPA life cycle where they develop L-DOPA-induced complications that are difficult to treat. Although dyskinesia are accepted as prototype for these complications and are the most commonly observed complication among many others, the underlying mechanisms are different for each type of complication. L-DOPA-induced dyskinesia (LID) will be used as a common term representing the whole range of complications in the rest of the thesis for simplification purposes. Based on published data, it has been estimated that PD patients treated for less than 5 years have an 11 % risk of developing dyskinesia while those treated for 6–9 years have a risk of 32 % and patients treated for more than 10 years have a risk of 89% (Fabbrini *et al.*, 2007).

Table 1. Clinical spectrum of L-DOPA-induced complications (Aquino & Fox, 2015).

Motor fluctuations	Predictable wearing-Off Unpredictable, sudden Offs Dose failure, beginning of dose worsening, end-of-dose rebound On-Off fluctuations
L-DOPA-induced dyskinesia	High-dose dyskinesia (mixture of chorea, dystonia and myoclonus) Chorea, dystonia Myoclonus Ocular dyskinesia Respiratory dyskinesia
Low-dose dyskinesia	Off-period dystonia Diphasic dyskinesia
Non-motor fluctuations	Autonomic symptoms Thermo-regulatory dysfunction, sphincter disturbances, abdominal bloating, Off-period sweating, urinary problems and urgency, constipation, dysphagia, dyspnea and stridor Sensory symptoms Pain, numbness, paresthesia, akathisia and restless legs

The underlying mechanisms of LID are still not fully known. It is generally accepted that LID does not occur in patients (or in experimental animals) that have not been previously treated with dopaminergic medications. The processes by which the brain cells are sensitized, such administration of dopaminergic therapy modifies the response to the subsequent dopaminergic medications, is called

priming. Following priming, the development of LID largely depends on two supplementary factors, the pulsatile administration of L-DOPA and the degree of dopaminergic denervation in the striatum (Del Sorbo & Albanese, 2008). Current views suggest that both pre-synaptic (i.e., production, storage, controlled release, and reuptake of DA by nigrostriatal neurons) and post-synaptic (i.e., status of receptors and second messenger signaling pathways in striatal neurons) compartments are critical for the induction and maintenance of dyskinesia [reviewed elsewhere (Cenci & Lundblad, 2006; Cenci, 2007; Calabresi *et al.*, 2015; Mosharov *et al.*, 2015; Wang & Zhang, 2016; Borgkvist *et al.*, 2018)].

Serotonin hypothesis

5-HT system has a role in pathological events, which could explain some of the clinical manifestations and L-DOPA related complications in PD [reviewed recently in (Carta & Bjorklund, 2018)]. Despite the fact that 5-HT neurons can utilize L-DOPA in advance to synthesize and release DA, they lack feedback control mechanism, which enables the fine-tuning of the synaptic DA levels. It has been suggested that this uncontrolled release leads to excessive synaptic DA peaks, and thus contribute to swings in DA levels following administration of L-DOPA (de la Fuente-Fernandez *et al.*, 2004; Pavese *et al.*, 2006; Carlsson *et al.*, 2007; Lindgren *et al.*, 2010). This so called ‘serotonin hypothesis’ was supported by the studies of pharmacological manipulations of the 5-HT system in animal models of PD [reviewed in (Carta & Tronci, 2014)]. Among currently available clinical pharmaceutical interventions, eltoprazine, a 5-HT_{1A/B} receptor agonist and buspirone, a partial agonist of 5-HT_{1A} have been tested and found to have only modest effect in abolishing dyskinesia with unclear consequences on the motor function in PD patients (Bomasang-Layno *et al.*, 2015; Svenningsson *et al.*, 2015). Although the preclinical findings were promising, translation of these data to the clinical setting was less encouraging most likely due to the hypothesis being only one-dimensional. Moreover, excessive extracellular DA levels cannot explain motor improvements or unwanted effects by low doses L-DOPA. Indeed, the interaction between L-DOPA and 5-HT system is complex and may involve several other mechanisms. The details of impairment of 5-HT transmission by L-DOPA and its clinical implications has been reviewed recently in (Migueluez *et al.*, 2017).

Effect of L-DOPA on natural history of PD

DA generated from L-DOPA is partly metabolized to form reactive oxygen species, which has created a substantial amount of worry about the early use of L-DOPA with regard to possible toxic effect for DA neurons, despite powerful

symptom relieving effect (Olanow *et al.*, 2004). The first use of L-DOPA is frequently delayed because of these theoretical concerns about its toxicity or the risk of drug-induced motor complications (Olanow, 2009). Around the year 2000, the fear of L-DOPA-induced motor complications resulted in “L-DOPA phobia” among patients and doctors (Kurlan, 2005). Consequently, clinicians started to choose DA agonists as the first line of treatment because of their possible neuroprotective effects and in order to delay the long-term complications (Olanow *et al.*, 2001; Weiner & Reich, 2008). There are ten DA agonists that have been marketed for PD so far. Bromocriptine, cabergoline, dihydroergocryptine, lisuride and pergolide are ergot derivatives, and apomorphine, priribedil, pramipexole, ropinirole, rotigotine are non-ergot derivatives. Currently, only non-ergot derivatives are used in the clinical practice owing to their better side effect profiles. As a result, L-DOPA, DA agonists or some other medications including anticholinergics, amantadine, MAO-B inhibitors (selegiline, rasagiline) may be used either as initial treatment in the early stages of PD or as combination therapy in advanced PD. More recently, a shift towards initial use of L-DOPA appears to be occurring (Lang & Marras, 2014; Zhang & Tan, 2016).

As reviewed elegantly in (Olanow, 2015), in spite of *in vitro* data showing that L-DOPA as an oxidizing agent, which can be toxic to the DA neurons, no evidence of L-DOPA toxicity has been observed in normal, DA-lesioned or oxidatively stressed animals in animal models. In regards to pathological studies in humans, it is not possible to exclude but there is again no direct evidence for toxicity of L-DOPA (Quinn *et al.*, 1986; Olanow & Obeso, 2011; Parkkinen *et al.*, 2011). In parallel, two natural history human studies showed no evidence to suggest that patients primarily receiving L-DOPA were disadvantaged compared to those with delayed use, in terms of rate of disease progression with respect to disability and mortality (Diamond & Markham, 1990; Group *et al.*, 2014). Moreover, in two prospective double-blind trials evaluating patients with untreated PD randomized to initial treatment with either L-DOPA or a DA agonist (pramipexole or ropinirole), L-DOPA receiving patients had significant improvements in the unified Parkinson's disease rating scale (UPDRS) at all time points, although the rate of decline of the biomarker was greater (Parkinson Study, 2002; Whone *et al.*, 2003). These findings suggest that L-DOPA has no detrimental effect on the clinical progression despite possible toxicity on DA neurons.

To assess the effect of L-DOPA on the course of PD, the ELLDOPA study (Early vs. Late L-DOPA) was conducted by the Parkinson Study Group (Fahn *et al.*, 2004). This was a randomized, double-blind, placebo-controlled trial, evaluating 361 patients with early PD who were assigned to receive L-DOPA (in combination with carbidopa) at a daily dose 150 mg, 300 mg, or 600 mg, or a matching placebo over a period of 9 months, followed by 2 weeks of drug washout. The 2 weeks L-DOPA washout provided an untreated PD state at the end of the study. The

primary outcome was a change in UPDRS scores between baseline and 42 weeks. Furthermore, 142 subjects were examined with neuroimaging studies at baseline and at 9 months to assess striatal DAT density. The clinical data showed similar results as observed in previous studies that L-DOPA either slows the progression of PD or has a prolonged effect on the symptoms of the disease. Unfortunately, it was not possible to exclude the fact that patients were experiencing a longer duration of symptomatic response to L-DOPA that had extended beyond the two-week washout period. In contrast to the clinical outcome of the study, the imaging data indicated that dopaminergic function showed a greater deterioration in the L-DOPA treated group. Moreover, the subjects receiving the highest dose of L-DOPA had considerably more LID, high blood pressure, infection, headache, and nausea compared to placebo. As a result, the ELLDOPA study provided conflicted results and could not clarify whether L-DOPA was adversely affecting disease progression or not (Olanow, 2015).

The optimal timing for the initiation of L-DOPA and the use of other medications such as DA agonists, MAO-B inhibitor, COMT inhibitors still remain unclear and rely mostly on personal preferences. I personally try to avoid L-DOPA as an initial therapy for young-onset (before 40 years of age) PD patients, since these groups appear to have an increased risk for LID. This decision is however made after an open discussion with the patients and their relatives. There is no doubt that L-DOPA is the most effective antiparkinsonian agent to date and therefore should be used when there is a genuine need for reducing disability. Although the concerns about toxicity of L-DOPA cannot be excluded scientifically, complications related to L-DOPA seem to be related to the non-physiological restoration of striatal DA, rather than a specific toxic effect. This view was strongly supported with clinical studies of continuous delivery of L-DOPA using intestinal gel showing marked reduction of motor complications (Kurlan *et al.*, 1986; Stocchi *et al.*, 2005; Nyholm *et al.*, 2008; Olanow *et al.*, 2014; Wirdefeldt *et al.*, 2016).

Aims

Taken together, L-DOPA is a pivotal player in the DA synthesis machinery and even though L-DOPA is proven to be the most effective therapy to date, its use has many long-term consequential complications for PD patients. In light of this, different strategies are emerging with the central goal of restoring the malfunctioning DA system. Based on this premise, the primary objective of this thesis was to investigate mechanisms behind the dysfunctional DA signaling at multiple levels i.e. from BBB transport kinetics of L-DOPA and its metabolites as well as the role of presynaptic DA and 5-HT neurons to the postsynaptic striatal responses in relation to these neurons. Thus, the specific aims of the thesis was

- to tease apart the contribution of the pre- and postsynaptic compartments in the pathophysiology of LIDs in the parkinsonian brain,
- to directly investigate DA release properties from 5-HT terminals both in the parkinsonian striatum and after neuronal transplantation in 6-OHDA lesioned rats,
- to obtain proof-of-concept for the utility of a prediction model for BBB transport kinetics of L-DOPA and its metabolites in the extracellular fluid in the brain.

Materials and methods

Animals

Young adult female Sprague-Dawley rats weighing between 225–250 g on arrival from Charles River (Kisslegg, Germany) were used in all experiments included in this thesis. The animals were housed 2-3 per cage under a 12-h light/12-h dark cycle with free access to food and water. For blood sampling studies in *Paper III*, the animals were fasted overnight before the operation day to avoid competition of proteins with L-DOPA for the LAT1. All experimental procedures were performed according to the regulations set by the ethical committee for use of laboratory animals in the Lund-Malmö region.

Experimental protocols

In *Paper I*, two groups of animals were injected with rAAV5 vectors expressing either the TH knockdown construct or its scrambled control. A third group received striatal 6-OHDA lesion and finally a fourth group of rats were followed as non-treated intact animals. Animals in each group were then divided into 6 subsets. The first subset was directly killed and the brains were fixed for histological analysis. The second subset was included in the microdialysis experiment and then killed for histological analysis. Two additional subsets were included in biochemical analysis either at baseline or after a single dose of L-DOPA challenge. The final two subsets were allocated into behavioral test paradigms with chronic L-DOPA (presynaptic induction of dyskinesia) or apomorphine (postsynaptic induction of dyskinesia) treatment regimens and then killed for histological analysis.

In *Paper II*, while the first group of animals received a unilateral 6-OHDA lesion in the medial forebrain bundle (MFB), others were retained as intact controls. Animals that had a complete lesion were then treated with daily injections of L-DOPA for 28 days to induce AIMs, equivalent to peak dose dyskinesia seen in PD patients. The dyskinetic animals were then allocated into three different groups: Two groups of animals were transplanted with fetal tissue prepared as single-cell

suspensions, predominantly dopaminergic and serotonergic cells, respectively. The third group of dyskinetic rats did not receive any graft and were followed as 6-OHDA-lesion group. Functional benefits of transplantation were assessed using behavioral tests, microdialysis and PET imaging during the *in vivo* follow up period and using histological or biochemical end-points with termination at 8–14 months after grafting.

In *Paper III*, we used a protocol of simultaneous blood sampling and online-microdialysis in intact rats. The animals were divided into two experimental groups. The first group of animals was used in the pharmacokinetic dose-finding experiment, which led to the definition of the required dose of L-DOPA to be used in the real prediction experiments. We then simultaneously collected blood samples and brain dialysates from other animals to develop and test the prediction model.

Animal models of PD used in the thesis

6-OHDA (*Paper I, II*)

6-OHDA is a neurotoxin, which is selectively taken up by dopaminergic neurons via the DAT. Injection of 6-OHDA into the MFB causes an almost complete destruction of nigral dopaminergic neurons and thus full dopaminergic denervation in the striatum (Fibiger *et al.*, 1972). To achieve a less severe degeneration of the DA system, the toxin is delivered to the striatum in smaller doses in three deposits distributed along the rostrocaudal axis. This approach is useful in mimicking different stages of PD (Kirik *et al.*, 1998).

Functional TH knockdown (*Paper II*)

We have used viral vector mediated long-term short-hairpin RNA (shRNA) expression to block *in vivo* DA synthesis by targeted silencing of TH which is known to be the rate-limiting enzyme in the synthesis of DA, selectively in the nigrostriatal projection system (Hommel *et al.*, 2003). For this purpose, the rAAV5 vectors expressing shRNA sequences were generated as previously described (Ulusoy *et al.*, 2009).

This technology provided us a novel animal model where DA synthesis is knockdown without destruction of the presynaptic terminals. In this approach, the DA synthesis machinery is functionally silenced in a targeted manner in nigral DA neurons, whereas the structural integrity of the cells and their terminals are

maintained. This unique experimental system allowed us to explore the specific contribution of the presynaptic compartment in the induction and maintenance of LIDs in *Paper I*.

Surgical procedures

Choice of anesthetic

An injectable anesthetic with a 20:1 mixture of fentanyl citrate (Fentanyl) and medetomidin hydrochloride (Dormitor) (Apoteksbolaget) was used for both the viral vector injections and 6-OHDA lesion surgeries. The rats were anesthetized with 1–2% isoflurane mixed with 0.4 L/min O₂ and 1 L/min N₂O for cell transplantation, blood sampling and microdialysis experiments.

Stereotactic frame coordinates for different targets (*Paper I, II, III*)

Different coordinates were used according to the need for targeting of diverse regions according to the atlas of Paxinos and Watson (Paxinos *et al.*, 2007). Table 2 summarizes the stereotactic coordinates used followed in the entire thesis. The reason for using an altered microdialysis coordinates for *Paper II* was to target the mid point of three transplant deposits.

Table 2. Stereotactic frame coordinates.

Different coordinates (relative to the bregma) are used in different experiments throughout the thesis work.

	Target	TB	AP	ML	DV*
AAV-shTH (<i>Paper I</i>)	SN	-2.3	-5.2	-2.0	-7.2
6-OHDA (<i>Paper I</i>)	STR	0.0	+1.0, -0.1, -1.2	-3.0, -3.7, -4.5	-5.0
6-OHDA (<i>Paper I, II</i>)	MFB	-2.3	+1.2	-4.4	-7.8
Transplantation (<i>Paper II</i>)	STR	-2.3	+1.4, +0.5 +0.5	-2.5, -2.2, -3.7	-5, -3.5
Microdialysis (<i>Paper I, III</i>)	STR	-2.3	+0.6	-3.0	-5.5
Microdialysis (<i>Paper II</i>)	STR	-2.3	+1.1	-2.7	-5.5

AP: anteroposterior, DV: dorsoventral ML: mediolateral, MFB: medial forebrain bundle, TB: tooth bar. AAV-shTH: shRNA expression to knockdown TH. SN: substantia nigra. STR: striatum. *relative to dural surface.

6-OHDA lesion (*Paper I, II*)

The rats received unilateral injections of 6-OHDA (Sigma-Aldrich AB, Sweden; 3 mg/ml free base dissolved in 0.9% w/v NaCl with 0.2 mg/mL L-ascorbic acid) into the right MFB using a stereotaxic apparatus (Stoelting, Wood Dale, IL, USA) and 10 mL Hamilton syringe, (*Paper I* and *II*). For striatal lesions, the toxin was delivered into the striatum by injecting a total of 21 µg 6-OHDA dissolved in ascorbate-saline (0.02%) using three coordinates, in (*Paper I*).

Viral vector injection (*Paper I*)

Viral vector injections were performed into the SN using 5-µL Hamilton syringe fitted with a glass capillary with a tip diameter of about 60–80 µm. Two microliters of the buffer containing the appropriate number of viral particles was injected at a speed of 0.4 µL /min. The needle was withdrawn slowly over 5 min after completion of the injection.

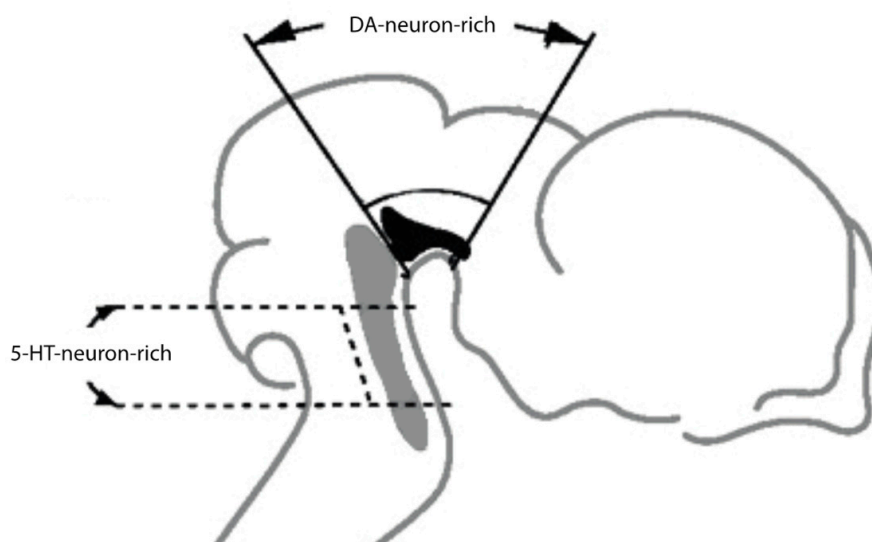


Figure 7

Illustration of ventral mesencephalon in rat embryo. Tissue pieces include either DA- or 5-HT-neuron-rich grafts in accordance with different microdissection approaches (Modified from Carlsson et al., 2007).

Cell transplantation (*Paper II*)

All transplantation procedures were performed using fetal cells dissected from embryonic day 14 rat embryos, based on a micro transplantation protocol using glass capillaries attached to a 5 µL Hamilton syringe, as described previously (Carlsson et al., 2007). Tissue pieces obtained from the ventral mesencephalon region (rich in DA neurons) or from the dorsal pontine raphe region (rich in 5-HT neurons) as indicated in Figure 7 were incubated in 0.1% trypsin/0.05% DNase in

DMEM at 37°C for 20 min, and rinsed before being mechanically dissociated to a single cell suspension, centrifuged, and re-suspended to a concentration of 100,000–150,000 cells/ml for DA-neuron-rich grafts and 80,000–140,000 cells/ml for 5-HT-neuron-rich grafts. The viability of the cells was 97% for both tissue preparations. A total of 3 ml from the final cell suspension was distributed over three injection tracts in the lesioned striatum. Two 0.5 ml deposits (-5 to -3.5 mm below dura) were delivered along each tract.

Microdialysis (*Paper I, II, III*)

Microdialysis is an *in vivo* sampling technique that allows the quantification of various substances (e.g., neurotransmitters, peptides, electrolytes) in blood and tissue. We used a specialized online microdialysis (OMD) setup directly coupled to an HPLC detection system (Figure 8).

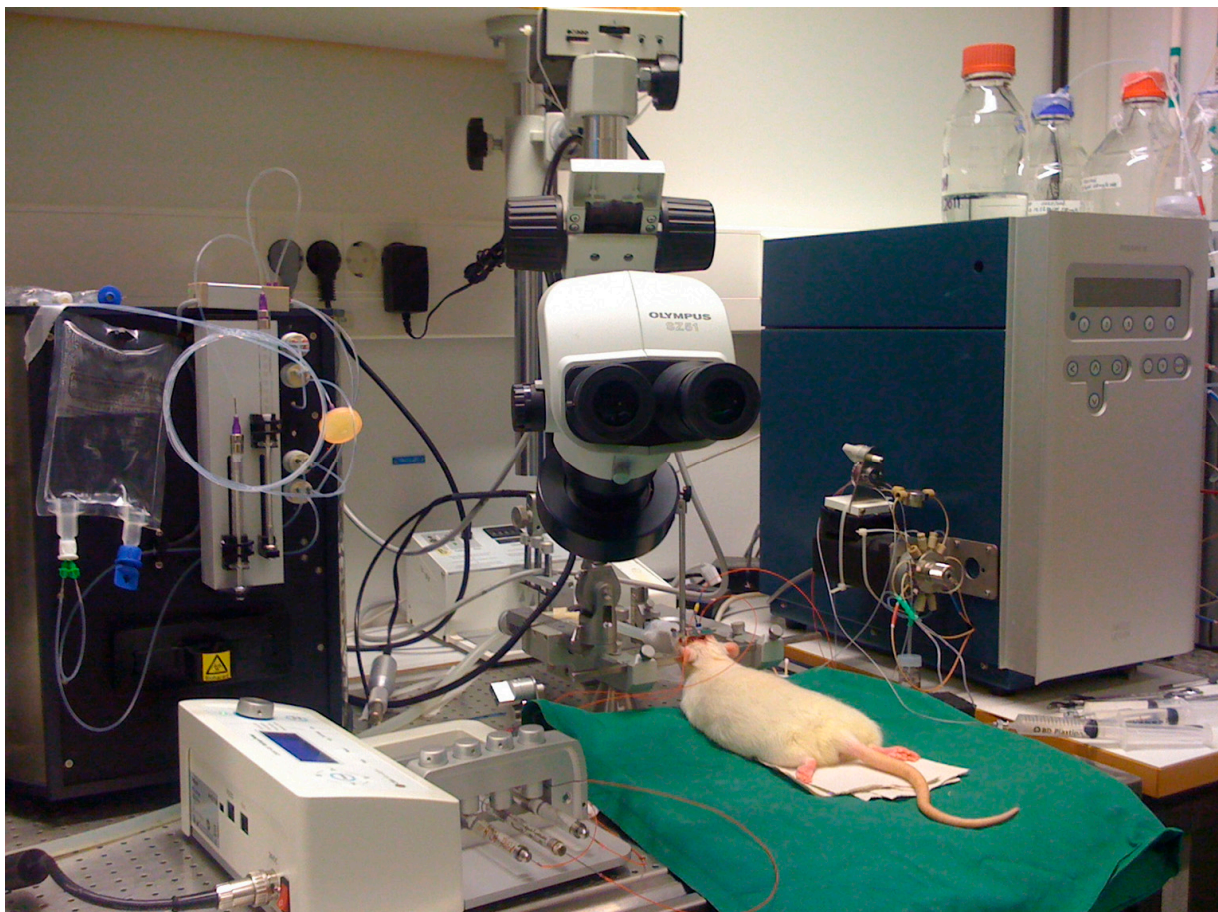


Figure 8
Online microdialysis (OMD) setup coupled to an HPLC system in a rat under gas anesthesia. (Picture from the own archive).

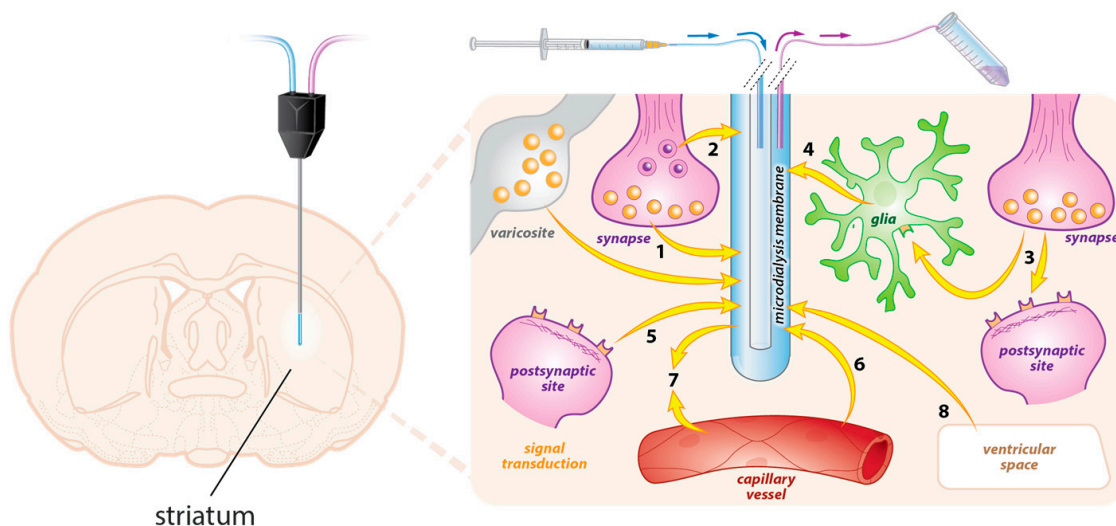


Figure 9

Schematic illustration of microdialysis. The probe is inserted into the striatum and kept there with the help of a probe holder. Ringer solution is run via microdialysis pump through the probe where the pores in the probe membrane allow exchange of monoamines from the surrounding extracellular fluid. Dialysate samples are analyzed online in the HPLC system coupled directly to the outlet of the microdialysis probe. Note that the information obtained from microdialysis in the brain comes from the perisynaptic structures (1 and 2), intrasynaptic events (3), the astroglial cells (4), the postsynaptic site (5), vascular structures (6 and 7) and ventricular space (8). Figure by Krzysztof Kucharz [modified from (Kehr & Karolinska, 1999)].

The microdialysis probe consisted of a tubular dialysis membrane with inlet and outlet tubes for perfusion and sample collection, respectively. During the microdialysis experiment, the inside of the membrane was perfused with fluid by the help of a microdialysis pump. In a typical microdialysis experiment, a series of samples will first be obtained for the determination of basal levels (Figure 9). Repeated samples will then be collected until stable baseline levels are achieved. This equilibration period takes about one hour. Depending upon the experimental protocol, the probe can then be used for sampling as well as for drug delivery. A liquid switch can also be used for delivery of different perfusates into the region dialyzed. To prevent oxidization of neurotransmitters studied, an antioxidant solution containing acetic acid, EDTA, L-cysteine, and ascorbic acid, was mixed with the dialysate at the outlet of the probe (Thorre *et al.*, 1997). The different perfusates and drug manipulations used in this thesis, and their readouts and interpretations regarding DA and serotonin metabolism are listed in Table 3.

The dialysates were directly analyzed on Alexys online monoamine analyzer microdialysis system (Antec Leyden) consisting of a DECADE II electrochemical detector and VT-3 electrochemical flow cell. Two different mobile phases—optimized for the detection of the respective metabolites—were used in each of the two flow paths. The first mobile phase (50 mM phosphoric acid, 8 mM NaCl, 0.1 mM EDTA, 12.5% methanol, 500 mg/L octane sulfate; pH 6.0) was used for the

detection of DA, and 5-HT using a 1 mm × 50-mm column with 3 μm particle size (ALF- 105) at a flow rate of 75 μL/min. The second mobile phase (50 mM phosphoric acid, 50 mM citric acid, 8 mM NaCl, 0.1 mM EDTA, 10% methanol, 600 mg/L octane sulfate; pH 3.2) was used for the detection of 3-OMD, DOPA, DOPAC, HVA, and 5-hydroxyindolacetic acid (5-HIAA), which passed through a 1 mm × 150-mm column with 3-μm particle size (ALF- 115) at a flow rate of 100 μL/min. The dialysate samples were transferred via 5-μL loops simultaneously into each flow path and analyzed by the online HPLC at 12.5 min time bins. The chromatograms were analyzed using the Clarity Chromatographic Station (version 2.7.03.498; DataApex). The probes were withdrawn to check the membrane integrity and animals were killed at the end of the experiment.

Table 3.

Microdialysis protocols for diverse readouts from the striatal monoamine neurotransmitter system used in different experiments throughout the thesis work.

Perfusate	Drug, injected to the animal	Readout	Interpretation	Paper(s)
mRL	none	DA, HVA, DOPAC	Baseline DA levels and its metabolism in ECF of striatum	I, II
mRL	none	5-HT, 5-HIAA	Baseline 5-HT levels and its metabolism in ECF of striatum	II
mRL with 100mM KCl	none	DA, 5-HT	Readily releasable pool of striatal DA and 5-HT	I, II
mRL	NSD-1015 (AADC blocker)	DOPA	Accumulation of DOPA in 90 min represents <i>in vivo</i> TH activity	I
mRL	Nomifensine (DAT blocker)	DA	DA levels in the synaptic cleft	II
mRL	L-DOPA	DOPA, 3-OMD, DA, HVA, DOPAC	BBB transport kinetics of DOPA and its striatal metabolism	III

mRL: modified Ringer Lactate.

Simultaneous blood sampling and microdialysis (*Paper III*)

This unique approach of simultaneous blood sampling and microdialysis enabled us to correlate between blood and brain ECF levels of individual metabolites after administration of exogenous L-DOPA in rats (*Paper III*). From a methodological perspective, cannulation of the tail artery was done first followed by the insertion of the microdialysis probe. After applying gas anesthesia, the surrounding tissue of the tail artery was dissected carefully. A polyethylene tubing was inserted through a small incision to the tail artery. After the confirmation of secure blood flow into the tubing, the distal part of the artery was permanently tied (Figure 10). The tubing was then flushed with heparin to keep the line open during the surgical procedure of microdialysis probe insertion and equilibration period. The rats were then placed into a stereotactic frame and with the help of a holder, the microdialysis probe were inserted into the striatum. A volume of 60 microliter

blood were sampled every 10 min for 2 hours manually. Following collection of two consecutive blood samples under the baseline conditions, animals were injected with L-DOPA and 18 more samples collected during the following 3 hours, while maintaining the total amount of blood collection from any animal under 1.5 ml (and replacing the withdrawn volume with saline to keep hemodynamic physiology of the animals intact). Five minutes after collection, blood samples were centrifuged for 1 min using a mini centrifuge. We then carefully transferred the supernatant (serum) to a 0.5 ml Eppendorf tube and added additional amount of perchloric acid so that the final concentration of perchloric acid is 0.01 M. The mixture then was transferred to a filter unit of 0.22 μm and spun for another 1 min to obtain the filtered plasma, which was rapidly frozen on dry ice and kept at -80°C until further processing.

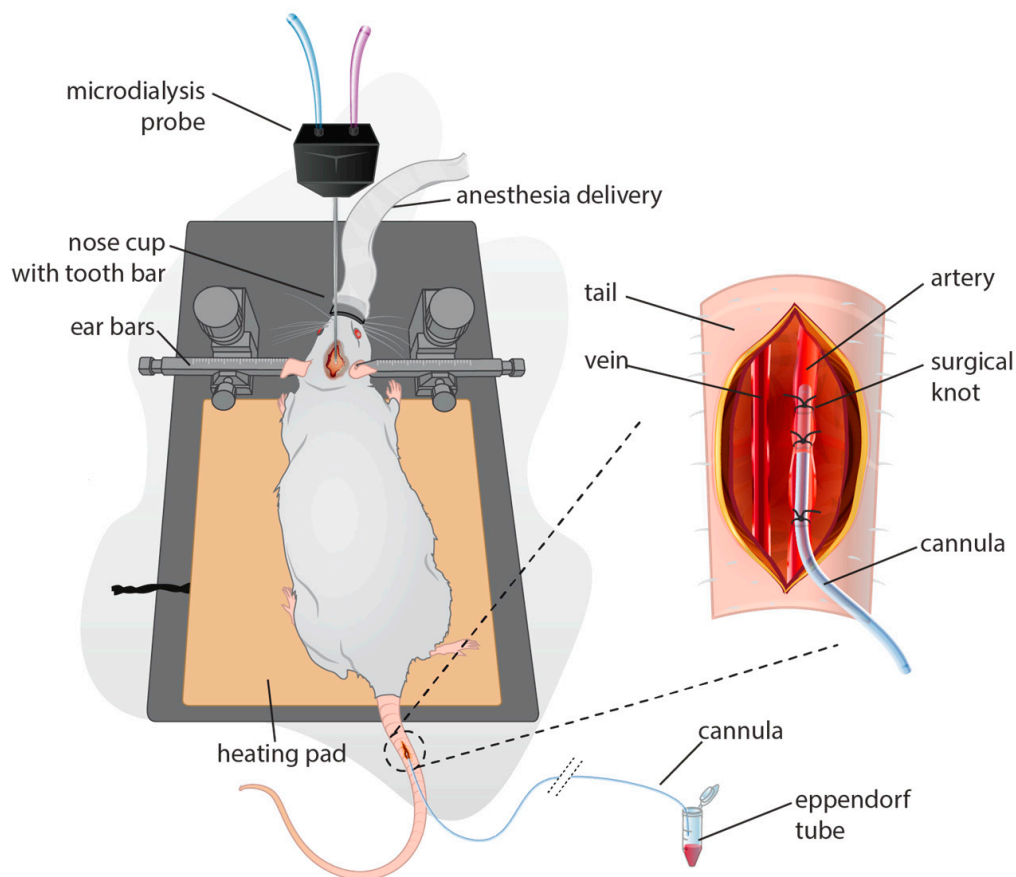


Figure 10

Illustration of simultaneous blood sampling from the tale artery and microdialysis through striatum that is coupled directly to a HPLC system (Online microdialysis, OMD) in a rat. Figure by Krzysztof Kucharz.

Behavioral tests

Amphetamine rotation test (*Paper I, II*)

Three weeks after 6-OHDA lesion, the animals were challenged with D-amphetamine (2.5 mg/kg, i.p.). This test was used as a screen for the selection of animals for further experimentation. Animals displaying rotational asymmetry of 6 full body turns/min (mean over 90 min) were selected for characterization using the cylinder test and then dyskinesia induction by daily L-DOPA injections.

Cylinder test (*Paper II*)

The cylinder test was used to assess the symmetrical use forelimb use, balance capabilities and exploratory behavior of the animal. The animals were allowed to move freely in a clear glass cylinder during video recording. Mirrors are placed behind the cylinder to allow for observation of all forelimb contacts on the glass wall. The videotapes are evaluated by an observer blinded to the identity of the animals and the number of left and right paw touches on the cylinder wall are counted separately for at least 20 contacts. Data was expressed as left paw touches as % of total if the 6-OHDA lesion was made on the right side as previously described (Barger & Dale, 1910).

Apomorphine and L-DOPA–Induced AIMs (*Paper I, II*)

The animals included in the behavioral experiments were treated chronically either with different doses of L-DOPA [administered subcutaneous (s.c.) together with 10 mg/ kg benserazide] over a 3 week period or apomorphine (dissolved in 0.2 mg/mL ascorbate-saline and administered s.c.) over a 15 day treatment period. The evaluation of the abnormal involuntary movements (AIMs) was performed according to the rat dyskinesia scale (Winkler *et al.*, 2002). Briefly, the animals were placed individually in transparent plastic cages with a grid lid so that the rater can visualize every movement. The rater was blinded to the identity of the animals and performed the scoring for each animal every 20 min following L-DOPA injection. The AIMs were classified into three subtypes according to their topographic distribution as forelimb, orolingual, and axial dyskinesia (Figure 11). Locomotive dyskinesia displayed as contralateral rotations were scored separately.

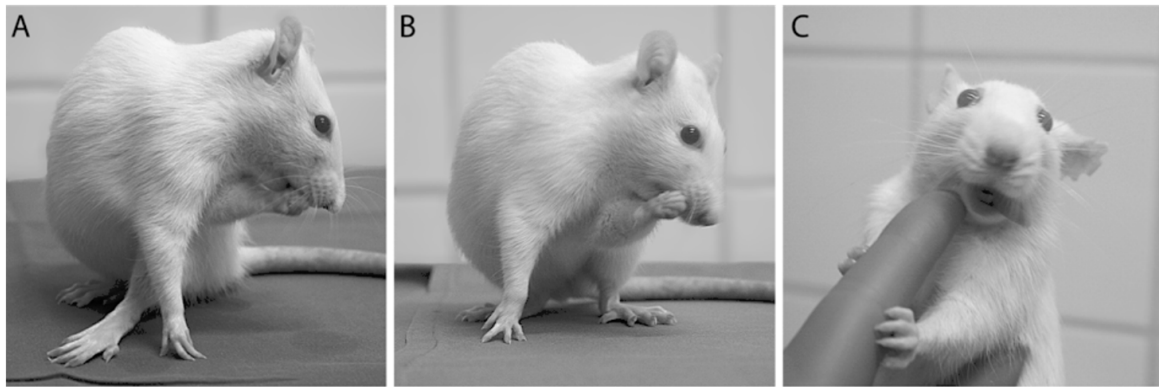


Figure 11

AIMs in rat showing axial (A), forelimb (B) and orolingual (C) dyskinesia induced by chronic injections of L-DOPA in combination with benserazide.

The severity of each AIM subtype was scored from 0 to 4 (0: no abnormal behaviors detected, 1: occasional AIMs, i.e. present less than 50% of the time; 2: frequent AIMs, i.e. present more than 50% of the time; 3: continuous AIMs, but interrupted by sensory stimuli and 4: continuous AIMs, not interrupted by sensory stimuli). Half-points were used when the behavior of the animal were clearly in between the two defined points. The data was calculated as time- integrated total scores and represented by sum of the orolingual, limb and axial subtypes.

PET Imaging (*Paper II*)

We utilized [^{18}F]fallypride positron emission tomography (PET) imaging as a means to estimate occupancy of the D_2R pool *in vivo* by calculating the binding potential (BP) of the ligand to the receptors in the presence and absence of L-DOPA. [^{18}F]fallypride ligand was chosen because this tracer has been used to assess $\text{D}_2/\text{D}_3\text{R}$ occupancy in rats, baboon and human striatum (Guggenheim, 1913; Waser & Lewandowski, 1921). Moreover, this ligand has been shown to be suitable for the measurement of amphetamine effects on $\text{D}_2/\text{D}_3\text{R}$ ligand binding in the striatum (Fahn, 2015). Rats were scanned on a dedicated small animal PET scanner (MicroPET Focus 220, Siemens Medical Solutions USA, Inc.). Radiochemical production and data analysis are performed by our collaborators at Commissariat à l'énergie atomique (CEA), Institut d'imagerie biomédicale (I2BM), Molecular Imaging Research Center (MIRCent), Fontenay aux Roses in France.

Postmortem analyses

High performance liquid chromatography (HPLC) (*Paper I, II, III*)

Offline HPLC analysis was utilized to assess the total tissue levels of DA, serotonin (5-HT), and their metabolites. For this purpose, the animals were decapitated and the brains were rapidly dissected. After a brief rinse with an ice-cold saline solution, the brains were placed on a brain matrix. A 2-mm slice containing the striatum was dissected out from the surrounding tissue. The tissue was rapidly frozen on dry ice and kept at -80°C until further processing. The midbrain samples from those animals were fixed in 4% paraformaldehyde overnight for immunohistochemical detection of viral transduction and treated in the same way as described under the histological analysis section below. For the analysis, striatal tissue samples were sonicated in 18 mL/mg ice-cold homogenization buffer (20 mM Tris acetate, pH 6.1) and centrifuged at $20,000 \times g$ for 10 min at 4°C . The supernatant was filtered through a PVDF filter ($0.45\mu\text{m}$; Uni-filter) and used for HPLC analysis to determine of the total tissue concentration of DA, 5-HT and their metabolites.

Moreover serum contents of DOPA, 3-OMD, DOPAC and HVA were also measured by HPLC. On the analysis day, they were filtered directly through a PVDF filter ($0.45\mu\text{m}$; Uni-filter) and spun down for an additional 3 min at 10,000 rpm. Each sample (either tissue or plasma) was injected by a cooled autosampler (AS100) into Alexys Monoamine Analyzer (Antec Leyden, Netherlands) consisting of a DECADE II electrochemical detector and VT-3 electrochemical flow cell. The mobile phase (50 mM phosphoric acid, 50 mM citric acid, 8 mM NaCl, 0.1 mM EDTA, 12.5 % methanol, 600 mg/L octane sulfate; pH 3.1) passed through a $1\text{mm} \times 150\text{mm}$ column with $3\text{-}\mu\text{m}$ particle size (ALF-115) (Antec Leyden, Netherlands) at a flow rate of $100 \mu\text{L}/\text{min}$ for the determination of monoamines. The peaks were analyzed using the Clarity Chromatographic Station (DataApex).

***In vitro* DA binding assay (*Paper II*)**

We used the gold-standard *in vitro* receptor assays to directly determine the K_d and B_{max} values for the $D_1\text{R}$ and $D_2\text{R}$ to confirm the PET imaging findings. For this purpose, we analyzed the brains of intact and 6-OHDA lesioned rats killed either under baseline or 1 hr after L- DOPA injection at the peak of dyskinesia. Striatal tissue from these brains was processed for $D_1\text{R}$ and $D_2\text{R}$ binding using [^3H]SCH23390 or [^3H]raclopride ligands respectively. The dissected tissue were kept on dry ice and stored at -80°C until further use. On the day of analysis, the

samples were homogenized using ultrasonic disintegrator in ice-cold assay buffer (50 mM Tris-HCl, 120 mM NaCl, 1 mM EDTA, 5 mM KCl, 1.5 mM CaCl₂, 4 mM MgCl₂, pH 7.4). The homogenate was diluted in ice-cold buffer and dispensed into two 96 well plates (MultiScreenHTS FB, membrane pore size, 1.0/ 0.65 mm durapore, opaque, Millipore). One of the plates was used for D₁R binding assay while the other one was used for D₂R assay. A total of 50 and 350 mg of tissue lysate was used for each well in D₁R and D₂R binding assays, respectively. Two different radioactive ligands ([³H]SCH23390 for D₁R and [³H]raclopride for D₂R, PerkinElmer) were used at eight different concentrations (ranging between 0.5–15 or 1–30 nM) for each assay. In order to determine the non-specific binding, 100 mM SCH23390 or 300 mM haloperidol was used for each concentration in the two assays, where the unlabeled compound was added to the homogenate 30 min prior to the incubation with the tritiated ligand. Plates were incubated for 2 h at room temperature and then were filtered by using MultiScreen vacuum manifold (Millipore) and allowed to air-dry for 24 h. Next day, the plates were punched using a MultiScreen Punch Kit (Millipore) in order to isolate the tissue bound membranes, which were then collected individually in scintillation vials. The vials were instantly filled with LSC cocktail (Ultima Gold, PerkinElmer). Forty-eight hours later, the radioactive decay was determined in each vial using a liquid scintillation counter (Beckman LS 6500). Data obtained in the wells treated with the cold compounds was used to measure the non-specific binding under each condition, while the corresponding wells without the unlabeled compound gave the total binding.

Histological Analysis (*Paper I, II*)

After the rats were deeply anesthetized, they were then perfused through the ascending aorta first with 50 mL physiological saline at room temperature over 1 min and then by 250 mL ice-cold 4% paraformaldehyde (PFA) for 5 min. Brains were post-fixed in 4% PFA solution for 2 h before being transferred into 25% sucrose solution for cyroprotection, where they were kept until they had sunk (typically within 24–48hrs). The brains were then sectioned in the coronal plane on a freezing microtome at a thickness of 35 μm. Sections were collected in six series and stored at –20 °C in a phosphate buffer containing 30% glycerol and 30% ethylene glycol until further processing.

Immunohistochemical stainings were performed on free-floating sections. For this purpose, brain sections were first rinsed with potassium-PBS (KPBS), and then endogenous peroxidase activity was quenched by incubation in a mixture of 3% H₂O₂ and 10% methanol in KPBS for 30 min. After three rinsing steps in KPBS, nonspecific binding sites were blocked by incubation in KPBS containing 5% normal serum matched to the species used to raise the corresponding secondary

antibody and 0.25% Triton-X. Samples were then incubated overnight at room temperature in primary antibody solution containing 5% serum and 0.25% Triton-X (see materials and methods section in *Paper I, II* and *III* for details of primary antibodies used).

On the second day, the sections were rinsed in KPBS and then incubated for 1h at room temperature in 1:200 dilution of appropriate biotinylated secondary antibody solutions. After rinsing, the sections were treated with avidin-biotin-peroxidase complex (ABC Elite kit; Vector Laboratories) and the color reaction was developed by incubation in 25 mg/mL 3,3'-diaminobenzidine and 0.005% H₂O₂. To increase the contrast in the FosB and c-Fos staining 2.5 mg/mL Nickel sulfate was added in the DAB solution before the color reaction. Sections were mounted on chrome- alum coated glass slides, dehydrated and cover-slipped with DPX mounting media (Sigma).

Image Analysis (*Paper I*)

The optical intensity of the TH- and VMAT₂-positive fibers as well as the numbers of c-Fos and FosB positive cells of the striatum were analyzed on images captured using a 10× Plan-Fluor objective (Numerical aperture = 0.30) on a Nikon Eclipse 90i microscope equipped with a Nikon DS-Q1Mc camera using NIS software (NIS Elements AR 3.0; Nikon). The c-Fos and FosB positive cells were counted from 0.5 mm × 0.5 mm tiff formatted images analyzed using the ImageJ software (Version 1.42i, NIH). After background subtraction, the numbers of cells specifically labeled with c-Fos and FosB were counted using the particle analysis tool. The density of immunopositive c-Fos and FosB profiles was expressed as number of cells/mm².

Confocal Microscopy (*Paper I*)

The triple immunohistochemical staining was visualized on a Nikon Eclipse 90i microscope equipped with a D-eclipse C1 confocal camera (Nikon). The high power confocal images were captured using a 60× Plan-Apo objective (Numerical aperture = 1.4) on a single plane using sequential acquisition. The low power images were taken using a 4× Plan-Fluor objective (numerical aperture = 0.13) as z-stacks of eight focal planes penetrating 6–8 μm from the surface of the section in sequential acquisition mode. Confocal images were captured and pseudo-colored using EZ-C1 software (gold version 3.9). The z-stack images were then processed for maximal intensity projection on an NIS-Elements AR software (version 3.10).

Stereological Analysis (*Paper I, II*)

The TH-positive and VMAT₂-positive cell numbers in the SN were estimated using an unbiased stereological quantification method by using the optical fractionator principle (Lindvall & Bjorklund, 1974; Albin *et al.*, 1989). All quantifications were undertaken blinded to the identity of the sections by a coding system. Upon completion of the quantification of batches, samples were moved to a database for further analysis using appropriate statistical and graphical tools. The borders for the region of interest was defined by using a 4× objective, whereas the actual counting was performed using a 60× Plan-Apo oil objective (Numerical aperture = 1.4) on a Nikon 80i microscope equipped with an X-Y motorized stage, a z axis motor and a high-precision linear encoder (Heidenhein). All three axes and the input from the digital camera were controlled by a PC computer running the NewCast Module in VIS software (Visio- pharm A/S), which carries out the procedure with a random start and systematic sampling routine. The sampling interval in the x-y axis was adjusted so that at least 100 cells were counted for each SN. Coefficient of error attributable to the sampling was calculated according to Gundersen and Jensen (Gundersen & Jensen, 1987) and values ≤ 0.10 were accepted.

Statistical analysis

The statistical analyses of behavioral, microdialysis, histological and imaging data were performed using either SPSS statistical software (SPSS Inc. Chicago IL) (*Paper I, II, III*) or R software (*Paper II*). A parametric test was selected when the dependent variable was measured on a continuous scale (microdialysis, histological, imaging and prediction data; *Paper I, II, III*), whereas a non-parametric test was selected when the dependent variable's level of measurement was nominal (categorical) or ordinal (AIMs data, *Paper I*). Statistical significance was set at $P < 0.05$. As well as the details of the tests used, and the results of statistical analyses were presented in the respective *Papers*.

Mathematical modeling for prediction of brain ECF levels of L-DOPA and its metabolites (*Paper III*)

We used blood levels of DOPA and its metabolites as input values to the model for the prediction of corresponding brain extracellular fluid (ECF) levels based on the data obtained by simultaneous blood sampling and microdialysis in intact rats. We formulated a simple approach for predicting the metabolite concentrations in the

brain when only the corresponding blood metabolites were observed. In what follows, a *test* sample was used to denote an animal for which we have observed the blood metabolite concentrations, and wish to predict the brain metabolite concentrations. Similarly, *training* samples referred to animals which we have observed both blood and brain metabolite concentrations. The prediction of brain metabolite concentrations for a test sample was carried out in two steps: first, constrained regression was used to model the observed blood metabolite concentrations as a linear combination of the corresponding concentrations in a collection of training samples. Second, the obtained regression coefficients were used to calculate the same linear combination of the brain metabolite concentrations in the training samples, which formed the predicted values of the brain metabolite concentrations in the test sample. The implicit assumption of this approach is that if two animals show similar behavior in terms of the blood metabolite concentrations, their brain metabolite concentrations will also be similar (*See Figure 2, Paper III*). Our collaborators in the Centre for Mathematical Sciences at the Faculty of Engineering, in Lund University carried out this prediction analysis.

Results

Presynaptic dopaminergic compartment determines LID (*Paper I*)

Mechanisms of L-DOPA-induced dyskinesia

The motor symptoms such as bradykinesia, rigidity and tremor encountered in PD are caused by the progressive loss of dopaminergic neurons in the SN (Fearnley & Lees, 1991). Degeneration of these neurons causes decreased DA content in their target region, namely the striatum (Marsden, 1990). L-DOPA, the natural precursor of DA, replaces this dopaminergic deficit effectively and improves quality of life in patients with PD. Essentially all Parkinson patients will eventually require the use of L-DOPA as a symptomatic therapy and are expected to develop motor complications related to L-DOPA within a decade. These complications include motor fluctuations and AIMs i.e. dyskinesia.

LID are known to be caused by both presynaptic and postsynaptic mechanisms. Presynaptic mechanisms include events related to the production, storage, controlled release and reuptake of DA by dopaminergic neurons. On the other hand, postsynaptic mechanisms include the status of DA receptors and second messenger pathways in the striatal MSNs.

The aim of *Paper I* was to investigate whether pre- or postsynaptic sites play a critical role in pathophysiology of LID in the parkinsonian brain. Our hypothesis was that response of postsynaptic striatal neurons remains under the control of the presynaptic DA terminals even in dyskinetic animals. The difficulty here was to find the best suitable animal model to dissect out pre- and post-synaptic mechanisms. Traditional animal models utilizing 6-OHDA induce both pre- and post-synaptic changes. Synaptic changes secondary to the dopaminergic denervation and long-term drug treatment adds to the complexity in finding an appropriate model.

Therefore, we used a novel tool that was developed in our lab where TH, known to be the rate limiting enzyme in the synthesis of DA, was selectively knocked down by a short-hairpin RNA-mediated construct (shTH) using a recombinant adeno-

associated virus carrying AAV5 capsid protein (rAAV5) (Ulusoy *et al.*, 2009). In this unique animal model, the structural integrity of the DA cells and their terminals are maintained, which in turn allowed us to specifically explore the role of the presynaptic compartment in the development and maintenance of LID.

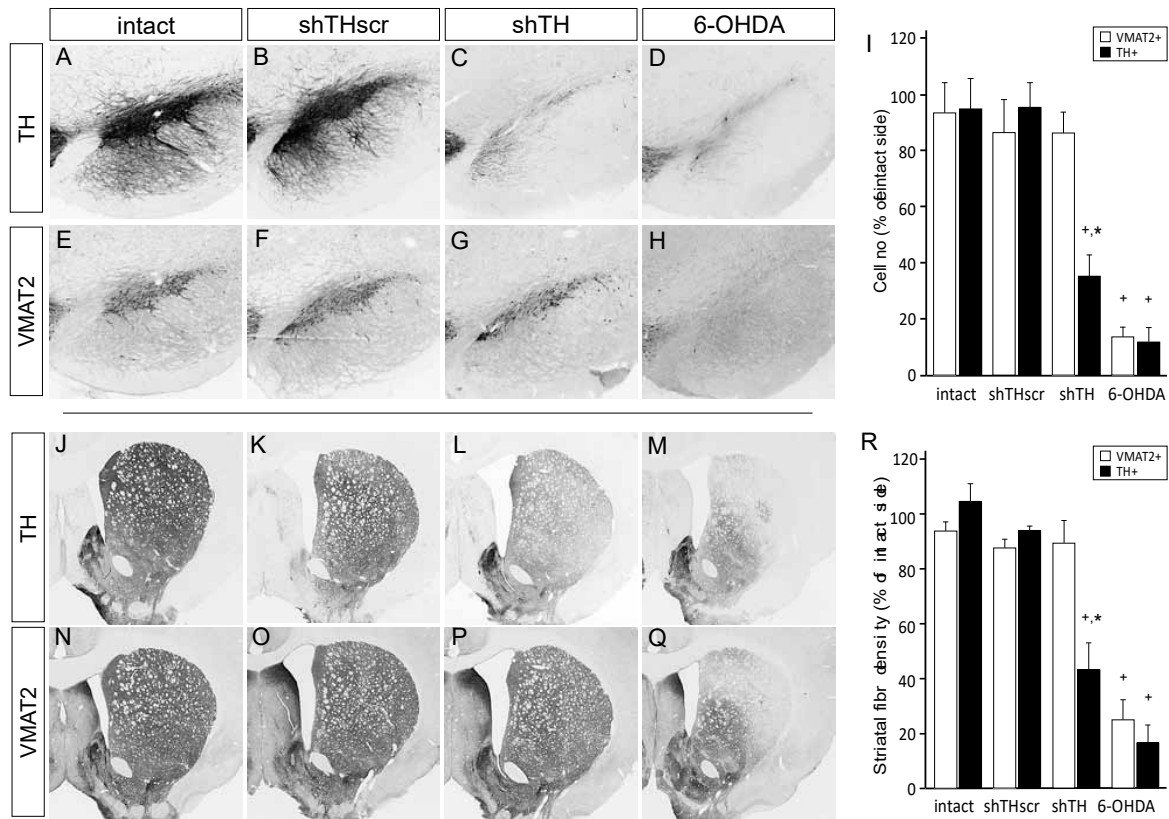


Figure 12

Down-regulation of TH by rAAV-mediated shRNA expression in the SN and striatum without changing VMAT₂ expression. While control groups showed no change either in TH- or VMAT₂ expression (A, B, E, F, J, K, N, O), active knockdown group (shTH) showed a reduced TH protein in the cell bodies (C) and at the terminals (L). VMAT₂ expression on the other side remained unchanged (G and P), confirming that TH knockdown was selective and induced no structural change in the dopaminergic neurons. Note that 6-OHDA lesion group as being the positive control showed decrease in both TH and VMAT₂ expression at both cellular (D, H) and terminal level (M, Q). Data are analyzed by two way factorial ANOVA [I, group vs. phenotypic marker effect $F(7,27) = 16.497$, $P < 0.0001$; R, group vs. phenotypic marker effect $F(7,27) = 26.841$, $P < 0.0001$], followed by Tukey's HSD post hoc. Error bars represent SEM. *Different from intact and shTHscr control group within the same phenotypic marker; +TH-positive cells or fiber density different from the corresponding VMAT₂-positive cells or fiber density in the same group.

shTH Expression in nigral DA neurons effectively down-regulates TH expression in the absence of structural damage

Maintenance of the long-term down-regulation of TH expression in the SN and striatum was confirmed with both histological and biochemical analyses. At the histological level, stereology showed that while 6-OHDA lesion led to 88.0 and 86.3% decrease in TH- and VMAT₂-positive cells respectively in the SN. In comparison, stereological analysis from shTH-expressing rats showed a 64.6 % decrease in TH-positive cells while VMAT₂-positive neurons were not different from normal controls (Figure 12, A-I). Image analyses of striatal fiber terminals also showed comparable results (Figure 12, J-R) with an obvious dissociation between the two markers in the shTH-expressing rats. This finding confirmed that dopaminergic cells, which no longer expressed the TH enzyme, still remained viable throughout the experiment.

We then analyzed striatal tissue content of DA, 5-HT and their metabolites by HPLC at the biochemical level under baseline conditions and in a separate cohort of animals after L-DOPA treatment. Baseline DA levels in the shTH and 6-OHDA groups were significantly lower than the control groups on the injected side. L-DOPA administration resulted in significant recovery of DA levels only in the shTH group confirming that the DA machinery in these animals was intact and functionally capable of handling exogenously administered L-DOPA. This capacity was lost in the 6-OHDA because of the structural damage to the terminals. 5-HT turnover was unchanged confirming that the experimental changes in the DA system were specific (*See Paper II, Figure 2*).

shTH Expression in nigral DA neurons induces a significant dopaminergic denervation in the striatum

We performed the microdialysis experiment using an online HPLC system with high sensitivity to prove that extracellular DA concentration in the shTH group was reduced (*See Paper I, Figure S2* for illustration of the system). Baseline extracellular DA concentrations were found to be reduced by 69.6 and 57.7% in the shTH and 6-OHDA groups respectively (Figure 13, A, B). Despite these comparable results in the two treatment groups, the readily releasable pool of DA, as measured upon the application of high concentration of KCl in the dialysate revealed a milder reduction of DA in the shTH group (69.4 vs. 94.5%) (Figure 13, C). Moreover, the i.p. injection of NSD-1015 (AADC inhibitor) led to a decreased DOPA accumulation rate in both treatment groups (71.4% in shTH and 87.2% in 6-OHDA groups) confirming that *in vivo* TH enzyme activity was decreased in both treatment groups compared to control groups (Figure 13, D, E).

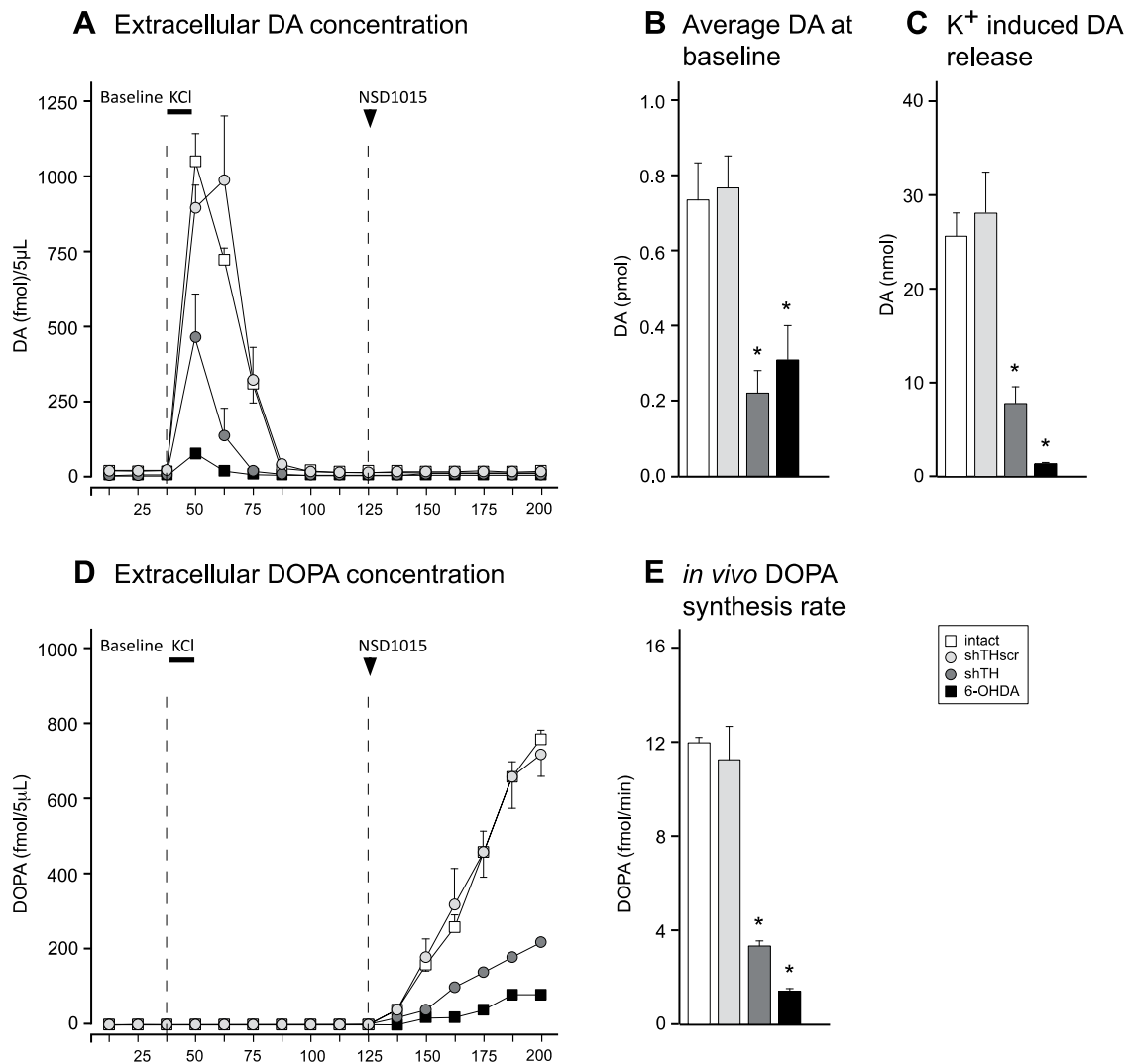


Figure 13

Three-phase microdialysis protocol. In phase I, extracellular DA concentrations were monitored under baseline conditions (A, B). In phase II we applied high concentration of KCl in dialysate to measure readily releasable DA pool in the terminals (A, C). We inhibited AADC enzyme by i.p. injection of NSD-1015 in phase III, which in turn induces DOPA accumulation and reflects *in vivo* TH enzyme activity (D, E). Statistical comparisons were performed by one-way ANOVA [B, $F(3,10) = 11.975$, $P < 0.01$; C, $F(3,10) = 19.354$, $P < 0.0001$; E, $F(3,10) = 126.806$, $P < 0.0001$] followed by Tukey's HSD post hoc test. Error bars represent \pm SEM. *different from intact and shTHscr controls.

shTH expression prevents LID by modulating primed striatal neurons

As the biochemical results suggested that shTH expression maintained a very good buffering capacity for the newly synthesized DA after administration of exogenous L-DOPA, we expected that these animals would be resistant to the development of LID. In fact, chronic treatment with L-DOPA in an escalating dose regimen of 6, 12, and 24 mg/kg s.c. over a 3-week treatment period supported the abovementioned view since shTH expressing animals remained similar to the control group while the 6-OHDA lesion group developed severe dyskinesia as evaluated by the AIMs scale (Figure 14A). In contrary, as the extracellular DA

levels were decreased in both treatment groups (shTH and 6-OHDA), we expected the induction of dyskinesia after treatment with apomorphine, a direct D₁R/D₂R agonist targeting the postsynaptic site (Figure 14B). Apomorphine was administered at escalating doses of 0.1, 0.2 and 0.5 mg/kg over three 5-day blocks. As anticipated, both treatment groups developed dyskinesia though with different levels of severity. The control groups remained non-dyskinetic.

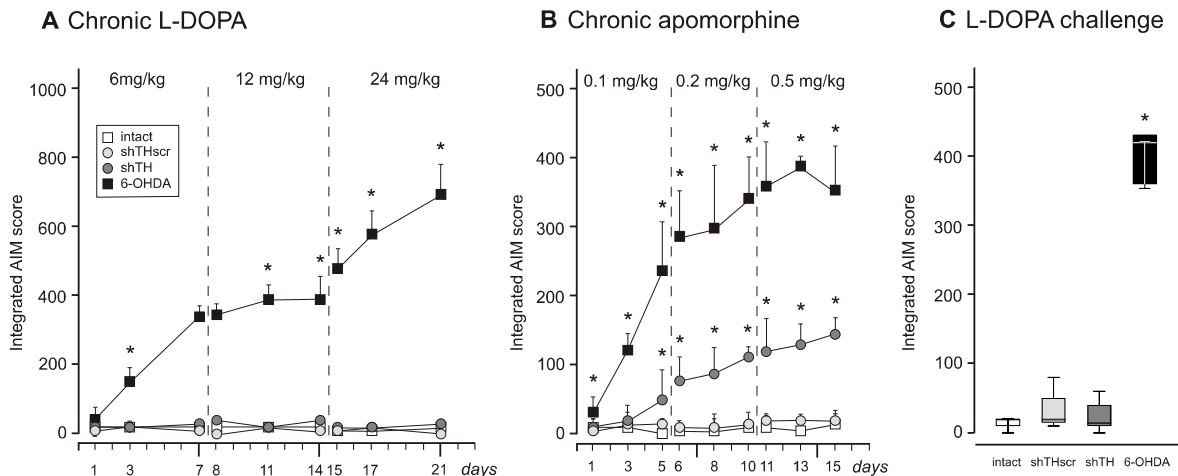


Figure 14

Chronic L-DOPA and apomorphine injections using a dose-escalating regimen to induce dyskinesia in control (intact and shTHscr) and treatment (shTH and 6-OHDA) groups. The animals were scored three times at each dose level for the development of AIMs. (A) The development of LID increases with increasing doses of L-DOPA over 21 days only in the 6-OHDA treatment group. (B) The induction of dyskinesia via DA receptor stimulation increases with increasing doses of apomorphine treatment in both the 6-OHDA and shTH treated groups. (C) Animals that were subjected to the apomorphine sensitization regimen were challenged with a single dose of 24 mg/kg L-DOPA (in combination with 10mg/kg benserazide). Data are shown as median values in □ all panels. In A and B, the error bars show 75% percentiles, whereas in C box plots mark the 50% percentiles and the whiskers indicate 95% percentiles. Statistical comparisons in A and B were performed using Friedman test, time effect $P < 0.0001$, group effect $P < 0.0001$. Individual comparisons in A, B, and C were performed by Kolmogorov-Smirnov test and P values were compensated for false discovery rates. *Different from intact and shTHscr controls.

Finally, we administered a single high dose of L-DOPA (24 mg/kg) in a subset of animals in the shTH and 6-OHDA treatment groups, which have been chronically treated with apomorphine and also exhibited clear dyskinetic behavior. Interestingly, all animals in the 6-OHDA group responded to L-DOPA with equally severity of the dyskinesia score, while no animals in the shTH group displayed any abnormal behavior (Figure 14C). In addition, these behavioral findings were validated with immunohistochemistry for FosB and c-fos, immediate early gene markers (See Paper I, Figure 5). These findings provided the evidence that presynaptic DA terminals retain the functional control of postsynaptic striatal neurons even after the establishment of dysplastic changes in these neurons and further showed that dyskinetic behavior could be reversed even after priming.

Postsynaptic differential receptor occupancy underlies LID (*Paper II*)

L-DOPA exerts its effect after conversion into DA by the AADC enzyme and this conversion occurs mainly in remaining dopaminergic terminals in early PD. As the disease progresses, more terminals become degenerated and this conversion shifts to other neuronal and non-neuronal compartments (Porrás *et al.*, 2014). One of the most critical AADC pool becomes 5-HT neurons, which share similar properties with DA neurons: not only for having AADC enzyme but also VMAT₂ transport protein (Carta *et al.*, 2007). This machinery of AADC/VMAT₂ enables 5-HT neurons to not only synthesize DA from exogenously administered L-DOPA but also to store it in vesicles. However, 5-HT terminals lack control mechanisms such as DAT and D₂R auto-receptors that causes uncontrolled release of DA towards the postsynaptic compartment. As such, it has been proposed that the uncontrolled rise of DA beyond physiological levels might be the reason for LID (Carta & Bezard, 2011; Navailles & De Deurwaerdere, 2011). Unfortunately however, there are not direct measurements tackling this question, and therefore the precise mechanisms are still not known. The aim of *Paper II* was to investigate the role of 5-HT terminals in the development of LID. The data was obtained from direct striatal measurements of DOPA and DA in the ECF using OMD and from analyses of DA receptor occupancy using PET imaging and in-vitro DA binding assay. After induction of LID in 6-OHDA lesioned rats upon daily i.p. injections L-DOPA (6 mg/kg, in combination with 10 mg/kg benserazide) for a period of 4 weeks, animals were transplanted either with DA-neuron rich or 5-HT-neuron-rich grafts. Two groups of animals kept as intact- and lesion-controls.

DA- and 5-HT-neuron-rich act as divergent both in histological features and in behavioral character

The transplantation of VM cells into the striatum allowed for the survival of numerous dopaminergic neurons and the re-innervation of the host striatal tissue (*See Figure 2C in Paper II*). These ‘DA-neuron-rich’ grafts included on the average, 5515±984 TH-positive cells as well as a smaller proportion of 5-HT positive neurons with a total estimate count of 1527 ±475 cells. The transplantation of more caudal tissue, however (Figure 7), gave rise to only 5-HT positive neurons with an average of 4169± 773 cells with no dopaminergic component. These ‘5-HT-neuron-rich’ grafts were able to form an intense supra-normal axon terminal network in the dorsal striatum, which was shown by SERT immunohistochemical staining (*See Paper II, Figure 2L*).

Behavioral characterization of the grafted animals showed that while 5-HT-neuron-rich grafts were ineffective in reversing motor deficit, DA-neuron-rich grafts improved limb use, as measured by the cylinder test, significantly at 12 weeks post transplantation (Figure 15A). In contrast, the challenge dose of L-DOPA in these previously primed dyskinetic animals resulted in a significant reduction in the AIMs scores with DA-neuron-rich grafts and 5-HT-neuron-rich grafts (Figure 15B). Co-treatment of the animals with 5-HT rec 1A and 1B agonists (0.1 mg/kg 8-OH-DPAT and 1.75 mg/kg CP-94253) reduced AIMs score significantly in all animals as previously shown (Carlsson *et al.*, 2007).

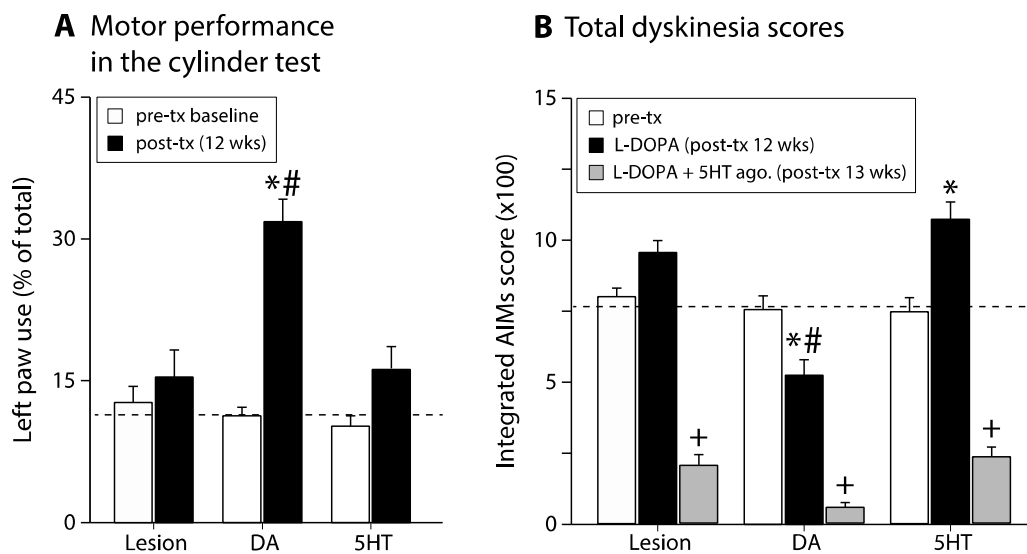


Figure 15 Behavioral characterization of the dyskinetic animals grafted with DA-rich or 5-HT-rich tissues. Motor performance evaluated by limb-use in cylinder test was improved only in the animals with DA-neuron-rich grafts ($p < 0.0083$) (A). In parallel, while DA-rich grafts were able to modulate LID with a significant reduction by 30.6%, 5-HT-neuron-rich grafts in contrast, were ineffective or even aggravated the AIMs by 43.7% ($p < 0.0033$) (B). Co-treatment with 5-HT rec 1A and 1B agonists reduced LID significantly in all groups.

Conversion of exogenously administered L-DOPA into DA occurs in other cellular compartments (e.g. 5-HT neurons) in degeneration of dopaminergic terminals

We performed an OMD protocol to measure extracellular levels of DA and 5-HT after KCl stimulation to demonstrate that a new releasable pool of DA would emerge following exogenous administration of L-DOPA in the denervated striatum, which would be increased even after in the 5-HT grafted animals. The KCl stimulation was done both prior to and 60 min after injection of 12 mg/kg L-DOPA (in combination with 10 mg/kg benserazide). This dose has been chosen on the basis of previous data showing that 12 mg/kg results in stable blood DOPA levels for at least three hours (Cederfjall *et al.*, 2012). We found that under baseline conditions 5-HT-neuron-rich grafts had none or a minimal releasable pool

of DA and this was not different compared to the 6-OHDA-lesion group (Figure 16). On the other hand, DA-neuron-rich grafts comprised a clearly notable releasable pool at about 10% of the capacity of the intact striatum. After L-DOPA administration, we detected a burst of DA in the 5-HT-grafted animals upon KCl challenge and the magnitude of DA released from 5-HT terminals were similar to that obtained from DA-neuron-rich grafts. This provided direct *in vivo* evidence that 5-HT terminals became an ectopic source for DA synthesis after L-DOPA administration. Interestingly, the L-DOPA challenge was effectively buffered in intact and DA-rich-grafted animals possibly by the efficient re-uptake in the presence of a dense DA terminal network in the vicinity of the serotonergic terminals.

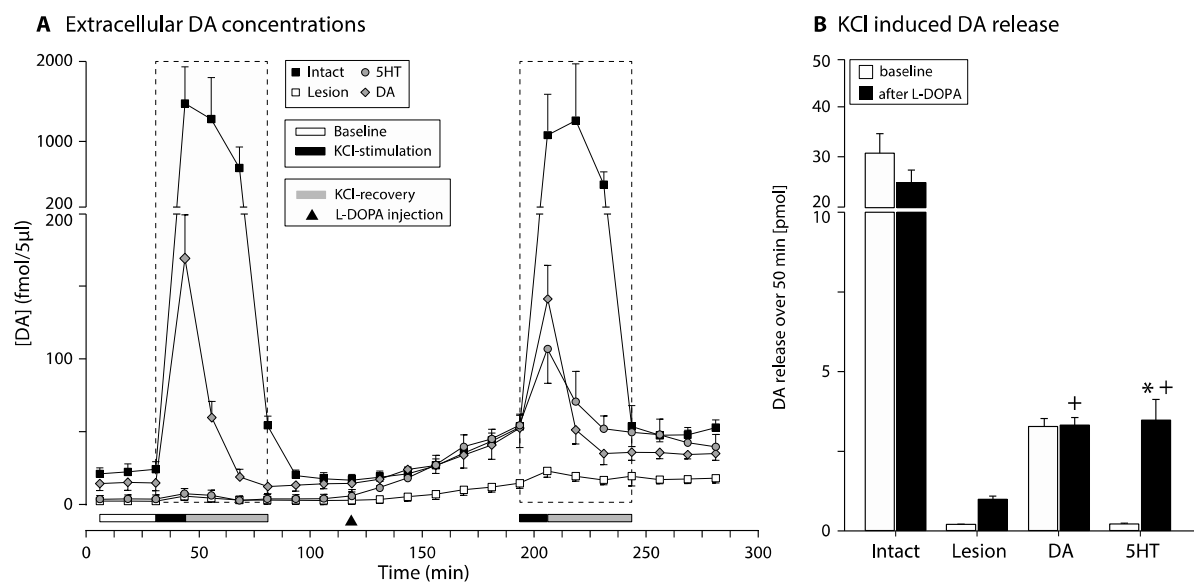


Figure 16 Quantification of the releasable pool of DA in baseline conditions and after systemic administration of 12 mg/kg L-DOPA (in combination with 10 mg/kg benserazide) showed that a new pool of DA release site emerged in the 5-HT grafted animals after L-DOPA challenge ($p < 0.001$).

DA released from serotonergic terminals does not reach supra-physiological levels

To investigate how extracellular DA levels were changed upon L-DOPA administrations in the absence of KCl challenge (i.e. under physiological conditions), we performed OMD in a group of awake and freely moving rats that were naïve to L-DOPA and evaluated AIMS simultaneously. As expected, both intact animals and DA-rich grafted rats were able to maintain stable DA with minimal changes upon L-DOPA challenge (Figure 17). On the contrary, the shift in DA levels was greater in 6-OHDA lesion group and 5-HT-neuron-rich grafted animals, but never reached supra-physiological levels. Intriguingly, these animals

were severely dyskinetic despite similar ECF DA levels compared to intact and DA-rich grafted animals. Taken together, there was no indication that supra-physiological DA levels underlie LID in the parkinsonian state.

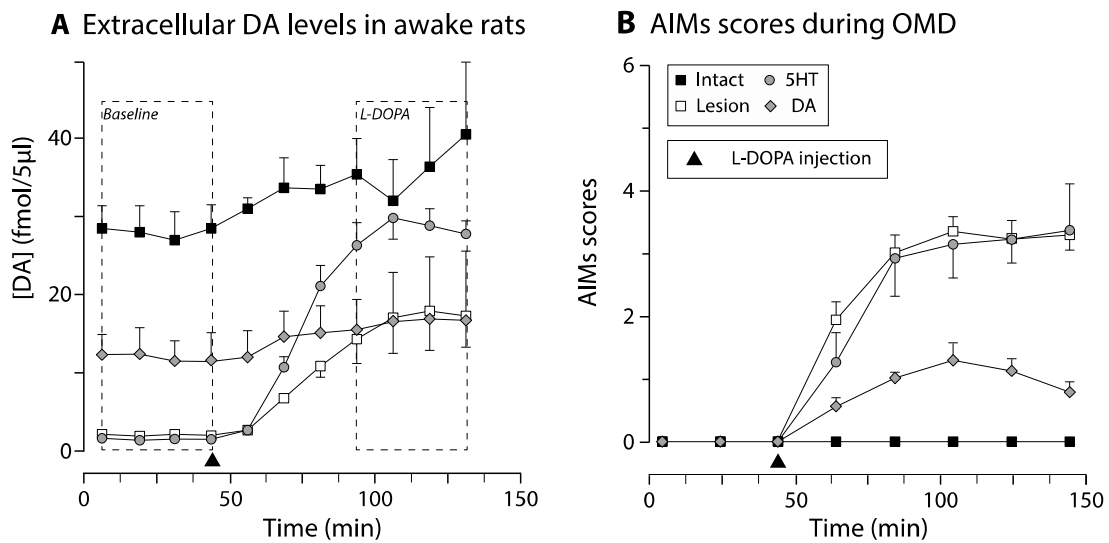


Figure 17
OMD (A) in baseline conditions before and after administration of L-DOPA in freely moving awake animals showed that dyskinesia (B) seen in 6-OHDA lesioned and 5-HT-grafted animals occur in the absence of supra-physiological DA levels in the striatum.

Differential DA receptor activation contributes to LID

To investigate whether DA released from serotonergic terminals resulted in abnormal receptor activation in the striatal neurons at the post-synaptic level, we studied DA receptors upon the administration of L-DOPA. The abnormal activation theory would be plausible based on so called ‘serotonin hypothesis’ suggesting that DA released from 5-HT terminals would be uncontrolled (Carlsson *et al.*, 2007). In addition, our KCl-challenge microdialysis experiments confirmed the emergence of a new pool of DA after L-DOPA-challenge, proving that the substrate for this abnormal release mechanism existed. However it is also important to note that the microdialysis experiment only shows extracellular DA diffusing in the extrasynaptic space and those taken up by the probe. Therefore, a different measurement modality was required to determine the level of activation of DA receptors. For this purpose, we used [^{18}F]fallypride PET imaging to estimate D_2R occupancy *in vivo* by calculating the BP before and after L-DOPA (Figure 18). In the absence of L-DOPA, animals with unilateral 6-OHDA lesions showed an increased BP compared to the contralateral intact side where DA from preserved terminals to the striatum competes with [^{18}F]fallypride. DA-neuron-rich grafts normalized this abnormally high BP. This suggested that grafted DA cells

were able to reconstitute normal DA signaling at the receptor site. As predicted, 5-HT-neuron-rich grafts lacked this ability under baseline conditions.

Administration of L-DOPA did not result in significant differences in the BP for 6-OHDA in lesion controls and DA-neuron-rich grafted animals. On the other hand, we had expected that L-DOPA administration would significantly alter BP in 5-HT-grafted animals because of the newly generated DA pool in the nigrostriatal terminals. However, we found that L-DOPA administration did not result any change in the BP in these animals (Figure 18). This finding supported the interpretation that DA released from 5-HT terminals resulted in low occupancy as a result of low DA concentrations at D2R containing sites. We have demonstrated that [¹⁸F]fallypride was displaceable upon DA release in additional experiments by using amphetamine challenge (See Paper II, Figure 8).

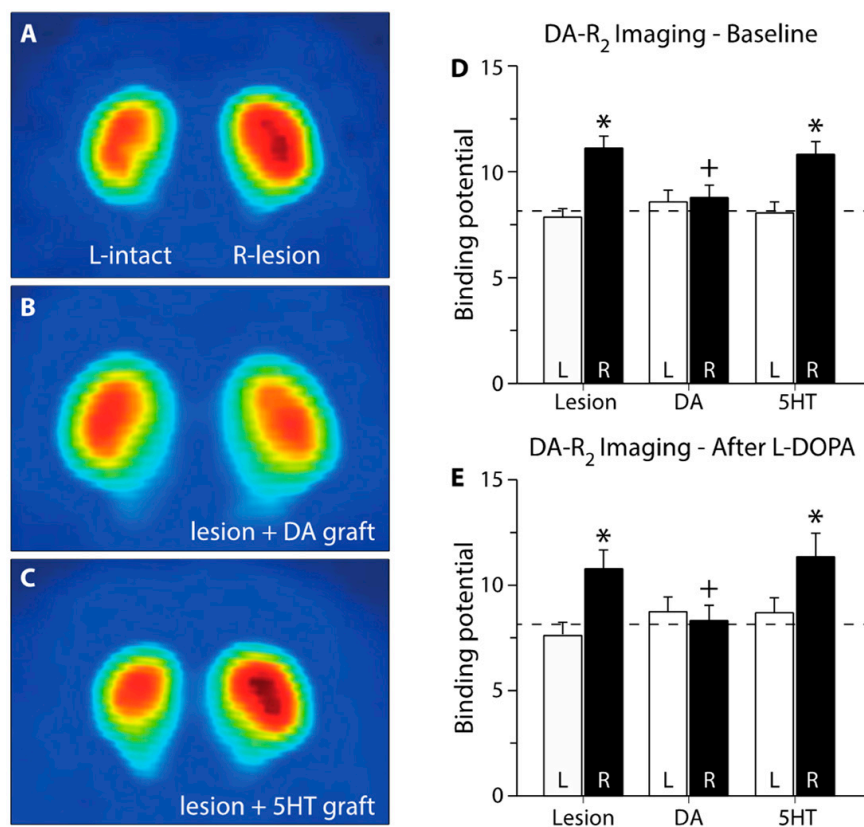


Figure 18

Assessment of striatal D₂R occupancy using PET imaging. A subset of animals (n = 28) were subjected to two [¹⁸F]fallypride PET imaging experiments between 4–7 months after grafting. The first examination was done under baseline conditions whereas the second one was performed starting 30 min after L-DOPA treatment. This radioligand binds to the D₂ receptors. The signal is increased when the endogenous ligand is lost, as seen in the 6-OHDA-lesion group under baseline conditions (A). The abnormally increased binding is completely normalized in DA grafted rats (B), but remained unchanged in the 5-HT-grafted animals (C). The imaging data was quantified using Logan plots to determine the BP in the striatal tissue (D; two-way ANOVA F(5,55) = 6.70, p,0.001; followed by pairwise comparison adjusted using Bonferroni, p,0.008). L-DOPA injection did not result in any change in the BP (E; two-way ANOVA F(5,55) = 3.15, p = 0.15). *: Different from intact side; +: different from 6-OHDA lesion group.

To further dissect DA receptor occupancy at sub-receptor level, we used *in vitro* receptor assays to directly determine K_d and B_{max} values for D_1R and D_2R by using [3H]SCH23390 and [3H]raclopride respectively (Figure 19). We used striatal tissue from intact and 6-OHDA lesioned rats killed either under baseline or 1-hr after L-DOPA injection using the peak dose for dyskinesia. The results showed that the primary site of activity for the newly synthesized DA was at the D_2R while no significant change occurred at the D_1R in the intact striatum. This suggested a selective activation of the D_2R by DA released from endogenous terminals. On the other hand, in the lesioned striatum where DA is released mainly from ectopic 5-HT terminals upon L-DOPA administration, no changes occurred at the D_2R site.

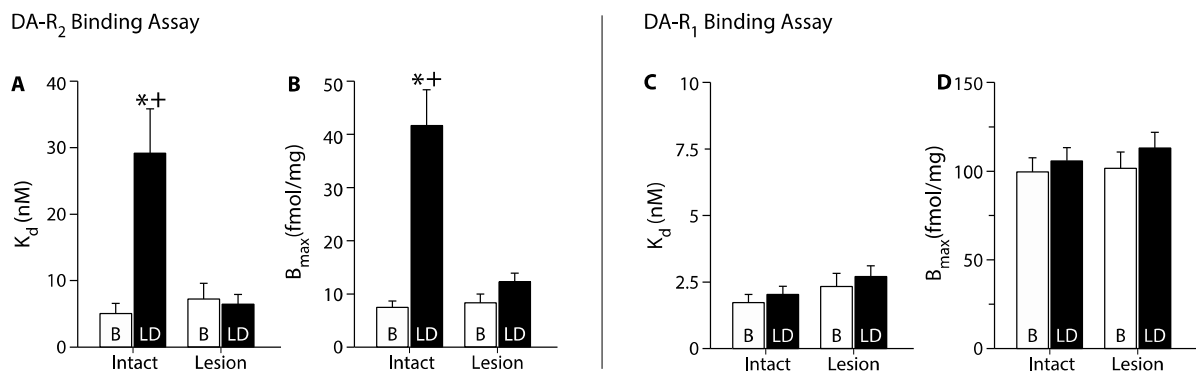


Figure 19

In vitro receptor binding assay was performed for D_2R (A,B) and D_1R (C,D) and analyzed using a generalized non-linear model. In panel A and B, post-hoc comparisons between B and LD in the D_2R in the intact brain is p , 0.001 for K_d and .002 for B_{max} , respectively and posthoc comparisons between LD injected intact and lesioned brains is p , 0.001 for K_d and .003 for B_{max} , respectively. L: left (intact) side, R: right side, B: Baseline; LD: L-DOPA treatment, K_d : binding affinity, B_{max} : Receptor density. *: Different from intact side; +: different from 6-OHDA lesion group.

BBB transport kinetics L-DOPA towards optimization of therapeutic and diagnostic use (*Paper III*)

L-DOPA is probably one of the most effective drugs that have ever been developed. Its mechanism of action is rather simple. It enters into the blood stream after its absorption from the intestines. The co-administration of AADC inhibitors (i.e. carbidopa or benserazide) blocks peripheral conversion to DA and thus allows L-DOPA to enter into the brain via the LAT1 transport protein (Kageyama *et al.*, 2000). In the early stages of PD, L-DOPA is taken up effectively, converted into DA, stored in the vesicles and released towards postsynaptic receptor sites in the nigrostriatal DA system. As the presynaptic neurodegeneration progresses, PD patients experience response fluctuations and abnormal involuntary movements, i.e. dyskinesia (Ahlskog & Muentner, 2001). Both pre- and postsynaptic mechanisms have been postulated to underlie LID. However, there is a clear lack

of knowledge regarding pharmacokinetics of L-DOPA especially transport kinetics through BBB and it is not possible to tailor the use of this drug in the clinical practice to overcome its long-term complications. Towards this end, we performed simultaneous measurements of L-DOPA, DA and their main metabolites such as 3-OMD, DOPAC and HVA in the blood and brain ECF via blood sampling and microdialysis respectively to better understand the biological variation in the response to L-DOPA administration in ten healthy rats (Figure 20). Such integrated data is pivotal to developing and utilizing learning algorithms to model the kinetics of BBB transport as it pertains to L-DOPA metabolism (*Paper III*).

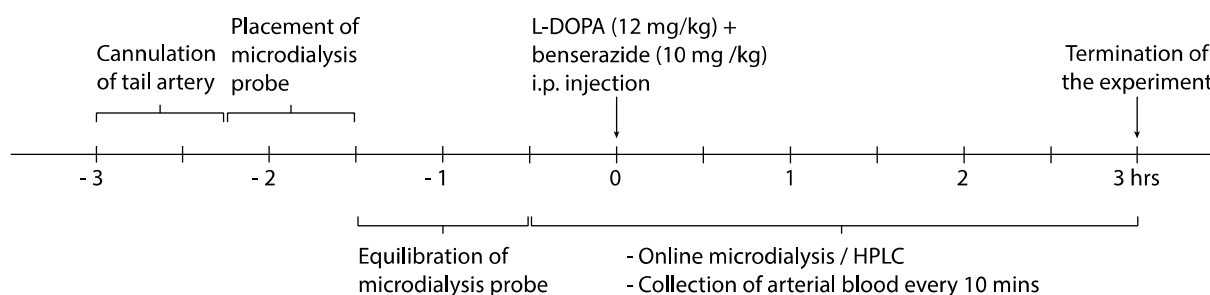


Figure 20
Experimental design of simultaneous blood sampling and OMD.

Blood and brain ECF levels of L-DOPA and its metabolites are correlated

Administration of 12 mg/kg L-DOPA (in combination with 10 mg/kg benserazide) led to an early peak in blood levels of DOPA that is followed by a steady decrease during the next 3 hours (Figure 21A). DOPA levels in the brain ECF, however, increased gradually over 2 hours (Figure 21B). The transport kinetics for the immediate product of L-DOPA, namely 3-OMD was different. It showed a continuous linear increase throughout the sampling (Figure 21A). This increase however, was sigmoidal shaped in the brain ECF and appeared after a 1-hour delay from the injection time point (Figure 21B).

The endpoint metabolite in the central DA metabolic pathway, HVA exhibited a similar pattern of increase in blood and brain ECF upon administration of L-DOPA, with the blood compartment shifting to the right in the time curve (Figure 21A, C). For the intermediary metabolite, DOPAC, a sigmoidal shaped increase with saturation around 2 hours was observed after L-DOPA administration (Figure 21C). It was not possible to reliably quantify blood levels of DOPAC in a robust and reproducible manner (Figure 21A). We also measured 5-HIAA, the metabolite of 5-HT metabolism, to examine whether the changes observed in our study were

specific for the DA metabolism pathway and showed that this did not change throughout the experiment (Figure 21C).

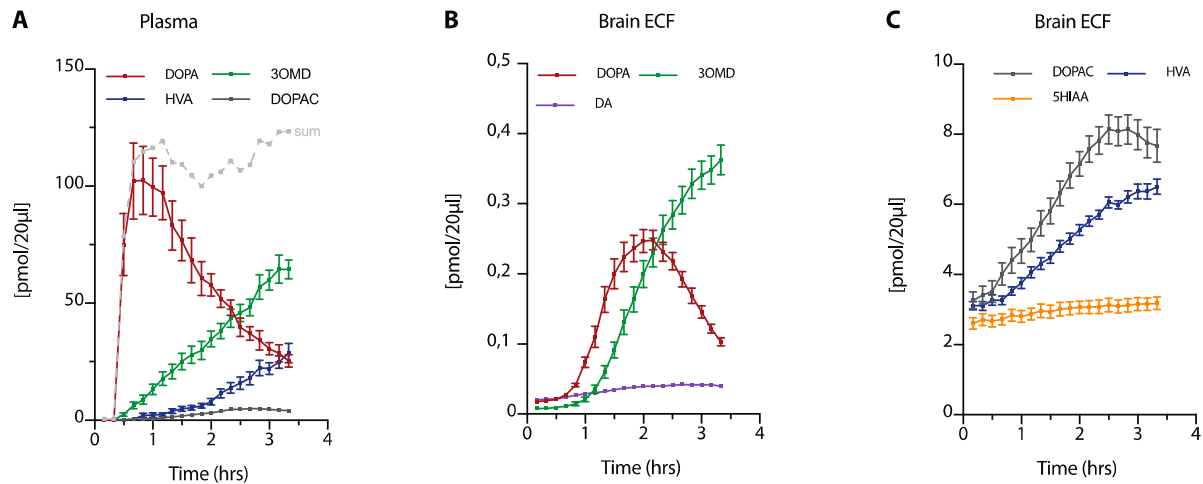


Figure 21

Blood and brain ECF levels of DOPA and its metabolites after systemic administration of 12 mg/kg L-DOPA (in combination with 10 mg/kg benserazide). While panel A displays blood levels, B and C panels depict the brain ECF levels of respective metabolites. In addition to L-DOPA and its metabolites, we measured 5-HIAA, the metabolite of 5-HT metabolism, for specificity of the experiment (C).

Brain ECF levels of DOPA and its metabolites predict low error rates by utilizing machine learning algorithms

We evaluated the performance of our model when different sets of input (blood) measurements were used to estimate the regression coefficients. For prediction of each of the three metabolites (DOPA, 3-OMD and HVA) where we measured both blood and ECF concentrations, we investigated the effects of using only the corresponding blood metabolite as the input, as well as using all the blood metabolites. In its simplest mode, i.e. prediction of brain levels of a given metabolite by using the blood data only from the same metabolite, we were able to predict the brain levels of a given metabolite with satisfactory estimations in some but not all cases as we found that this one-to-one pairing resulted in high errors (defined here as scaled RMSE values) and outliers. Examples of good predictions and over/under estimations are shown in Figure 22.

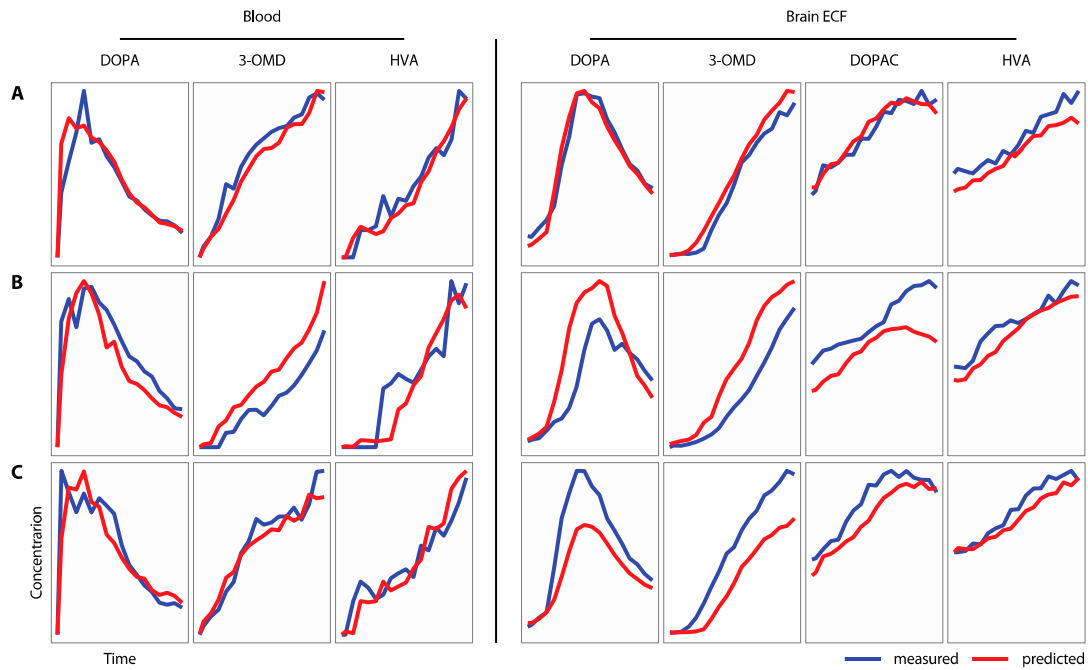


Figure 22

The figure displays the representative examples with accurate estimation (A), overestimation (B) and underestimation (C) of the DOPA (and other metabolite) levels in blood and brain ECF compartment.

Using blood data from the combination of all three metabolites, i.e., DOPA, 3-OMD and HVA, to predict the individual levels in the brain ECF gave better results than using single metabolites. This was evident in the improvement in the range of scaled RMSE values in all metabolites and by statistically significant in the group median values for HVA (Welch t test, $p=0,038$; Figure 23A). Moreover, the model performed a comparable prediction for DOPAC, even though its blood data was missing. Using the combination of all three metabolites as input function gave the best estimations compared to using only blood data of HVA (Figure 23B). Combining the error values across all metabolites and test animals showed the best performance when using blood data from all three metabolites as input function (Figure 23C).

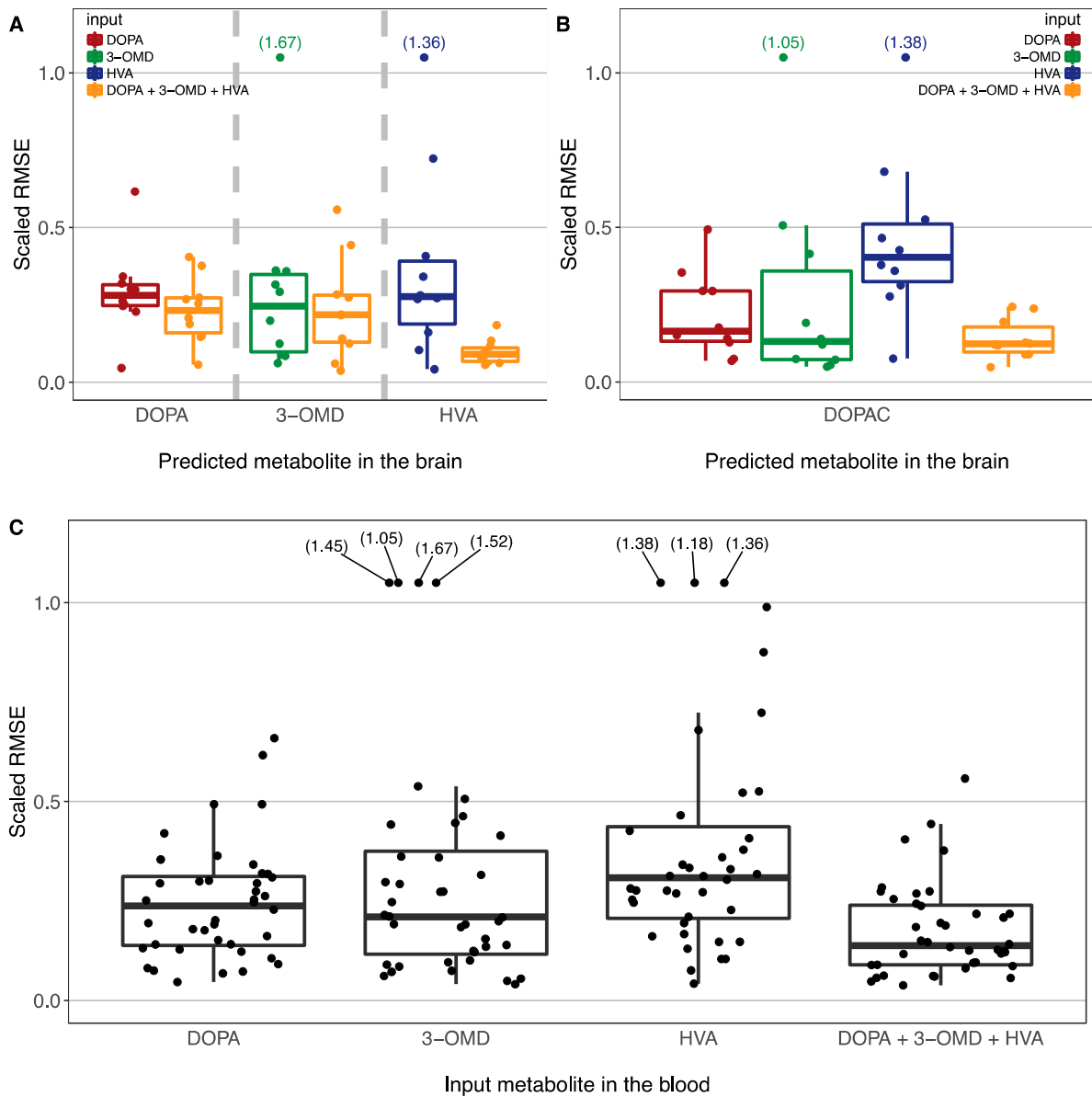


Figure 23

The figure depicts the performance of our predictive model with different input values and target ECF metabolites. (A) Scaled RMSE values for prediction of ECF DOPA, 3-OMD and HVA levels, using either the same metabolite or a combination of metabolites as input values. (B) Scaled RMSE values for prediction of ECF DOPAC levels, using either individual blood metabolites or a combination of DOPA, 3-OMD and HVA as input values. (C) Scaled RMSE values summarized for all ECF metabolites, using either individual blood metabolites or a combinations of DOPA, 3-OMD and HVA as input values. Scaled RMSE values above 1 are indicated in parentheses. (RMSE: Root mean squared error, lower values correspond to better performance).

Discussion and future directions

The most prominent feature of PD is the age-related and progressive degeneration of nigrostriatal dopaminergic neurons. This leads to a dopaminergic denervation, that gives rise to the cardinal motor symptoms (Dexter & Jenner, 2013). Moreover, serotonergic and noradrenergic neurotransmissions are also damaged during the course of the disease, causing non-motor problems (Schapira *et al.*, 2017). The DA deficit occurring as a consequence of dopaminergic degeneration could effectively be replaced by L-DOPA, thus making this drug a commander in the treatment of PD (You *et al.*, 2018). Other therapies such as MAO-B or COMT inhibitors and DA agonists play a less pivotal role. Every patient with PD will require the use of L-DOPA eventually. In spite of its proven efficacy, L-DOPA therapy comes with long-term problems in the form of response variations, motor fluctuations and involuntary movements. It has been argued that with the contemporary standards of the acceptable range of side effects, it is unlikely that L-DOPA would get an approval for clinical use today. Nevertheless, L-DOPA remains the most efficient drug in the treatment of PD at present and brings an obligation for the research community to better understand its mechanism of action not only on dopaminergic neurotransmission but also in other neuronal and non-neuronal compartments (i.e. serotonin neurons and glial cells respectively). This thesis work aims to study presynaptic (at both BBB-transport and dopaminergic-terminal level) and postsynaptic events coupled to L-DOPA therapy and provide new insights for future directions to both clinical and preclinical researchers.

Problems associated with L-DOPA therapy have been well studied though there are currently no available solutions to the problem: (1) Upon its administration via oral intake, it is taken up mostly in the small intestines. It has a rather erratic absorption, which contributes to the initial basis for response variation among individuals with PD. (2) Following this stage, L-DOPA is transferred into the blood stream with the help of a special transport protein, LAT1. Here comes the second problem in the form of competition with dietary proteins. (3) Peripheral conversion of L-DOPA into DA constitutes the third problem that DA itself cannot cross BBB because of its polar nature. Thus, we need to block AADC enzyme with additional drugs i.e. benserazide, carbidopa. (4) An additional problem here is the dosage of these blockers especially during the advanced phase of PD. Since there are ready formulation of L-DOPA and benserazide (or carbidopa) available

in the market, it will unlikely be possible to make fine adjustment of these blockers. It remains quite plausible that many patients take higher doses than required and the consequences of this have not been well studied. (5) L-DOPA then becomes an attractive substrate for COMT enzyme, which converts it to an inert metabolite, 3-OMD. This conversion takes place mainly in the liver and muscles. As a result only 10-15% of orally administered L-DOPA reaches the brain. (6) An additional problem that arises again is the competition of L-DOPA with these metabolites and blood proteins while being transferred across the BBB. It is the LAT1 transporter again which is responsible for the carriage into the brain. (7) When L-DOPA is in the brain, it is taken up both by neuronal (i.e., DA and 5-HT neurons as well as interneurons) and non-neuronal cells (i.e., astrocytes, glial cells, endothelial cells) where it could be converted to DA to finally reach the postsynaptic site where its actions are exerted. This conversion mainly occurs in DA neurons, however, as the dopaminergic degeneration progresses, it shifts to other cells. This could be implicative of a good phenomenon with the creation of a new pool of releasable DA. Unfortunately, the cells creating this pool lack release and uptake control mechanisms in addition to not making proper synapses so that DA could be concentrated to an extent where it can exert its action on the receptors. (8) As a result of this false neurotransmission, disabling motor fluctuations and dyskinesia develops because of peri-synaptic (both pre- and postsynaptic) mechanisms. In this chapter, all experimental outcomes are consolidated from this work and I will make a case for pre- and post-synaptic dysregulation of DA signaling in PD.

The relative contribution of the pre- vs. postsynaptic mechanisms in the induction and maintenance of LID is a central yet unresolved research question. This is important not only from the pathophysiological point of view but also for the development of new therapies towards this disabling clinical problem. There is data supporting involvement of both presynaptic and postsynaptic compartments. However, the difficulty lies in assessing the impact of individual compartment, which stems from the inability to dissociate the alterations induced by each part independently. Our approach of the functional TH knockdown (*Paper I*), i.e. viral vector-mediated long-term shTH expression, allowed us to generate a hypodopaminergic yet functional presynaptic compartment, creating changes attributed to the DA denervation on postsynaptic striatal cells. For comparison, we used the 6-OHDA-toxin model in which DA terminals were structurally destructed, leading to a combined pre- and postsynaptic dysfunction. Using the shTH model, we showed that chronic stimulation of postsynaptic D₁/D₂ receptors, by a direct DA agonist, apomorphine, induced AIMs while L-DOPA did not elicit any LID. Furthermore, we also showed that high-dose L-DOPA challenge failed to cause LID in the animals that were previously primed with chronic apomorphine administration. These observations were confirmed at the histological level with

immediate early gene activation. As a result, our data confirmed that the response of postsynaptic striatal neurons to the stimulation of DA receptors is controlled by presynaptic activity and thus the integrity of the presynaptic machinery determines the induction and the maintenance of LID. The clinical translation of this conclusion is that recovery of the presynaptic DA machinery by cell- or gene-based therapies can prevent or even reverse the development of LID in PD patients.

The nigrostriatal DA terminals provide a buffering capacity for exogenously administered L-DOPA and as such continuous dopaminergic stimulation without fluctuations of DA levels in the synaptic cleft. This is the likely mechanism by which cell-based therapies restore motor function and abolish dyskinesia (Winkler *et al.*, 2005). In contrast to animal studies, human trials however resulted in disabling graft-induced dyskinesia (GID) in PD patients (Freed *et al.*, 2001; Olanow *et al.*, 2003). Further research is required to unravel mechanisms of graft-induced dyskinesia. Unwanted contamination of 5-HT neurons in the grafts has been suggested as one of the mechanisms contributing to the GID. Our experimental model in *Paper II*, has allowed for the comparison of DA and 5-HT neurons with regards to the supply of a releasable DA pool, stimulation of postsynaptic receptors and reversing LID. We presented the first direct measurements proving that 5-HT terminals synthesize, store and release DA upon administration of L-DOPA, and thus providing an ectopic source of readily releasable DA pool in the parkinsonian state. However, in contrast to what has been proposed before, the extracellular DA levels measured by OMD never exceeded physiological concentrations seen in intact animals. Moreover, our PET experiments showed that *in vivo* D₂R occupancy in the striatum was not altered. This finding was in line with the behavioral findings in animals grafted with 5-HT neurons.

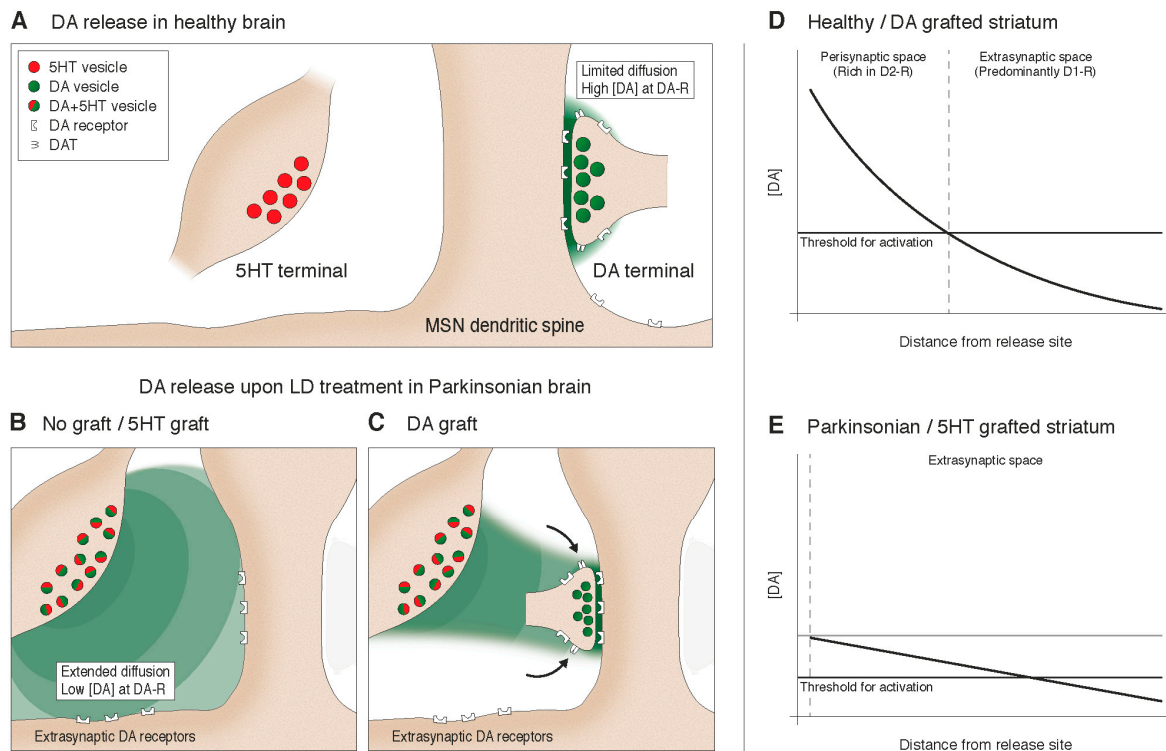


Figure 24

False DA neurotransmission via serotonergic terminals as a proposed mechanism for LID in the Parkinsonian brain. Healthy brain (A), as well as the DA graft (C), has the ability to release DA at high concentration at the synaptic site and control the spread by way of the uptake sites creating a sharp gradient in DA concentration (D). DA released from 5-HT terminals, however, results in not only a wider diffusion (B) but also fails to create the selectivity in the activation pattern leading to an abnormal dopaminergic signaling (E) (Figure from *Paper II*).

Complementary *in vitro* binding assays provided further data supporting our working hypothesis i.e. differential DA receptor occupancy underlies LID (Figure 24). This hypothesis proposes that in the intact brain (or DA-cell grafted striatum), DA release from the presynaptic site results in a sharp increase in synaptic DA concentrations and as such provides an appropriate stimulation of intra-synaptic receptors and limited diffusion of DA towards unwanted stimulation of receptors (i.e. D₁R) located far from the synaptic cleft. These receptors are supposed to be selectively activated after phasic discharges of DA under physiological conditions. On the other hand, DA originated from 5-HT terminals, does not reach to sufficient concentrations required to stimulate D₂R containing sites. Moreover, because of the lack of clearance mechanisms via DAT, DA diffuses to the extrasynaptic sites, thus providing continuous D₁R stimulation. Such abnormal stimulation of D₁R upon exogenous administration of L-DOPA has been linked to LID in previous studies (Dumartin *et al.*, 1998; Muriel *et al.*, 1999; Di Rocco & Werner, 2000; Dumartin *et al.*, 2000; Gonon *et al.*, 2000). A therapeutic method diminishing DA release from 5-HT terminals might be effective in decreasing

LID, however, in order to re-establish motor function, it is necessary to provide an additional pool of DA. This could successfully be achieved by enriching the dopaminergic terminal density especially in the denervated striatal regions that are highly innervated by 5-HT terminals.

Besides the abovementioned complex central pharmacodynamics, L-DOPA has also problematic peripheral pharmacokinetics partially underlying the motor complications attributed to its long-term use. In spite of tremendous data regarding peripheral metabolism of L-DOPA, direct measurements relating to BBB transport are limited. Such understanding would help us to better predict brain metabolism of L-DOPA with noninvasive techniques such as blood sampling. The last part of this thesis (*Paper III*) enlightens transport kinetics of L-DOPA upon exogenous administration in healthy rats with direct measurements of the main metabolites by using a special experimental setup where we simultaneously sampled blood and brain ECF to relate these two compartments. We have shown that our model provides a valuable tool to assess the BBB transport kinetics of L-DOPA under therapeutic administration conditions. One of the most important outcomes of this study was that one should take into account not only DOPA but also HVA, 3-OMD and DOPAC for predicting brain metabolism. This preclinical data is a good premise for a follow-up clinical study in PD patients to better understand L-DOPA metabolism and explain biological variations to predict L-DOPA related long-term complications in PD patients.

Acknowledgements

In this section, I would like to acknowledge people who have influenced my scientific formation and helped in one way or another in the delivery of this thesis. I studied Medicine together in the same years at Hacettepe University in Ankara with my supervisor Prof. Deniz Kirik, who chose to move Sweden during his medical studies. I chose to take a more conservative way and finish medical studies to become a specialist in neurology and finally to undertake a sub-specialization in movement disorders at my university. In spite of this quite ideal clinical career, I was always craving the need for doing research even from the early years during my residency training. All of a sudden, my paths crossed with Prof. Bülent Elibol. He was my mentor in many aspects, ranging from clinical to academic aspects; he guided me to better understand the complexities of life... I will never forget the evenings when we were sitting outside the lab after a long session of microscopy, looking at the stars in the sky in the middle of night and dreaming on publishing our results. I would cherish those moments forever in my life. I would also like to thank one additional professor, Turgay Dalkara, who developed our neuroscience unit at the Hacettepe University and turned it into a huge neuroscience institute. A quote from Prof. Dalkara that I always remember: ‘A good scientist is the one who tries to disprove his/her own hypothesis’.

Bülent and I kept following the studies performed by Deniz, and decided to contact him for a post-doc position in which I would have the possibility to do full-time research to satisfy my scientific curiosity. He replied instantly and accepted me to his lab without any hesitation. This opened a new chapter in my life: ‘Sweden’. Luckily, my wife also found a perfect lab for her further studies in HIV so with that; Sweden welcomed us as a family. The first thing that drew my attention about Deniz was that he never complained about being busy and working with him was like a charm. Besides juggling many collaborations with external people, he would always ensure that the lab was running smoothly. I think that the most outstanding feature of Deniz is that he knows all the techniques used in his lab to a level of perfection, regardless of whether it is related to advanced physics, imaging techniques, mathematics or analytical chemistry. I would like to extend my heartfelt gratitude to Deniz for accepting me to his lab, for all the scientific and para-scientific fruitful discussions and for being there whenever I needed guidance.

I would like to also acknowledge my co-supervisors, Prof Håkan Widner and Prof Per Odin. Besides his scientific guidance, Håkan introduced me to my current clinic in Hässleholm by contacting the neurologist, Magnus Esbjörnsson. I also owe a big thank you to Magnus for covering my absence at the clinic, so that I was able to complete the last part of my experiments and to write my thesis. Similarly, I am thankful to my immediate director Joakim Planck and our administrative task scheduler, Gunilla Juhlin, from Hässleholm hospital for facilitating my research.

Before going into scientific thanks, I should mention my friends that made my life colorful and joyful during my research career. Birgül, you are my lifetime sister, we have grown and walked the corridors of medical and research profession together. Gül, you will forever remain my student even when you become a professor in the near future. Being your mentor has been a real privilege and I am grateful for this opportunity. Sanaz, Erik and Rana, I hope that our synergy and thoughtfulness on each other will continue for the rest of our lives.

To work at the lab with the members of BRAINS and TNU has been enriching and collaborative. The support and companionship amongst you all made me never feel alone. I would like to thank you all, past and present members of these teams, with especial thanks to Ayse Ulusoy for introducing me to the lab and the work you've done in our shared paper. Manolo Carta for introducing me to the microdialysis field and teaching behavioral evaluations in rats. Charlotte Sonesson for shedding light to the dark labyrinth of mathematics in our studies. Erik Cederfjäll for our fruitful collaboration in our microdialysis studies, to Hélène Hall and Natalie Landeck for our blood sampling and microdialysis studies, to Rana Soyulu-Kucharz for her guidance in molecular techniques, to Sanaz Gabery for her assistance in stereology studies and to Rachel Cheong for all those excellent proof-reading that kept going 24/7.

I am also grateful to Åsa Petersen, Anna S Hansen, Barbara Baldo, Gabrielle Callander, Jo Beldring Henningsen, Kerstin Buck, Sandra Cuellar-Baena, Sofia Hult Lundh, Umar Sajjad. Special thanks to Jenny Månsson, Eva Nordin, Sara Freoul, Hülya Leeb-Lundberg for all things administrative, to Krzysztof Kucharz and Anders Mårtensson for helping me to find my way in the IT world, and to Priya Patel, Merve Özgür for allowing me to supervise you. I believe that Lund University's research success relies on the lab engineer-concept, which before I had arrived to Lund, was unfamiliar to me. I cannot thank enough Anneli Josefsson, Ulla Samuelsson, Ulrika Sparrhult-Björk, Ulrika Schagerlöf and Björn Anzelius, for their excellent guidance in my experiments.

The last but not the least, my mother, father and brother. You make my life meaningful. Your approval and pride gives me the motivation I need for everything that I do.

Babam; bana lise yıllarımda evden uzakta okurken yazdığın 'Yiğit Oğlum' başlıklı mektuplar hayatımın geri kalanına ışık tuttu. Senden hayat karşısında dik durmayı ve prensiplerime sonuna kadar bağlı kalmayı öğrendim. Annem; bana vicdanlı olmayı ve karşılıksız sevmeyi öğrettin. Sana layık bir evlat olmayı başarabildiysem ne mutlu bana. Abim, kardeşliğimiz can yoldaşlığına dönüştü. Hayatın zorluklarını göğüslerken seni her zaman yanımda hissettim. Üçünüz benim için arkamda yıkılmaz bir dağ gibisiniz.

Ada, you turned us into a family and Maya, you completed our family. The greatest privilege and happiness in my life is to see you both blossom. I hope that you continue to be happy throughout your lives and I want you to know that it will always be my highest duty to support you unconditionally.

Finally, to Gülşen. You are my soulmate. I am grateful for your endurance during the difficult times. Your sense of humor makes my life joyous. It is amazing to witness how you have evolved from a young and ambitious medical student to a competent professional and a loving mother throughout the years. This is the magic in life. I will forever love you.

References

- Abercrombie, E.D., Bonatz, A.E. & Zigmond, M.J. (1990) Effects of L-dopa on extracellular dopamine in striatum of normal and 6-hydroxydopamine-treated rats. *Brain research*, 525, 36-44.
- Adler, C.H., Singer, C., O'Brien, C., Hauser, R.A., Lew, M.F., Marek, K.L., Dorflinger, E., Pedder, S., Deptula, D. & Yoo, K. (1998) Randomized, placebo-controlled study of tolcapone in patients with fluctuating Parkinson disease treated with levodopa-carbidopa. Tolcapone Fluctuator Study Group III. *Archives of neurology*, 55, 1089-1095.
- Agnati, L.F., Fuxe, K., Zoli, M., Ozini, I., Toffano, G. & Ferraguti, F. (1986) A correlation analysis of the regional distribution of central enkephalin and beta-endorphin immunoreactive terminals and of opiate receptors in adult and old male rats. Evidence for the existence of two main types of communication in the central nervous system: the volume transmission and the wiring transmission. *Acta physiologica Scandinavica*, 128, 201-207.
- Ahlskog, J.E. & Muentner, M.D. (2001) Frequency of levodopa-related dyskinesias and motor fluctuations as estimated from the cumulative literature. *Movement disorders : official journal of the Movement Disorder Society*, 16, 448-458.
- Albanese, A., Altavista, M.C. & Rossi, P. (1986) Organization of central nervous system dopaminergic pathways. *Journal of neural transmission. Supplementum*, 22, 3-17.
- Albin, R.L., Young, A.B. & Penney, J.B. (1989) The functional anatomy of basal ganglia disorders. *Trends in neurosciences*, 12, 366-375.
- Aquino, C.C. & Fox, S.H. (2015) Clinical spectrum of levodopa-induced complications. *Movement disorders : official journal of the Movement Disorder Society*, 30, 80-89.
- Arai, R., Karasawa, N. & Nagatsu, I. (1996) Aromatic L-amino acid decarboxylase is present in serotonergic fibers of the striatum of the rat. A double-labeling immunofluorescence study. *Brain research*, 706, 177-179.
- Ballanger, B., Thobois, S., Baraduc, P., Turner, R.S., Broussolle, E. & Desmurget, M. (2006) "Paradoxical kinesia" is not a hallmark of Parkinson's disease but a general property of the motor system. *Movement disorders : official journal of the Movement Disorder Society*, 21, 1490-1495.
- Barger, G. & Dale, H.H. (1910) Chemical structure and sympathomimetic action of amines. *The Journal of physiology*, 41, 19-59.
- Baruzzi, A., Contin, M., Riva, R., Procaccianti, G., Albani, F., Tonello, C., Zoni, E. & Martinelli, P. (1987) Influence of meal ingestion time on pharmacokinetics of

- orally administered levodopa in parkinsonian patients. *Clinical neuropharmacology*, 10, 527-537.
- Birkmayer, W. (1969) [Experimental results of the combined treatment of parkinsonism using L-DOPA and a decarboxylase inhibitory agent (Ro 4-4602)]. *Wiener klinische Wochenschrift*, 81, 677-679.
- Birkmayer, W. & Hornykiewicz, O. (1998) The effect of l-3,4-dihydroxyphenylalanine (=DOPA) on akinesia in parkinsonism. *Parkinsonism & related disorders*, 4, 59-60.
- Birkmayer, W. & Hornykiewicz, O. (2001) The effect of l-3,4-dihydroxyphenylalanine (=DOPA) on akinesia in parkinsonism. 1961. *Wiener klinische Wochenschrift*, 113, 851-854.
- Björklund, A. & Lindvall, O. (1984) *Dopamine-containing systems in the CNS*. Elsevier, Amsterdam; Oxford.
- Blaschko, H. (1939) The specific actions of l-dopa decarboxylase. *The Journal of physiology*, 96, 50-51.
- Blaschko, H., Richter, D. & Schlossmann, H. (1937) The inactivation of adrenaline. *The Journal of physiology*, 90, 1-17.
- Bomasang-Layno, E., Fadlon, I., Murray, A.N. & Himelhoch, S. (2015) Antidepressive treatments for Parkinson's disease: A systematic review and meta-analysis. *Parkinsonism & related disorders*, 21, 833-842; discussion 833.
- Borgkvist, A., Lieberman, O.J. & Sulzer, D. (2018) Synaptic plasticity may underlie l-DOPA induced dyskinesia. *Current opinion in neurobiology*, 48, 71-78.
- Brown, P. & Marsden, C.D. (1998) What do the basal ganglia do? *Lancet*, 351, 1801-1804.
- Buddhala, C., Loftin, S.K., Kuley, B.M., Cairns, N.J., Campbell, M.C., Perlmutter, J.S. & Kotzbauer, P.T. (2015) Dopaminergic, serotonergic, and noradrenergic deficits in Parkinson disease. *Annals of clinical and translational neurology*, 2, 949-959.
- Burke, R.E. & O'Malley, K. (2013) Axon degeneration in Parkinson's disease. *Experimental neurology*, 246, 72-83.
- Cakmakli, G. & Topcuoglu, E. (2011) Bazal gangliyonların işlevsel anatomisi. In Elibol, B. (ed) *Hareket Bozuklukları*. Rotatip, pp. 19-30.
- Calabresi, P., Ghiglieri, V., Mazzocchi, P., Corbelli, I. & Picconi, B. (2015) Levodopa-induced plasticity: a double-edged sword in Parkinson's disease? *Philosophical transactions of the Royal Society of London. Series B, Biological sciences*, 370.
- Carlsson, A., Lindqvist, M. & Magnusson, T. (1957) 3,4-Dihydroxyphenylalanine and 5-hydroxytryptophan as reserpine antagonists. *Nature*, 180, 1200.
- Carlsson, T., Carta, M., Winkler, C., Björklund, A. & Kirik, D. (2007) Serotonin neuron transplants exacerbate L-DOPA-induced dyskinesias in a rat model of Parkinson's disease. *The Journal of neuroscience : the official journal of the Society for Neuroscience*, 27, 8011-8022.
- Carta, M. & Bezard, E. (2011) Contribution of pre-synaptic mechanisms to L-DOPA-induced dyskinesia. *Neuroscience*, 198, 245-251.

- Carta, M. & Bjorklund, A. (2018) The serotonergic system in L-DOPA-induced dyskinesia: pre-clinical evidence and clinical perspective. *Journal of neural transmission*.
- Carta, M., Carlsson, T., Kirik, D. & Bjorklund, A. (2007) Dopamine released from 5-HT terminals is the cause of L-DOPA-induced dyskinesia in parkinsonian rats. *Brain: a journal of neurology*, 130, 1819-1833.
- Carta, M. & Tronci, E. (2014) Serotonin System Implication in l-DOPA-Induced Dyskinesia: From Animal Models to Clinical Investigations. *Frontiers in neurology*, 5, 78.
- Cederfjall, E., Sahin, G. & Kirik, D. (2012) Key factors determining the efficacy of gene therapy for continuous DOPA delivery in the Parkinsonian brain. *Neurobiology of disease*, 48, 222-227.
- Cenci, M.A. (2007) Dopamine dysregulation of movement control in L-DOPA-induced dyskinesia. *Trends in neurosciences*, 30, 236-243.
- Cenci, M.A. & Lundblad, M. (2006) Post- versus presynaptic plasticity in L-DOPA-induced dyskinesia. *Journal of neurochemistry*, 99, 381-392.
- Chakravarthy, V.S., Joseph, D. & Bapi, R.S. (2010) What do the basal ganglia do? A modeling perspective. *Biological cybernetics*, 103, 237-253.
- Cotzias, G.C. (1968) L-Dopa for Parkinsonism. *The New England journal of medicine*, 278, 630.
- Cotzias, G.C., Van Woert, M.H. & Schiffer, L.M. (1967) Aromatic amino acids and modification of parkinsonism. *The New England journal of medicine*, 276, 374-379.
- Dahlstrom, A. & Fuxe, K. (1964) Localization of monoamines in the lower brain stem. *Experientia*, 20, 398-399.
- De Deurwaerdere, P., Ramsay, R.R. & Di Giovanni, G. (2017) Neurobiology and neuropharmacology of monoaminergic systems. *Progress in neurobiology*, 151, 1-3.
- de la Fuente-Fernandez, R., Sossi, V., Huang, Z., Furtado, S., Lu, J.Q., Calne, D.B., Ruth, T.J. & Stoessl, A.J. (2004) Levodopa-induced changes in synaptic dopamine levels increase with progression of Parkinson's disease: implications for dyskinesias. *Brain : a journal of neurology*, 127, 2747-2754.
- Del Sorbo, F. & Albanese, A. (2008) Levodopa-induced dyskinesias and their management. *Journal of neurology*, 255 Suppl 4, 32-41.
- DeLong, M. & Wichmann, T. (2009) Update on models of basal ganglia function and dysfunction. *Parkinsonism & related disorders*, 15 Suppl 3, S237-240.
- Dexter, D.T. & Jenner, P. (2013) Parkinson disease: from pathology to molecular disease mechanisms. *Free radical biology & medicine*, 62, 132-144.
- Di Rocco, A. & Werner, P. (2000) Levodopa induces a cytoplasmic localization of D1 dopamine receptors in striatal neurons in Parkinson's disease. *Annals of neurology*, 47, 136-137.

- Diamond, S.G. & Markham, C.H. (1990) Longitudinal study of effects of early levodopa treatment on disability and mortality in Parkinson's disease. *Advances in neurology*, 53, 399-403.
- Dumartin, B., Caille, I., Gonon, F. & Bloch, B. (1998) Internalization of D1 dopamine receptor in striatal neurons in vivo as evidence of activation by dopamine agonists. *The Journal of neuroscience : the official journal of the Society for Neuroscience*, 18, 1650-1661.
- Dumartin, B., Jaber, M., Gonon, F., Caron, M.G., Giros, B. & Bloch, B. (2000) Dopamine tone regulates D1 receptor trafficking and delivery in striatal neurons in dopamine transporter-deficient mice. *Proceedings of the National Academy of Sciences of the United States of America*, 97, 1879-1884.
- Ehringer, H. & Hornykiewicz, O. (1960) [Distribution of noradrenaline and dopamine (3-hydroxytyramine) in the human brain and their behavior in diseases of the extrapyramidal system]. *Klinische Wochenschrift*, 38, 1236-1239.
- Fabbrini, G., Brotchie, J.M., Grandas, F., Nomoto, M. & Goetz, C.G. (2007) Levodopa-induced dyskinesias. *Movement disorders : official journal of the Movement Disorder Society*, 22, 1379-1389; quiz 1523.
- Fahn, S. (2015) The medical treatment of Parkinson disease from James Parkinson to George Cotzias. *Movement disorders : official journal of the Movement Disorder Society*, 30, 4-18.
- Fahn, S., Oakes, D., Shoulson, I., Kieburtz, K., Rudolph, A., Lang, A., Olanow, C.W., Tanner, C., Marek, K. & Parkinson Study, G. (2004) Levodopa and the progression of Parkinson's disease. *The New England journal of medicine*, 351, 2498-2508.
- Fearnley, J.M. & Lees, A.J. (1991) Ageing and Parkinson's disease: substantia nigra regional selectivity. *Brain : a journal of neurology*, 114 (Pt 5), 2283-2301.
- Fibiger, H.C., Pudritz, R.E., McGeer, P.L. & McGeer, E.G. (1972) Axonal transport in nigro-striatal and nigro-thalamic neurons: effects of medial forebrain bundle lesions and 6-hydroxydopamine. *Journal of neurochemistry*, 19, 1697-1708.
- Floresco, S.B. (2015) The nucleus accumbens: an interface between cognition, emotion, and action. *Annual review of psychology*, 66, 25-52.
- Floresco, S.B., West, A.R., Ash, B., Moore, H. & Grace, A.A. (2003) Afferent modulation of dopamine neuron firing differentially regulates tonic and phasic dopamine transmission. *Nature neuroscience*, 6, 968-973.
- Fox, S.H. (2013) Non-dopaminergic treatments for motor control in Parkinson's disease. *Drugs*, 73, 1405-1415.
- Freed, C.R., Greene, P.E., Breeze, R.E., Tsai, W.Y., DuMouchel, W., Kao, R., Dillon, S., Winfield, H., Culver, S., Trojanowski, J.Q., Eidelberg, D. & Fahn, S. (2001) Transplantation of embryonic dopamine neurons for severe Parkinson's disease. *The New England journal of medicine*, 344, 710-719.
- Freitas, M.E. & Fox, S.H. (2016) Nondopaminergic treatments for Parkinson's disease: current and future prospects. *Neurodegenerative disease management*, 6, 249-268.

- Gonon, F. (1997) Prolonged and extrasynaptic excitatory action of dopamine mediated by D1 receptors in the rat striatum in vivo. *The Journal of neuroscience : the official journal of the Society for Neuroscience*, 17, 5972-5978.
- Gonon, F., Burie, J.B., Jaber, M., Benoit-Marand, M., Dumartin, B. & Bloch, B. (2000) Geometry and kinetics of dopaminergic transmission in the rat striatum and in mice lacking the dopamine transporter. *Progress in brain research*, 125, 291-302.
- Goto, Y. & Grace, A.A. (2005) Dopaminergic modulation of limbic and cortical drive of nucleus accumbens in goal-directed behavior. *Nature neuroscience*, 8, 805-812.
- Grace, A.A. (2000) The tonic/phasic model of dopamine system regulation and its implications for understanding alcohol and psychostimulant craving. *Addiction*, 95 Suppl 2, S119-128.
- Grace, A.A. & Bunney, B.S. (1984a) The control of firing pattern in nigral dopamine neurons: burst firing. *The Journal of neuroscience : the official journal of the Society for Neuroscience*, 4, 2877-2890.
- Grace, A.A. & Bunney, B.S. (1984b) The control of firing pattern in nigral dopamine neurons: single spike firing. *The Journal of neuroscience : the official journal of the Society for Neuroscience*, 4, 2866-2876.
- Greenacre, J.K., Coxon, A., Petrie, A. & Reid, J.L. (1976) Comparison of levodopa with carbidopa or benserazide in parkinsonism. *Lancet*, 2, 381-384.
- Grieder, T.E., George, O., Tan, H., George, S.R., Le Foll, B., Laviolette, S.R. & van der Kooy, D. (2012) Phasic D1 and tonic D2 dopamine receptor signaling double dissociate the motivational effects of acute nicotine and chronic nicotine withdrawal. *Proceedings of the National Academy of Sciences of the United States of America*, 109, 3101-3106.
- Group, P.D.M.C., Gray, R., Ives, N., Rick, C., Patel, S., Gray, A., Jenkinson, C., McIntosh, E., Wheatley, K., Williams, A. & Clarke, C.E. (2014) Long-term effectiveness of dopamine agonists and monoamine oxidase B inhibitors compared with levodopa as initial treatment for Parkinson's disease (PD MED): a large, open-label, pragmatic randomised trial. *Lancet*, 384, 1196-1205.
- Guggenheim, P. (1913) Dioxyphenylalanin, eine neue Aminosäure aus *Vicia faba*. *Zschr physiol Chem*, 88, 276-284.
- Guillot, T.S. & Miller, G.W. (2009) Protective actions of the vesicular monoamine transporter 2 (VMAT2) in monoaminergic neurons. *Molecular neurobiology*, 39, 149-170.
- Gundersen, H.J. & Jensen, E.B. (1987) The efficiency of systematic sampling in stereology and its prediction. *Journal of microscopy*, 147, 229-263.
- Heikkinen, H., Nutt, J.G., LeWitt, P.A., Koller, W.C. & Gordin, A. (2001) The effects of different repeated doses of entacapone on the pharmacokinetics of L-Dopa and on the clinical response to L-Dopa in Parkinson's disease. *Clinical neuropharmacology*, 24, 150-157.
- Hikida, T., Kimura, K., Wada, N., Funabiki, K. & Nakanishi, S. (2010) Distinct roles of synaptic transmission in direct and indirect striatal pathways to reward and aversive behavior. *Neuron*, 66, 896-907.
- Holtz, P. (1939) Dopadecarboxylase. *Naturwissenschaften*, 27, 724-725.

- Hommel, J.D., Sears, R.M., Georgescu, D., Simmons, D.L. & DiLeone, R.J. (2003) Local gene knockdown in the brain using viral-mediated RNA interference. *Nature medicine*, 9, 1539-1544.
- Hornykiewicz, O. (1958) The action of dopamine on the arterial blood pressure of the guinea-pig. *British journal of pharmacology and chemotherapy*, 13, 91-94.
- Hornykiewicz, O. (2002a) Dopamine miracle: from brain homogenate to dopamine replacement. *Movement disorders : official journal of the Movement Disorder Society*, 17, 501-508.
- Hornykiewicz, O. (2002b) L-DOPA: from a biologically inactive amino acid to a successful therapeutic agent. *Amino acids*, 23, 65-70.
- Hornykiewicz, O. (2010) A brief history of levodopa. *Journal of neurology*, 257, S249-252.
- Huot, P. & Fox, S.H. (2013) The serotonergic system in motor and non-motor manifestations of Parkinson's disease. *Experimental brain research*, 230, 463-476.
- Huot, P., Fox, S.H. & Brotchie, J.M. (2011) The serotonergic system in Parkinson's disease. *Progress in neurobiology*, 95, 163-212.
- Hyland, B.I., Reynolds, J.N., Hay, J., Perk, C.G. & Miller, R. (2002) Firing modes of midbrain dopamine cells in the freely moving rat. *Neuroscience*, 114, 475-492.
- Ikemoto, S., Yang, C. & Tan, A. (2015) Basal ganglia circuit loops, dopamine and motivation: A review and enquiry. *Behavioural brain research*, 290, 17-31.
- Iversen, S.D. & Iversen, L.L. (2007) Dopamine: 50 years in perspective. *Trends in Neurosciences*, 30, 188-193.
- Jankovic, J. (2008) Parkinson's disease: clinical features and diagnosis. *Journal of neurology, neurosurgery, and psychiatry*, 79, 368-376.
- Jansson, A., Descarries, L., Cornea-Hebert, V., Riad M, V., D., Bancila, M., Agnati, L. & Fuxe, K. (2002) *Transmitter-receptor mismatches in central dopamine, serotonin, and neuropeptide systems. Further evidence for volume transmission.* . Humana Press, Totowa, N.J.
- Kaakkola, S. (2000) Clinical pharmacology, therapeutic use and potential of COMT inhibitors in Parkinson's disease. *Drugs*, 59, 1233-1250.
- Kageyama, T., Nakamura, M., Matsuo, A., Yamasaki, Y., Takakura, Y., Hashida, M., Kanai, Y., Naito, M., Tsuruo, T., Minato, N. & Shimohama, S. (2000) The 4F2hc/LAT1 complex transports L-DOPA across the blood-brain barrier. *Brain research*, 879, 115-121.
- Karstaedt, P.J. & Pincus, J.H. (1992) Protein redistribution diet remains effective in patients with fluctuating parkinsonism. *Archives of neurology*, 49, 149-151.
- Kehr, J. & Karolinska (1999) *Modern Techniques in Neuroscience Research.*
- Kirik, D., Rosenblad, C. & Bjorklund, A. (1998) Characterization of behavioral and neurodegenerative changes following partial lesions of the nigrostriatal dopamine system induced by intrastriatal 6-hydroxydopamine in the rat. *Experimental neurology*, 152, 259-277.

- Koller, W., O'Hara, R., Weiner, W., Lang, A., Nutt, J., Agid, Y., Bonnet, A.M. & Jankovic, J. (1987) Relationship of aging to Parkinson's disease. *Advances in neurology*, 45, 317-321.
- Kopin, I.J. (1985) Catecholamine metabolism: basic aspects and clinical significance. *Pharmacological reviews*, 37, 333-364.
- Kurlan, R. (2005) "Levodopa phobia": a new iatrogenic cause of disability in Parkinson disease. *Neurology*, 64, 923-924.
- Kurlan, R., Rubin, A.J., Miller, C., Rivera-Calimlim, L., Clarke, A. & Shoulson, I. (1986) Duodenal delivery of levodopa for on-off fluctuations in parkinsonism: preliminary observations. *Annals of neurology*, 20, 262-265.
- Lang, A.E. (2007) The progression of Parkinson disease: a hypothesis. *Neurology*, 68, 948-952.
- Lang, A.E. & Marras, C. (2014) Initiating dopaminergic treatment in Parkinson's disease. *Lancet*, 384, 1164-1166.
- Lee, J., Zhu, W.M., Stanic, D., Finkelstein, D.I., Horne, M.H., Henderson, J., Lawrence, A.J., O'Connor, L., Tomas, D., Drago, J. & Horne, M.K. (2008) Sprouting of dopamine terminals and altered dopamine release and uptake in Parkinsonian dyskinesia. *Brain : a journal of neurology*, 131, 1574-1587.
- Leenders, K.L., Poewe, W.H., Palmer, A.J., Brenton, D.P. & Frackowiak, R.S. (1986) Inhibition of L-[18F]fluorodopa uptake into human brain by amino acids demonstrated by positron emission tomography. *Annals of neurology*, 20, 258-262.
- Lees, A. (2017) An essay on the shaking palsy. *Brain : a journal of neurology*, 140, 843-848.
- LeWitt, P.A. (2015) Levodopa therapy for Parkinson's disease: Pharmacokinetics and pharmacodynamics. *Movement disorders : official journal of the Movement Disorder Society*, 30, 64-72.
- Lindgren, H.S., Andersson, D.R., Lagerkvist, S., Nissbrandt, H. & Cenci, M.A. (2010) L-DOPA-induced dopamine efflux in the striatum and the substantia nigra in a rat model of Parkinson's disease: temporal and quantitative relationship to the expression of dyskinesia. *Journal of neurochemistry*, 112, 1465-1476.
- Lindgren, N., Xu, Z.Q., Herrera-Marschitz, M., Haycock, J., Hokfelt, T. & Fisone, G. (2001) Dopamine D(2) receptors regulate tyrosine hydroxylase activity and phosphorylation at Ser40 in rat striatum. *The European journal of neuroscience*, 13, 773-780.
- Lindvall, O. & Bjorklund, A. (1974) The organization of the ascending catecholamine neuron systems in the rat brain as revealed by the glyoxylic acid fluorescence method. *Acta physiologica Scandinavica. Supplementum*, 412, 1-48.
- Lindvall, O., Bjorklund, A. & Skagerberg, G. (1984) Selective histochemical demonstration of dopamine terminal systems in rat di- and telencephalon: new evidence for dopaminergic innervation of hypothalamic neurosecretory nuclei. *Brain research*, 306, 19-30.

- Lloyd, K.G., Davidson, L. & Hornykiewicz, O. (1975) The neurochemistry of Parkinson's disease: effect of L-dopa therapy. *The Journal of pharmacology and experimental therapeutics*, 195, 453-464.
- Mannisto, P.T. & Kaakkola, S. (1989) New selective COMT inhibitors: useful adjuncts for Parkinson's disease? *Trends in pharmacological sciences*, 10, 54-56.
- Markham, C., Diamond, S.G. & Treciokas, L.J. (1974) Carbidopa in Parkinson disease and in nausea and vomiting of levodopa. *Archives of neurology*, 31, 128-133.
- Marsden, C.D. (1990) Parkinson's disease. *Lancet*, 335, 948-952.
- Marsden, C.D. & Obeso, J.A. (1994) The functions of the basal ganglia and the paradox of stereotaxic surgery in Parkinson's disease. *Brain : a journal of neurology*, 117 (Pt 4), 877-897.
- Melamed, E., Hefti, F., Pettibone, D.J., Liebman, J. & Wurtman, R.J. (1981) Aromatic L-amino acid decarboxylase in rat corpus striatum: implications for action of L-dopa in parkinsonism. *Neurology*, 31, 651-655.
- Melamed, E., Ziv, I. & Djaldetti, R. (2007) Management of motor complications in advanced Parkinson's disease. *Movement disorders : official journal of the Movement Disorder Society*, 22 Suppl 17, S379-384.
- Migueluez, C., Benazzouz, A., Ugedo, L. & De Deurwaerdere, P. (2017) Impairment of Serotonergic Transmission by the Antiparkinsonian Drug L-DOPA: Mechanisms and Clinical Implications. *Frontiers in cellular neuroscience*, 11, 274.
- Mink, J.W. (1996) The basal ganglia: focused selection and inhibition of competing motor programs. *Progress in neurobiology*, 50, 381-425.
- Mirenowicz, J. & Schultz, W. (1996) Preferential activation of midbrain dopamine neurons by appetitive rather than aversive stimuli. *Nature*, 379, 449-451.
- Montagu, K.A. (1957) Catechol compounds in rat tissues and in brains of different animals. *Nature*, 180, 244-245.
- Mosharov, E.V., Borgkvist, A. & Sulzer, D. (2015) Presynaptic effects of levodopa and their possible role in dyskinesia. *Movement disorders : official journal of the Movement Disorder Society*, 30, 45-53.
- Mura, A., Jackson, D., Manley, M.S., Young, S.J. & Groves, P.M. (1995) Aromatic L-amino acid decarboxylase immunoreactive cells in the rat striatum: a possible site for the conversion of exogenous L-DOPA to dopamine. *Brain research*, 704, 51-60.
- Muriel, M.P., Bernard, V., Levey, A.I., Laribi, O., Abrous, D.N., Agid, Y., Bloch, B. & Hirsch, E.C. (1999) Levodopa induces a cytoplasmic localization of D1 dopamine receptors in striatal neurons in Parkinson's disease. *Annals of neurology*, 46, 103-111.
- Nagatsu, T., Levitt, M. & Udenfriend, S. (1964) Tyrosine Hydroxylase. The Initial Step in Norepinephrine Biosynthesis. *The Journal of biological chemistry*, 239, 2910-2917.
- Navailles, S. & De Deurwaerdere, P. (2011) Presynaptic control of serotonin on striatal dopamine function. *Psychopharmacology*, 213, 213-242.

- Nicola, S.M., Surmeier, J. & Malenka, R.C. (2000) Dopaminergic modulation of neuronal excitability in the striatum and nucleus accumbens. *Annual review of neuroscience*, 23, 185-215.
- Nutt, J.G. & Fellman, J.H. (1984) Pharmacokinetics of levodopa. *Clinical neuropharmacology*, 7, 35-49.
- Nutt, J.G., Woodward, W.R., Beckner, R.M., Stone, C.K., Berggren, K., Carter, J.H., Gancher, S.T., Hammerstad, J.P. & Gordin, A. (1994) Effect of peripheral catechol-O-methyltransferase inhibition on the pharmacokinetics and pharmacodynamics of levodopa in parkinsonian patients. *Neurology*, 44, 913-919.
- Nyholm, D. (2006) Enteral levodopa/carbidopa gel infusion for the treatment of motor fluctuations and dyskinesias in advanced Parkinson's disease. *Expert review of neurotherapeutics*, 6, 1403-1411.
- Nyholm, D., Lewander, T., Johansson, A., Lewitt, P.A., Lundqvist, C. & Aquilonius, S.M. (2008) Enteral levodopa/carbidopa infusion in advanced Parkinson disease: long-term exposure. *Clinical neuropharmacology*, 31, 63-73.
- Ohno, Y., Shimizu, S., Tokudome, K., Kunisawa, N. & Sasa, M. (2015) New insight into the therapeutic role of the serotonergic system in Parkinson's disease. *Progress in neurobiology*, 134, 104-121.
- Olanow, C.W. (2009) Can we achieve neuroprotection with currently available anti-parkinsonian interventions? *Neurology*, 72, S59-64.
- Olanow, C.W. (2015) Levodopa: effect on cell death and the natural history of Parkinson's disease. *Movement disorders : official journal of the Movement Disorder Society*, 30, 37-44.
- Olanow, C.W., Agid, Y., Mizuno, Y., Albanese, A., Bonuccelli, U., Damier, P., De Yebenes, J., Gershanik, O., Guttman, M., Grandas, F., Hallett, M., Hornykiewicz, O., Jenner, P., Katzenschlager, R., Langston, W.J., LeWitt, P., Melamed, E., Mena, M.A., Michel, P.P., Mytilineou, C., Obeso, J.A., Poewe, W., Quinn, N., Raisman-Vozari, R., Rajput, A.H., Rascol, O., Sampaio, C. & Stocchi, F. (2004) Levodopa in the treatment of Parkinson's disease: current controversies. *Movement disorders : official journal of the Movement Disorder Society*, 19, 997-1005.
- Olanow, C.W., Goetz, C.G., Kordower, J.H., Stoessl, A.J., Sossi, V., Brin, M.F., Shannon, K.M., Nauert, G.M., Perl, D.P., Godbold, J. & Freeman, T.B. (2003) A double-blind controlled trial of bilateral fetal nigral transplantation in Parkinson's disease. *Annals of neurology*, 54, 403-414.
- Olanow, C.W., Kieburtz, K., Odin, P., Espay, A.J., Standaert, D.G., Fernandez, H.H., Vanaganas, A., Othman, A.A., Widnell, K.L., Robieson, W.Z., Pritchett, Y., Chatamra, K., Benesh, J., Lenz, R.A., Antonini, A. & Group, L.H.S. (2014) Continuous intrajejunal infusion of levodopa-carbidopa intestinal gel for patients with advanced Parkinson's disease: a randomised, controlled, double-blind, double-dummy study. *The Lancet. Neurology*, 13, 141-149.
- Olanow, C.W. & Obeso, J.A. (2011) Levodopa toxicity and Parkinson disease: still a need for equipoise. *Neurology*, 77, 1416-1417.

- Olanow, C.W., Watts, R.L. & Koller, W.C. (2001) An algorithm (decision tree) for the management of Parkinson's disease (2001): treatment guidelines. *Neurology*, 56, S1-S88.
- Parkinson Study, G. (2002) Dopamine transporter brain imaging to assess the effects of pramipexole vs levodopa on Parkinson disease progression. *Jama*, 287, 1653-1661.
- Parkkinen, L., O'Sullivan, S.S., Kuoppamaki, M., Collins, C., Kallis, C., Holton, J.L., Williams, D.R., Revesz, T. & Lees, A.J. (2011) Does levodopa accelerate the pathologic process in Parkinson disease brain? *Neurology*, 77, 1420-1426.
- Pattij, T. & Vanderschuren, L.J. (2008) The neuropharmacology of impulsive behaviour. *Trends in pharmacological sciences*, 29, 192-199.
- Pavese, N., Evans, A.H., Tai, Y.F., Hotton, G., Brooks, D.J., Lees, A.J. & Piccini, P. (2006) Clinical correlates of levodopa-induced dopamine release in Parkinson disease: a PET study. *Neurology*, 67, 1612-1617.
- Paxinos, G., Watson, C. & Paxinos, G. (2007) *The rat brain in stereotaxic coordinates*. Elsevier Academic Press, Amsterdam ; Boston.
- Peter, D., Liu, Y., Sternini, C., de Giorgio, R., Brecha, N. & Edwards, R.H. (1995) Differential expression of two vesicular monoamine transporters. *The Journal of neuroscience : the official journal of the Society for Neuroscience*, 15, 6179-6188.
- Pickel, V.M., Nirenberg, M.J. & Milner, T.A. (1996) Ultrastructural view of central catecholaminergic transmission: immunocytochemical localization of synthesizing enzymes, transporters and receptors. *Journal of neurocytology*, 25, 843-856.
- Politis, M. & Niccolini, F. (2015) Serotonin in Parkinson's disease. *Behavioural brain research*, 277, 136-145.
- Porras, G., De Deurwaerdere, P., Li, Q., Marti, M., Morgenstern, R., Sohr, R., Bezard, E., Morari, M. & Meissner, W.G. (2014) L-dopa-induced dyskinesia: beyond an excessive dopamine tone in the striatum. *Scientific reports*, 4, 3730.
- Quinn, N., Parkes, D., Janota, I. & Marsden, C.D. (1986) Preservation of the substantia nigra and locus coeruleus in a patient receiving levodopa (2 kg) plus decarboxylase inhibitor over a four-year period. *Movement disorders : official journal of the Movement Disorder Society*, 1, 65-68.
- Rajput, A.H. (2001) Levodopa prolongs life expectancy and is non-toxic to substantia nigra. *Parkinsonism & related disorders*, 8, 95-100.
- Ramsey, A.J. & Fitzpatrick, P.F. (2000) Effects of phosphorylation on binding of catecholamines to tyrosine hydroxylase: specificity and thermodynamics. *Biochemistry*, 39, 773-778.
- Sahin, G. & Kirik, D. (2012) Efficacy of L-DOPA therapy in Parkinson's disease. In D'Mello, J.P.F. (ed) *Amino Acids in Human Nutrition and Health*.
- Sames, D., Dunn, M., Karpowicz, R.J., Jr. & Sulzer, D. (2013) Visualizing neurotransmitter secretion at individual synapses. *ACS chemical neuroscience*, 4, 648-651.

- Schapira, A.H.V., Chaudhuri, K.R. & Jenner, P. (2017) Non-motor features of Parkinson disease. *Nature reviews. Neuroscience*, 18, 435-450.
- Shaw, K.N., McMillan, A. & Armstrong, M.D. (1957) The metabolism of 3, 4-dihydroxyphenylalanine. *The Journal of biological chemistry*, 226, 255-266.
- Shepherd, D.M. & West, G.B. (1952) Hydroxytyramine (dopamine) and the suprarenal medulla. *The Journal of physiology*, 117, 67P-68P.
- Shutov, A.A. & Dondova, A.I. (2008) [Involvement of serotonergic system in the pathogenesis of non-motor symptoms of Parkinson's disease]. *Zhurnal neurologii i psikiatrii imeni S.S. Korsakova*, 108, 67-71.
- Spruill, W., Wade, W., DiPiro, J., Blouin, R. & Pruemer, J. (2014) Introduction to pharmacokinetics and pharmacokinetics *Concepts in Clinical Pharmacokinetics*. American Society of Health-System Pharmacists.
- Stayte, S. & Vissel, B. (2014) Advances in non-dopaminergic treatments for Parkinson's disease. *Frontiers in neuroscience*, 8, 113.
- Stocchi, F., Vacca, L., Ruggieri, S. & Olanow, C.W. (2005) Intermittent vs continuous levodopa administration in patients with advanced Parkinson disease: a clinical and pharmacokinetic study. *Archives of neurology*, 62, 905-910.
- Svenningsson, P., Rosenblad, C., Af Edholm Arvidsson, K., Wictorin, K., Keywood, C., Shankar, B., Lowe, D.A., Bjorklund, A. & Widner, H. (2015) Eltoprazine counteracts l-DOPA-induced dyskinesias in Parkinson's disease: a dose-finding study. *Brain : a journal of neurology*, 138, 963-973.
- T., H., M., M., A., B., S., K. & M., G. (1984) *Handbook of chemical neuroanatomy. Classical transmitters in the CNS, Part 1 Vol. 2 Vol. 2*.
- Thorre, K., Pravda, M., Sarre, S., Ebinger, G. & Michotte, Y. (1997) New antioxidant mixture for long term stability of serotonin, dopamine and their metabolites in automated microbore liquid chromatography with dual electrochemical detection. *Journal of chromatography. B, Biomedical sciences and applications*, 694, 297-303.
- Tokcaer, A. (2011) Hareket bozukluklarının patofizyolojisi. In Elibol, B. (ed) *Hareket bozukluklari*. Rotatip, pp. 31-41.
- Ulusoy, A., Sahin, G., Bjorklund, T., Aebischer, P. & Kirik, D. (2009) Dose optimization for long-term rAAV-mediated RNA interference in the nigrostriatal projection neurons. *Molecular therapy : the journal of the American Society of Gene Therapy*, 17, 1574-1584.
- Villalba, R.M., Mathai, A. & Smith, Y. (2015) Morphological changes of glutamatergic synapses in animal models of Parkinson's disease. *Frontiers in neuroanatomy*, 9, 117.
- Wade, D.N., Mearrick, P.T. & Morris, J.L. (1973) Active transport of L-dopa in the intestine. *Nature*, 242, 463-465.
- Wang, Q. & Zhang, W. (2016) Maladaptive Synaptic Plasticity in L-DOPA-Induced Dyskinesia. *Frontiers in neural circuits*, 10, 105.

- Waser, E. & Lewandowski, M. (1921) Untersuchungen in der Phenylalanin - Reihe I. Synthese des 1-3,4-Dioxy-phenylalanins (Studies on the phenylalanine series I. Synthesis of L-3,4-dihydroxyphenylalanine). *Helv chim Acta*, 4, 657-666.
- Weil-Malherbe, H. & Bone, A.D. (1957) Intracellular distribution of catecholamines in the brain. *Nature*, 180, 1050-1051.
- Weiner, W.J. & Reich, S.G. (2008) Agonist or levodopa for Parkinson disease?: ultimately, it doesn't matter; neither is good enough. *Neurology*, 71, 470-471.
- Whone, A.L., Watts, R.L., Stoessl, A.J., Davis, M., Reske, S., Nahmias, C., Lang, A.E., Rascol, O., Ribeiro, M.J., Remy, P., Poewe, W.H., Hauser, R.A., Brooks, D.J. & Group, R.-P.S. (2003) Slower progression of Parkinson's disease with ropinirole versus levodopa: The REAL-PET study. *Annals of neurology*, 54, 93-101.
- Wichmann, T. & DeLong, M.R. (2007) Anatomy and physiology of the basal ganglia: relevance to Parkinson's disease and related disorders. *Handbook of clinical neurology*, 83, 1-18.
- Williams, S.M. & Goldman-Rakic, P.S. (1998) Widespread origin of the primate mesofrontal dopamine system. *Cerebral cortex (New York, N.Y. : 1991)*, 8, 321-345.
- Wimalasena, K. (2011) Vesicular monoamine transporters: structure-function, pharmacology, and medicinal chemistry. *Medicinal research reviews*, 31, 483-519.
- Winkler, C., Kirik, D. & Bjorklund, A. (2005) Cell transplantation in Parkinson's disease: how can we make it work? *Trends in neurosciences*, 28, 86-92.
- Winkler, C., Kirik, D., Bjorklund, A. & Cenci, M.A. (2002) L-DOPA-induced dyskinesia in the intrastriatal 6-hydroxydopamine model of parkinson's disease: relation to motor and cellular parameters of nigrostriatal function. *Neurobiology of disease*, 10, 165-186.
- Wirdefeldt, K., Odin, P. & Nyholm, D. (2016) Levodopa-Carbidopa Intestinal Gel in Patients with Parkinson's Disease: A Systematic Review. *CNS drugs*, 30, 381-404.
- Wolf, M.E. & Roth, R.H. (1990) Autoreceptor regulation of dopamine synthesis. *Annals of the New York Academy of Sciences*, 604, 323-343.
- Yamada, H., Aimi, Y., Nagatsu, I., Taki, K., Kudo, M. & Arai, R. (2007) Immunohistochemical detection of L-DOPA-derived dopamine within serotonergic fibers in the striatum and the substantia nigra pars reticulata in Parkinsonian model rats. *Neuroscience research*, 59, 1-7.
- You, H., Mariani, L.L., Mangone, G., Le Febvre de Nailly, D., Charbonnier-Beaupel, F. & Corvol, J.C. (2018) Molecular basis of dopamine replacement therapy and its side effects in Parkinson's disease. *Cell and tissue research*.
- Zhang, J. & Tan, L.C. (2016) Revisiting the Medical Management of Parkinson's Disease: Levodopa versus Dopamine Agonist. *Current neuropharmacology*, 14, 356-363.
- Zoli, M., Jansson, A., Sykova, E., Agnati, L.F. & Fuxe, K. (1999) Volume transmission in the CNS and its relevance for neuropsychopharmacology. *Trends in pharmacological sciences*, 20, 142-150.



Presynaptic dopaminergic compartment determines the susceptibility to L-DOPA–induced dyskinesia in rats

Ayşe Ulusoy¹, Gurdal Sahin¹, and Deniz Kirik²

Brain Repair and Imaging in Neural Systems, Department of Experimental Medical Science, Lund University, BMC D11, 22184 Lund, Sweden

Edited* by Tomas G. M. Hökfelt, Karolinska Institutet, Stockholm, Sweden, and approved June 15, 2010 (received for review March 17, 2010)

Drug-induced dyskinesias in dopamine-denervated animals are known to depend on both pre- and postsynaptic changes of the nigrostriatal circuitry. In lesion models used thus far, changes occur in both of these compartments and, therefore, it has not been possible to dissect the individual contribution of each compartment in the pathophysiology of dyskinesias. Here we silenced the nigrostriatal dopamine neurotransmission without affecting the anatomical integrity of the presynaptic terminals using a short-hairpin RNA-mediated knockdown of tyrosine hydroxylase enzyme (shTH). This treatment resulted in significant reduction (by about 70%) in extracellular dopamine concentration in the striatum as measured by on-line microdialysis. Under these conditions, the animals remained nondyskinetic after chronic L-DOPA treatment, whereas partial intrastriatal 6-hydroxydopamine lesioned rats with comparable reduction in extracellular dopamine levels developed dyskinesias. On the other hand, apomorphine caused moderate to severe dyskinesias in both groups. Importantly, single-dose L-DOPA challenge in apomorphine-primed shTH animals failed to activate the already established abnormal postsynaptic responses. Taken together, these data provide direct evidence that the status of the presynaptic, DA releasing compartment is a critical determinant of both the induction and maintenance of L-DOPA–induced dyskinesias.

adeno-associated virus | dopamine | Parkinson's disease | RNA interference | shRNA

Treatment-induced motor complications are a major problem in management of patients suffering from Parkinson's disease (PD) (1). Dyskinesias induced by L-DOPA, in particular, constitute a significant challenge that impacts a higher proportion of the treated patients with treatment duration. Essentially all patients are expected to develop dyskinesias within a decade from onset of treatment (2). The underlying mechanisms of L-DOPA–induced dyskinesias (LIDs) are still not fully understood. Current views suggest that both presynaptic (i.e., production, storage, controlled release, and reuptake of dopamine by nigrostriatal dopaminergic neurons) and postsynaptic (i.e., status of receptors and second messenger signaling pathways in striatal neurons) components are critical in induction and maintenance of dyskinesias (3–5). However, the destruction of the presynaptic dopamine (DA) terminals, typically obtained by administration of a specific neurotoxin in animals, and the plastic changes induced in the postsynaptic striatal neurons occur at the same time. Moreover, synaptic changes secondary to chronic drug treatment further complicate the interpretation of the observations made in studies using animal models of PD (4–6).

The aim of this study was to tease apart the contribution of the pre- and postsynaptic compartments in the pathophysiology of LIDs in the parkinsonian brain. The abnormal response of the striatal neurons to DA receptor stimulation following chronic DA depletion could be determined solely by mechanisms intrinsic to the striatal cells or alternatively, the functional activity of the presynaptic compartment could determine whether or not L-DOPA treatment results in development of dyskinesias. We hypothesized that the response of the postsynaptic striatal neuron remains under the control of the presynaptic DA terminals even in dyskinetic

animals. However, this hypothesis could not be tested using the classical neurotoxin lesion paradigms.

Recent advances in *in vivo* gene transfer techniques using viral vectors and targeted silencing of specific gene expression using RNA interference mechanisms have created a unique opportunity to tackle this question (7–10). Combining these two technologies provides a tool to knockdown the tyrosine hydroxylase (TH) expression, known to be the rate-limiting enzyme in synthesis of DA, selectively in the nigrostriatal projection system (11, 12). Here, we have expressed a short-hairpin RNA-mediated TH knockdown construct (shTH) using a recombinant adeno-associated virus carrying AAV5 capsid protein (rAAV5). In this model, the DA synthesis machinery is functionally silenced in a targeted manner in nigral DA neurons, whereas the structural integrity of the cells and their terminals are maintained (12). This unique experimental system allowed us to explore the specific contribution of the presynaptic compartment in the induction and maintenance of LIDs.

Results

To provide conclusive data to prove or dispute the hypothesis, we first investigated whether two critical conditions were met following rAAV5-mediated shTH expression: (i) the structural integrity of the nigral DA neurons and their terminals needed to be maintained such that DA stores in these cells could be replenished by peripheral L-DOPA supplement; and (ii) under baseline conditions, extracellular DA levels *in vivo* had to be at subphysiological levels such that the postsynaptic cells would develop supersensitivity to direct DA receptor stimulation. Thus, we first tested the validity of these conditions.

Long-Term rAAV5-Mediated shTH Expression in Nigral DA Neurons Leads to a Functional Knockdown of DA Input in the Striatum. We verified the transduction efficacy and the specific TH knockdown by performing triple immunohistochemical staining against the DAergic markers TH and vesicular monoamine transporter-2 (VMAT2) as well as the GFP marker protein coexpressed by rAAV5-shTH and rAAV5-shTHscr vector constructs (Fig. S1). Injection of rAAV5 vectors encoding for both shTH and shTHscr resulted in expression of the transgene in vast majority of the cells. shTH expression led to specific down-regulation of the TH protein, whereas in the shTHscr group all three proteins were coexpressed in the DAergic neurons.

We confirmed the maintenance of long-term down-regulation of TH expression in the nigral DAergic neurons in the absence of

Author contributions: D.K. designed research; A.U. and G.S. performed research; A.U. and G.S. analyzed data; and A.U., G.S., and D.K. wrote the paper.

The authors declare no conflict of interest.

*This Direct Submission article had a prearranged editor.

¹A.U. and G.S. contributed equally to this work.

²To whom correspondence should be addressed. E-mail: deniz.kirik@med.lu.se.

This article contains supporting information online at www.pnas.org/lookup/suppl/doi:10.1073/pnas.1003432107/-DCSupplemental.

any structural damage using two sets of tools. First, at the histological level, we quantified the numbers of TH and VMAT2-positive cells in the substantia nigra pars compacta (SN) and the density of fiber innervation in the striatum. Estimation of the total number of nigral DAergic cells using stereological techniques showed that the TH- and VMAT2-positive cell population in the SN remained unchanged in the intact and shTHscr groups (Fig. 1 *A, B, E, F, and I*). As expected, the 6-OHDA lesion led to $88.0 \pm 5.2\%$ and $86.3 \pm 3.6\%$ decrease in TH- and VMAT2-positive cells in the SN, respectively (Fig. 1 *D and H*). In the shTH group, on the other hand, there was a $64.6 \pm 7.7\%$ reduction in TH-positive cells, whereas the VMAT2-positive neuron counts were not different from the normal controls confirming that the DAergic cells that no longer expressed the TH enzyme remained viable throughout the experiment (Fig. 1 *C and G*).

At the striatal terminal level, TH and VMAT2 fiber densities in the two control groups were not different between the two sides of the brain (Fig. 1 *J, K, N, O, and R*). There was a clear loss of both the TH- and VMAT2-positive fibers on the lesioned side in the 6-OHDA lesioned rats. Reduction in the fiber density in this group was $83.4 \pm 6.5\%$ and $74.9 \pm 7.3\%$ compared with the uninjected control side in TH and VMAT2 stained sections, respectively (Fig. 1 *M and Q*). The dissociation between the two markers was obvious in the shTH-expressing rats (Fig. 1 *L and P*), as TH-positive fiber density was reduced by $56.7 \pm 9.8\%$, whereas VMAT2-positive fiber density remained unchanged (Fig. 1 *R*).

The second set of analysis was carried out at the biochemical level. Striatal samples from each group were processed for HPLC analysis to measure the tissue content of DA, serotonin (5-HT), and their metabolites under baseline conditions, and in separate animals, after L-DOPA treatment (Fig. 2). The levels of DA on the uninjected side of the brain were not significantly different in any group, nor were they modified by L-DOPA treatment (Fig. 2*A*). On the injected side, however, DA levels in the shTH and 6-OHDA groups were lower than the control groups. Only in

the shTH group, L-DOPA administration resulted in significant reconstitution of DA levels. In fact, after L-DOPA treatment, the values were no longer different from controls providing evidence that complete reconstitution of DA stores were possible in the shTH treated animals. On the other hand, in the 6-OHDA group, where the terminals were structurally damaged and removed, this capacity was lost (Fig. 2*B*). Moreover, in the 6-OHDA, but not in the shTH group, DA turnover rates were abnormally high (Fig. 2*C*). 5-HT turnover was not modified in any of the groups illustrating that the changes in the DA system were specific (Fig. 2*D*). Complete list of all biochemical analysis is given in [Tables S1–S4](#).

rAAV5-Mediated Knockdown Leads to a Significant Decrease in the Extracellular DA Levels in the Striatum.

To test the validity of the second assumption, i.e., that the extracellular DA concentration in the shTH group in vivo would be reduced, we performed a microdialysis experiment using an online HPLC system with high sensitivity (design illustrated in Fig. S2). Using this system, we analyzed the extracellular DA and DOPA content in the striatum by using a three-phase microdialysis protocol. In phase I, we monitored the extracellular DA concentrations under baseline conditions (Fig. 3*A*), and found that they were reduced by $69.6 \pm 8.2\%$ and $57.7 \pm 12.5\%$ in the shTH and 6-OHDA groups, respectively (Fig. 3*B*). This suggested that, although the DA loss in the two experimental treatment groups is mechanistically different from each other, at the functional level, the extracellular DA depletion as measured by microdialysis were comparable. In phase II, we applied high concentration of KCl in dialysate and found that the readily releasable pool of DA was reduced by $69.4 \pm 7.0\%$ and $94.5 \pm 0.3\%$ in the shTH and 6-OHDA groups, respectively (Fig. 3*C*). In phase III, we inhibited the aromatic acid decarboxylase (AADC) enzyme in the brain by administering 3-hydroxybenzylhydrazine dihydrochloride (NSD-1015; 100 mg/kg i.p. injection) and monitored the in vivo build-up of DOPA in the striatum. Inhibition of the AADC enzyme led to accumulation of DOPA in all groups. However, the

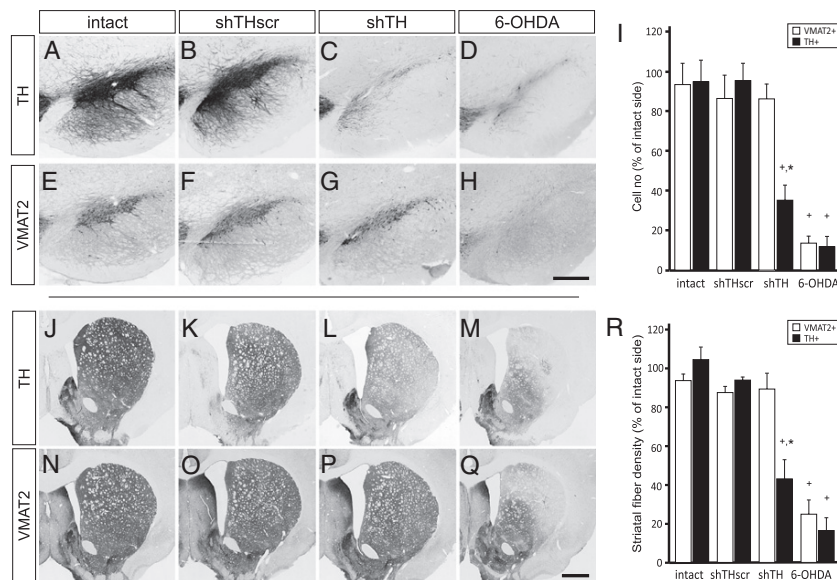


Fig. 1. Long-term down-regulation of TH by rAAV-mediated shRNA expression in the SN and striatum. Both TH and VMAT2 phenotypic markers were maintained at normal levels (intact; *A, E, J, and N*) after expression of scrambled control sequence (shTHscr; *B, F, K, and O*), whereas in the active knockdown group (shTH), TH protein was selectively reduced in the cell bodies (*C*) and at the fiber terminals (*L*), whereas the VMAT2 expression remained unchanged (*G* and *P*). In the 6-OHDA lesioned rats, on the other hand, neurodegeneration in the SN was accompanied with loss of both TH (*D* and *M*) and VMAT2 (*H* and *Q*) immunostaining. The magnitude and specificity of the down-regulation in TH enzyme is shown by stereological quantification of TH and VMAT2-positive cell numbers in the SN (*I*) and semiquantitative optical densitometry measurements in the striatum (*R*). Data are analyzed by two way factorial ANOVA [*I*, group vs. phenotypic marker effect $F(7,27) = 16.497$, $P < 0.0001$; *R*, group vs. phenotypic marker effect $F(7,27) = 26.841$, $P < 0.0001$], followed by Tukey's HSD post hoc. Error bars represent \pm SEM. *Different from intact and shTHscr control group within the same phenotypic marker; **TH-positive cells or fiber density different from the corresponding VMAT2-positive cells or fiber density in the same group. [Scale bars, 50 μ m (in *H* for *A–H*) and 100 μ m (in *Q* for *J–Q*).]

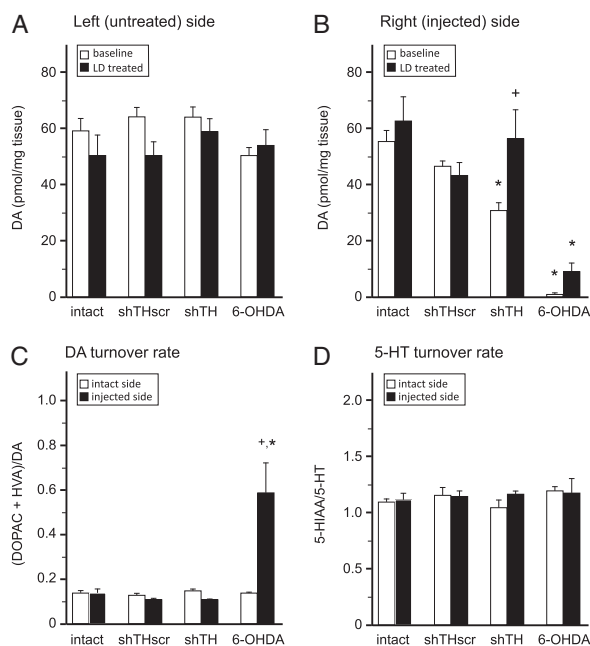


Fig. 2. Quantification of monoamines in striatal tissue samples using HPLC. Two groups of animals were analyzed to determine the concentrations of DA and its metabolites under baseline conditions or following L-DOPA treatment on the uninjected control side (A) and injected side (B). In addition the turnover rate for DA (C) and 5-HT (D) were calculated. Data are analyzed by two-way factorial ANOVA [B, treatment vs. group effect $F(7,37) = 13.479$, $P < 0.0001$; C, group vs. side effect $F(7,41) = 5.194$, $P < 0.0001$], followed by Tukey's HSD post hoc test. Error bars represent \pm SEM. *Different from intact and shTHscr control groups within the same condition (A and B) or side (C and D). **Different from baseline condition (B) or intact side (C).

rate was significantly decreased in shTH and 6-OHDA groups ($71.4 \pm 1.0\%$ and $87.2 \pm 0.5\%$, respectively; Fig. 3D and E).

Primed Striatal Neurons in Dyskinetic Rats Remain Responsive to Normal Modulation of Activity by DA Released from DAergic Terminals. The results of the biochemical analysis provided evidence that both assumptions held true in this experimental setting and thus allowed us to test the hypothesis that striatal neurons would remain responsive to modulation by DA terminals even after maladaptive plasticity had developed.

We addressed this issue in two consecutive steps. First, as the biochemical data suggested that shTH expressing rats had a very good buffering capacity for handling the newly synthesized DA upon exogenous L-DOPA administration, we expected that these animals would be resistant to develop dyskinesias despite chronic treatment with L-DOPA. The experimental results supported this view. L-DOPA treatment was carried out so that the animals received daily injections in an escalating dose regimen of 6, 12, and 24 mg/kg s.c. over a 3-wk treatment period. As expected, the 6-OHDA lesioned rats gradually developed dyskinesias in a time and dose dependent manner, as measured using a well established abnormal involuntary movements (AIMs) scale (Fig. 4A) (13, 14). On the other hand, the shTH group remained similar to the control groups and did not show any abnormal movements throughout the 3-wk testing period. Conversely, as the extracellular DA levels were reduced in both shTH and 6-OHDA treated rats, we expected that both groups would be sensitive to treatment with apomorphine, a direct D1/D2 receptor agonist, targeting the postsynaptic site. This was indeed the case. Apomorphine treatment was given at escalating doses (0.1, 0.2, and 0.5 mg/kg) over three 5-d blocks. During this treatment period not only the

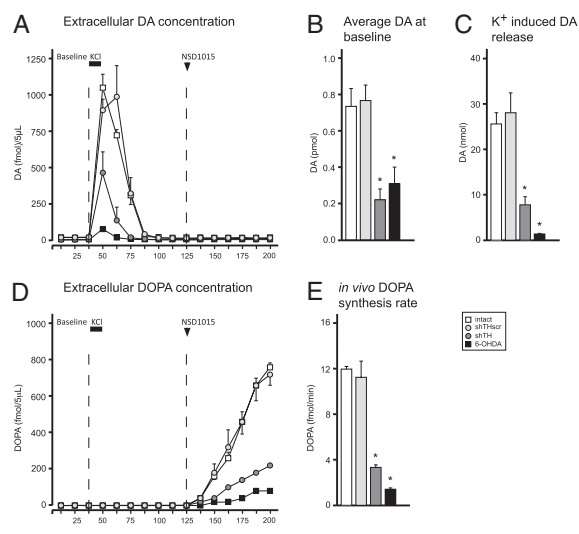


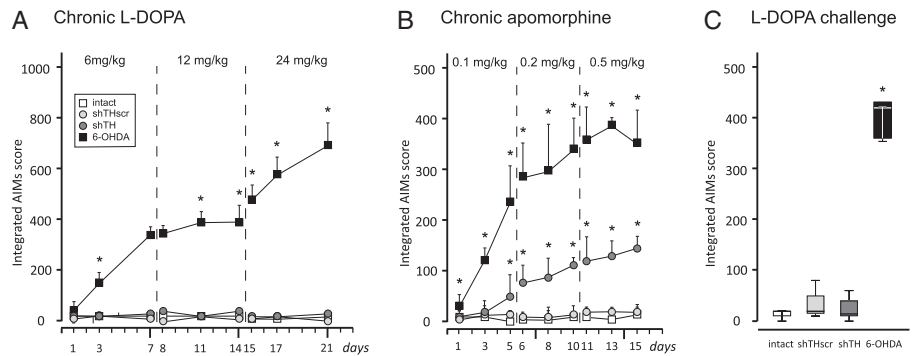
Fig. 3. Online in vivo microdialysis. Baseline (B) and KCl-induced (C) DA release were estimated by calculating the area under the curve in A at the respective time intervals. In the third phase, the animals received a systemic injection of NSD-1015, and in vivo accumulation of DOPA was monitored via the microdialysis probe (D) to estimate the DOPA synthesis rate (E). Statistical comparisons were performed by one-way ANOVA [B, $F(3,10) = 11.975$, $P < 0.01$; C, $F(3,10) = 19.354$, $P < 0.0001$; E, $F(3,10) = 126.806$, $P < 0.0001$] followed by Tukey's HSD post hoc test. Error bars represent \pm SEM. *Different from intact and shTHscr controls.

6-OHDA-lesioned rats, but also the shTH group, developed dyskinesias upon apomorphine treatment, albeit at different severities, whereas control groups did not exhibit any AIMs (Fig. 4B). In the shTH treated rats orolingual dyskinesias and axial dystonia were the predominant manifestations, whereas 6-OHDA lesioned animals displayed high frequency and severity of dyskinesias of all three components, involving also the abnormal limb movements. Both groups of animals developed similar level of locomotive dyskinesia, seen as full body rotation (Fig. S3).

These results led us to the second step where, after 15 d of apomorphine injections, we administered a single high dose of L-DOPA (24 mg/kg) in a subset of animals. In this scenario, both the shTH and 6-OHDA treated rats had been primed with apomorphine and displayed clear dyskinetic behaviors. As expected, in the 6-OHDA group, all of the animals responded to L-DOPA with equally severe dyskinesias, whereas in the shTH group no abnormal behaviors were seen (Fig. 4C). The shTH expressing treated control animals during the entire observation period of 150 min after the drug administration.

To generate the final data to support the hypothesis, we analyzed the immediate early gene expression in the striatum of all animals that received both drug treatments. For this purpose the striatal sections were immunostained using antibodies against FosB (to illustrate the effect of the chronic drug treatment) and against c-Fos (to illustrate the effect of the acute drug challenge on the last day), and quantified the numbers of immunopositive cells for each marker in the lateral, central, and medial striatum separately (the placement of regions of interest are shown in Fig. S4). Chronic L-DOPA treatment resulted in an increased number of FosB-positive nuclei in the 6-OHDA lesioned animals, which was most prominent in the central and lateral striatum (Fig. 5C and D; quantified in A). We did not observe any significant FosB induction in the shTH group (Fig. 5E–G), supporting the observations at the behavioral level, nor did we see FosB induction in intact and shTHscr control groups following chronic L-DOPA treatment (Fig. 5A).

Fig. 4. Induction of dyskinesias by daily L-DOPA and apomorphine treatment using a dose-escalation regimen. The animals were scored three times at each dose level for development of abnormal involuntary movements (AIMs). Chronic L-DOPA administration was carried out over 21 d of three 7-d treatment blocks or 6 mg/kg, 12 mg/kg, and 24 mg/kg (A). DA receptor stimulation was done by administration of apomorphine at 0.1, 0.2, and 0.5 mg/kg doses over 15 d (B). Some animals that have completed the apomorphine sensitization regimen were challenged with a single dose of 24 mg/kg L-DOPA on day 16 (C). Data are shown as median values in all panels. In A and B the error bars show 75% percentiles, whereas in C box plots mark the 50% percentiles and the whiskers indicate 95% percentiles. Statistical comparisons in A and B were performed using Friedman test, time effect $P < 0.0001$, group effect $P < 0.0001$. Individual comparisons in A, B, and C were performed by Kolmogorov-Smirnov test and P values were compensated for false discovery rates. *Different from intact and shTHscr controls.



Data are shown as median values in all panels. In A and B the error bars show 75% percentiles, whereas in C box plots mark the 50% percentiles and the whiskers indicate 95% percentiles. Statistical comparisons in A and B were performed using Friedman test, time effect $P < 0.0001$, group effect $P < 0.0001$. Individual comparisons in A, B, and C were performed by Kolmogorov-Smirnov test and P values were compensated for false discovery rates. *Different from intact and shTHscr controls.

Chronic apomorphine treatment, on the other hand, led to increased FosB-positive cells both in 6-OHDA and shTH, but not in the control groups (Fig. 5H). In the 6-OHDA group, the induction was almost exclusively in the lateral striatum (Fig. 5, compare K with I and J), whereas in the shTH treated rats, the FosB-positive cells were mostly in the medial and central areas (Fig. 5, compare L, M, and N). A single 24-mg/kg L-DOPA injection after chronic apomorphine treatment led to a comparable level of induction of c-Fos in the 6-OHDA group (Fig. 5Q and R; quantified in O), whereas in the shTH group, no acute c-Fos induction was seen after L-DOPA treatment (Fig. 5S–U). This observation constituted the final piece of evidence showing that presynaptic DA terminals could retain the functional control of the postsynaptic striatal neurons even after the establishment of dysplastic changes in these neurons.

Discussion

This study was designed to address a critical yet unanswered question regarding the relative contribution of the pre- and postsynaptic compartments in induction and maintenance of drug-induced dyskinesias in PD. The difficulty in assessing the impact of a single compartment on the occurrence of motor complications originates from the inability to dissociate changes induced by each compartment independently (15). Thus the novelty of our current approach was to use viral vector-mediated long-term shRNA expression to functionally knockdown DA synthesis, without destruction of the presynaptic terminals. As the manipulation is unilateral and involves only the nigral DA neurons, these rats eat and drink normally and maintain a normal general health status. Using this experimental model, we showed that chronic stimulation of the postsynaptic DA receptors by a direct D1/D2 agonist (apomorphine) induced dyskinesias, whereas administration of L-DOPA failed to induce any abnormal movements. Moreover, rats that have been already primed with apomorphine treatment did not display any dyskinesias upon an acute high dose challenge with L-DOPA. These behavioral observations were correlated with immediate early gene activation seen in the respective groups. Taken together, in the present model where the structural integrity of the DA terminals is maintained, the response of the postsynaptic striatal neurons to stimulation of DA receptors was strictly controlled by the presynaptic activity. Thus, it appears from our data that the state of the presynaptic machinery is a critical determinant of the induction and maintenance of the LIDs.

Experimental studies have thus far focused on changes that occur at the postsynaptic site as the leading mechanism for induction and maintenance of dyskinesias. The data supporting this view argue that upon lesion of DAergic input to the striatum, and following treatment with L-DOPA or direct DA-agonists, striatal neurons undergo dysplastic changes (16). Alterations in postsynaptic DA

receptors on striatal neurons have been formulated as denervation supersensitivity (17–19). Additionally there are also changes in the activity of other neurotransmitter systems such as glutamate, 5-HT, acetylcholine, and adenosine (16, 20–23). It is thought that the changes at the receptor level cause further modification of downstream cascades including second messenger systems and signaling pathways (3, 24). Based on the structural and functional changes described above, it has been argued that postsynaptic mechanisms are critical for the development of dyskinesias in PD.

The alternative view emphasizes the importance of the presynaptic compartment in the pathophysiology of motor complications following chronic L-DOPA treatment and is primarily based on observations in PD patients. In vivo PET studies comparing PD patients with and without dyskinesias did not reveal any specific changes in either D1 or D2 receptor binding potentials (25, 26). Furthermore, in a recent PET study it has been shown that PD patients with dyskinesias have reduced DA transporter expression, supporting the role of presynaptic alterations in the appearance of dyskinesias (27). Finally, clinical observations from DOPA-responsive dystonia show that, despite the fact that these patients have similar levels of striatal DA depletion, dyskinesias do not occur even after long-term (essentially life-long) L-DOPA treatment (28, 29). As these patients do not develop DA neurodegeneration, it appears that under conditions when the presynaptic DA compartment is structurally intact, dysplastic changes in the postsynaptic striatal neurons do not lead to development of motor complications. Thus, proponents of the so-called “presynaptic hypothesis of dyskinesias” argue that the postsynaptic plastic changes are secondary, rather than causally linked to LIDs (4).

The unregulated DA production and release via alternative routes following degeneration of the nigrostriatal neurons provide further evidence for the critical role of a functionally intact presynaptic DA terminals in the development of the LIDs. In the parkinsonian brain, as the presynaptic DAergic neurodegeneration progresses, other cell types start to take part in handling exogenously administered L-DOPA and its conversion to DA. In particular, 5-HT cells are known to play a critical role. These cells contain the enzymes AADC and VMAT2 and therefore possess not only the capability to convert L-DOPA to DA but also store it in synaptic vesicles as a false neurotransmitter (30). However, because they do not express D2 autoreceptors and DA transporter, which are essential for the normal autoregulatory feedback control of DA release from the presynaptic terminal, their activity leads to uncontrolled swings in extracellular DA concentrations (31). Importantly, it has been recently shown that DA released from 5-HT terminals was responsible for the appearance of LIDs in parkinsonian rats (32). Furthermore, either a lesion of 5-HT system by specific toxins, or pharmacological silencing of these neurons by selective 5-HT1A and 5-HT1B agonists dramatically reduced or even completely abolished LIDs in 6-OHDA le-

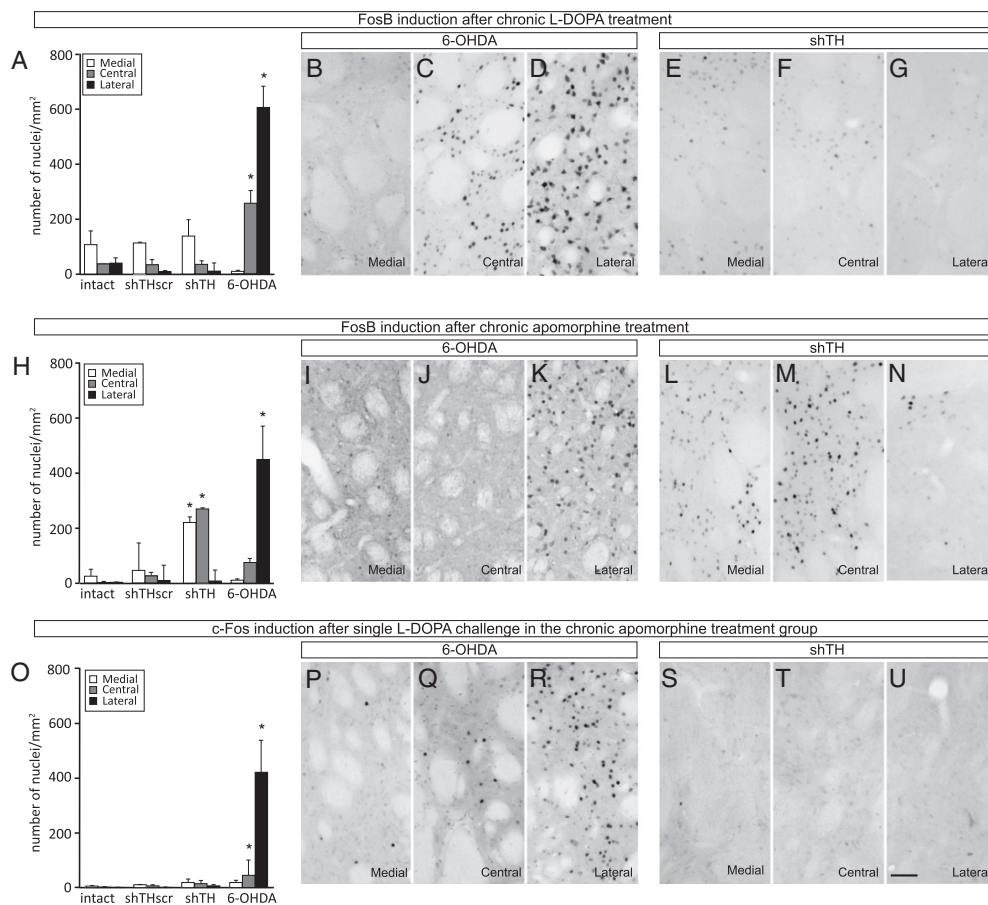


Fig. 5. Analysis of FosB and c-Fos induction following L-DOPA and apomorphine treatment. The numbers of c-Fos and FosB-positive cells were assessed on three coronal sections in the striatum as shown in Fig. S4. (A–G) FosB induction after chronic L-DOPA treatment; (H–N) FosB induction after chronic apomorphine treatment; (O–U) c-Fos induction in the striatum after a single dose 24 mg/kg L-DOPA challenge in the animals that were primed with chronic apomorphine treatment. Note that the FosB and c-Fos photomicrographs in *Middle* and *Bottom* rows are taken from adjacent series of sections processed from the same animal. The contrast between 6-OHDA lesions and rAAV5-mediated TH knockdown is illustrated with two panels under each condition representing the medial, central, and lateral striatal expression of the two gene products. Quantification of the FosB (A and H) and c-Fos (O) positive nuclei after chronic L-DOPA (A), chronic apomorphine (H), and acute L-DOPA (O) treatments are illustrated as bar graphs. Statistical comparisons for each striatal area were performed by one-way ANOVA [A, lateral striatum $F(3,21) = 47.425$, $P < 0.0001$; central striatum $F(3,21) = 6.065$, $P < 0.05$; H, lateral striatum $F(3,14) = 8,124$, $P < 0.005$; central striatum $F(3,14) = 3.478$, $P < 0.05$; medial striatum $F(3,14) = 3,719$, $P < 0.05$; O, lateral striatum $F(3,13) = 4.977$, $P < 0.05$] followed by Tukey's HSD post hoc test. Error bars represent \pm SEM. *Different from the number of positive-nuclei from the corresponding striatal region in other groups. (Scale bar, 50 μ m in U for B–G, I–N and P–U.)

sioned rats and MPTP-treated monkeys (33). These studies point to the deterministic role of the presynaptic DA releasing compartment on the occurrence of dyskinesias.

To compare the pathophysiological mechanisms of dyskinesias, we used two different experimental models. On one hand, the TH knockdown approach allowed us to generate a functional presynaptic DA depletion creating an isolated postsynaptic dysfunction. On the other hand, the 6-OHDA lesion model, which disrupted DAergic input structurally, led to a combined pre- and postsynaptic dysfunction. The validity of the comparison, however, depends on the assumption that the presence of DAergic neuronal death is the main difference between these two conditions. The preserved release of factors from the DA neurons and terminals (e.g., BDNF and glutamate) in the shTH group might, however, contribute to the behavior seen in TH knockdown animals. In addition, there is evidence to suggest that structural destruction of the DA terminals can generate changes in postsynaptic neurons, which involves modifications of spine morphology and distribution, as well as alterations in synapse structure and changes in electrophysiological and electrochemical properties of the cells (34–37). It is not clear, at this point, if the shRNA expression that silence DA

production chronically results in development of similar changes over time. Nevertheless, some of the changes that are seen in 6-OHDA lesioned rats such as the reduction in spine numbers and alterations in miniature excitatory postsynaptic currents in medium spiny neurons have been shown to occur in reserpinized rats, which leads to DA depletion that last several days or weeks (38–40). In our experiments all behavioral tests were carried out 6–8 mo after transduction, which argues that such secondary modifications should have taken place at the time of analysis.

Finally, strong evidence supporting the presynaptic hypothesis comes from transplantation studies. In animal models of PD, embryonic ventral mesencephalon rich in DA neurons results in reconstitution of the DA terminal network capable of restoring feedback-controlled release of DA in the striatum (41). Importantly DA cell rich grafts have been shown to improve LIDs in these animals (42). On the contrary, transplantation of 5-HT neurons, which cannot release DA in a regulated fashion, worsens the dyskinesic side effects of L-DOPA medication (43, 44). It is probable that the worsening of dyskinesias in grafted patients might be a consequence of abnormal DA handling in the presynaptic com-

partment(s) possibly due to presence of serotonin neurons in the graft and/or ongoing inflammatory processes in the host brain (45).

In conclusion, by using a model system allowing us to functionally deplete striatal DA while maintaining the structural integrity of the presynaptic compartment, we have shown that postsynaptic plastic changes caused by DA receptor stimulation occur as a consequence of the lack of DA and do not require structural damage to the presynaptic DAergic terminals (46). Importantly, although dyskinesias may be elicited as a function of the intrinsic cellular changes of the postsynaptic compartment, the striatal neurons respond normally to regulated DA release from an adequate presynaptic compartment. These observations have implications for the interpretation of the concept of priming and support the view that this phenomenon may be the direct consequence of loss of DA while essentially nonphysiological DAergic pharmacotherapy merely unravels this behavior. Reconstitution of the DA machinery by cell- or gene-based therapies can reverse or even prevent development of L-DOPA-induced dyskinesias in PD patients.

Methods

A total of 117 young female Sprague–Dawley rats were used for rAAV5 vector injections and $3 \times 7 \mu\text{g}$ striatal 6-OHDA lesions. rAAV5 vector constructs carried

1. Obeso JA, Olanow CW, Nutt JG (2000) Levodopa motor complications in Parkinson's disease. *Trends Neurosci* 23 (10, Suppl):S2–S7.
2. Ahlskog JE, Muenter MD (2001) Frequency of levodopa-related dyskinesias and motor fluctuations as estimated from the cumulative literature. *Mov Disord* 16:448–458.
3. Cenci MA, Lundblad M (2006) Post- versus presynaptic plasticity in L-DOPA-induced dyskinesia. *J Neurochem* 99:381–392.
4. de la Fuente-Fernández R (2007) Presynaptic mechanisms of motor complications in Parkinson disease. *Arch Neurol* 64:141–143.
5. Linazasoro G (2007) Pathophysiology of motor complications in Parkinson disease: Postsynaptic mechanisms are crucial. *Arch Neurol* 64:137–140.
6. Lee CS, Kumar A (2004) Reply to: PET studies and pathophysiology of motor fluctuations in Parkinson's disease. *Brain* 127:E16.
7. Lundberg C, et al. (2008) Applications of lentiviral vectors for biology and gene therapy of neurological disorders. *Curr Gene Ther* 8:461–473.
8. Carthew RW, Sontheimer EJ (2009) Origins and Mechanisms of miRNAs and siRNAs. *Cell* 136:642–655.
9. Ulusoy A, Björklund T, Hermening S, Kirik D (2008) In vivo gene delivery for development of mammalian models for Parkinson's disease. *Exp Neurol* 209:89–100.
10. Grimm D (2009) Small silencing RNAs: State-of-the-art. *Adv Drug Deliv Rev* 61:672–703.
11. Hommel JD, Sears RM, Georgescu D, Simmons DL, DiLeone RJ (2003) Local gene knockdown in the brain using viral-mediated RNA interference. *Nat Med* 9:1539–1544.
12. Ulusoy A, Sahin G, Björklund T, Aebischer P, Kirik D (2009) Dose optimization for long-term rAAV-mediated RNA interference in the nigrostriatal projection neurons. *Mol Ther* 17:1574–1584.
13. Winkler C, Kirik D, Björklund A, Cenci MA (2002) L-DOPA-induced dyskinesia in the intrastriatal 6-hydroxydopamine model of parkinson's disease: Relation to motor and cellular parameters of nigrostriatal function. *Neurobiol Dis* 10:165–186.
14. Lundblad M, et al. (2002) Pharmacological validation of behavioural measures of akinesia and dyskinesia in a rat model of Parkinson's disease. *Eur J Neurosci* 15:120–132.
15. Nadjar A, Gerfen CR, Bezard E (2009) Priming for l-dopa-induced dyskinesia in Parkinson's disease: A feature inherent to the treatment or the disease? *Prog Neurobiol* 87:1–9.
16. Hirsch EC (2000) Nigrostriatal system plasticity in Parkinson's disease: Effect of dopaminergic denervation and treatment. *Ann Neurol* 47 (4 Suppl 1):S115–S120.
17. Pycock CJ, Marsden CD (1977) Central dopaminergic receptor supersensitivity and its relevance to Parkinson's disease. *J Neurol Sci* 31:113–121.
18. Rinne UK, et al. (1990) Positron emission tomography demonstrates dopamine D2 receptor supersensitivity in the striatum of patients with early Parkinson's disease. *Mov Disord* 5:55–59.
19. Antonini A, et al. (1994) [^{11}C]raclopride and positron emission tomography in previously untreated patients with Parkinson's disease: Influence of L-dopa and lisuride therapy on striatal dopamine D2-receptors. *Neurology* 44:1325–1329.
20. Guerra MJ, Liste I, Labandeira-Garcia JL (1997) Effects of lesions of the nigrostriatal pathway and of nigral grafts on striatal serotonergic innervation in adult rats. *Neuroreport* 8:3485–3488.
21. Chase TN, Oh JD (2000) Striatal dopamine- and glutamate-mediated dysregulation in experimental parkinsonism. *Trends Neurosci* 23 (10, Suppl):S86–S91.
22. Pisani A, et al. (2001) Role of tonically-active neurons in the control of striatal function: Cellular mechanisms and behavioral correlates. *Prog Neuropsychopharmacol Biol Psychiatry* 25:211–230.
23. Fredduzzi S, et al. (2002) Persistent behavioral sensitization to chronic L-DOPA requires A2A adenosine receptors. *J Neurosci* 22:1054–1062.
24. Calon F, et al. (2000) Dopamine-receptor stimulation: Biobehavioral and biochemical consequences. *Trends Neurosci* 23 (10, Suppl):S92–S100.
25. de la Fuente-Fernández R, et al. (2004) Levodopa-induced changes in synaptic dopamine levels increase with progression of Parkinson's disease: Implications for dyskinesias. *Brain* 127:2747–2754.
26. Linazasoro G, et al. (2009) Levodopa-induced dyskinesias in parkinson disease are independent of the extent of striatal dopaminergic denervation: A pharmacological and SPECT study. *Clin Neuropharmacol* 32:326–329.
27. Troiano AR, et al. (2009) PET demonstrates reduced dopamine transporter expression in PD with dyskinesias. *Neurology* 72:1211–1216.
28. Nygaard TG, Marsden CD, Fahn S (1991) Dopa-responsive dystonia: Long-term treatment response and prognosis. *Neurology* 41:174–181.
29. Nutt JG, Nygaard TG (2001) Response to levodopa treatment in dopa-responsive dystonia. *Arch Neurol* 58:905–910.
30. Arai R, Karasawa N, Geffard M, Nagatsu T, Nagatsu I (1994) Immunohistochemical evidence that central serotonin neurons produce dopamine from exogenous L-DOPA in the rat, with reference to the involvement of aromatic L-amino acid decarboxylase. *Brain Res* 667:295–299.
31. Carta M, Carlsson T, Kirik D, Björklund A (2007) Dopamine released from 5-HT terminals is the cause of L-DOPA-induced dyskinesia in parkinsonian rats. *Brain* 130:1819–1833.
32. Bishop C, et al. (2009) Contribution of the striatum to the effects of 5-HT1A receptor stimulation in L-DOPA-treated hemiparkinsonian rats. *J Neurosci Res* 87:1645–1658.
33. Muñoz A, et al. (2008) Combined 5-HT1A and 5-HT1B receptor agonists for the treatment of L-DOPA-induced dyskinesia. *Brain* 131:3380–3394.
34. Galarraga E, Bargas J, Martínez-Fong D, Aceves J (1987) Spontaneous synaptic potentials in dopamine-denervated neostriatal neurons. *Neurosci Lett* 81:351–355.
35. Nitsch C, Riesenberger R (1995) Synaptic reorganization in the rat striatum after dopaminergic deafferentation: An ultrastructural study using glutamate decarboxylase immunocytochemistry. *Synapse* 19:247–263.
36. Ingham CA, Hood SH, Taggart P, Arbuthnott GW (1998) Plasticity of synapses in the rat neostriatum after unilateral lesion of the nigrostriatal dopaminergic pathway. *J Neurosci* 18:4732–4743.
37. Picconi B, et al. (2003) Loss of bidirectional striatal synaptic plasticity in L-DOPA-induced dyskinesia. *Nat Neurosci* 6:501–506.
38. Day M, et al. (2006) Selective elimination of glutamatergic synapses on striatopallidal neurons in Parkinson disease models. *Nat Neurosci* 9:251–259.
39. Shen W, Flajolet M, Greengard P, Surmeier DJ (2008) Dichotomous dopaminergic control of striatal synaptic plasticity. *Science* 321:848–851.
40. Taverna S, Iljic E, Surmeier DJ (2008) Recurrent collateral connections of striatal medium spiny neurons are disrupted in models of Parkinson's disease. *J Neurosci* 28:5504–5512.
41. Moukhlès H, Furni C, Nieoullon A, Daszuta A (1994) Regulation of dopamine levels in intrastriatal grafts of fetal mesencephalic cell suspension: An in vivo voltammetric approach. *Exp Brain Res* 102:10–20.
42. Lee CS, Cenci MA, Schulzer M, Björklund A (2000) Embryonic ventral mesencephalic grafts improve levodopa-induced dyskinesia in a rat model of Parkinson's disease. *Brain* 123:1365–1379.
43. Carlsson T, Carta M, Winkler C, Björklund A, Kirik D (2007) Serotonin neuron transplants exacerbate L-DOPA-induced dyskinesias in a rat model of Parkinson's disease. *J Neurosci* 27:8011–8022.
44. Carlsson T, et al. (2009) Impact of grafted serotonin and dopamine neurons on development of L-DOPA-induced dyskinesias in parkinsonian rats is determined by the extent of dopamine neuron degeneration. *Brain* 132:319–335.
45. Hedlund E, Perlmann T (2009) Neuronal cell replacement in Parkinson's disease. *J Intern Med* 266:358–371.
46. Kim DS, Palmiter RD, Cummins A, Gerfen CR (2006) Reversal of supersensitive striatal dopamine D1 receptor signaling and extracellular signal-regulated kinase activity in dopamine-deficient mice. *Neuroscience* 137:1381–1388.

Supporting Information

Ulusoy et al. 10.1073/pnas.1003432107

SI Methods

Experimental Design. A total of 117 young adult female Sprague-Dawley rats weighing between 225–250 g were obtained from Charles River. The animals were housed under a 12-h light/12-h dark cycle with free access to food and water. All surgical procedures were performed according to the regulations set by the ethical committee for use of laboratory animals in Lund-Malmö region.

The animals were divided into four experimental groups. Two groups of animals were injected with rAAV5 vectors expressing either the TH knockdown construct (shTH group; $n = 32$) or its scrambled control (shTHscr group; $n = 27$), a third group that received striatal 6-hydroxydopamine lesion (6-OHDA group; $n = 26$) and finally a fourth group of rats ($n = 23$) were followed as nontreated intact animals. All animals were allowed to survive for 5 mo before any other treatment was initiated. At that time point, animals in each group were divided into 6 subsets. The first subset consisting of 14 animals (shTH $n = 4$, shTHscr $n = 4$, 6-OHDA $n = 3$, intact $n = 3$) was directly killed and the brains were fixed for histological analysis. The second subset, consisting of 14 animals (shTH $n = 3$, shTHscr $n = 3$, 6-OHDA $n = 4$, intact $n = 4$) was included in the microdialysis experiment and then killed for histological analysis. Two additional subsets consisting of a total of 37 animals (shTH $n = 6 + 6$, shTHscr $n = 5 + 4$, 6-OHDA $n = 4 + 3$, intact $n = 4 + 5$) were included in biochemical analysis either at baseline or after a single dose L-DOPA challenge. Two final subsets consisting of a total of 43 animals were allocated into behavioral test paradigms with chronic L-DOPA (presynaptic induction of dyskinesias) or Apomorphine (postsynaptic induction of dyskinesias) treatment regimens (shTH $n = 8 + 5$, shTHscr $n = 6 + 5$, 6-OHDA $n = 7 + 5$, intact $n = 4 + 3$, respectively) and then killed for histological analysis.

Constructs and rAAV5 Virus Production. The rAAV5 vectors expressing short hairpin RNA (shRNA) sequences were generated as previously described (1). Briefly, an siRNA matching the rat TH mRNA at 790–810bp location and the corresponding scrambled siRNA sequence (denoted as shTH and shTHscr, respectively) were inserted into the transfer plasmid for vector production. The sequences for these shRNAs were as follows: shTH (5'-aacggctactgtgctaccgagttcaagagactcggtagccacagctaccgtt-3') and shTHscr (5'-gcgctcagtcaggctacagattcaagagaactctgactgactgacgcgc-3'). These sequences were cloned into an AAV transfer vector in two steps. First, the shRNA sequences were placed downstream of the H1 promoter. In the second step, XhoI-SacI fragments containing the H1-shRNA sequences were cloned into the pTR-UF11 backbone plasmid containing the AAV2 inverted terminal repeats. The insertion was carried out by removing PYF441 enhancer and HSV-tk promoter driven *NeoR* gene on the original backbone plasmid (pTR-UF11), which was downstream of GFP driven by a CMV enhancer hybrid CBA promoter. rAAV5 vectors were produced in 293 cells in cell factories with a confluency of 70–80%. The transfection was carried out using the Calcium-phosphate method and included the appropriate transfer plasmid (as detailed above) and the pXYZ5 packaging plasmid, encoding for the AAV5 capsid proteins in trans (2, 3). Transfected cells were incubated for 3 d before being harvested by PBS-EDTA. The cell pellet was lysed and crude lysates were purified first by ultracentrifugation (1.5 h at $350,000 \times g$ at 18 °C) in a discontinuous iodixanol gradient, and then by ion-exchange chromatography using FPLC as described earlier (1). The virus suspension was then concentrated using a concentrator (Ultra 100kDa MWCO; Millipore Amicon) at $1,500 \times g$ and 18 °C in two consecutive steps by adding lactated ringer. The titers

of the vector preparations were determined using TaqMan quantitative PCR. The stock batch titers were $3.7E12$ and $3.6E13$ gc/mL for shTH and shTHscr, respectively. The injected solution was adjusted to the target concentration [as determined in (1)] by a dilution from the stocks in PBS buffer. The final injected solution was retitered before use and confirmed to have $1.3E12$ and $1.7E12$ gc/mL for the vector encoding for shTH and shTHscr, respectively.

Stereotaxic Surgeries. Viral vector injection and 6-OHDA lesion surgeries were performed under 20:1 mixture of fentanylcitrate (Fentanyl) and medetomidin hydrochloride (Dormitor) (Apo-teksbolaget) prepared as an injectable anesthetic. rAAV5 vector injections were made into substantia nigra using 5- μ L Hamilton syringe fitted with a glass capillary with a tip diameter of about 60–80 μ m. Two microliters of the buffer containing the appropriate number of viral particles was injected at a speed of 0.4 μ L/min. The needle was withdrawn slowly 5 min after completion of the injection. Coordinates used for SN injections were anteroposterior (AP): -5.2 mm and mediolateral (ML): -2.0 mm relative to the bregma and dorsoventral (DV): -7.2 mm from the dural surface, according to the atlas of Paxinos and Watson (4). The tooth bar was adjusted to -2.3 mm in all nigral injections. 6-OHDA lesions were placed into the right striatum by injecting a total of 21 μ g 6-OHDA dissolved in ascorbate-saline (0.02%) delivered in three deposits distributed along the rostrocaudal axis. The coordinates were AP: $+1.0$, -0.1 , -1.2 mm and ML: -3.0 , -3.7 , -4.5 mm, respectively, relative to the bregma and DV: -5.0 mm from the dural surface (5). The tooth bar was set to 0.0 mm. A volume of 2 μ L per site was injected at a rate of 0.4 μ L/min. The needle was left in place for 5 min after completion of each injection.

Microdialysis Experiment. The in vivo DOPA synthesis and DA release parameters in the striatum were assessed using a microdialysis protocol. For this purpose, the rats were anesthetized with 1–2% isoflurane mixed with O₂ and N₂O and placed in a stereotaxic frame. Microdialysis probes used in this experiment had a 3-mm membrane length and 0.5-mm outer diameter (Agnthos Microdialysis). The probes were inserted into the striatum with the help of a holder and placed at AP: $+0.6$ mm, ML: -3.0 mm relative to bregma and DV: -5.5 mm from the dural surface. The tooth bar was set to -2.3 mm.

The probes were connected to a syringe infusion pump (Model 100; CMA Microdialysis) via polyethylene tubing and perfused with normal ringer solution containing 145 mM NaCl, 3 mM KCl and 1.3 mM CaCl₂ at a constant rate of 1 μ L/min. The dialysates were directly analyzed on Alexys online monoamine analyzer microdialysis system (Antec Leyden) consisting of a DECADE II electrochemical detector and VT-3 electrochemical flow cell. The outlet of the microdialysis probe was connected to a 14-port external valve that can direct the dialysate into two separate flow paths (Fig. S2). Two different mobile phases—optimized for the detection of the respective metabolites—were used in each of the two flow paths. The first mobile phase (50 mM phosphoric acid, 8 mM NaCl, 0.1 mM EDTA, 12.5% methanol, 500 mg/L octane sulfate; pH 6.0) was used for the detection of DA and 5-HT ran through a 1 mm \times 50-mm column with 3 μ m particle size (ALF-105) at a flow rate of 75 μ L/min. The second mobile phase (50 mM phosphoric acid, 50 mM citric acid, 8 mM NaCl, 0.1 mM EDTA, 10% methanol, 600 mg/L octane sulfate; pH 3.2) was used for the detection of DOPA, DOPAC, HVA, and 5-HIAA, which passed through a 1 mm \times 150-mm column with 3- μ m particle size (ALF-115) at a flow rate of 100 μ L/min. The dialysate samples were

transferred via 5- μ L loops simultaneously into each flow path and analyzed by the online HPLC at 12.5 min time bins.

One hour of equilibration was followed by analysis of three baseline samples before the dialysate was changed to a modified ringer lactate solution containing high KCl (51 mM NaCl, 100 mM KCl, and 1.3 mM CaCl₂) for 12.5 min to stimulate the readily releasable pool of DA and then switched back to the normal ringer lactate solution. After analyzing serial samples for six more time bins (i.e., until $t = 125$ min), the animals were i.p. injected with 100 mg/kg of NSD-1015 (Sigma-Aldrich) to block the AADC enzyme activity. The dialysate samples were analyzed for another 75 min following the NSD-1015 treatment while the newly synthesized DOPA accumulated in the brain. The chromatograms were analyzed using the Clarity Chromatographic Station (version 2.7.03.498; DataApex). The probes were withdrawn at the end of the procedure and animals were allowed to recover and kept alive for another 10 d before killing.

Apomorphine and L-DOPA-Induced AIMS. The animals included in the behavioral experiments were treated as follows: L-DOPA treatment regimen was carried as consecutive weekly escalating doses of 6, 12, and 24 mg/kg daily L-DOPA administered s.c. together with 10 mg/kg benserazide over a 3-wk period. AIMS were evaluated three times (the first, third or fourth, and the final day) at each dose level. On the 22nd day of the treatment the animals were injected with a final dose of 24 mg/kg L-DOPA 2 h before death. The apomorphine treatment regimen was carried out as three consecutive 5-d escalating doses of 0.1, 0.2, and 0.5 mg/kg daily apomorphine injections (dissolved in 0.2 mg/mL ascorbate-saline and administered s.c.) over a 15-d treatment period. A group of animals from the 6-OHDA group ($n = 4$) and intact group ($n = 3$) were used as sham controls and received s.c. injection of 0.2 mg/mL ascorbate-saline for 3 wk. The evolution of AIMS was monitored on alternating days during the treatment period (i.e., on first, third, and last days of each dose). On day 16, a subset of the animals received a single challenge dose of 24 mg/kg L-DOPA, to test the ability to trigger AIMS via the presynaptic mechanism in apomorphine primed animals and killed 2 h after the drug administration.

The evaluation of the AIMS were performed according to the rat dyskinesia scale as described previously (6, 7). Briefly, the animals were placed individually in transparent plastic cages with a grid lid so that every movement can be visualized in detail. A researcher blinded to the identity of the animals scored them every 10 or 20 min following apomorphine or L-DOPA injections, respectively. The AIMS were classified into three subtypes according to their topographic distribution as forelimb, orolingual, and axial dyskinesias. Locomotive dyskinesia displayed as contralateral rotations were scored separately. The severity of each AIM subtype was scored from 0 to 4 (0, no abnormal behaviors detected; 1, occasional AIMS, i.e., present less than 50% of the time; 2, frequent AIMS, i.e., present more than 50% of the time; 3, continuous AIMS, but interrupted by strong sensory stimuli; and 4, continuous AIMS, not interrupted by strong sensory stimuli). Half-points were used where the behavior of the animal were clearly in between the two defined points. The data are calculated as time-integrated scores and represented by sum of the orolingual, limb and axial subtypes.

Biochemical Assays. A total of 37 animals were killed for HPLC analysis to assess the total tissue levels of DA, serotonin (5-HT), and their metabolites either at baseline ($n = 19$) or 150 min after a single 12 mg/kg L-DOPA injection ($n = 18$). For this purpose, the animals were decapitated and the brains were rapidly dissected. After a brief rinse with an ice-cold saline solution, the brains were placed on a brain slicer. A 2-mm slice containing the head of striatum and nucleus accumbens was dissected out from the surrounding tissue. This sample was then quickly dissected into two parts; one containing the ventromedial striatum together

with nucleus accumbens and the other containing the rest of the dorsal striatal tissue within that segment. The tissue was rapidly frozen on dry ice and kept at -80°C until further processing. The midbrain samples from those animals were fixed in 4% paraformaldehyde overnight for immunohistochemical detection of viral transduction and treated in the same way as described under the histological analysis section below.

At the time of analysis striatal tissue samples were sonicated in 18 mL/mg ice-cold homogenization buffer (20 mM Tris acetate, pH 6.1) and centrifuged at $20,000 \times g$ for 10 min at 4°C . The supernatant was filtered through a PVDF filter (0.45 μ m; Uni-filter) and used for HPLC analysis for determination of the total tissue concentration of DA, 5-HT, and their metabolites. Briefly, 20 μ L of each sample was injected by a cooled Spark Midas autosampler (Spark Holland) into an ESA Coulochem III coupled to an electrochemical detector set to a potential of +350 mV. The mobile phase (5 g/L Na acetate, 30 mg/L Na₂-EDTA, sodium octane sulphonic acid 100mg/L, 10% methanol, pH 4.2) was delivered at a flow rate of 0.5 mL/min to a reversed phase C18 column (particle size 3 μ m, 4.0 mm \times 100 mm, Chromtech). The peaks were analyzed by using the Clarity Chromatographic Station (DataApex). The amounts were expressed as nmol/mg tissue.

Histological Analysis. Rats were deeply anesthetized with 1.2 mL sodium pentobarbital (Apoteksbolaget). They were perfused through the ascending aorta first with 50 mL physiological saline at room temperature over 1 min and then by 250 mL ice-cold 4% paraformaldehyde (PFA) for 5 min. Brains were postfixed in 4% PFA solution for 2 h before being transferred into 25% sucrose solution for cyroprotection, where they were kept until they had sunk (typically within 24–48hrs). The brains were then sectioned in the coronal plane on a freezing microtome at a thickness of 35 μ m. Sections were collected in six series and stored at -20°C in a phosphate buffer containing 30% glycerol and 30% ethylene glycol until further processing.

Immunohistochemical stainings were performed on free-floating sections. For this purpose, brain sections were first rinsed with potassium-PBS (KPBS), and then endogenous peroxidase activity was quenched by incubation in a mixture of 3% H₂O₂ and 10% methanol in KPBS for 30 min. After three rinsing steps in KPBS, nonspecific binding sites were blocked by incubation in KPBS containing 5% normal serum matched to the species used to raise the corresponding secondary antibody and 0.25% Triton-X. Samples were then incubated overnight at room temperature in primary antibody solution containing 5% serum and 0.25% Triton-X. The primary antibodies used for immunohistochemical staining were as follows: mouse anti-TH (working dilution 1:2,000, MAB318; Millipore), rabbit anti-VMAT2 (working dilution 1:1,000, AB1767; Millipore), chicken anti-GFP (working dilution 1:5,000, ab13970; Abcam), goat anti-FosB (working dilution 1:1,000, SC-48X; Santa Cruz) and rabbit anti-c-Fos (working dilution 1:1,000, PC05; Oncogene). On the second day, the sections were rinsed in KPBS and then incubated for 1h at room temperature in 1:200 dilution of appropriate biotinylated secondary antibody solutions (horse anti-mouse for TH antibody, goat anti-rabbit for c-Fos and VMAT2 antibodies, sheep anti-goat for FosB antibody; Vector Laboratories). After rinsing, the sections were treated with avidin-biotin-peroxidase complex (ABC Elite kit; Vector Laboratories) and the color reaction was developed by incubation in 25 mg/mL 3,3'-diaminobenzidine and 0.005% H₂O₂. To increase the contrast in the FosB and c-Fos staining 2.5 mg/mL Nickel sulfate was added in the DAB solution before the color reaction. Sections were mounted on chrome-alum coated glass slides, dehydrated and cover-slipped with Depex mounting media (Sigma).

TH, GFP, and VMAT2 triple immunohistofluorescence was carried out as above with the exception that the biotinylated secondary antibodies were replaced with fluorophore conjugated

variants (Dylight 488 conjugated donkey-anti-chicken, cy3 conjugated donkey-anti-mouse conjugated, and cy5 conjugated donkey-anti-rabbit; Jackson Immunoresearch) and H₂O₂ quenching, ABC and DAB reaction steps were excluded. The sections were directly mounted on chrome-alum coated glass slides and cover-slipped using PVA-DABCO (Sigma).

Image Analysis. The optical intensity of the TH- and VMAT2-positive fibers as well as the numbers of c-Fos and FosB positive cells of the striatum were analyzed on images captured using a 10× Plan-Fluor objective (Numerical aperture = 0.30) on a Nikon Eclipse 90i microscope equipped with a Nikon DS-Q1Mc camera using NIS software (NIS Elements AR 3.0; Nikon). The fiber density measurements were performed at four rostrocaudal levels through the striatum (*i*) anteroposterior (AP), +2.16; (*ii*) AP, +0.84; (*iii*) AP, -0.3; (*iv*) AP, -0.9 relative to bregma. For the c-Fos and FosB positive cells the images were captured from three rostrocaudal striatal levels (*i*) AP, +1.20; (*ii*) AP, -0.26; and (*iii*) AP, -1.30; relative to bregma (Fig S4) according to the rat brain atlas of Paxinos and Watson (4). To estimate the specific TH and VMAT2 staining density, the optical intensity readings were corrected for nonspecific background, as measured from the corpus callosum for each animal. The fiber densities were expressed as the percent of intact side. The c-Fos and FosB positive cells were counted from 0.5 mm × 0.5 mm TIFF formatted images analyzed using the ImageJ software (Version 1.42i, NIH). After background subtraction, the numbers of cells specifically labeled with c-Fos and FosB were counted using the particle analysis tool. The density of immunopositive c-Fos and FosB profiles was expressed as number of cells/mm².

Confocal Microscopy. The triple immunohistochemical staining was visualized on a Nikon Eclipse 90i microscope equipped with a D-eclipse C1 confocal camera (Nikon). The high power confocal images were captured using a 60× Plan-Apo objective (Numerical aperture = 1.4) on a single plane using sequential acquisition. The low power images were taken using a 4× Plan-Fluor objective (numerical aperture = 0.13) as z-stacks of eight focal planes penetrating 6–8 μm from the surface of the section in sequential acquisition mode. Confocal images were captured and pseudo-colored using EZ-C1 software (gold version 3.9). The z-stack

images were then processed for maximal intensity projection on an NIS-Elements AR software (version 3.10).

Stereological Analysis. The TH-positive and VMAT2-positive cell numbers in the SN were estimated using an unbiased stereological quantification method by using the optical fractionator principle (8, 9). All quantifications were done after blinding the identity of the sections by a coding system. Upon completion of the quantification of batches, samples were moved to a database for further analysis using appropriate statistical and graphical tools. The borders for the region of interest was defined by using a 4× objective, whereas the actual counting was performed using a 60× Plan-Apo oil objective (Numerical aperture = 1.4) on a Nikon 80i microscope equipped with an X-Y motorized stage, a z axis motor and a high-precision linear encoder (Heidenhein). All three axes and the input from the digital camera were controlled by a PC computer running the NewCast Module in VIS software (Visio-pharm A/S), which carries out the procedure with a random start and systematic sampling routine. The sampling interval in the x-y axis was adjusted so that at least 100 cells were counted for each SN. Coefficient of error attributable to the sampling was calculated according to Gundersen and Jensen (10) and values ≤0.10 were accepted.

Statistical Analysis. Statistical significance for the group comparisons for stereological cell counts, fiber density measurements and the HPLC data were analyzed by using two-way factorial ANOVA, followed by post hoc comparisons using Tukey HSD test. One-way ANOVA test was performed to compare results from microdialysis measurements and the quantification of immediate-early gene markers, followed by Tukey HSD post hoc test. The above-mentioned data were represented as mean ± SE of mean. As AIM scores are not parametric data, they are presented as median ± 75% confidence interval. The final L-DOPA challenge scores were represented as a box-plot chart where the whiskers represent 95% percentiles of the median. The comparisons of the dyskinesia scores were performed using Friedman test followed by individual comparisons using Kolmogorov-Smirnov test and corrected for false discovery rate. Statistical significance was set at $P < 0.05$. All statistical analysis was performed using SPSS statistical software (Version 17).

1. Ulusoy A, Sahin G, Björklund T, Aebischer P, Kirik D (2009) Dose optimization for long-term rAAV-mediated RNA interference in the nigrostriatal projection neurons. *Mol Ther* 17:1574–1584.
2. Zolotukhin S, et al. (1999) Recombinant adeno-associated virus purification using novel methods improves infectious titer and yield. *Gene Ther* 6:973–985.
3. Grimm D (2002) Production methods for gene transfer vectors based on adeno-associated virus serotypes. *Methods* 28:146–157.
4. Paxinos G, Watson C (2007) *The Rat Brain in Stereotaxic Coordinates* (Academic Press, London), 2nd Ed.
5. Kirik D, Rosenblad C, Björklund A (1998) Characterization of behavioral and neurodegenerative changes following partial lesions of the nigrostriatal dopamine system induced by intrastriatal 6-hydroxydopamine in the rat. *Exp Neurol* 152:259–277.
6. Lundblad M, et al. (2002) Pharmacological validation of behavioural measures of akinesia and dyskinesia in a rat model of Parkinson's disease. *Eur J Neurosci* 15: 120–132.
7. Winkler C, Kirik D, Björklund A, Cenci MA (2002) L-DOPA-induced dyskinesia in the intrastriatal 6-hydroxydopamine model of parkinson's disease: Relation to motor and cellular parameters of nigrostriatal function. *Neurobiol Dis* 10:165–186.
8. West MJ (1999) Stereological methods for estimating the total number of neurons and synapses: Issues of precision and bias. *Trends Neurosci* 22:51–61.
9. Schmitz C, Hof PR (2005) Design-based stereology in neuroscience. *Neuroscience* 130: 813–831.
10. Gundersen HJ, Jensen EB (1987) The efficiency of systematic sampling in stereology and its prediction. *J Microsc* 147:229–263.

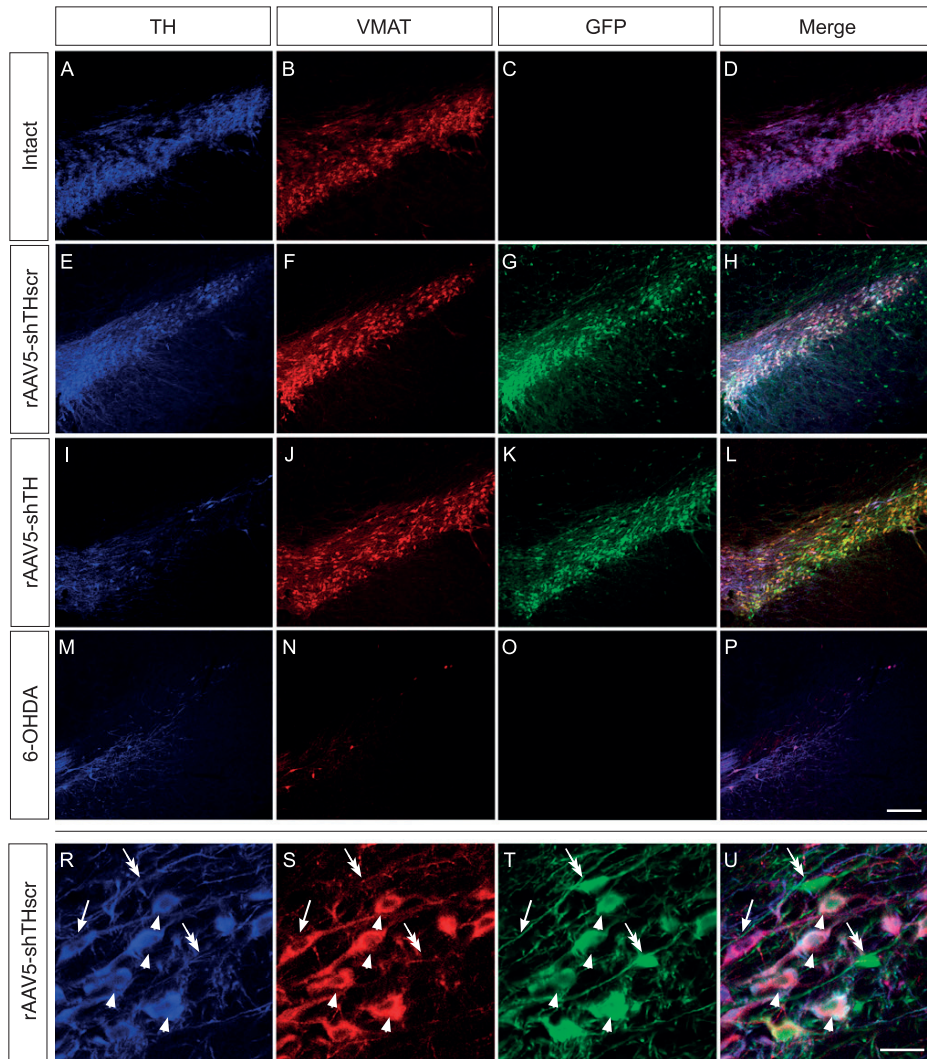


Fig. S1. Transgene expression and transduction efficacy following rAA5 mediated shRNA expression in the rat nigra. As the vector constructs express not only the shRNA but also the GFP marker protein, multilabeling using fluorescent immunohistochemistry allowed us to assess the transduction efficiency in the target cell population in the ventral midbrain. Confocal microscopical images are obtained from the substantia nigra after triple staining for TH pseudocolored in *blue* (Left), VMAT2 pseudocolored as *red* (Center Left), the GFP shown in *green* (Center Right) and the merged panels (Right) on the intact side (A–D), rAAV5-shTHscr (E–H), rAAV5-shTH (I–L) vector injected sides or in 6-OHDA lesioned rats (M–P). High power images obtained from rAAV5-shTHscr injected midbrain illustrates the colocalization of the three markers showing high efficiency of targeting the transgene to DA neurons (R–U). Injection of rAAV5-shTH (I–L) and rAAV5-shTHscr (E–H) leads to a robust GFP expression in the TH and VMAT2-positive neurons in the SN with high transduction efficiency. shTH expression led to specific down-regulation of the TH protein (I), whereas in the shTHscr group all three proteins are readily detectable giving the white color in the merged panels (H, U). Arrowheads show some of the triple labeled cells expressing the GFP marker gene, TH and VMAT2, arrow shows a nontransduced DAergic neuron expressing TH and VMAT2 but not GFP and two double arrows show GFP-positive transduced cells that are negative for both DAergic markers. (Scale bar, 200 μ m in P for A–P and 30 μ m in U for R–U.)

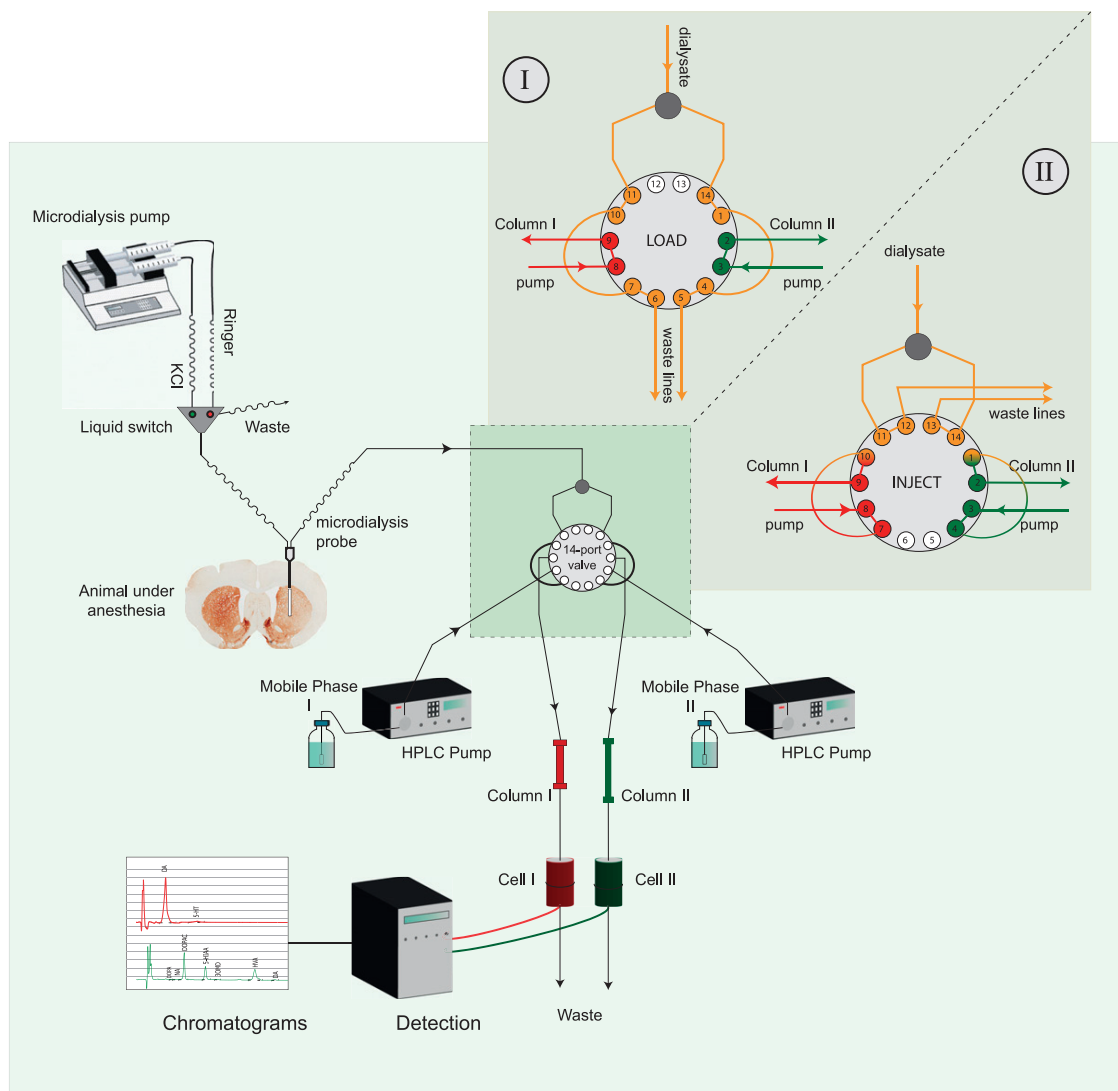


Fig. S2. Illustration of the ALEXYS Online Monoamine Analyzer. The microdialysis pump directs the ringer solution and the KCl solution to a liquid switch where depending on the experimental phase, either one of the solution is manually selected to flow into the microdialysis probe. We have, in this study, stereotaxically inserted the probe into the striatum of rats to measure extracellular levels of monoamines and their metabolites. The output dialysate collected from the striatum flows into 14-port injector valve and splits into two equal portions, eventually to be directed into two different columns for separate electrochemical detection. This separation allows acquiring increased time resolution and decreased sample volume. Two different valve positions define the flow paths of the mobile phases and the dialysate sample. When the valve is in load position (detailed in *I*) the dialysate is parallel loaded into two loops with 5- μ L volume. The valve changes to the inject position at predefined time intervals. The residual volume exceeding 5 μ L is disposed through waste lines. In the inject position (detailed in *II*) 5 μ L dialysate sample is transferred from the loop to the columns. In this context we have used two different columns allowing us to detect NA, DA, and 5-HT in column 1 and NA, DOPA, DOPAC, 5-HIAA, 3-OMD, HVA and DA in column 2, simultaneously. Columns are connected to separate electrochemical cells and the signal is then detected and monitored as chromatograms.

Apomorphine-induced rotation

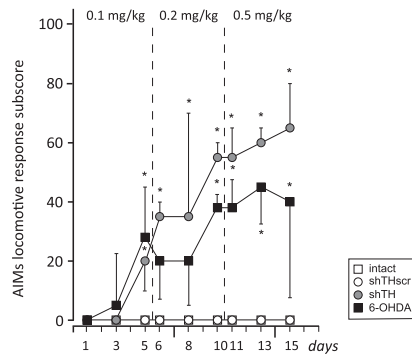


Fig. 53. Induction of locomotive dyskinesia observed as rotational behavior after daily apomorphine treatment using a dose-escalation regimen. Animals were scored three times at each dose level for development of AIMs by using a dedicated rating scale. Three subtypes of AIMs (forelimb, orolingual, and axial) are reported as integrated AIMs scores in Fig. 4. Locomotive behaviors were distinguished as circular movements contralateral to the lesioned side and were rated from 0 (absent) to 4 (continuous rotation, not interrupted by repeated strong sensory stimuli) every 10 min after each dose of apomorphine injections. In the shTH group there was slow onset but a continuous sensitization in the frequency of rotational response with escalating apomorphine doses. In the 6-OHDA lesion group, the overall response was not different from the shTH group, although the magnitude of the response was blunted with higher doses most likely due to severe axial dyskinesia seen in this group. Data are shown as median values in all groups. Error bars show 75% percentiles. Individual comparisons were performed by Kolmogorov-Smirnov test and *P* values were compensated for false discovery rates. *different from intact and shTHscr controls.

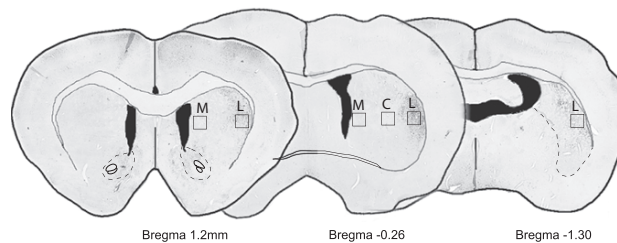


Fig. 54. Illustration of regions of interest used for quantification of the numbers of c-Fos and FosB-positive cells. The analysis was carried out on three coronal sections in the striatum at levels +1.2 mm, -0.26 mm, and -1.3 mm from bregma. Digital images were taken from the lateral striatum on all three levels, central striatum at the second level, and in the medial striatum at the first two levels as shown in the delineated squares.

Table S1. DA and DA metabolite levels in the dorsal striatum

	DA		DOPAC		HVA		(DOPAC + HVA)/DA	
	Baseline	L-DOPA	Baseline	L-DOPA	Baseline	L-DOPA	Baseline	L-DOPA
Right (injected)								
intact	55,533 ± 4,130	62,905 ± 8,761	4,596 ± 324	9,699 ± 1,043	2,773 ± 245	18,201 ± 3,073	0.135 ± 0.019	0.447 ± 0.032
shTHscr	46,774 ± 2,053	43,496 ± 4,614	3,182 ± 230	6,375 ± 262	2,126 ± 107	13,566 ± 1,022	0.114 ± 0.007	0.470 ± 0.052
shTH	31,012 ± 2,865*	56,587 ± 10,413	2,109 ± 162*	8,389 ± 1,664	1,242 ± 91*	12,535 ± 2,330	0.109 ± 0.005	0.372 ± 0.029
6-OHDA	1,099 ± 662*	9,218 ± 3,031	202 ± 99*	3,976 ± 1,080*	162 ± 62*	9,086 ± 3,157	0.588 ± 0.135*	1.558 ± 0.317*
Left (uninjected)								
intact	59,449 ± 4,502	50,571 ± 7,359	5,098 ± 168	6,666 ± 1,059	3,021 ± 231	14,577 ± 1,529	0.138 ± 0.011	0.437 ± 0.042
shTHscr	64,422 ± 3,444	50,589 ± 4,862	5,052 ± 396	7,211 ± 359	3,127 ± 143	14,930 ± 1,500	0.128 ± 0.009	0.444 ± 0.036
shTH	64,332 ± 3,684	59,117 ± 4,741	5,545 ± 304	10,316 ± 1,504	3,594 ± 201	16,004 ± 1,483	0.144 ± 0.009	0.445 ± 0.036
6-OHDA	50,649 ± 2,965	54,222 ± 5,678	4,914 ± 453	9,363 ± 2,530	2,887 ± 51	19,673 ± 5,364	0.151 ± 0.005	0.519 ± 0.084

Table contains two panels showing the right (injected) side and left (uninjected) side. Levels of DA, DOPAC, HVA and DA turnover rate in the dorsal striatum are illustrated under baseline conditions as well as in a group of animals that received a single dose of 12 mg/kg L-DOPA (plus 10 mg/kg benserazide) and killed 150 min after injection. The levels of DA, DOPAC, HVA, 5-HT and 5-HIAA are represented as fmol/mg tissue. Statistical group comparisons were performed using one-way ANOVA, if significant followed by Tukey HSD post hoc analysis. 5-HIAA, 5-hydroxyindoleacetic acid, 5-HT, serotonin; 6-OHDA, 6-hydroxydopamine; DA, dopamine; DOPAC, 3,4-dihydroxyphenylacetic acid; HVA homovanilic acid; scr, scrambled; shRNA, short hairpin RNA; shTH, short-hairpin RNAs targeting the rat TH mRNA.

*Different from intact controls.

Table S2. DA and DA metabolite levels in the ventral striatum including nucleus accumbens

	DA		DOPAC		HVA		(DOPAC + HVA)/DA	
	Baseline	L-DOPA	Baseline	L-DOPA	Baseline	L-DOPA	Baseline	L-DOPA
Right (injected)								
intact	40,261 ± 6,159	39,970 ± 7,648	4,449 ± 588	7,631 ± 1,696	2,427 ± 419	12,045 ± 1,776	0.181 ± 0.010	0.500 ± 0.021
shTHscr	35,503 ± 1,623	25,247 ± 7,242	3,403 ± 242	5,607 ± 2,423	1,837 ± 61	9,350 ± 3,507	0.149 ± 0.011	0.535 ± 0.123
shTH	29,239 ± 3,395	40,741 ± 3,213	2,745 ± 205	9,027 ± 1,223	1,412 ± 95*	11,400 ± 1,202	0.146 ± 0.007	0.502 ± 0.062
6-OHDA	5,934 ± 2,826	25,806 ± 2,817	929 ± 432*	7,812 ± 1,299	488 ± 174*	11,399 ± 2,878	0.313 ± 0.047*	0.729 ± 0.079
Left (uninjected)								
intact	45,689 ± 3,509	42,185 ± 1,797	5,241 ± 408	8,221 ± 600	2,429 ± 80	13,600 ± 1,441	0.177 ± 0.018	0.517 ± 0.048
shTHscr	39,317 ± 2,724	29,525 ± 1,448	4,392 ± 333	6,274 ± 794	1,905 ± 110	11,011 ± 3,258	0.163 ± 0.013	0.579 ± 0.091
shTH	35,374 ± 3,294	33,422 ± 3,706	4,134 ± 356	8,130 ± 1,373	2,083 ± 113	10,756 ± 1,881	0.179 ± 0.013	0.551 ± 0.049
6-OHDA	40,748 ± 2,902	40,130 ± 1,262	5,901 ± 434	10,322 ± 1,729	2,300 ± 148	17,856 ± 3,783	0.203 ± 0.008	0.695 ± 0.112

Table contains two panels showing the right (injected) side and left (uninjected) side. Levels of DA, DOPAC, HVA and DA turnover rate in the ventral striatum including nucleus accumbens are illustrated under baseline conditions as well as in a group of animals that received a single dose of 12 mg/kg L-DOPA (plus 10 mg/kg benserazide) and killed 150 min after injection. The levels of DA, DOPAC, HVA, 5-HT and 5-HIAA are represented as fmol/mg tissue. Statistical group comparisons were performed using one-way ANOVA, if significant followed by Tukey HSD post hoc analysis. 5-HIAA, 5-hydroxyindoleacetic acid, 5-HT, serotonin; 6-OHDA, 6-hydroxydopamine; DA, dopamine; DOPAC, 3,4-dihydroxyphenylacetic acid; HVA homovanilic acid; scr, scrambled; shRNA, short hairpin RNA; shTH, short-hairpin RNAs targeting the rat TH mRNA.

*Different from intact controls.

Table S3. 5HT and 5HIAA levels in the dorsal striatum

	5HT		5HIAA		5HIAA/5HT	
	Baseline	L-DOPA	Baseline	L-DOPA	Baseline	L-DOPA
Right (injected)						
intact	1,010 ± 57	1,080 ± 314	1,078 ± 28	2,264 ± 232	1.097 ± 0.064	2.411 ± 0.404
shTHscr	791 ± 66	1,121 ± 300	914 ± 81	2,240 ± 271	1.160 ± 0.053	2.326 ± 0.303
shTH	970 ± 109	1,059 ± 246	1,013 ± 113	1,870 ± 180	1.049 ± 0.034	2.088 ± 0.235
6-OHDA	752 ± 201	1,229 ± 138	811 ± 133	2,958 ± 206	1.198 ± 0.125	2.432 ± 0.110
Left (uninjected)						
intact	1,359 ± 95	1,102 ± 181	1,503 ± 80	2,063 ± 235	1.122 ± 0.030	2.233 ± 0.194
shTHscr	1,476 ± 136	953 ± 100	1,694 ± 149	2,140 ± 306	1.155 ± 0.067	2.559 ± 0.166
shTH	1,384 ± 144	880 ± 90	1,618 ± 171	1,927 ± 156	1.174 ± 0.067	2.347 ± 0.205
6-OHDA	1,408 ± 117	1,237 ± 89	1,635 ± 95	2,606 ± 113	1.177 ± 0.038	2.117 ± 0.074

Table contains two panels showing the right (injected) side and left (uninjected) side. Levels of 5-HT, 5-HIAA and serotonin turnover rate in the dorsal striatum under baseline conditions and after L-DOPA injection were also measured to assess the specificity of the changes in the DAergic system. The levels of DA, DOPAC, HVA, 5-HT and 5-HIAA are represented as fmol/mg tissue. Statistical group comparisons were performed using one-way ANOVA, if significant followed by Tukey HSD post hoc analysis. 5-HIAA, 5-hydroxyindoleacetic acid, 5-HT, serotonin; 6-OHDA, 6-hydroxydopamine; DA, dopamine; DOPAC, 3,4-dihydroxyphenylacetic acid; HVA homovanilic acid; scr, scrambled; shRNA, short hairpin RNA; shTH, short-hairpin RNAs targeting the rat TH mRNA.

*Different from intact controls.

Paper II



Differential Dopamine Receptor Occupancy Underlies L-DOPA-Induced Dyskinesia in a Rat Model of Parkinson's Disease

Gurdal Sahin^{1*}, Lachlan H. Thompson^{1,2}, Sonia Lavisse³, Merve Ozgur¹, Latifa Rbah-Vidal³, Frédéric Dollé⁴, Philippe Hantraye^{3,9}, Deniz Kirik^{1,9}

1 Brain Repair And Imaging in Neural Systems (BRAINS) Unit, Department of Experimental Medical Science, Lund University, Lund, Sweden, **2** Florey Institute of Neuroscience and Mental Health, The University of Melbourne, Victoria, Australia, **3** Commissariat à l'énergie atomique (CEA), Institut d'imagerie biomédicale (I²BM), Molecular Imaging Research Center (MIRCent), Fontenay aux Roses, France, **4** Commissariat à l'énergie atomique (CEA), Institut d'imagerie biomédicale (I²BM), Service Hospitalier Frédéric Joliot, Orsay, France

Abstract

Dyskinesia is a major side effect of an otherwise effective L-DOPA treatment in Parkinson's patients. The prevailing view for the underlying presynaptic mechanism of L-DOPA-induced dyskinesia (LID) suggests that surges in dopamine (DA) via uncontrolled release from serotonergic terminals results in abnormally high level of extracellular striatal dopamine. Here we used high-sensitivity online microdialysis and PET imaging techniques to directly investigate DA release properties from serotonergic terminals both in the parkinsonian striatum and after neuronal transplantation in 6-OHDA lesioned rats. Although L-DOPA administration resulted in a drift in extracellular DA levels, we found no evidence for abnormally high striatal DA release from serotonin neurons. The extracellular concentration of DA remained at or below levels detected in the intact striatum. Instead, our results showed that an inefficient release pool of DA associated with low D2 receptor binding remained unchanged. Taken together, these findings suggest that differential DA receptor activation rather than excessive release could be the underlying mechanism explaining LID seen in this model. Our data have important implications for development of drugs targeting the serotonergic system to reduce DA release to manage dyskinesia in patients with Parkinson's disease.

Citation: Sahin G, Thompson LH, Lavisse S, Ozgur M, Rbah-Vidal L, et al. (2014) Differential Dopamine Receptor Occupancy Underlies L-DOPA-Induced Dyskinesia in a Rat Model of Parkinson's Disease. PLoS ONE 9(3): e90759. doi:10.1371/journal.pone.0090759

Editor: Patrick Callaerts, VIB & Katholieke Universiteit Leuven, Belgium

Received: December 18, 2013; **Accepted:** February 3, 2014; **Published:** March 10, 2014

Copyright: © 2014 Sahin et al. This is an open-access article distributed under the terms of the Creative Commons Attribution License, which permits unrestricted use, distribution, and reproduction in any medium, provided the original author and source are credited.

Funding: The authors would like to acknowledge the Swedish Research Council (K2009-61P-20945-03-1), Swedish Parkinson Foundation (grant no. 334/10), the European Research Council (ERC) Starting Grant (TreatPD, 242932) and European Union 6th Framework Program project Diagnostic Molecular Imaging (DiMI, LSHB-CT-2005-512146). The funders had no role in study design, data collection and analysis, decision to publish, or preparation of the manuscript.

Competing Interests: The authors have declared that no competing interests exist.

* E-mail: Gurdal.Sahin@med.lu.se

⁹ These authors contributed equally to this work.

Introduction

Parkinson's disease (PD) is a neurodegenerative disorder affecting nearly 1% of the general population older than 60 years of age. It is characterized by loss of dopaminergic innervation in the striatum, which is responsible for motor symptoms such as bradykinesia, tremor and rigidity [1]. The most efficient treatment strategy for PD is replacement of dopamine (DA) by exogenous supplement of its precursor L-DOPA. In spite of its efficiency, long-term use of L-DOPA is associated with serious side effects consisting of motor response fluctuations and emergence of drug-induced involuntary movements, so called L-DOPA-induced dyskinesia (LID). These side effects are troublesome and limit utility of L-DOPA in patients [2]. The extent of dopaminergic neurodegeneration in the substantia nigra (SN) leading to denervation of their striatal targets is one of the major risk factors in the development of LID [3]. L-DOPA exerts its effect after conversion into DA by the aromatic amino acid decarboxylase (AADC) enzyme, which primarily occurs in residual DA terminals early in the disease. As the degeneration progresses, synthesis of

DA from exogenously administered L-DOPA is gradually shifted to other cellular compartments (e.g. serotonergic neurons and non-neuronal cells). Importantly, however, these cells lack appropriate controlled release and reuptake mechanisms, therefore cannot buffer extracellular DA levels. Normally DA concentration is strictly regulated in the synaptic cleft by dopamine transporter (DAT) and the activity of presynaptic DA type 2 receptors (D2R). This helps DA to exert its effect on the post-synaptic neurons in an efficient and highly controlled manner. However, as the degeneration progresses, the number of residual dopaminergic terminals becomes insufficient to maintain this function, which results in reduced DA concentration at the synaptic sites accompanied with larger sphere of diffusion in the extracellular space [reviewed in [4]].

Postsynaptic mechanisms (i.e., status of DA receptors and second messenger signaling pathways in striatal neurons) are also known to be critical in pathophysiology of LID. The imbalance between the stimulation of D1 and D2 receptors results in a loss of synergistic activity between the direct and indirect output pathways [5,6]. Moreover, these receptor-level modifications are

caused not only by the disease itself but are also aggravated by L-DOPA treatment. Abnormal activation of striatal neurons, especially the D1R rich sub-population has been linked to alterations in transcriptional and translational factors (DARPP32, ERK1/2, CREB and δ FosB), which in turn are thought to be responsible from the emergence of LID and serve as molecular markers of maladaptive plasticity in the striatum [7].

There is an increasing interest in the presynaptic mechanisms of LID. In particular, the role of the serotonergic compartment has gained considerable attention [8–12]. The so-called pre-synaptic serotonergic mechanism of LID stipulates that the L-DOPA precursor can be taken up by the serotonergic terminals and converted to DA, which is then stored and released from vesicles as false neurotransmitter. Serotonergic cells rely on the activity of the AADC enzyme and the vesicular monoamine transporter-2 (VMAT2) for synthesis and storage of serotonin (5HT). Thus the machinery for processing exogenously administered L-DOPA to DA is present in these cells, just as it is in dopaminergic neurons [13–16]. One critical distinction, however, is the release control mechanisms. Both DA and 5HT neurons retain the extracellular concentrations of their natural neurotransmitters by way of autoreceptors that can sense and regulate the amount released and uptake sites that can clear the synaptic cleft after discharge. When DA is generated in serotonergic terminals, on the other hand, this critical control mechanism becomes compromised. In support of this view, lesioning the serotonin neurons or pharmacological suppression of their activity produce near complete suppression of dyskinesia in the rat and monkey models of PD [10,17]. Thus, it is plausible to expect that DA release from 5HT terminals would result in an uncontrolled rise in extracellular DA concentrations beyond physiological levels, which might cause worsening of dyskinesia. Despite circumstantial data to support this model, to date, there is no direct evidence showing that release from 5HT terminals indeed results in supra-physiological DA concentrations in the striatum, or abnormally high occupancy of DA receptors at the appropriate post-synaptic site.

Materials and Methods

Animals

A total of 250 young adult female Sprague-Dawley rats weighing between 225–250 g were obtained from Charles River (Kisslegg, Germany). The animals were housed under a 12 h light/12 h dark cycle with free access to food and water. All surgical procedures were performed according to the regulations set by the ethical committee for use of laboratory animals in Lund-Malmö region. The protocol was approved by the Malmö/Lund Committee for Animal Experiment Ethics (Permit Number: M268–08).

Experimental design

The schematic time-line and design of the experiment is presented in Figure 1. In the beginning of the study, 220 animals received a unilateral 6OHDA lesion in the medial forebrain bundle (MFB) while 30 others were retained as intact controls. Starting 3 weeks post-lesion, the animals were screened for completeness of the lesion of the ascending dopaminergic pathway using amphetamine-induced rotational asymmetry. 60% of the rats exhibited more than six full-body turns per minute ipsilateral to the DA-lesioned side and were considered completely lesioned. These animals were then treated with daily injections of L-DOPA for 28 days to induce abnormal involuntary movements (AIMs), equivalent to peak dose dyskinesia seen in PD patients. At the end of this induction phase, 62% of animals (n = 82) exhibited stable

AIMs and were retained in the study. The dyskinetic animals were then allocated into three different groups: Two groups of animals were transplanted with fetal tissue prepared as single-cell suspensions. One group received cells from the anterior segment of the ventral mesencephalon (VM) containing high numbers of dopaminergic and low numbers of serotonergic neuroblasts (referred to as DA grafts, n = 29). The second group was grafted with tissue dissected from the dorsal pontine raphe region (referred to as 5HT-grafts; n = 31), which contained high numbers of serotonergic cells but no or very few dopaminergic neuroblasts. The third group of dyskinetic rats did not receive any graft and were followed as 6OHDA lesion group (n = 22). After this point animals were kept under twice weekly injection of L-DOPA (maintenance phase) until the end of the experiment. Functional benefits of transplantation was assessed using the cylinder test for spontaneous forelimb use and AIMs test for evaluation of L-DOPA induced involuntary movements both before and three-months after the transplantation. After the completion of behavioral analyses, sub-groups of animals were subjected to one of three different microdialysis protocols for assessment of neurotransmitter release, or PET imaging to monitor the D2R occupancy during the *in vivo* follow up period. Finally, tissue were collected for either histological or biochemical end-points at termination 8–14 months after grafting (Fig. 1).

Surgical procedures

Female Sprague Dawley rats received unilateral injections of 6OHDA (Sigma-Aldrich AB, Sweden; 3 μ g/ μ l free base dissolved in 0.9% w/v NaCl with 0.2 mg/mL L-ascorbic acid) into the right medial forebrain bundle using a stereotaxic apparatus (Stoelting, Wood Dale, IL, USA) and 10 μ l Hamilton syringe. Operations were performed under 20:1 mixture of fentanyl citrate (Fentanyl) and medetomidin hydrochloride (Dormitor). Both drugs obtained from Apoteksbolaget, Sweden and prepared as injectable anesthetics. The antero-posterior (AP) and medio-lateral (ML) coordinates were +1.2 mm and –4.4 mm relative to bregma. The injection was made at a dorsoventral (DV) position of –7.8 mm from the surface of the dura and the tooth bar was set to –2.3 mm. The toxin was injected at a rate of 1 μ l/mL and the syringe was kept in place for an additional 3 min to allow diffusion before it was slowly retracted.

For cell transplantation, the rats were anesthetized with 1–2% isoflurane mixed with 0.4 L/min O₂ and 1 L/min N₂O and placed in a stereotaxic frame. All transplantation procedures were performed using fetal cells dissected from embryonic day 14 rat embryos, based on a micro transplantation protocol using glass capillaries attached to a 5 μ l Hamilton syringe, as described previously [10]. Tissue pieces obtained from the VM region (rich in DA neurons) or from the dorsal pontine raphe region (rich in 5HT neurons) were incubated in 0.1% trypsin/0.05% DNase in DMEM at 37°C for 20 min, and rinsed, then mechanically dissociated to a single cell suspension, centrifuged, and resuspended to a concentration of 100,000–150,000 cells/ μ l for DA neuron rich grafts and 80,000–140,000 cells/ μ l for 5HT neuron rich grafts. The viability of the cells were >97% for both tissue preparations. A total of 3 μ l from the final cell suspension was distributed over three injection tracts in the lesioned striatum (AP: +1.4, +0.5 and +0.5; ML: –2.5, –2.2, and –3.7, from bregma; tooth bar = –2.3). Two 0.5 μ l deposits (–5 to –3.5 mm below dura) were delivered along each tract.

Behavioral tests

Three weeks after 6OHDA lesion, the animals were challenged with D-amphetamine (2.5 mg/kg, i.p.). This test was used as a

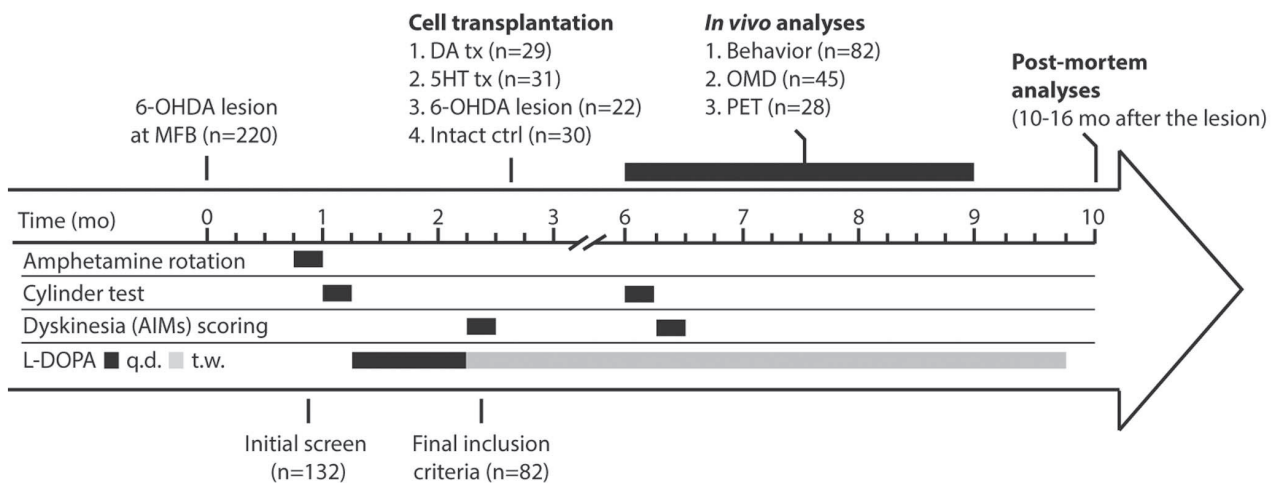


Figure 1. Experimental design. A total of 220 animals were lesioned with 6OHDA to remove the ascending dopamine (DA) projections unilaterally. The completeness of the lesions was confirmed with behavioral analysis and animals fulfilling the inclusion criteria were subjected to chronic daily L-DOPA treatment for induction of dyskinesia. Animals were then allocated to one of three groups balanced according to behavioral scores to receive either DA or serotonin (5HT)-rich tissue grafts or were followed as 6OHDA lesion group. Post-grafting follow up was about 7 months during which time animals underwent follow-up behavioral assessments with intervals as indicated under the study time-line. A sub-set of animals was then subjected to online microdialysis (OMD) for measurement of DA and 5HT release from the grafted neurons under baseline or after L-DOPA treatment or [^{18}F]fallypride PET imaging before termination. *Post mortem* analysis included both histological and biochemical end-points (q.d.: once a day, t.w.: twice a week)-
 doi:10.1371/journal.pone.0090759.g001

screen for selection of animals for further experimentation. Animals displaying rotational asymmetry of ≥ 6 full body turns/min (mean over 90 min) were selected for characterization using the cylinder test and then dyskinesia induction by daily L-DOPA injections.

For assessment of forelimb use in the cylinder test, the animals were allowed to move freely in a clear glass cylinder during video recording. Mirrors were placed behind the cylinder to be able to observe all forelimb contacts on the glass wall. The videotapes were evaluated by an observer blinded to the identity of the animals and the number of left and right paw touches on the cylinder wall were counted separately for at least 20 contacts. Data are expressed as left paw touches as % of total.

In order to establish stable L-DOPA-induced AIMs (induction phase), L-DOPA methyl ester (6 mg/kg; Research Organics, Cleveland, Ohio) combined with the peripheral DOPA decarboxylase inhibitor, benserazide (10 mg/kg, Sigma-Aldrich, Sweden) was dissolved in physiological saline and administered daily to each rat as an i.p. injection for a period of 4 weeks. The evaluation of the AIMs was performed according to the rat dyskinesia scale [3]. Briefly, the animals were placed individually in transparent plastic cages with a grid lid so that the rater can visualize every movement. A researcher blinded to the identity of the animals scored each animal every 20 min following the L-DOPA injection. The AIMs were classified into three subtypes according to their topographic distribution as forelimb, orolingual, and axial dyskinesia. Locomotive dyskinesia displayed as contralateral rotations were scored separately. The severity of each AIM subtype was scored from 0 to 4 (0: no abnormal behaviors detected, 1: occasional AIMs, i.e. present less than 50% of the time; 2: frequent AIMs, i.e. present more than 50% of the time; 3: continuous AIMs, but interrupted by sensory stimuli and 4: continuous AIMs, not interrupted by sensory stimuli). Half-points were used when the behavior of the animal were clearly in between the two defined points. The data are calculated as time-

integrated total scores and represented by sum of the orolingual, limb and axial subtypes.

To evaluate the effect of the 5HT receptor agonists on L-DOPA induced dyskinesia, selective 5-HT_{1A} agonist, 8-OH-DPAT ((\pm)-8-hydroxy-2-dipropylaminotetralin hydrobromide; TOCRIS, Sweden), and the 5-HT_{1B} agonist, CP-94253 (TOCRIS, Sweden) were injected subcutaneously 5 min before L-DOPA. The drugs were administered in combination at a dose of 0.1 mg/kg and 1.75 mg/kg for 8-OH-DPAT and CP-94253, respectively.

PET imaging study

A total of 28 rats were used for PET imaging starting from 6 months after transplantation and allocated in one of 3 groups on the basis of the dyskinesia scores and cylinder tests: 6OHDA lesion group (n=9), DA-graft (n=8) and 5HT-graft (n=11) groups. [^{18}F]fallypride ligand was chosen for the PET imaging session because this tracer has been used to access D₂/D₃R occupancy in rats, baboon and human striatum [18,19] and its ^{18}F -labelling enables successive PET scan sessions. Moreover, this ligand has been shown suitable for measurement of amphetamine effects on D₂/D₃ ligand binding in striatum [20,21]. L-DOPA treatment (6 mg/kg) was continued throughout the PET imaging period at the maintenance dose regimen. Each animal was imaged twice on two separate days: once under baseline conditions and a second time starting 30 min following an L-DOPA challenge (12 mg/kg). PET scans under baseline conditions were carried out 2 days after the preceding L-DOPA maintenance dose. Rats undergoing a PET scan in combination with the L-DOPA challenge did not receive the second maintenance injection within the same week.

Rats were scanned on a dedicated small animal PET scanner (MicroPET Focus 220, Siemens Medical Solutions USA, Inc.). Anaesthesia was induced by 4% isofluorane and maintained by 2 to 2.5% of isofluorane in a mixture of 100% O₂. Before scanning, the caudal vein was catheterized with a 26-gauge catheter for intravenous injection of the [^{18}F]fallypride ligand. During imaging, the head of each rat was fixed in a homemade

stereotactic frame compatible with PET acquisition and the animals were maintained at 37°C using a heating blanket. Two dynamic PET scans were performed on each day of imaging. The second scan started 15 min following completion of the first one. Rats from different groups were allocated to first or second imaging slot on a given day and received either baseline or L-DOPA challenge protocol on alternative days 2 weeks apart, so that each group were represented equally as many times in first or second scan time and in either order of the two scan protocols.

Radiolabeled tracer was injected as a single bolus concomitantly with the start of PET acquisition. The injected dose was adjusted to inject similar mass of radiotracer into each separate rat (0.944 ± 0.28 mCi; 0.486 ± 0.198 nmol).

Rats were sacrificed the day after their last PET experiment; the brain was removed and stored at -80°C .

To study competition of [^{18}F]fallypride binding in the striatal region with endogenous dopamine levels, four additional female Sprague-Dawley intact rats were scanned five times with a two-week wash-out interval between scans: one scan at baseline and four scans following increasing doses of amphetamine. Rats were subcutaneously injected with 0.1, 0.2, 1 and 2.5 mg/kg amphetamine 30 mins prior to tracer injection. These rats also underwent blocking studies (pre-saturation experiments) with a large excess of unlabeled fallypride (154.3 ± 3.89 nmol) injected 30 minutes prior to [^{18}F]fallypride in order to achieve full receptor occupancy. Displacement and receptor occupancy values (%) were calculated based on BP values measured under baseline and pre-saturation conditions.

Radiochemistry

Ready-to-inject, >99% radiochemically pure [^{18}F]fallypride (*N*-((2*S*)-1-(2-propenyl)-2-pyrrolidinyl)methyl)-5-(3-[^{18}F]fluoropropyl)-2,3-dimethoxybenzamide) was prepared from cyclotron-produced [^{18}F]fluoride (Cyclone-18/9 cyclotron, IBA, Louvain-la-Neuve, Belgium) on the basis of already published standard conditions [22] using a tosyloxy-for-fluorine nucleophilic aliphatic substitution in a commercially available TRACERLabTM FX-FN synthesizer (GEMS, Buc, France)[23]. [^{18}F]fallypride, as an ethanolic (15%) physiological saline (aq. 0.9% NaCl) solution (10–12 GBq batches, 10 mL-volume), is routinely obtained within 45 minutes starting from 30–35 GBq of [^{18}F]fluoride (28–40% non-decay-corrected overall isolated yields) with specific radioactivities ranging from 222 to 333 GBq/ μmol . Quality controls were performed on an aliquot of the ready-to-inject [^{18}F]fallypride preparation, in compliance with the in-house quality control/assurance specifications.

PET data analysis

Dynamic emission scans were acquired in list-mode format over 120 min. The data files were displayed as 3D sinograms with a maximum ring difference of 47 and a span of 3. The acquired data were then sorted into 31 time-frames [1*15 s, 5*30 s, 1*45 s, 6*1 min, 1*1.5 min, 4*2 min, 1*3.5 min, 5*5 min, 1*7.5 min, 6*10 min]. Finally, each emission sinogram was normalized, corrected for attenuation and radioactivity decay, and reconstructed using Fourier rebinning and 2-dimensional ordered-subsets expectation maximization (16 subsets, 4 iterations).

Time frames collected were summed to create an integrated image. In order to define volumes of interest (VOIs) using anatomical landmarks, rats underwent as well a T2-weighted MR imaging that was used for PET/MRI co-registration. To this aim, rats were placed on a 7 Tesla MR system (Varian-Agilent Technologies, USA) equipped with a gradient coil reaching 600 mT/m (120 μs rise time), a radiofrequency birdcage 1H coil

for transmission, and a 4-channel surface receive coil and T2-weighted images were acquired over a total acquisition time of 9 minutes. PET/MRI co-registration was then performed using the in-house image processing software Anatomist (<http://www.brainvisa.info>). Striatal VOI were delineated using the microPET Data analysis software ASIPro (ASIPro VM, Siemens) and ROI drawn over 13 to 15 continuous planes.

To measure *in vivo* the fraction of [^{18}F]fallypride non-specific binding, a 10-voxel-diameter spherical region of interest (voxel size of 0.47; 0.47; 0.796 mm) was drawn over the cerebellum, in a region devoid of D2R. The mean activity concentration values in all VOIs (left and right striata, cerebellum) were then calculated and plotted over time yielding regional time-activity curves. These curves were then normalized to the injected dose and body weight and expressed as standardized uptake values (SUVs).

Kinetic modelling analysis was performed using the PMOD software package (version 2.95; PMOD Technologies). D2R occupancy by the released DA in each set of experiments was estimated by calculating the distribution volume ratio (DVR) using the Logan noninvasive method [24]. This method which yields an estimate of specific binding (BP) through the relationship $\text{DVR} = \text{BP} + 1$, assuming the existence of a reference region, such as the cerebellum, which is almost devoid of dopamine receptor and can be used to assess the pharmacokinetics of the radiotracer in the absence of a specific compartment. For each PET experiment, BP was calculated based on 9 regression points, starting after an equilibrium time of 42.5 min post-injection.

Microdialysis experiments

The *in vivo* DOPA synthesis and DA release parameters in the striatum were assessed using a high resolution and sensitivity microdialysis protocol. For this purpose, the rats were anesthetized with 1–2% isoflurane mixed with 0.4 L/min O_2 and 1 L/min N_2O and placed in a stereotaxic frame. Microdialysis probes with a 3 mm membrane and 0.5 mm outer diameter (Agnthos Microdialysis, Sweden) were used. The probes were inserted into the striatum with the help of a holder and placed at AP: +1.1 mm, ML: -2.7 mm relative to bregma and DV: -5.5 mm from the dural surface. The tooth bar was set to -2.3 mm. This position corresponded to a position between the three graft deposits in the transplanted rats. The probes were connected to a syringe infusion pump (Model 100; CMA Microdialysis, Sweden) via polyethylene tubing and perfused with normal ringer solution containing 145 mM NaCl, 3 mM KCl and 1.3 mM CaCl_2 at a constant rate of 1 $\mu\text{L}/\text{min}$. To prevent oxidization of neurotransmitters studied here, an antioxidant solution containing 1 M acetic acid, 0.27 mM EDTA, 33 mM L-cysteine, and 5 mM ascorbic acid, was mixed with the dialysate at the outlet of the probe [25].

The samples were transferred via 5 μL loops simultaneously into two flow paths and were directly analyzed at 12.5 min time bins using Alexys online monoamine analyzer HPLC system (Antec Leyden, The Netherlands) consisting of a DECADE II electrochemical detector and VT-3 electrochemical flow cell. The precise technical description of the setup has been published earlier [26]. Briefly, the outlet of the microdialysis probe was connected to a 14-port external valve that can direct the dialysate into two separate flow paths. Two different mobile phases – optimized for the detection of the respective metabolites – were used in each of the two flow paths. The first mobile phase (50 mM phosphoric acid, 8 mM NaCl, 0.1 mM EDTA, 12.5% methanol, 500 mg/L octane sulphate; pH 6.0) used for the detection of DA and 5HT ran through a 1 mm \times 50 mm column with 3 μm particle size (ALF-105) at a flow rate of 75 $\mu\text{L}/\text{min}$. The second mobile phase (50 mM phosphoric acid, 50 mM citric acid, 8 mM

NaCl, 0.1 mM EDTA, 10% methanol, 600 mg/L octane sulphate; pH 3.2) was used for the detection of DOPA, DOPAC, HVA and 5-HIAA, which passed through a 1 mm×150 mm column with 3 µm particle size (ALF-115) at a flow rate of 100 µL/min.

We designed three different online microdialysis (OMD) protocols to address different questions relating to the hypothesis tested in this study:

OMD Protocol 1. KCl-induced DA and 5HT release in the striatum. This protocol was implemented to measure the releasable pool of DA and 5HT in the striatum after grafting and to determine how these pools were affected upon L-DOPA administration. The placement of the microdialysis probe was followed by one hour of equilibration period before collection of a total of 23 samples over 5 hours (i.e., each analysis point corresponded to a sampling interval of 12.5 min). Three baseline samples were collected before the dialysate was changed to a modified ringer lactate solution containing high KCl (51 mM NaCl, 100 mM KCl and 1.3 mM CaCl₂) for a single sampling interval in order to stimulate the readily releasable pool of DA and 5HT, and then switched back to the normal ringer lactate solution. The burst of neurotransmitter release was evident in the sample with high KCl while the recovery took place during the following three sampling intervals. These 4 consecutive samples were, therefore, analyzed together to estimate the total KCl-induced release by calculating the area under the curves. After waiting for additional three time bins, 12 mg/kg L-DOPA (plus 10 mg/kg benserazide hydrochloride) was injected systemically. A second challenge with KCl was then applied during the 6th time bin (62.5–80 min after L-DOPA administration) and data analyzed for four consecutive sampling intervals as described above.

OMD Protocol 2. Extracellular DA levels under physiological conditions. For this purpose, we designed an OMD protocol in freely moving rats where we first obtained measurements in baseline and then injected these animals with 12 mg/kg L-DOPA (plus 10 mg/kg benserazide hydrochloride)—which lead to peak dose dyskinesia that lasted for about 2 hours—and continued sampling the extracellular DA levels during this time without any other intervention or drug treatment.

OMD Protocol 3. Extracellular DA levels after blockade of the DAT by nomifensine. This protocol was performed in anesthetized animals, as in Protocol 1. In this experiment, measurements in baseline conditions were followed by 12 mg/kg L-DOPA (plus 10 mg/kg benserazide hydrochloride) injection, and 75 min later, the dialysis solution was switched to modified ringer lactate containing 25 µM of nomifensine and samples were analyzed for an additional 2 hours.

In vitro dopamine receptor binding assay

Two groups of rats (DA denervated rats, n=12; intact rats, n=12) were treated with L-DOPA+benserazide (n=7 and 7 for the two groups, respectively) or processed as non-injected controls (n=5 per group). Sixty minutes later the animals were decapitated and striatum was dissected by removing striatum from the surrounding tissue. The dissected tissue were kept on dry ice and stored at -80°C until further use. On the day of analysis, the samples were homogenized using ultrasonic disintegrator in ice-cold assay buffer (50 mM Tris-HCl, 120 mM NaCl, 1 mM EDTA, 5 mM KCl, 1.5 mM CaCl₂, 4 mM MgCl₂, pH 7.4). The homogenate was diluted in ice-cold buffer and dispensed into two 96 well plates (MultiScreen_{HTS} FB, membrane pore size, 1.0/0.65 µm durapore, opaque, Millipore). One of the plates was used for D1R binding assay while the other one was used for D2R assay. A total of 50 and 350 µg of tissue lysate was used for each

well in D1R and D2R binding assays, respectively. Two different radioactive ligands ([³H]SCH23390 for D1R and [³H]raclopride for D2R, PerkinElmer) were used at eight different concentrations (ranging between 0.5–15 or 1–30 nM) for each assay. In order to determine the non-specific binding, 100 mM SCH23390 or 300 mM haloperidol was used for each concentration in the two assays, where the unlabeled compound was added to the homogenate 30 min prior to the incubation with the tritiated ligand. Plates were then incubated for 2 h at room temperature. Plates were then filtered by using MultiScreen vacuum manifold (Millipore) and allowed to air-dry for 24 h. Next day, the plates were punched using a MultiScreen Punch Kit (Millipore) in order to isolate the tissue bound membranes, which were then collected individually in scintillation vials. The vials were instantly filled with LSC cocktail (Ultima Gold, PerkinElmer). Fourty-eight hours later, the radioactive decay was determined in each vial using a liquid scintillation counter (Beckman LS 6500). Data obtained in the wells treated with the cold compounds was used to measure the non-specific binding under each condition, while the corresponding wells without the unlabeled compound gave the total binding.

Histological analysis

Rats were deeply anesthetized with 300 mg/kg sodium pentobarbital (Apoteksbolaget, Sweden) and perfused through the ascending aorta with 50 mL physiological saline at room temperature over 1 min followed by 250 mL ice-cold 4% paraformaldehyde (PFA) over 5 min. Brains were post-fixed in 4% PFA solution for 2 h before being transferred into 25% sucrose solution for cryoprotection, where they were kept until they had sunk (typically within 24–48 hrs). The brains were then sectioned in the coronal plane on a freezing microtome at a thickness of 35 µm. Sections were collected in 6 series and stored at -20°C in a phosphate buffer containing 30% glycerol and 30% ethylene glycol until further processing.

Immunohistochemical stainings were performed on free-floating sections. For this purpose, brain sections were first rinsed with potassium-phosphate buffered saline (KPBS), and then endogenous peroxidase activity was quenched by incubation in a mixture of 3% H₂O₂ and 10% methanol in KPBS for 30 min. After a series of rinsing steps in KPBS, non-specific binding sites were blocked by incubation in KPBS containing 0.25% Triton-X and 5% normal serum matched to the species used to raise the corresponding secondary antibody. Samples were then incubated overnight at room temperature in primary antibody solution containing 5% serum and 0.25% Triton-X. The primary antibodies used for immunohistochemical staining were as follows: mouse anti-TH (MAB318, Millipore; working dilution 1:2000), rabbit anti-5HT (20080, Immunostar; working dilution 1:10,000), mouse anti-SERT (MAB 1564, Millipore; working dilution 1:1000) and goat anti-pan-FosB (SC-48X, Santa Cruz Biotechnology; working dilution 1:15000). On the second day, the sections were rinsed in KPBS and then incubated for 1 h at room temperature in 1:200 dilutions of appropriate biotinylated secondary antibody solutions (horse anti-mouse, goat anti-rabbit and sheep anti-goat for antibodies as appropriate; Vector Laboratories, USA). After rinsing, the sections were treated with avidin-biotin-peroxidase complex (ABC Elite kit, Vector Laboratories) and the color reaction was developed by incubation in 25 mg/mL 3,3'-diaminobenzidine and 0.005% H₂O₂. In order to increase the contrast in the FosB staining 2.5 mg/mL Nickel sulphate was added in the DAB solution prior to the color reaction. Sections were mounted on chrome-alum coated glass slides, dehydrated and cover-slipped with Depex mounting media (Sigma).

Stereological analysis

The numbers of TH- and 5HT-immunoreactive cell numbers in the striatum were estimated using an unbiased stereological quantification method by employing the optical fractionator principle [27]. All quantifications were done after blinding the identity of the sections by a coding system. The borders for the region of interest was defined by using a 4x objective, whereas the actual counting was performed using a 60x Plan-Apo oil objective (Numerical aperture = 1.4) on a Nikon 80i microscope equipped with an X-Y motorized stage, a Z-axis motor and a high-precision linear encoder (Heidenhein). All three axes and the input from the digital camera that were controlled by a Computer Assisted Toolbox Software (New CAST) module in VIS software (Visiopharm A/S, Denmark), which carries out the procedure with a random start and systematic sampling routine. The sampling interval in the X-Y axis was adjusted so that at least 100 cells were counted in each grafted striatum. Upon completion of the quantification of batches, samples were moved to a database for further analysis using appropriate statistical and graphical tools. Coefficient of error attributable to the sampling was calculated according to Gundersen and Jensen [28] and values ≤ 0.10 were accepted.

Image analysis

The numbers of FosB/ δ FosB immunoreactive cells in the striatum were analyzed on images captured using a 10x Plan-Fluor objective on a Nikon BXA microscope equipped with a Olympus DX72 camera using cellSens standard 1.5 software (Olympus Corporation). The images were captured from the striatal level corresponding to AP +1.20 relative to bregma according to the rat brain atlas of Paxinos and Watson [29]. The quantification was carried out using TIFF formatted images analyzed by using the ImageJ software (Version 1.42i, NIH). After background subtraction, the total numbers of profiles specifically labeled with FosB/ δ FosB were counted using the particle analysis tool. The density of immunopositive FosB/ δ FosB profiles was expressed as number of immunoreactive cellular profiles per mm^2 .

Statistical analysis

The statistical analysis pertaining to the behavioral, histological microdialysis and imaging data were conducted using the SPSS statistical package for Mac version 19 (SPSS Inc., Chicago). Initial analysis was conducted using two-way ANOVA and the general linear model. When ANOVA gave significant effects this was followed by pairwise comparisons adjusted using Bonferroni correction.

Estimation of the maximum binding (B_{max}) and the binding affinity (K_d) of the D1 and D2 ligands in the *in vitro* receptor binding assays were analysed using generalized nonlinear least squares using [the gnls function in] the nlme 3.1–106 [30] package in R software, version 2.15.2 [31]. The model was

$$\text{Bound} = (1 - \text{Type}) * \alpha_{i} * \text{Conc} \div (\beta_{i} + \text{Conc}) + \gamma_{i} * \text{Conc} + \epsilon$$

Where *Bound* is the concentration of chemically bound ligand after adding *Conc* to the sample. *Type* is an indicator being zero if only Hot ligand is added and 1 if Cold and Hot ligand is added. α_{i} is the asymptotical maximum of bound ligand for treatment *i* ($i = 1, \dots, 4$), β_{i} is the half-saturation constant for treatment *i*, and γ_{i} is the unspecific non-saturable binding in treatment *i*. ϵ is normally distributed with variance propor-

tional to a power function fitted value in order to obtain homoscedasticity. Comparisons of estimates between groups were adjusted for multiple comparisons using the package multcomp v 1.2–15 [32].

Results

The precise mechanism of action by which serotonin (5HT) neurons contribute to LID in the parkinsonian striatum and how transplantation of DA neurons alleviate it while 5HT neurons worsen LID was investigated. In order to obtain results that can be unambiguously interpreted, we compared behavioral, biochemical and imaging data from intact rats and 6OHDA lesioned dyskinetic animals with that obtained from dyskinetic parkinsonian rats that received either one of two types of grafts: DA neuron-rich grafts obtained from the VM region or 5HT neuron-rich tissue obtained from the dorsal pontine raphe region of day 14 rat embryos. All animals were characterized with respect to motor behavioral deficits in the cylinder test and response to L-DOPA in the abnormal involuntary movements (AIMs) scale. Subsets of animals from each group were subjected to one of three different microdialysis protocols for assessment of extracellular DA and 5HT levels, or PET imaging to monitor dopamine D2 receptor (D2R) occupancy during the *in vivo* follow up period, and histological and biochemical end-points at termination 8–14 months after grafting (Fig. 1).

The 6OHDA toxin applied in the MFB caused a near complete lesion of the midbrain dopaminergic system, therefore removing the ascending projections to the striatum (compare Fig 2A and 2B), whereas the serotonergic projections from the raphe nucleus remained intact, or in some cases were partially affected, as visualized by immunohistochemical staining of the serotonergic axon terminals using antibodies against 5HT (Fig 2E, F) or the serotonin transporter (SERT; Fig 2I, J). Transplantation of VM cells into the striatum gave rise to a new innervation source as numerous dopaminergic neurons survived and re-innervated the depleted host striatum (Fig 2C). These grafts contained, on the average, 5515 ± 984 TH-positive cells as well as a smaller contribution of 5HT expressing neurons (1527 ± 475 cells; Fig 2M), constituting about 1.42 and 0.49% of the total number of cells grafted in these animals, respectively (Fig 2N). When a more caudal tissue piece was used for the grafting, however, the contribution of the DA neurons was near completely abolished (as this region does not give rise to DA neurons during embryonic development), whereas the number of 5HT neurons was increased to 4169 ± 772 corresponding to about 1.45% of total cells grafted in this group (Fig 2G, H and quantified in M, N). Importantly, in the absence of the DA neurons, the grafted 5HT neurons formed an intense supra-normal axon terminal network in the dorsal striatum, where the serotonergic innervation would otherwise be sparse (Fig 2L, compare with I–K).

The most important difference between the two types of grafts in the context of this study was the differential ability of DA neuron-rich grafts to alleviate both the motor deficits induced by 6OHDA lesion as well as the dyskinesia induced by pulsatile administration of L-DOPA in the lesioned animals. Here, we documented the functional effects of the DA grafts by assessing forelimb use in the cylinder test. As expected, the 6OHDA lesion group displayed a deficit in use of the left (affected) forelimb, which remained unchanged in the follow-up period. There was no change in cylinder test performance after 5HT grafts, whereas the DA neurons were able to establish a functional improvement in the DA-neuron grafted animals (Fig 3A). Secondly, as the animals were subjected to chronic daily L-DOPA treatment, all animals

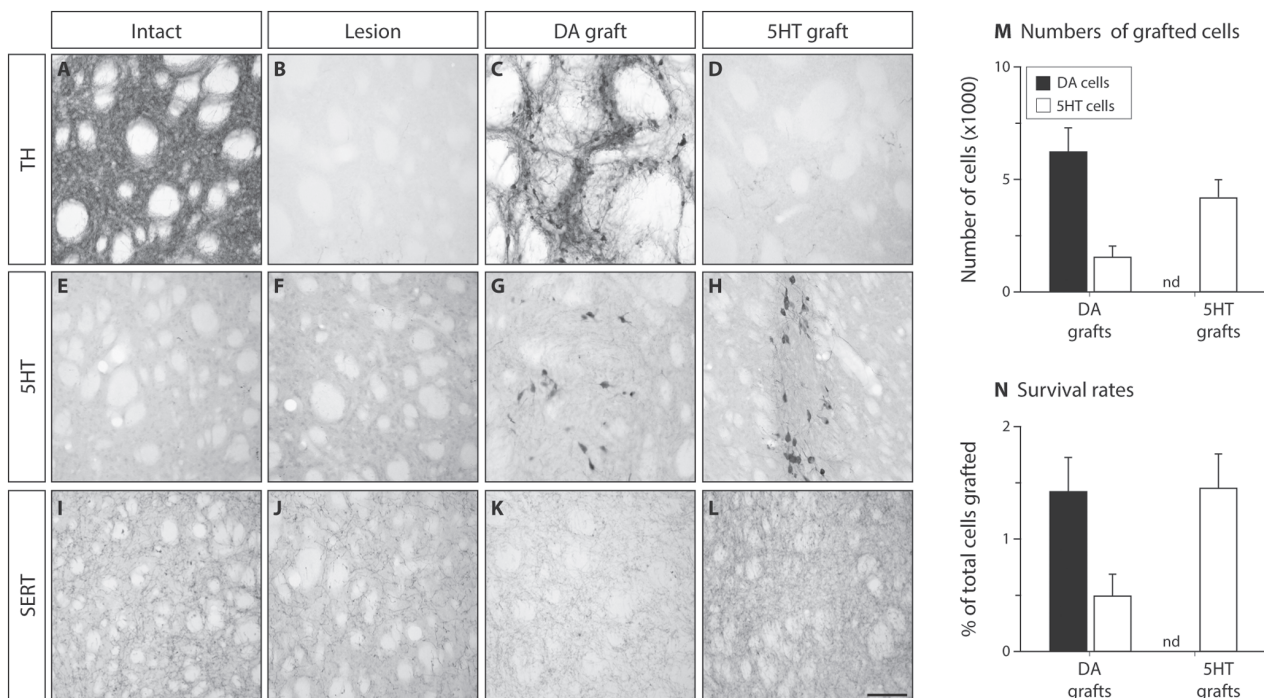


Figure 2. Histological characterization of the grafts. Striatal sections from fixed tissue were stained against tyrosine hydroxylase (TH), serotonin (5HT) or serotonin transporter (SERT) using immunohistochemistry. The 6OHDA lesion caused a complete lesion of the dopamine (DA) terminals in the striatum (compare A and B). VM tissue known to be rich in DA cells resulted in survival of over 6,000 TH positive cells in these long-term grafts (C, M), while 5HT grafts had no TH-positive cells (D). Immunostainings with 5HT showed numerous serotonergic cells (over 4,000) in the 5HT grafts (H), and about 1500 cells in the DA grafts (G, M). These numbers correspond to survival rates of 1.42–1.45% of the total grafted cells and illustrate excellent graft survival in both groups (N). As 5HT antibodies do not stain the serotonergic terminals well, we processed an additional set slides for SERT immunohistochemistry and confirmed that the 5HT grafts provided an intense fiber terminal network above the level seen in the intact striatum (compare I and L), whereas neither the 6OHDA lesion nor the DA grafts had a detectable effect (J, K). nd: not detected. Scale bar in panel L represents 50 μ m and applies to all panels. doi:10.1371/journal.pone.0090759.g002

had moderate-to-severe dyskinesia that could be seen as orolingual and limb hyperkinesia, axial dystonia and locomotive dyskinesia. Using a well-established rating scale [3] the L-DOPA-induced dyskinesia was quantified on three occasions; first prior to transplantation, secondly at 12 weeks post grafting when the motor improvement was documented in the cylinder test and a week later after co-injection of L-DOPA and a mixture of 5HT-1A and 1B receptor agonists (Fig 3B). We found that DA neuron rich grafts reduced dyskinesia by 30.6% while in the 5HT grafted group there was a 43.7% increase from the baseline evaluation. Thus, at 3 months after grafting, the 5HT group had 2-fold higher dyskinesia scores as compared with DA grafted animals. In all groups, dyskinesia could be substantially reduced or blocked by co-administration of the 5HT1A and 1B agonists (8-OH-DPAT and CP-94253, respectively) at doses affecting primarily the pre-synaptic auto-receptors (Gray bars in Fig 3B) [10]_ENREF_18. The residual dyskinesia in these animals was largely due to the differences between the duration of action of the agonists and L-DOPA – as the effect of the agonists waned off, abnormal movements became detectable at the end of the peak dose dyskinesia curve (Fig 3C). Of note, the reduction of dyskinesia in the DA neuron-rich grafts was accompanied with normalization of δ Fos-B immunoreactive nuclei in the striatum whereas 5HT neurons lacked the ability to mediate a similar effect (Fig 4). These findings confirmed that the grafts were functional and had differential effects on motor performance and response to L-DOPA.

Investigation of whether DA released from 5HT neurons contributed to worsening of dyskinesia via a mechanism that involved fluctuations of extracellular DA concentrations with swings into the supra-physiological levels, required us to probe a series of important factors. The first step was to demonstrate that a new releasable pool of DA would emerge following systemic administration of L-DOPA in the denervated striatum, which would be increased even further in the 5HT grafted animals. For this purpose, we performed an online microdialysis (OMD) study in order to measure the extracellular levels of DA and 5HT that can be recovered by KCl stimulation (Fig 5A, C). The KCl challenges were done both under baseline conditions (i.e., prior to L-DOPA) and 60 min after injection of 12 mg/kg L-DOPA and 10 mg/kg benserazide hydrochloride which results in stable blood L-DOPA levels for at least three hours [33]. The total releasable pool of DA was estimated by calculating the area under the curve over 3 time bins (12.5 min each) following each KCl administration (Fig 5B). We found that under baseline conditions, 5HT grafts had no or minimal releasable pool of DA and was not different from the 6OHDA lesion group, whereas the DA neuron rich grafts re-constituted a clearly distinguished releasable pool, albeit at about 10% of the capacity of the intact striatum. The situation was different after the L-DOPA administration. Here, we detected a burst of DA in the 5HT-grafted animals upon KCl challenge (Fig 5). The magnitude of DA released from 5HT terminals was similar to that obtained from DA-grafted animals, suggesting that 5HT terminals became a major source of DA after L-DOPA

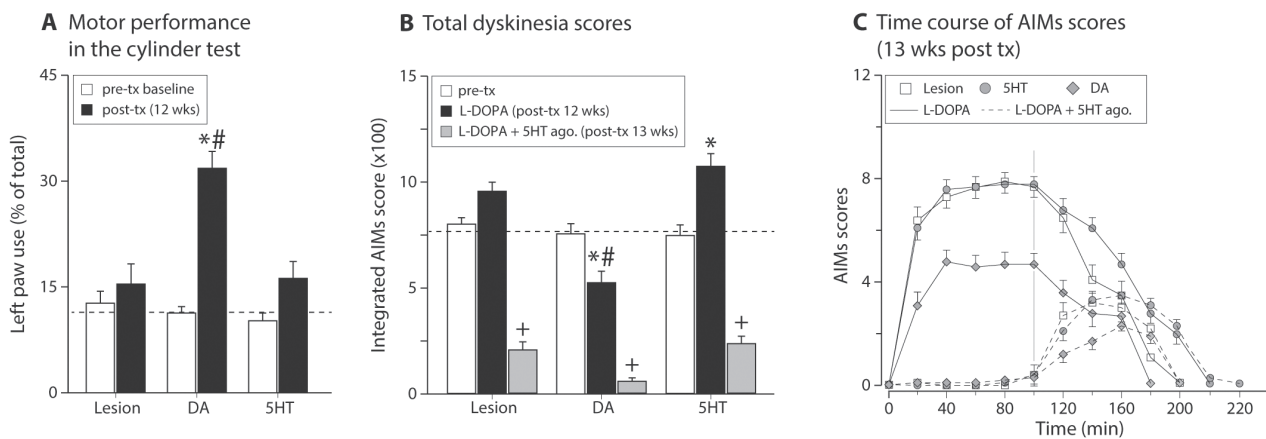


Figure 3. Behavioral characterization of the grafted animals. Cylinder test is a well-established spontaneous motor test based on limb-use asymmetry known to be sensitive to graft-induced functional recovery (A). All animals were severely impaired in the use of left forelimb (contralateral to the lesion side, open bars in A). 5HT grafts were functionally ineffective, whereas DA grafts ameliorated the limb use deficit significantly at 12 weeks after grafting (Two-way ANOVA $F(5,163)=16.75$, $p<0.001$; followed by pairwise comparison adjusted using Bonferroni, $p<0.0083$). The animals were then challenged with L-DOPA to assess if the grafts were able to modulate the dyskinesia that were established prior to transplantation (B; two-way ANOVA $F(8,245)=63.48$, $p<0.001$; followed by pairwise comparison adjusted using Bonferroni, $p<0.0033$). DA-cell rich grafts reduced the dyskinesia, while 5HT cells were ineffective or even aggravated the dyskinesia. Co-treatment of the animals with 5HT receptor 1A and 1B agonists (0.1 mg/kg 8-OH-DPAT and 1.75 mg/kg CP-94253) reduced the dyskinesia significantly in all groups (B). The residual abnormal movements were primarily due to differential duration of action of L-DOPA and the agonists (C). tx: transplantation, *: different from pre-tx baseline; +: different from post-tx 12 wks; #: different from 6OHDA lesion and 5HT groups. doi:10.1371/journal.pone.0090759.g003

administration in these animals (Fig. 5B). Importantly, exogenously administered L-DOPA caused no change in DA release in the intact striatum or the DA-grafted animals, suggesting that the dopaminergic terminals in these animals were able to keep the extracellular levels of DA unchanged and effectively buffer the newly synthesized DA in the tissue. Stability of the dopaminergic tone was maintained despite the fact that the 5HT terminals were involved in conversion of L-DOPA to DA in intact controls and DA-grafted rats (Fig. 5C), as KCl-induced 5HT release was diminished after L-DOPA administration in essentially all groups (change varied between 25–60%; Fig 5C, D). These observations illustrated that L-DOPA administration would involve an ectopic

DA synthesis in 5HT terminals under all circumstances but that this would be effectively buffered by efficient re-uptake in the presence of a dense DA terminal network in the vicinity of the serotonergic terminals.

Next, we investigated how extracellular DA levels were changed upon L-DOPA administration under physiological conditions (i.e. in the absence of KCl challenge). For this purpose, we performed OMD in awake and freely moving rats that were naïve to L-DOPA. We first obtained measurements at baseline and then injected these animals with 12 mg/kg L-DOPA – which lead to peak dose dyskinesia that lasted for about 2 hours – and continued sampling the extracellular DA levels during this time period

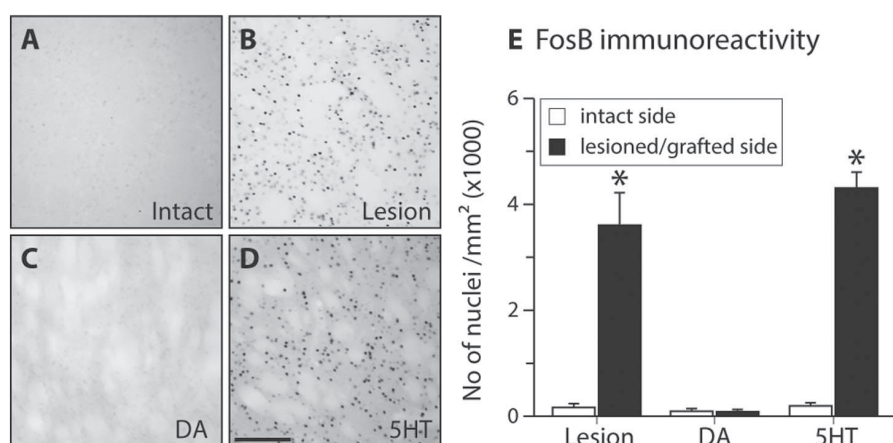


Figure 4. Analysis of FosB induction. The numbers of FosB/δFosB -positive cells in the striatum were assessed on a single coronal section corresponding to level +1.2 mm from bregma. Digital images were taken from the dorsolateral striatum. 6OHDA lesion group and 5HT graft animals showed significant increase in the induction number of FosB/δFosB positive profiles while in DA grafts this remained very low and similar to intact striatum (Two-way ANOVA $F(5,46)=75.05$, $p<0.001$; followed by pairwise comparison adjusted using Bonferroni, $p<0.0083$). *: Different from intact side and DA grafts. Scale bar in panel D represents 50 μm and applies to all panels. doi:10.1371/journal.pone.0090759.g004

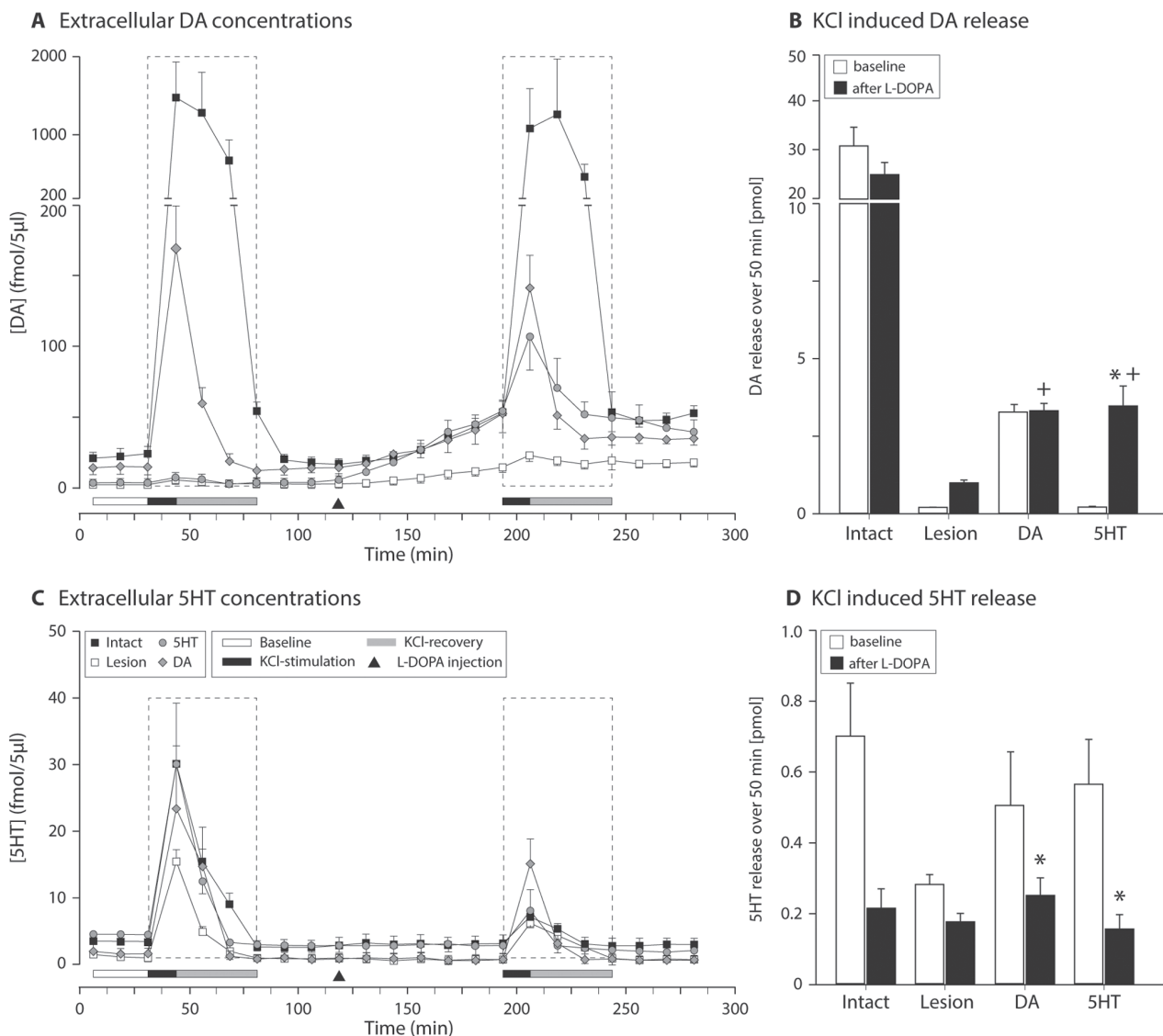


Figure 5. Assessment of releasable pool of DA and 5HT in the grafted animals using on-line microdialysis. Extracellular (extra-synaptic) DA levels were measured in DA depleted rats, in animals with DA and 5HT grafts as well as intact controls under anesthesia (A). This protocol included baseline assessment followed by KCl-induced release both prior to and following L-DOPA administration. Quantification of total releasable DA by KCl showed that a new pool of DA release sites emerged in the 5HT grafted animals after L-DOPA treatment, whereas this capacity was not measurable in the absence of L-DOPA (B, two-way ANOVA $F(5,23)=28.75$, $p<0.001$; followed by pairwise comparison adjusted using Bonferroni, $p<0.0083$). Simultaneous measurement of 5HT release is shown in C and quantified in D. *: different from baseline; +: different from 6OHDA lesion group, comparisons are made excluding intact rats. doi:10.1371/journal.pone.0090759.g005

(OMD results are shown in Fig. 6A, B, while the corresponding dyskinesia rating is given in Fig. 6C, D). The results were interesting: As expected, DA levels in the intact controls and DA-grafted animals were stable with minimal changes upon L-DOPA challenge. In the 6OHDA lesioned animals, DA levels at baseline were very low (about 8% of intact), and started to rise after L-DOPA before stabilizing at about the same level as in the DA grafted animals (Fig. 6A), despite that the 6OHDA lesion group had more severe dyskinesia while DA grafts reduced them in the transplanted group. Moreover, in the 5HT-grafted animals – where the dyskinesia was most severe – the changes in extracellular DA levels followed a similar drift as in 6OHDA lesion group, but reached levels comparable to that seen in the intact animals

(Fig 6B). There was however no indication that DA released from the serotonergic terminals reached supra-physiological levels.

To establish whether DA released from serotonergic terminals resulted in abnormal, post-synaptic activation of the striatal neurons – as a basis to induce and/or worsen dyskinesia – we investigated whether the occupancy of DA receptors upon L-DOPA administration in these animals surpassed normal physiological levels. This would be reasonable to expect based on the earlier stated hypothesis postulating that DA released from 5HT terminals would be uncontrolled and thus could exceed the physiological levels normally seen in the intact striatum [10]. Moreover, the results from the KCl-challenge experiments described above confirmed that a new pool of DA had indeed

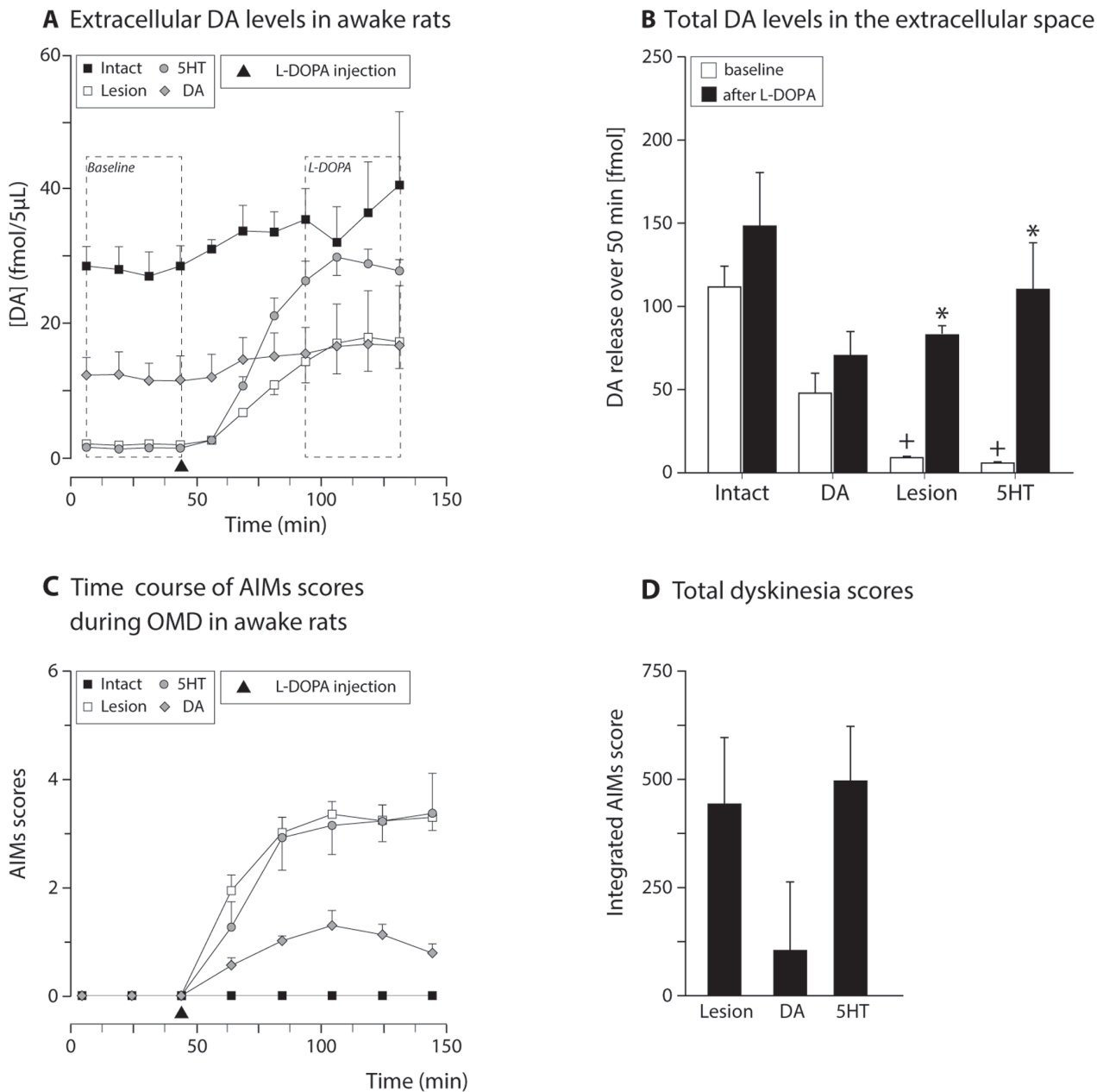


Figure 6. Assessment of changes in extracellular DA levels following L-DOPA injection. Animals were subjected to on-line microdialysis measurements either under baseline conditions, or following a systemic injection of 12 mg/kg L-DOPA without any perturbation of the release sites using release-inducing drugs. Time course data is shown in A, while quantification of the two phases (4 time bins in each case) is given in panel B (Two-way ANOVA, $F(7,27) = 12.15$, $p < 0.001$; followed by pairwise comparison adjusted using Bonferroni, $p < 0.0071$). Panel C illustrates the dyskinesia rating scores obtained during the OMD experiment as the animals were sampled in awake and freely moving state. Panel D shows the integrated AIMs data from this session (One-way ANOVA, $F(2,10) = 13.11$, $p = 0.003$; followed by pairwise comparison adjusted using Bonferroni, $p < 0.017$). Note that the dyskinesia seen in lesion and 5HT groups occur in the absence of supra-normal DA levels as detected by the probe in the striatum *: Different from baseline; +: different from intact; #: different from lesion and 5HT groups. doi:10.1371/journal.pone.0090759.g006

emerged after L-DOPA administration in these animals, confirming that the substrate for this abnormal release mechanism existed. Demonstration of the presence of supra-physiological DA in the 5HT grafted animals, however, required a different measurement technique than microdialysis as this method would only inform on extracellular DA that diffuses in the extra-synaptic space and is taken up by the probe, as opposed to DA levels at the specific

release sites, which in turn determines the level of activation of DA receptors (i.e., their occupancy by DA). Therefore, we utilized [^{18}F]fallypride PET imaging as a means to estimate occupancy of the D2R pool *in vivo* by calculating the binding potential (BP) of the ligand to the receptors in the presence and absence of L-DOPA (Fig. 7). Under baseline conditions (i.e., in the absence of L-DOPA), animals with unilateral 6OHDA lesions showed increased

[¹⁸F]fallypride ligand binding to D2R's compared with the contralateral intact side, where dopamine from the preserved ascending projection to the striatum competes with [¹⁸F]fallypride at the D2R binding (Fig. 7A). The DA-neuron rich grafts completely normalized this abnormally high binding suggesting that these cells can re-constitute a normal DA signaling at the appropriate receptor sites in the living animal (Fig. 7B), while the 5HT grafts lacked this ability (Fig. 7C). We expected that the administration of L-DOPA in the 5HT-grafted animals would significantly alter the BP of [¹⁸F]fallypride tracer, if indeed it resulted in abnormally high DA levels in the peri-synaptic space. However, we found that the administration of L-DOPA did not result in any change in the BP obtained in these animals (compare BP values in Fig. 7D and E).

The [¹⁸F]fallypride PET imaging data were at odds with the expected results but supported the interpretation that DA released from 5HT terminals (both in the presence of a 5HT graft and in the DA denervated striatum) resulted in low concentrations of DA at the D2R containing sites thus a low occupancy of these receptors. In order to demonstrate the displacement of [¹⁸F]fallypride, we performed additional experiments where we determined the dose-response relationship between amphetamine-induced DA release and changes in [¹⁸F]fallypride BP. In occupancy studies using amphetamine challenge, BP values were compared to baseline values. Dose dependent decreases in [¹⁸F]fallypride BP (−2.36%, −9.32%, −12.48%, and −17.93%) were seen in the striatum following 0.1, 0.2, 1 and 2.5 mg/kg

doses of amphetamine, corresponding to 38.3–434.3 fmols DA released in the extracellular space in intact rats, respectively (Fig. 8A–B). In addition, full saturation studies using a large excess of unlabeled fallypride injected prior to the radiotracer indicated that 88.31% of the [¹⁸F]fallypride *in vivo* binding relates to specific (displaceable) binding to dopamine receptors. Moreover, up to about 20% of the receptor pool was sensitive to displacement by endogenous DA released in the extracellular space after amphetamine treatment. The two parameters (extracellular DA levels and % changes in BP) correlated with one another and suggested a logarithmic relationship (Fig. 8C), note however the data are obtained in different animals due to technical difficulty of simultaneous measurements.

To confirm the above PET imaging results obtained *in vivo*, we used the gold-standard *in vitro* receptor assays to directly determine the K_d and B_{max} values for the D1 and D2 receptors. For this purpose, we analyzed the brains of a separate group of intact and 6OHDA lesioned rats killed either under baseline or 1 hr after L-DOPA injection at the peak of dyskinesia. Striatal tissue from these brains was processed for D1R and D2R receptor binding using [³H]SCH23390 or [³H]raclopride ligands (Fig. 7F–I). Comparison between baseline and post-L-DOPA conditions in the intact brain showed that the primary site of activity for the newly synthesized DA was at the D2R (Fig. 7F,H), while no significant change occurred at the D1R (Fig. 7G,I). This suggested a selective activation of the D2R by DA after released from the endogenous terminals. In the lesioned striatum, where DA release is

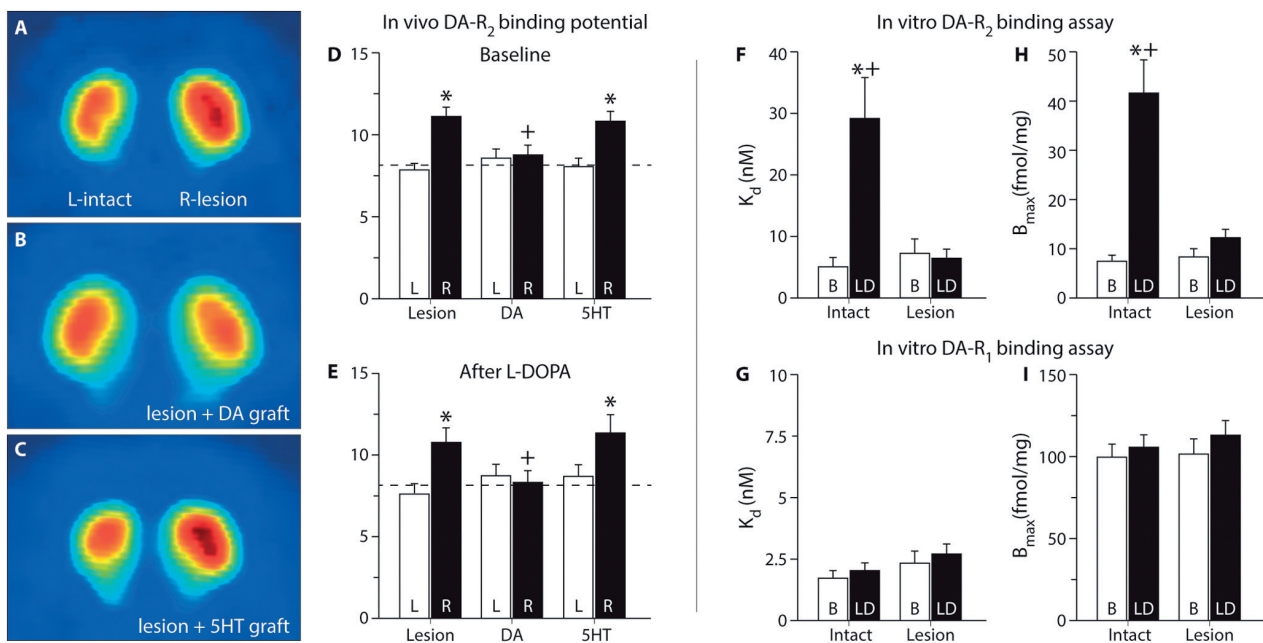


Figure 7. Assessment of striatal dopamine D2 receptor occupancy using positron emission tomography imaging. A subset of animals (n = 28) were subjected to two [¹⁸F]fallypride PET imaging experiments between 4–7 months after grafting. The first examination was done under baseline conditions whereas the second one was performed starting 30 min after L-DOPA treatment. This radioligand binds to the D2 receptors. The signal is increased when the endogenous ligand is lost, as seen in the 6OHDA lesion group under baseline conditions (A). The abnormally increased binding is completely normalized in DA grafted rats (B), but remained unchanged in the 5HT-grafted animals (C). The imaging data was quantified using Logan plots to determine the binding potential in the striatal tissue (D; two-way ANOVA F (5,55) = 6.70, p < 0.001; followed by pairwise comparison adjusted using Bonferroni, p < 0.008). L-DOPA injection 30 min after L-DOPA treatment did not result in any change in the binding potential (E; two-way ANOVA F (5,55) = 3.15, p = 0.15). *In vitro* receptor binding assay was performed for D2R (F,H) and D1R (G,I) and analyzed using a generalized non-linear model. In panel F and H, post-hoc comparisons between B and LD in the intact brain is p < 0.001 for K_d and < 0.002 for B_{max}, respectively and post-hoc comparisons between LD injected intact and lesioned brains is p < 0.001 for K_d and < 0.003 for B_{max}, respectively. L: left (intact) side, R: right side, B: Baseline; LD: L-DOPA treatment, K_d: binding affinity, B_{max}: Receptor density. *: Different from intact side; +: different from 6OHDA lesion group. doi:10.1371/journal.pone.0090759.g007

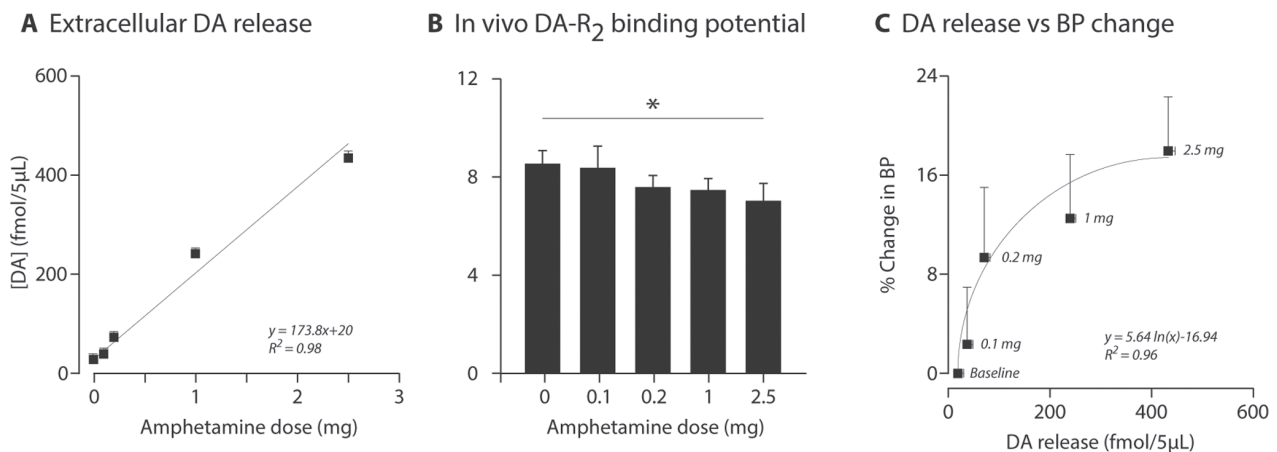


Figure 8. The relationship between dose of systemic amphetamine administration, DA concentrations and [¹⁸F]fallypride binding potential. Extracellular DA levels following different doses of amphetamine measured using online microdialysis (A). Note the tight and linear correlation between the two parameters. In animals pre-treated with the same doses of amphetamine, the binding potential (BP) for [¹⁸F]fallypride was reduced (B, *: effect of dose, one-way repeated ANOVA $F(3,9) = 6.99$, $p = 0.006$). The relationship between extracellular DA concentration and BP followed a logarithmic curve (C). The formulas indicated in panels A and C refer to the best fit for the respective data. doi:10.1371/journal.pone.0090759.g008

predominantly from the ectopic serotonergic terminals, the results were different as no change occurred at the D2R.

Taken together, these findings lead us to consider an alternative hypothesis to the previously held model (see discussion). In order to further substantiate the evidence to support this hypothesis, and demonstrate the magnitude of difference in DA released from DA-neurons and that released from 5HT-neurons, we carried out a third microdialysis study where we monitored the DA captured by the microdialysis probe after blockade of DAT by nomifensine (Fig. 9). Inhibition of the re-uptake sites by nomifensine resulted in a rapid and dramatic rise in the amount of DA captured by the microdialysis probe and revealed the true difference in the amount of DA that is generated at the synaptic site in the intact striatum and re-constituted after grafting DA neurons versus the very low levels in the 6OHDA lesion group and 5HT-grafted animals (time line shown in Fig. 9A). We found that the total amounts of DA recovered in DA grafted animals and in the intact rats were 5.2–8.9, and 16.2–28.1 fold higher than the lesioned and 5HT-grafted groups, respectively (Fig. 9B).

Discussion

DA released from serotonin neurons as a false neurotransmitter is a key factor in the induction of LID in the 6OHDA rat model of PD. However, the precise mechanism accounting for this event has not been demonstrated. The so-called pre-synaptic serotonergic mechanism of LID stipulates that an abnormally high and uncontrolled DA release might be the underlying pathophysiological event contributing to induction and maintenance of dyskinesia in animal models of PD [34,35]. Here we designed experiments to directly test the validity of the hypothesis that upon administration of exogenous L-DOPA, DA released from serotonergic terminals reaches supra-physiological levels and whether DA released as a false neurotransmitter is associated with abnormally high occupancy of DA receptors on the striatal neurons.

For this purpose, we compared the *in vivo* DA release properties and D2R occupancy under 4 conditions: (1) intact striatum where the DA terminal network is intense and far above the endogenous 5HT terminal density; (2) lesioned striatum with near complete loss of DA innervation while the 5HT fiber terminals are at least

partially retained; (3) denervated striatum grafted with 5HT neurons in which the total 5HT fiber density is enhanced beyond the sparse network present endogenously; and (4) denervated striatum transplanted with DA-neuron rich grafts that partially re-constitutes the normal DA terminal network, and in fact also contained some 5HT neurons as well.

Although the data we obtained confirmed that 5HT terminals were recruited to ectopically synthesize and store DA upon L-DOPA administration, the level of extracellular DA measured by OMD did not exceed those seen in intact animals – either in parkinsonian rats or in animals where grafts rich in 5HT neurons generated a supra-normal serotonergic terminal density in the dopamine denervated striatum. Moreover, [¹⁸F]fallypride PET imaging showed that the D2R occupancy in the striatum was in fact not altered in either group of animals, suggesting that DA originating from serotonergic terminals could not have contributed to a large increase in DA bound to D2R.

Exogenous L-DOPA induced a KCl-releasable pool of DA accumulating in the serotonergic terminals originating from the 5HT grafts comparable to what we measured in DA grafts suggesting that in the presence of L-DOPA, the serotonergic terminal network served as a potent source of DA comparable to that generated by conventional VM grafts. Importantly, however, enriching the DA synthesizing compartment in the denervated striatum by DA- or 5HT-grafts had distinctly different functional consequences. First, DA grafts reduced dyskinesia and improved normal motor performance, whereas 5HT grafts appeared ineffective in reducing motor impairments and worsened dyskinesia. Secondly, under baseline conditions, DA grafts reconstituted extracellular DA levels, which remained stable even after administration of L-DOPA peripherally. 5HT grafts, on the other hand, not only lacked the ability to normalize DA neurotransmission, but also failed to buffer the newly formed extracellular DA upon L-DOPA challenge as the DA levels in the striatum started to drift. The OMD measurements showed that although DA levels increased by 19 to 27-fold in lesioned animals, the peak levels reached at about 2 hours after L-DOPA administration still remained within the normal physiological range. These findings are in agreement with data reported by Lindgren and collaborators [11]. Third, while DA grafts were efficient in normalizing the

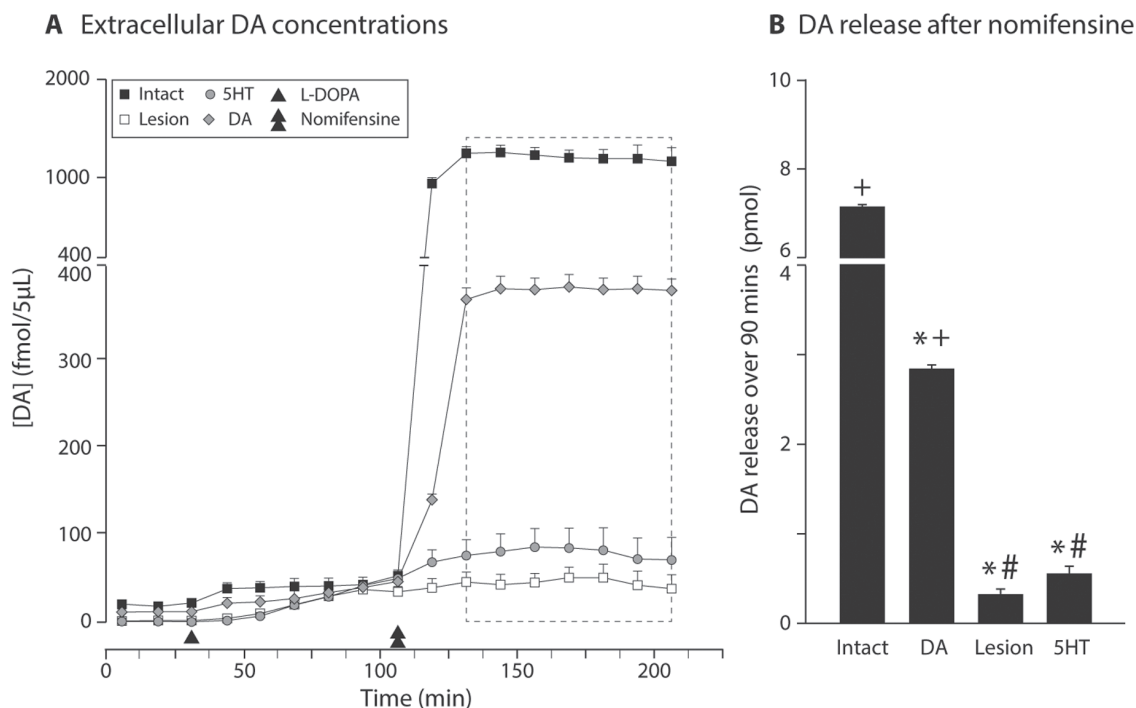


Figure 9. Assessment of changes in extracellular DA levels following L-DOPA injection and nomifensine treatment. Anesthetized animals were subjected to OMD measurements first under baseline for 37.5 min (3 time bins), and then injected systemically with 12 mg/kg L-DOPA. At 125 min, they received nomifensine (DAT blocker) using the reverse dialysis method. The time course data shown from this experiment is shown in A and quantification of the plateau phase after nomifensine (7 time bins over about 90 min) is given in panel B. (One-way ANOVA $F(3,15) = 166.48$, $p < 0.001$; followed by pairwise comparison adjusted using Bonferroni, $p < 0.0083$). *: Different from intact; +: different from lesion; #: different from DA graft.

doi:10.1371/journal.pone.0090759.g009

BP for [^{18}F]fallypride in the striatum, 5HT grafts were ineffective in mediating a similar correction even after L-DOPA administration. The latter finding, in particular, suggested that DA released from the 5HT terminals was inefficient in re-constituting dopaminergic neurotransmission, at least via the D2R mediated pathway.

In both PD patients and 6-OHDA lesioned animals, where there is a severe loss of dopaminergic terminals in the striatum, synaptic DA concentrations remain at very low levels of L-DOPA. Two characteristic features of this phenomenon might have an impact on occurrence and severity of dyskinesia. First, DA neurotransmission is re-constituted, albeit at insufficient levels, only in the presence of peripheral L-DOPA. Second, each L-DOPA treatment causes a short-term increase in DA levels exposing the striatal neurons to a transient DA-receptor stimulation. Thus, the post-synaptic neurons maintain an abnormal exposure and response to DA stimulation. The characteristics of generation of DA in the striatum might still be one of the critical factors in expression of dyskinesia in lesioned animals, as a recent study found differences in peak striatal DA concentrations between non-dyskinetic and dyskinetic rats, although data in both groups remained below levels measured in normal rats [11]. Given that we have not been able to show the presence of an excessive DA release from serotonergic terminals and that maladaptive plasticity in the striatal neurons persisted, it is plausible that the pathophysiological basis of LID in these animals relies on a transient activation of super-sensitive receptors. Stocchi and colleagues (1995) showed that the benefits of continuous dopamine stimulation were obtained despite that the blood levels of L-DOPA

in these patients were higher during continuous infusion as compared with the intermittent oral administration, supporting the view that dyskinesia was probably related to the pulsatile nature of the stimulation rather than the level of L-DOPA *per se* [36].

It is notable that in the experimental conditions studied here, D2R occupancy at sub-physiological levels might be part of a mechanism that gave rise to severe dyskinetic behaviors in parkinsonian animals that have a rich serotonergic terminal network in the striatum. Therefore, another mechanism, not mutually exclusive of the aforementioned, might relate to the precise activation profile of DA receptors in the striatum. It is well known that activation of D1R provoke severe dyskinesia, while the use of D2R agonists do not cause the same side effects [6,37–42]. Thus, a differential activation of the two-receptor subtypes by DA might be the cause of the substantially different behavioral outcomes. Our findings in this experiment suggest that abnormal behavioral outcomes (such as occurrence of dyskinesia) could be seen when D2R activation fails, while the D1R binding properties remain unaltered.

DA receptors (at least the D1R type) are known to be located on the soma and dendrites of striatal neurons where dopaminergic neurons do not normally make synaptic contacts [43,44]. Our OMD data showed similar levels of DA in the extracellular space in the 5HT-grafted L-DOPA treated animals and the intact rats. Therefore, it appears that the extra-synaptic DA-receptor occupancy would be comparable in these two scenarios. This raises the possibility that activation of extra-synaptic D1R, in the absence of appropriate D2R activation, could be one of the underlying

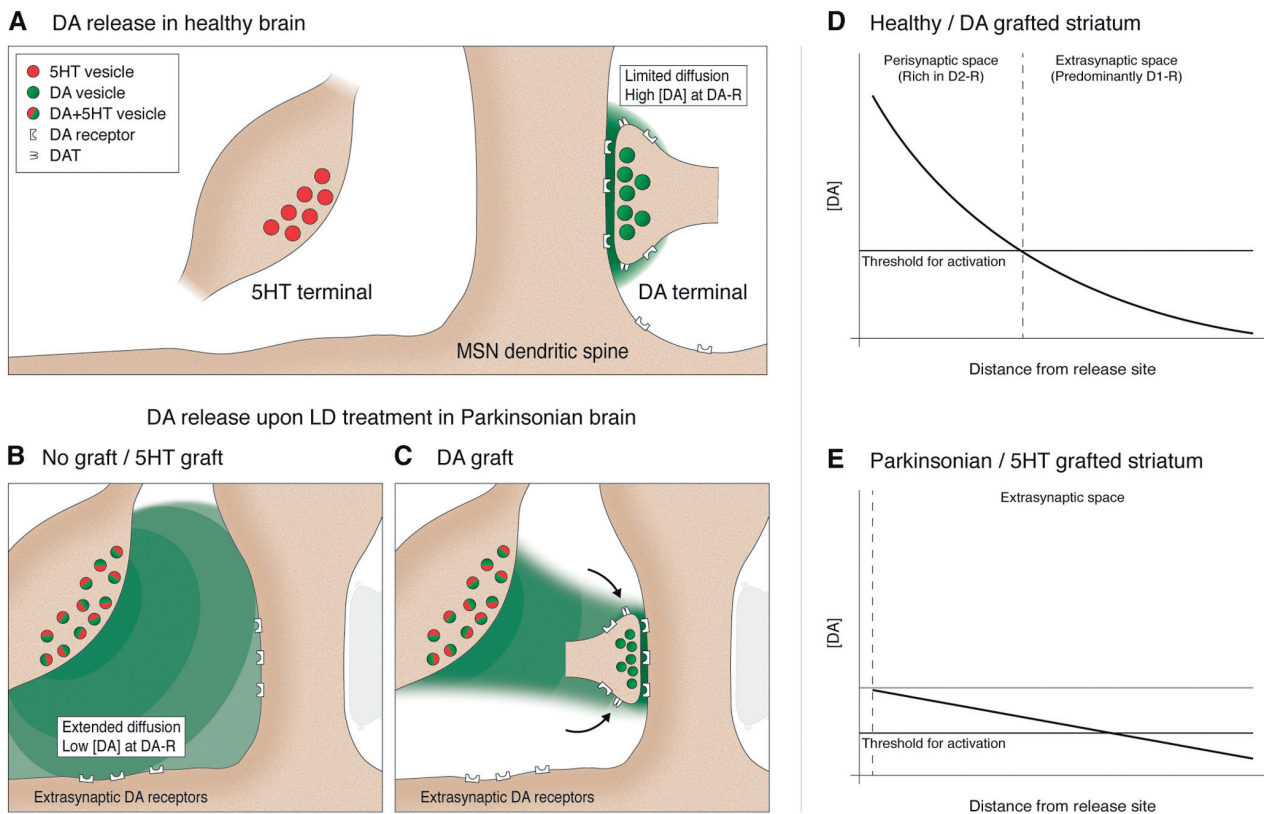


Figure 10. Serotonergic mechanisms for induction of L-DOPA induced dyskinesia in Parkinson's disease. Two distinct properties of dopamine (DA) release from the dopaminergic nerve terminals in the healthy brain (A) distinguish it from the dopaminergic neurotransmission seen in Parkinson's disease (PD) (B). The ability to release DA at high concentration at the synaptic site and control the spread by way of the uptake sites creates a sharp gradient in DA concentration as a function of distance providing selectivity in the receptors activated (D). Extrasynaptic DA-receptors are typically activated only after burst discharges (not illustrated in this figure). Lack of appropriate synaptic specializations at the correct target locations and the absence of re-uptake sites for DA makes the serotonergic nerve terminals behave differently upon L-DOPA administration (B). DA released from these terminals as a false neurotransmitter results in not only a wider diffusion but also fails to create the selectivity in the activation pattern leading to an abnormal dopaminergic signaling (E). Note that under these circumstances the threshold for activation of receptors may also be altered. Nevertheless, dopamine-neuron rich grafts re-establish the proper synaptic release mechanisms, limit the diffusion of DA in the extracellular space and therefore restore physiological neurotransmission (C, D). doi:10.1371/journal.pone.0090759.g010

reasons for occurrence of LID, and 5HT-neuron mediated DA release might lead to this unwanted outcome.

The effect of L-DOPA on D2R occupancy has been studied using another PET ligand, [^{11}C]raclopride, where the investigators found that the BP values after L-DOPA treatment was lower and this was reversed by use of selective 5-HT $_{1A}$ agonist, 8-OH-DPAT [45]. Although the characteristics of the [^{11}C]raclopride and [^{18}F]fallypride tracers are reported to be similar [46], we cannot rule out that displacement of [^{11}C]raclopride would be achieved at lower levels of re-constitution of DA in the striatum. In a series of additional experiments done in healthy rats, we found that there is strong relationship between amphetamine induced DA release and % decrease in [^{18}F]fallypride BP obtained by PET imaging (Fig 8). In addition, the study by Nahimi and colleagues used an acute challenge paradigm and administered high dose L-DOPA (50 mg/kg) to animals prior to imaging. The dose selected in that study would not be possible to implement in a chronic treatment paradigm like the one we used here, as it would result in self-mutilation in animals and in fact is much higher than clinically applied doses in man.

Our current working hypothesis (illustrated in Fig. 10) proposes the following mechanism: In the intact brain or the DA grafted

striatum (Fig. 10A, C), DA release from the appropriate sites results in a sharp rise in DA concentrations at the release site, followed by a rapid clearance via the DAT, thus creating a limited sphere of influence with a sharp concentration gradient as a function of distance and a brief time window of activation after each release event (Fig. 10D), providing a temporal and spatial selectivity to the physiological neurotransmission [47–49]. It follows that, under normal conditions, extra-synaptic D1R are activated selectively after burst discharges [49], whereas, DA released from 5HT terminals would neither create sufficiently high concentrations at D2R containing sites, nor would it be able to establish a clearance mechanism (i.e., lack selectivity in the activation pattern) (Fig. 10B). DA release from compartments that do not contain functional DAT causes DA to persist in the extracellular space much longer [50,51]. This would cause DA to diffuse much further in the extracellular space and act on the D1R with a wider sphere of influence (Fig. 10E). Such abnormal activation of D1R by L-DOPA has been linked to abnormal internalization of D1R in the striatum [38,52,53]. On the other hand, restoration of a new DA-neuron based terminal release network would establish an appropriate synaptic release mechanism, normalize the D2R occupancy, control the leakage of DA in

the extra-synaptic space, and thus also restore the normal activation pattern of D1R (Fig. 10C).

A logical interpretation of this outcome can be based on the differential ultrastructural properties of the two types of terminals. DA neurons are known to innervate their striatal target cells at very high intensity forming not only synaptic contacts but also a dense axon lattice. Detailed electron microscopy studies investigating dopaminergic synapses demonstrated that majority of pre-synaptic DA terminals either make synaptic contacts with the spine neck of the striatal target neurons or reside in close proximity to these specialized sites [54–56]. By contrast, serotonergic terminals make proper synaptic contacts infrequently. Instead 5HT release typically occurs from varicosities located *en-passant* to the 5HT receptor bearing sites [57]. Therefore it is plausible that the serotonergic terminal network – either endogenous or those established by the grafted neurons – release DA at sites further away from the release sites normally generated by DA neurons. As a consequence, while DA may be released in an uncontrolled manner from serotonergic terminals and diffuse further due to lack of uptake sites, it fails to reach sufficient concentration locally at the D2R containing sites. In support of this view, the insufficiency of the DA released from serotonergic terminals as compared with that originating from the dopaminergic neurons became evident in our OMD experiments upon blockade of the re-uptake sites with nomifensine.

DA terminals provide both continuous dopaminergic stimulation and a buffering capacity in the areas they innervate. It is likely that this is the underlying mechanism by which dopaminergic grafts reduce dyskinesia and abolish an abnormal response pattern of the striatal neurons [10,58–60]. Normalization of δ FosB expression after reconstitution of the appropriate DA release sites is an important indicator of this difference [61]. Here we demonstrated both retention of abnormal accumulation of δ FosB and a concomitant persistence of dyskinesia in both the DA denervated rats and the 5HT-grafted animals. The relationship between Δ FosB and dyskinesia has been well documented [7,62–64] and reduction of δ FosB expression by antisense oligonucleotide treatment has been shown to reduce the severity of dyskinesia in rats [62]. Moreover, striatal δ FosB induction occurs in dynorphin containing projection neurons of the direct pathway and is mediated by D1R activation [7,37,65].

The pre-synaptic dopamine-releasing compartment has a strong impact on the behavior of the post-synaptic striatal neurons. When striatal dopamine production is inhibited by knockdown of the TH enzyme – causing a functional DA depletion without a structural disintegration of the synaptic terminals – pulsatile administration of exogenous L-DOPA fails to induce dyskinesia [26]. Under these experimental conditions, even when dyskinesia is induced by direct

DA-receptor stimulation by chronic apomorphine treatment and striatal FosB/ δ FosB expression is elevated, re-constitution of substantial DA neurotransmission from endogenous terminals upon L-DOPA supplement fails to elicit dyskinesia. These results support the view that DA released from proper synaptic contacts with appropriate auto-receptor control mechanisms and re-uptake sites introduces very low or no risk for induction of dyskinesia in rats, despite providing higher levels of DA release than achieved via serotonergic terminals.

Taken together, our results suggest that in cases where dyskinesia is troublesome and there is an abundance of serotonergic terminals in areas of the striatum lacking dopamine terminals, the side effects of L-DOPA are induced not because of excessive DA production but rather a limited dopaminergic stimulation primarily targeting extra-synaptic receptor sites that persists only intermittently. In other words, the abnormality of DA release from serotonin neurons not only has a quantitative insufficiency, but also a qualitative abnormality, such as lack of appropriate gradients from release sites, specificity of activation in subsets of receptors needed to mediate appropriate actions and inability to buffer the extracellular levels of DA to mediate normal neurotransmission. A therapeutic intervention dampening DA release from the serotonergic terminals might be effective in reducing dyskinesia, however in order to achieve substantial functional restoration in these cases, it would be necessary to provide an additional pool of DA that can normalize the activation pattern of DA receptors (increase occupancy at D2R and reduce activation of extrasynaptic D1R) and sustain this activity over a long term, e.g., by enriching the dopaminergic terminal density in denervated regions of striatum especially in areas that receive 5HT innervation.

Acknowledgments

The authors wish to thank Anneli Josefsson, Ulla Samuelsson, Ulrika Sparrhult-Björk and Ulrika Schagerlöf for their excellent technical assistance, Tomas Björklund for advice in D2 receptor assay, Fredrik Nilsson for designing the generalized non-linear model for analysis of the D1 and D2 receptor assays and Erik Ahlm Cederfjäll for the art design of Figure 9. Authors are also grateful to Martine Guillemier, Marion Chaigneau and Diane Houitte for expert technical assistance with animal handling during PET experiments.

Author Contributions

Conceived and designed the experiments: PH DK. Performed the experiments: GS LHT SL MO LRV. Analyzed the data: GS SL PH DK. Contributed reagents/materials/analysis tools: GS SL FD PH DK. Wrote the paper: GS SL PH DK.

References

- Fahn S (2003) Description of Parkinson's disease as a clinical syndrome. *Annals of the New York Academy of Sciences* 991: 1–14.
- Kim DS, Palmiter RD, Cummins A, Gerfen CR (2006) Reversal of supersensitive striatal dopamine D1 receptor signaling and extracellular signal-regulated kinase activity in dopamine-deficient mice. *Neuroscience* 137: 1381–1388.
- Winkler C, Kirik D, Björklund A, Cenci MA (2002) L-DOPA-induced dyskinesia in the intrastriatal 6-hydroxydopamine model of parkinson's disease: relation to motor and cellular parameters of nigrostriatal function. *Neurobiology of disease* 10: 165–186.
- Rice ME, Patel JC, Cragg SJ (2011) Dopamine release in the basal ganglia. *Neuroscience* 198: 112–137.
- Gerfen CR, Miyachi S, Paletzki R, Brown P (2002) D1 dopamine receptor supersensitivity in the dopamine-depleted striatum results from a switch in the regulation of ERK1/2/MAP kinase. *The Journal of neuroscience: the official journal of the Society for Neuroscience* 22: 5042–5054.
- Aubert I, Guigoni C, Hakansson K, Li Q, Dovero S, et al. (2005) Increased D1 dopamine receptor signaling in levodopa-induced dyskinesia. *Annals of neurology* 57: 17–26.
- Westin JE, Vercammen L, Strome EM, Konradi C, Cenci MA (2007) Spatiotemporal pattern of striatal ERK1/2 phosphorylation in a rat model of L-DOPA-induced dyskinesia and the role of dopamine D1 receptors. *Biological psychiatry* 62: 800–810.
- Navailles S, Bioulac B, Gross C, De Deurwaerdere P (2010) Serotonergic neurons mediate ectopic release of dopamine induced by L-DOPA in a rat model of Parkinson's disease. *Neurobiology of disease* 38: 136–143.
- Garcia J, Carlsson T, Dobrossy M, Nikkiah G, Winkler C (2011) Impact of dopamine to serotonin cell ratio in transplants on behavioral recovery and L-DOPA-induced dyskinesia. *Neurobiology of disease* 43: 576–587.
- Carlsson T, Carta M, Winkler C, Björklund A, Kirik D (2007) Serotonin neuron transplants exacerbate L-DOPA-induced dyskinesias in a rat model of Parkinson's disease. *The Journal of neuroscience: the official journal of the Society for Neuroscience* 27: 8011–8022.

11. Lindgren HS, Andersson DR, Lagerkvist S, Nissbrandt H, Cenci MA (2010) L-DOPA-induced dopamine efflux in the striatum and the substantia nigra in a rat model of Parkinson's disease: temporal and quantitative relationship to the expression of dyskinesia. *Journal of neurochemistry* 112: 1465–1476.
12. Eskow KL, Dupre KB, Barnum CJ, Dickinson SO, Park JY, et al. (2009) The role of the dorsal raphe nucleus in the development, expression, and treatment of L-dopa-induced dyskinesia in hemiparkinsonian rats. *Synapse* 63: 610–620.
13. Tanaka H, Kamari K, Maeda T, Tomiyama M, Suda T, et al. (1999) Role of serotonergic neurons in L-DOPA-derived extracellular dopamine in the striatum of 6-OHDA-lesioned rats. *Neuroreport* 10: 631–634.
14. Ng KY, Chase TN, Colburn RW, Kopin IJ (1970) L-Dopa-induced release of cerebral monoamines. *Science* 170: 76–77.
15. Everett GM, Borcherding JW (1970) L-DOPA: effect on concentrations of dopamine, norepinephrine, and serotonin in brains of mice. *Science* 168: 847–850.
16. Arai R, Karasawa N, Geffard M, Nagatsu T, Nagatsu I (1994) Immunohistochemical evidence that central serotonin neurons produce dopamine from exogenous L-DOPA in the rat, with reference to the involvement of aromatic L-amino acid decarboxylase. *Brain research* 667: 295–299.
17. Munoz A, Li Q, Gardoni F, Marcello E, Qin C, et al. (2008) Combined 5-HT1A and 5-HT1B receptor agonists for the treatment of L-DOPA-induced dyskinesia. *Brain: a journal of neurology* 131: 3380–3394.
18. Constantinescu CC, Coleman RA, Pan ML, Mukherjee J (2011) Striatal and extrastriatal microPET imaging of D2/D3 dopamine receptors in rat brain with [(1)(8)F]fallypride and [(1)(8)F]desmethoxyfallypride. *Synapse* 65: 778–787.
19. Christian BT, Narayanan TK, Shi B, Mukherjee J (2000) Quantitation of striatal and extrastriatal D-2 dopamine receptors using PET imaging of [(18)F]fallypride in nonhuman primates. *Synapse* 38: 71–79.
20. Mukherjee J, Christian BT, Narayanan TK, Shi B, Collins D (2005) Measurement of d-amphetamine-induced effects on the binding of dopamine D-2/D-3 receptor radioligand, 18F-fallypride in extrastriatal brain regions in non-human primates using PET. *Brain Res* 1032: 77–84.
21. Slifstein M, Kegeles LS, Xu X, Thompson JL, Urban N, et al. (2010) Striatal and extrastriatal dopamine release measured with PET and [(18)F] fallypride. *Synapse* 64: 350–362.
22. Mukherjee J, Yang ZY, Das MK, Brown T (1995) Fluorinated benzamide neuroleptics—III. Development of (S)-N-[(1-allyl-2-pyrrolidinyl)methyl]-5-(3-[18F]fluoropropyl)-2, 3-dimethoxybenzamide as an improved dopamine D-2 receptor tracer. *Nuclear medicine and biology* 22: 283–296.
23. Kuhnast B, Hinnen F, Dollé F (2009) Production of [18F]Fallypride on a TRACERLab FX-FN synthesizer. *J Label Compounds Radiopharm* 52 (Suppl. 1): S286.
24. Logan J, Fowler JS, Volkow ND, Wang GJ, Ding YS, et al. (1996) Distribution volume ratios without blood sampling from graphical analysis of PET data. *Journal of cerebral blood flow and metabolism: official journal of the International Society of Cerebral Blood Flow and Metabolism* 16: 834–840.
25. Thorre K, Pravda M, Sarre S, Ebinger G, Michotte Y (1997) New antioxidant mixture for long term stability of serotonin, dopamine and their metabolites in automated microbore liquid chromatography with dual electrochemical detection. *Journal of chromatography B, Biomedical sciences and applications* 694: 297–303.
26. Ulusoy A, Sahin G, Kirik D (2010) Presynaptic dopaminergic compartment determines the susceptibility to L-DOPA-induced dyskinesia in rats. *Proceedings of the National Academy of Sciences of the United States of America* 107: 13159–13164.
27. West MJ (1999) Stereological methods for estimating the total number of neurons and synapses: issues of precision and bias. *Trends Neurosci* 22: 51–61.
28. Gundersen HJ, Jensen EB (1987) The efficiency of systematic sampling in stereology and its prediction. *J Microsc* 147: 229–263.
29. Paxinos G, Watson C (1997) *The Rat Brain in Stereotaxic Coordinates*. Sydney: Academic Press.
30. Pinheiro J, Bates D (2000) *Mixed-effects models in S and S-PLUS*. New York, NY [u.a.]: Springer.
31. R-Core-Team (2012) *R: A Language and Environment for Statistical Computing*.
32. Hothorn T, Bretz F, Westfall P (2008) Simultaneous inference in general parametric models. *Biom J* 50: 346–363.
33. Cederfjall E, Sahin G, Kirik D (2011) Key factors determining the efficacy of gene therapy for continuous DOPA delivery in the Parkinsonian brain. *Neurobiology of disease*.
34. Carta M, Bezard E (2011) Contribution of pre-synaptic mechanisms to L-DOPA-induced dyskinesia. *Neuroscience* 198: 245–251.
35. Navailles S, De Deurwaerdere P (2011) Presynaptic control of serotonin on striatal dopamine function. *Psychopharmacology* 213: 213–242.
36. Stocchi F, Vacca L, Ruggieri S, Olanow CW (2005) Intermittent vs continuous levodopa administration in patients with advanced Parkinson disease: a clinical and pharmacokinetic study. *Arch Neurol* 62: 905–910.
37. Darmopil S, Martin AB, De Diego IR, Ares S, Moratalla R (2009) Genetic inactivation of dopamine D1 but not D2 receptors inhibits L-DOPA-induced dyskinesia and histone activation. *Biological psychiatry* 66: 603–613.
38. Muriel MP, Bernard V, Levey AI, Laribi O, Abrous DN, et al. (1999) Levodopa induces a cytoplasmic localization of D1 dopamine receptors in striatal neurons in Parkinson's disease. *Annals of neurology* 46: 103–111.
39. St-Hilaire M, Landry E, Levesque D, Rouillard C (2005) Denervation and repeated L-DOPA induce complex regulatory changes in neurochemical phenotypes of striatal neurons: implication of a dopamine D1-dependent mechanism. *Neurobiology of disease* 20: 450–460.
40. Levey AI, Hersch SM, Rye DB, Sunahara RK, Niznik HB, et al. (1993) Localization of D1 and D2 dopamine receptors in brain with subtype-specific antibodies. *Proceedings of the National Academy of Sciences of the United States of America* 90: 8861–8865.
41. Yung KK, Bolam JP, Smith AD, Hersch SM, Ciliax BJ, et al. (1995) Immunocytochemical localization of D1 and D2 dopamine receptors in the basal ganglia of the rat: light and electron microscopy. *Neuroscience* 65: 709–730.
42. Mela F, Marti M, Bido S, Cenci MA, Morari M (2012) In vivo evidence for a differential contribution of striatal and nigral D1 and D2 receptors to L-DOPA induced dyskinesia and the accompanying surge of nigral amino acid levels. *Neurobiology of disease* 45: 573–582.
43. Hersch SM, Ciliax BJ, Gutekunst CA, Rees HD, Heilman CJ, et al. (1995) Electron microscopic analysis of D1 and D2 dopamine receptor proteins in the dorsal striatum and their synaptic relationships with motor corticostriatal afferents. *The Journal of neuroscience: the official journal of the Society for Neuroscience* 15: 5222–5237.
44. Caille I, Dumartin B, Bloch B (1996) Ultrastructural localization of D1 dopamine receptor immunoreactivity in rat striatonigral neurons and its relation with dopaminergic innervation. *Brain research* 730: 17–31.
45. Nahimi A, Holtzmann M, Landau AM, Simonsen M, Jakobsen S, et al. (2012) Serotonergic modulation of receptor occupancy in rats treated with L-DOPA after unilateral 6-OHDA lesioning. *Journal of neurochemistry* 120: 806–817.
46. Laruelle M (2000) Imaging synaptic neurotransmission with in vivo binding competition techniques: a critical review. *Journal of cerebral blood flow and metabolism: official journal of the International Society of Cerebral Blood Flow and Metabolism* 20: 423–451.
47. Chergui K, Suaud-Chagny MF, Gonon F (1994) Nonlinear relationship between impulse flow, dopamine release and dopamine elimination in the rat brain in vivo. *Neuroscience* 62: 641–645.
48. Suaud-Chagny MF, Dugast C, Chergui K, Msghina M, Gonon F (1995) Uptake of dopamine released by impulse flow in the rat mesolimbic and striatal systems in vivo. *Journal of neurochemistry* 65: 2603–2611.
49. Gonon F (1997) Prolonged and extrasynaptic excitatory action of dopamine mediated by D1 receptors in the rat striatum in vivo. *The Journal of neuroscience: the official journal of the Society for Neuroscience* 17: 5972–5978.
50. Giros B, Jaber M, Jones SR, Wightman RM, Caron MG (1996) Hyperlocomotion and indifference to cocaine and amphetamine in mice lacking the dopamine transporter. *Nature* 379: 606–612.
51. Jones SR, Gainetdinov RR, Wightman RM, Caron MG (1998) Mechanisms of amphetamine action revealed in mice lacking the dopamine transporter. *The Journal of neuroscience: the official journal of the Society for Neuroscience* 18: 1979–1986.
52. Dumartin B, Caille I, Gonon F, Bloch B (1998) Internalization of D1 dopamine receptor in striatal neurons in vivo as evidence of activation by dopamine agonists. *The Journal of neuroscience: the official journal of the Society for Neuroscience* 18: 1650–1661.
53. Dumartin B, Jaber M, Gonon F, Caron MG, Giros B, et al. (2000) Dopamine tone regulates D1 receptor trafficking and delivery in striatal neurons in dopamine transporter-deficient mice. *Proceedings of the National Academy of Sciences of the United States of America* 97: 1879–1884.
54. Freund TF, Powell JF, Smith AD (1984) Tyrosine hydroxylase-immunoreactive boutons in synaptic contact with identified striatonigral neurons, with particular reference to dendritic spines. *Neuroscience* 13: 1189–1215.
55. Moss J, Bolam JP (2008) A dopaminergic axon lattice in the striatum and its relationship with cortical and thalamic terminals. *The Journal of neuroscience: the official journal of the Society for Neuroscience* 28: 11221–11230.
56. Sesack SR, Aoki C, Pickel VM (1994) Ultrastructural localization of D2 receptor-like immunoreactivity in midbrain dopamine neurons and their striatal targets. *The Journal of neuroscience: the official journal of the Society for Neuroscience* 14: 88–106.
57. Descarries L, Soghomonian JJ, Garcia S, Doucet G, Bruno JP (1992) Ultrastructural analysis of the serotonin hyperinnervation in adult rat neostriatum following neonatal dopamine denervation with 6-hydroxydopamine. *Brain Res* 569: 1–13.
58. Lee CS, Cenci MA, Schulzer M, Bjorklund A (2000) Embryonic ventral mesencephalic grafts improve levodopa-induced dyskinesia in a rat model of Parkinson's disease. *Brain: a journal of neurology* 123 (Pt 7): 1365–1379.
59. Carlsson T, Winkler C, Lundblad M, Cenci MA, Bjorklund A, et al. (2006) Graft placement and uneven pattern of reinnervation in the striatum is important for development of graft-induced dyskinesia. *Neurobiology of disease* 21: 657–668.
60. Lane EL, Winkler C, Brundin P, Cenci MA (2006) The impact of graft size on the development of dyskinesia following intrastriatal grafting of embryonic dopamine neurons in the rat. *Neurobiology of disease* 22: 334–345.
61. Carlsson T, Carta M, Munoz A, Mattsson B, Winkler C, et al. (2009) Impact of grafted serotonin and dopamine neurons on development of L-DOPA-induced dyskinesias in parkinsonian rats is determined by the extent of dopamine neuron degeneration. *Brain: a journal of neurology* 132: 319–335.
62. Andersson M, Hilbertson A, Cenci MA (1999) Striatal fosB expression is causally linked with L-DOPA-induced abnormal involuntary movements and the

- associated upregulation of striatal prodynorphin mRNA in a rat model of Parkinson's disease. *Neurobiology of disease* 6: 461–474.
63. Pavon N, Martin AB, Mendiola A, Moratalla R (2006) ERK phosphorylation and FosB expression are associated with L-DOPA-induced dyskinesia in hemiparkinsonian mice. *Biological psychiatry* 59: 64–74.
64. Cao X, Yasuda T, Uthayathas S, Watts RL, Mouradian MM, et al. (2010) Striatal overexpression of DeltaFosB reproduces chronic levodopa-induced involuntary movements. *The Journal of neuroscience: the official journal of the Society for Neuroscience* 30: 7335–7343.
65. Moratalla R, Elibol B, Vallejo M, Graybiel AM (1996) Network-level changes in expression of inducible Fos:Jun proteins in the striatum during chronic cocaine treatment and withdrawal. *Neuron* 17: 147–156.

